The thesis committee for David Michael Wald
certifies that this is the approved version of the following thesis:

Experimental Investigation of Crushing Capacity of I-Girder Webs Containing Post-Tensioning Ducts

APPROVED BY
SUPERVISING COMMITTEE:

James O. Jirsa, Supervisor

Oguzhan Bayrak

Experimental Investigation of Crushing Capacity of I-Girder Webs Containing Post-Tensioning Ducts

by

David Michael Wald, B.S.Arch.E.

Thesis

Presented to the Faculty of the Graduate School of

The University of Texas at Austin

in Partial Fulfillment

of the Requirements

for the Degree of

Master of Science in Engineering

The University of Texas at Austin

December 2012

Dedication

To my family for their love and support

Acknowledgements

Firstly, this project could not have been made possible without the generous support of the Texas Department of Transportation. TxDOT's unwavering commitment to ensuring the safety, economy, and effectiveness of the state's transportation structures helped to guide the goals of this study.

To my supervisor, Dr. James O. Jirsa, and my advisor, Dr. Oguzhan Bayrak, I extend my sincerest gratitude for their feedback and guidance in completing my work. My passion to excel at research could not have been founded without their influence. Additional thanks go to Bijan Khaleghi, Steve Seguirant, and Chris White for their technical expertise imparted as members of this project's external advisory panel.

To the many student researchers contributing to this project – friends and colleagues – I offer my thanks for their devotion to their work and assistance in aiding in the development and accomplishment of my research endeavors. It was a pleasure to work with Katie Schmidt, Trang Nguyen, James Felan, and Josh Massey. Special thanks must be given to Andy Moore – it was a great privilege and learning experience to again work with such a capable and knowledgeable individual.

The day-to-day operations of this research study could not have been achieved without the hard work of the administrative and technical staff at Ferguson Lab. Many thanks go to Barbara Howard, Eric Schell, Mike Wason, and Dennis Fillip. To Andrew Valentine and Blake Stasney, whose aide and oversight I cannot speak highly enough of, I especially thank and commend for helping in test preparations five to ten times a day.

Lastly, to my parents and sister, I cannot express how deeply your undying love, support, and commitment to me have truly meant, not only during my time performing research, but all of the time. I could not be where I am today without you.

December, 2012

Experimental Investigation of Crushing Capacity of I-Girder Webs Containing Post-Tensioning Ducts

David Michael Wald, M.S.E.

The University of Texas at Austin, 2012

SUPERVISOR: James O. Jirsa

The shear capacity of a post-tensioned, concrete I-girder may be influenced if the crushing capacity of the web is reduced by ducts for the tendons. An experimental investigation was conducted on compressively-loaded, high-strength concrete panels with embedded post-tensioning ducts to better understand the parameters influencing girder web crushing behavior. The panels were intended to represent portions of a girder web subjected to shear-induced, principal compressive stresses. Material properties and construction procedures utilized in the fabrication and erection of bridge members in the field were considered.

The primary goal of this study was to assess the impacts of various parameters on web crushing capacity. The results were needed to determine which variables should be considered for shear testing of full-scale girders. The parameters considered in the panel test program were duct type, grouting, member thickness, and the inclusion of confining reinforcement near the ducts.

Notable findings from this study indicate that 1) elements with plastic ducts exhibit lower capacities than those with steel ducts, 2) a significant size effect exists

when determining crushing capacity, and 3) the presence of a small amount of reinforcement placed near a duct through a member's thickness can greatly improve its capacity.

Results indicated that American design codes may be severely unconservative in their handling of ducts when designing for shear. Recommendations to refine and expand the standard approach for reducing web crushing capacity were developed. Additionally, a new means of estimating web crushing capacity was introduced.

Table of Contents

List of Tables

List of Figures

CHAPTER 1
Introduction

1.1 BACKGROUND

The advent of spliced girder technology in the U.S. gives bridge designers an economical alternative to using segmental box girder or steel construction in order to achieve longer bridge spans. Spliced girder bridges take advantage of post-tensioning for load-resistance and provide continuity between multiple pretensioned girders that will be further linked via cast-in-place splices. The usefulness of these types of bridges is evident; however, the practical implementation of spliced girder construction requires understanding all of the components of design. Understanding the behavior of a post-tensioned girder in general is paramount.

The presence of post-tensioning ducts in girder webs is known to have an adverse effect on girder shear strength. The void created by a duct serves as a discontinuity in the flow path of principal compressive stresses induced by the application of shear force. With a lack of material within a duct that is of equal stiffness to the surrounding concrete, the compressive stress flow deviates from a straight path. This directional shift generates tensile stresses across the thickness of a web that cause splitting and reduce the web's crushing capacity.

The reduction in web crushing strength of a girder may be considered by utilizing an effective web width for shear calculations that is reduced from the gross web width. This effective width accounts for a loss in compressive capacity proportional to the size of the duct in a given web. Different design codes throughout the world require various reductions in web width based not only on duct and web sizes, but on the presence of grout and occasionally the duct material. Larger ducts in a given web result in greater stress flow deviation while the addition of grout in a duct can reduce the deviation.

Meanwhile, ducts can be made of either steel or high-density polyethylene (HDPE) plastic, each of which may affect web crushing behavior differently.

The discrepancies between different code equations accounting for the presence of ducts is concerning. Equations used in U.S. practice are not as conservative as those used elsewhere. Further, consideration of how much to reduce web widths has often been determined through the testing of small, uniaxially-compressed, concrete panel and prism specimens containing ducts that are intended to mimic portions of a web experiencing crushing behavior in a full girder. These tests may not be adequately scaled and often fail to reflect the multitude of practical design or construction choices. Thus, they do not capture the range of behavior that may result. Virtually no testing has been conducted on specimens with plastic ducts which are becoming increasingly popular for use in post-tensioning applications due to their superior corrosion protection and low-friction properties compared to steel ducts.

1.2 RESEARCH OBJECTIVES

The desire to implement spliced girder technology in the state of Texas led to the commissioning of Texas Department of Transportation (TxDOT) Project 0-6652 to be conducted at the Ferguson Structural Engineering Laboratory at The University of Texas at Austin. The initial phase of this project required an examination of the general shear behavior of post-tensioned girders and of the influence of incorporating ducts within member cross-sections. Ultimately, a lack of consistency in known approaches for shear design of post-tensioned girders instigated the need to develop a sounder basis for future applications. In advance of load-testing full-scale, post-tensioned girders to achieve this goal, an extensive preliminary study on representative component test specimens was initiated.

The study outlined in this document addresses the impact that post-tensioning ducts in I-girder webs have on web crushing strength through the load-testing of concrete panels containing ducts. These specimens were fabricated and tested to achieve the following objectives:

1. Develop accurate representations of the portions of an I-girder web containing a post-tensioning duct subjected to compressive stresses resulting from the application of shear loads.
2. Initiate a testing protocol analogous to those used in past research studies which have helped guide current design provisions.
3. Create simple and relatively inexpensive test specimens that can be used to quickly capture the relative impact of many design variations in an effort to understand and possibly improve current strength behavior. Many individual test results can be qualitatively and quantitatively compared without having to create and test much more expensive, full-scale girders with the same wide range of variables and modifications.
4. Use data from panel tests to optimize the design of girders that will be tested to verify results of the simple tests.
5. Use data to verify the validity and accuracy of current code equations.

1.3 SCOPE OF RESEARCH

An extensive literature review was conducted primarily covering constructability requirements for using post-tensioning ducts and current code treatments of ducts for shear design and calculations. Four structural design codes were consulted: 1) ACI 318-11 Building Code, 2) AASHTO LRFD Bridge Design Specifications, 6th Ed. (2012), 3) JSCE 3 (2002), and 4) Eurocode 2 (2004). The primary bridge design code used in the U.S. is the AASHTO LRFD document. The effectiveness of the specifications for determining the crushing capacity of panel or prism tests and for estimating the shear capacity of previously-tested, full-scale, post-tensioned girders was considered. Additionally, a database of ducted panel and prism test results was compiled from seven references. The methodologies previously used for panel testing were investigated to incorporate successful techniques in the current study. Results were examined to determine critical testing variables and document the areas where tests were needed.

The experimental program consisted of 100 uniaxial compression tests of high-strength concrete panels with ducts. The results from these tests were compared with reported research results and with code equations to assess the influence of each test variable prior to moving on to girder tests.

1.4 RESEARCH OVERVIEW: CHAPTER OUTLINE

In Chapter 2, a background review of past research on web crushing capacity and current construction and shear design approaches for handling post-tensioning ducts in girder webs are discussed. Various code reductions for web crushing strength are addressed along with a brief overview of code effectiveness at conservatively estimating girder shear strength. Extensive coverage of the findings and uses of previous panel and prism testing with ducts is provided.

In Chapter 3, the materials, methods, and testing procedures utilized for the current research are outlined. The test setup is explained, and a comprehensive walkthrough of the experimental process is outlined from specimen fabrication and test preparation through loading to failure.

In Chapter 4, the application of and basis for each of the major test variables in this study are described. The results obtained from panel testing are presented along with a discussion of testing observations and light analysis.

In Chapter 5, an analytical interpretation of the panel test results is presented. Emphasis is placed on the relative importance of major test variables in determining overall specimen capacities. Efforts are described to develop more complete approaches to estimate web crushing capacities. As a whole, the results are given context with a brief discussion of expectations for girder behavior and preliminary girder test observations from the next phase of this project.

In Chapter 6, the major findings from this research study are highlighted. Conclusions drawn from this work provide a basis for future compression tests of panels and shear tests of full-scale, post-tensioned girders.

CHAPTER 2
Background

2.1 OVERVIEW

Comprehensive background information pertaining to the treatment of post-tensioning ducts in I-girder webs when considering the phenomenon of web crushing is provided in this chapter. An extensive literature review was conducted gathering information on numerous code provisions for shear design and on construction applications where post-tensioning ducts are used. As such, the means by which ordinary prestressed girder designs are modified for post-tensioned applications with ducts introduced are explored. Then, a historical palette of research investigations aimed at understanding web crushing mechanisms and garnering capacities via small-scale testing is presented. The findings from previous studies serve as the guidance and inspiration for work in the present study. As will be seen, the basis for the experimental program and selection of test specimens, covered within Chapters 3 and 4, is derived from the distinction between various test cases.

2.2 INFLUENCE OF POST-TENSIONING DUCTS IN I-GIRDER WEBS

The presence of a post-tensioning duct in the web of an I-girder may have a detrimental effect on the girder's overall shear capacity. Notably, the web crushing capacity of a girder can be reduced due to the existence of the duct as a discontinuous element in the path of a shear-induced, principal compressive stress flow. In lowering the web crushing capacity of a girder, it may become more likely that the overall shear capacity is controlled by its crushing capacity rather than its shear-tension resistance. If and when this happens, the girder's capacity is reduced compared to what it would have been in a case without a duct. It is worth noting that a girder may be adequately designed with its capacity limited to that for web crushing. However, web crushing is an

undesirable mode of member failure due to the sudden, non-ductile manner in which the load-resisting capabilities are lost in such a case.

As illustrated by Leonhardt (1969), the trajectory of principal compressive stresses flowing through a post-tensioned girder web tends to deviate from linearity given the existence of an embedded duct (Figure 2-1). The amount of this deviation largely depends on the duct diameter-to-web thickness ratio, δ (i.e. the size of the duct in the girder web), and the presence or lack of grout within the duct. Stresses diverge more severely as duct size is increased. Without grout, a duct serves as an empty void that can carry no load; only the concrete at the sides of the duct may resist compressive forces. Compressive stresses bend around the empty duct while transverse tensile stresses develop to satisfy equilibrium across the web's thickness near the duct. In the presence of grout, compressive stresses in the web are attracted toward the grout-filled duct, thus reducing the net stress deviation and tension developed in the vicinity of the duct. The deviation depends largely on the relative stiffnesses of the grout and surrounding concrete. If a grouted duct is extremely stiff, such a large portion of load is then attracted toward the duct that the compressive stress flow actually funnels into the duct rather than bending around it while the field of transverse tension generated in equilibrium migrates away from the duct.

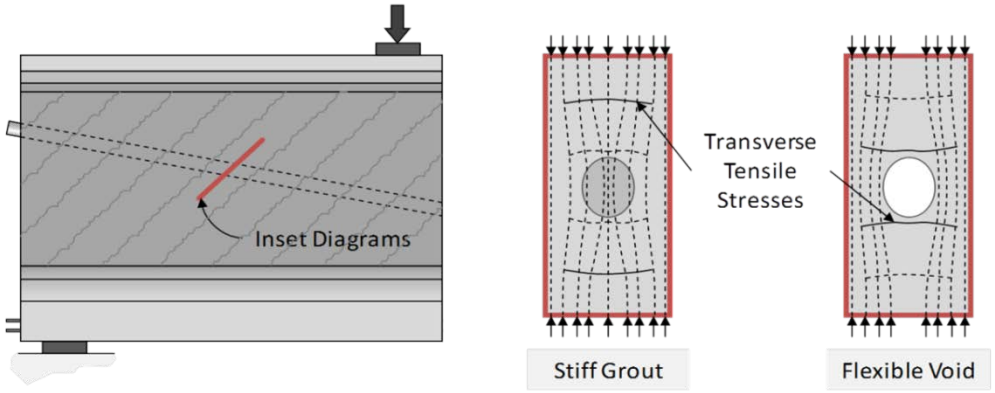

Figure 2-1: Principal Compressive Stress Flow in the Presence of a Grouted or Empty Duct (Adapted from Muttoni, Burdet, and Hars (2006) and Leonhardt (1969))

The existence of transverse tensile stresses through the thickness of the web reduces the crushing capacity of the web. The lack of homogeneity in materials at the level of the duct already lessens crushing capacity below that based on the gross width of a concrete-only section. Without consideration of tension, crushing capacity might simply be computed based on the net width of concrete at the level of the duct plus some fraction of the remainder of the web if the duct is grouted (and likely contingent upon the grout strength/stiffness). In reality, the action of tension produced by deviation in the direction of compression in the web can reduce crushing capacity more than would be expected.

2.3 PROVISIONS FOR SHEAR CALCULATIONS AND CONSTRUCTION WITH DUCTS

The use of post-tensioning ducts for bridge construction has necessitated modifications to shear design provisions and the development of practical fabrication procedures for efficient and manageable concreting. Understanding the basics of design and construction with ducts is vital in fully appreciating the impact of duct usage, recognizing the interaction between the design and construction processes, and eventually formulating and assessing test parameters within past and present web crushing studies.

2.3.1 Code Approaches to Web Crushing and Web Width Reduction

Many of the major structural design codes covering shear resistance of prestressed concrete beams address the presence of a post-tensioning duct in the web of an I-girder very similarly. Each of these codes calls for a reduction in the width of the web useful for web crushing resistance via equations of the same form, often with some correlation to results from the testing of panels or prisms containing ducts.

Design codes modify shear equations to account for the presence of ducts by replacing the gross web width with a reduced, effective web width. The effective web width is computed by subtracting some fraction of the total of all duct diameters aligned side-by-side in the cross section from the gross width as:

$$b_{eff} = b_w - k \cdot \Sigma\phi \qquad \textbf{Equation 2-1}$$

where:

b_{eff} = effective web width available to resist shear accounting for presence of ducts

b_w = gross web width

k = diameter correction factor, varied per code

ϕ = nominal duct diameter

The reduction depends on the type of duct used and whether or not ducts are grouted. When directly applied, the effective width is equivalent to the full width of a non-post-tensioned web having the same crushing capacity as that of a wider web containing a duct.

Unfortunately, there is a lack of agreement from one code to the next concerning how much of a ducted web should be considered ineffective for shear resistance. The fraction of the duct to be removed is presented as a constant in the general effective web width formula, referred to throughout this document as the k-factor or "diameter correction factor" (Muttoni, Burdet, and Hars 2006). It has been one of the primary goals of past web crushing research to identify appropriate and conservative k-factors for incorporating the effects of grouted steel ducts, empty steel ducts, grouted plastic ducts, or empty plastic ducts into design codes.

The following sections outline the means by which four major structural design codes adjust shear capacities of girders containing ducts in the web. For each code, k-factors are provided. Also included are discussions on how certain codes explicitly handle the potential for web crushing to control shear capacity.

2.3.1.1 ACI 318-11

The American Concrete Institute's Building Code makes no reduction for the presence of ducts on the shear capacity of flexural members. This is largely due to the fact that post-tensioning is a technique more widely used in bridge fabrication, and ACI 318 is principally applicable to building construction. Consequently, any shear

calculations performed using this code are based on the assumption that members have completely solid cross-sections, with full web widths available to resist shear forces. In comparison to other code shear calculation procedures, this is the least conservative.

It is also important to recognize how ACI 318 accounts for the possibility of web crushing in beam design. Section 11.4.7.9 of the code places a limit on the maximum contribution of transverse steel to the total, nominal shear capacity of a member. The limit given is:

$$V_s = 8\sqrt{f_c'}\,b_w d \qquad \textbf{Equation 2-2}$$

where:

f_c' = compressive strength of concrete [psi]

b_w = gross web width [in.]

d = distance from the extreme compression fiber to the centroid of the longitudinal tension reinforcement [in.]

The code assumes that if an excessive amount of shear reinforcement is provided in a member such that the steel contribution is in excess of the limit, a shear failure would more likely be attributed to crushing of the web rather than yielding of the reinforcement. Since transverse reinforcement is only expected to improve the shear-tension resistance of a member, but not its shear-compression capacity, the code enforces the steel contribution cap to stop designers from adding excess reinforcement that would end up providing no benefit to overall capacity.

2.3.1.2 AASHTO LRFD Bridge Design Specifications, 6th Ed. (2012)

Shear provisions for girders with ducts in the web are defined in two separate ways within Section 5 of the AASHTO LRFD Bridge Design Specifications herein referred to as AASHTO. The general shear design requirements are applicable in a majority of circumstances, including research. The shear provisions for segmental girders obviously have specialized use that may otherwise be irrelevant here, but differ in their treatment of ducts and must be considered.

2.3.1.2.1 General Shear Design

The general shear design provisions are highly comprehensive, with shear equations based upon the Modified Compression Field Theory (MCFT) of Vecchio and Collins (1986). For the sake of discussion, only a few of the major formulas are presented. The interested reader may refer to the code itself or seek other sources to understand the details, development, and use of the entirety of the shear provisions. In §5.8.3.3, the overall shear capacity of a girder is determined to be the lesser of:

$$V_n = V_c + V_s + V_p \qquad \textbf{Equation 2-3}$$

or $$V_n = 0.25 f_c' b_v d_v + V_p \qquad \textbf{Equation 2-4}$$

where:

V_n = nominal shear resistance [kips]

V_c = shear resistance contribution of concrete [kips]

V_s = shear resistance contribution of steel [kips]

V_p = vertical component of effective prestressing force [kips]

b_v = effective web width (= b_{eff} as defined earlier) [in.]

d_v = effective shear depth [in.]

The shear resistance contributions of the concrete (using general procedures) and steel (with transverse steel oriented at 90° to a member's longitudinal axis) are defined as:

$$V_c = 0.0316 \beta \sqrt{f_c'} b_v d_v \qquad \textbf{Equation 2-5}$$

and $$V_s = \frac{A_v f_y d_v \cot\theta}{s} \qquad \textbf{Equation 2-6}$$

where:

β = factor indicating ability of diagonally cracked concrete to transmit tension and shear

A_v = area of transverse reinforcement [in^2]

f_y = yield strength of transverse reinforcement [ksi]

θ = angle of inclination of diagonal compressive stresses

s = spacing of transverse reinforcement [in.]

Unlike the ACI 318 approach for considering the potential for web crushing by limiting the maximum amount of shear reinforcement, AASHTO institutes an upper limit on the shear stress that can be handled by the section. This is done by incorporating the 0.25 factor into Equation 2-4. Overall shear capacity may be controlled by this equation, which does not even consider the contribution of transverse steel. If this is the case, the equation assumes that a member experiencing shears higher than the calculated resistance would fail via web crushing rather than by yielding of transverse reinforcement.

Of all codes that do reduce the web width when ducts are present, AASHTO is the least conservative based on its general shear provisions. The general provisions call for k-factors of 0.25 and 0.5 for grouted and empty ducts, respectively, in §5.8.2.9. The duct type does not play a role in determining which k-factor to use. It is also interesting to note that an effective web width is used not only in the limiting shear equation for web crushing to control (Equation 2-4) but also in the formula for the concrete shear contribution (Equation 2-5). Effective web widths and k-factors have been developed to reflect a reduction in web crushing capacity rather than shear-tension capacity. Consequently, the use of an effective web width in Equation 2-5 is questionable given that the term V_c only contributes to shear-tension capacity.

2.3.1.2.2 Shear Design of Segmental Girders

AASHTO includes separate shear design provisions for segmental box girders that are more conservative than the general provisions regarding treatment of ducts in webs. Section 5.8.6.1 of the code specifies that the effective web width for calculation should utilize k-factors of 0.5 and 1.0 when using grouted and empty ducts, respectively.

Ultimately, the increase in k-factors has to do with the presence of fewer girder webs resisting shear in a segmental box girder bridge than in a regular I-girder bridge. More girders are typically utilized within a single span of an I-girder bridge than in a segmental box girder bridge, and thus there is less redundancy in the latter system. This generates the need for a more restrictive design and thus a greater reduction of the web width for computation.

2.3.1.3 JSCE No. 3 (2002)

Japanese specifications for the shear design of prestressed concrete members require a reduction in the web width given δ greater than 0.125. Section 6.3.3-4i of this code states:

> "In cases when the diameter of a duct in prestressed concrete members is equal to or greater than 1/8 of the width of the web, the width used in [concrete shear contribution equation] shall be appropriately reduced (from the actual width, b_w). It is recommended that the web width may be reduced to ($b_w - 1/2\Sigma\phi$), i.e. by an amount equal to one-half the sum of all the diameters of the ducts 'ϕ' spaced in the cross section."

JSCE No. 3, referred elsewhere simply as JSCE, allows for the same web width reduction regardless of duct type or grouting. A k-factor of 0.5 is given, which is consistent with those k-factors from the most conservative of codes dealing with grouted metal ducts.

2.3.1.4 Eurocode 2 (2004)

The provisions within Eurocode 2, referred elsewhere simply as Eurocode, for the design of members with shear reinforcement are by far the most conservative when accounting for the presence of ducts. Not only does this code give the highest k-factors overall, but it is the only set of specifications that addresses the use of plastic ducts. Section 6.2.3-6 in Part 1-1 of the code outlines the principal requirements for ducted

members. As with many other codes, the k-factor for the case of grouted, metal ducts is 0.5. This is applied only if δ is greater than 0.125, as was done in the Japanese code. For the use of all empty ducts or plastic ducts, a k-factor of 1.2 is required. This is a heightened value "introduced to take account of splitting of the concrete struts due to transverse tension." There is no suggestion of a lower limit of δ for this provision. Also, the code permits that the k-factor be dropped from 1.2 to 1.0 "if adequate transverse reinforcement [through the web thickness] is provided." The code, however, does not comment on what amount or type of reinforcement is sufficient for this purpose.

2.3.1.5 Summary of Codes

Each of the primary design codes consulted reduces the web width of a girder available to resist shear. The web width is reduced by some fraction of the sum of duct diameters placed horizontally in the web by using a k-factor that varies depending on grouting and/or duct type. Table 2-1 summarizes the k-factors from each code for the different combinations of duct type and grouting.

Table 2-1: Summary of Concrete Shear Design Code k-factors

	Steel Ducts		**Plastic (HDPE) Ducts**	
	Grouted	***Empty***	***Grouted***	***Empty***
ACI 318-11	0			
AASHTO 2012 General	0.25	0.5	0.25	0.5
AASHTO 2012 Segmental	0.5	1	0.5	1
JSCE No. 3 2002	0.5			
Eurocode 2 2004	0.5	1.2*	1.2*	1.2*

* *Use 1.0 if adequate transverse reinforcement across web is provided*

American codes are the least conservative overall with regards to reducing web widths to account for ducts. ACI 318 does not reduce web widths at all, but is not intended to be used for bridge design applications. The general provisions of AASHTO call for reductions in the web width, but the reductions are not as significant as those required in international codes. Provisions in AASHTO for segmental construction

specify larger k values, but are not used as often. JSCE requires the same web width reduction in all situations, which may not be adequate for some cases. Eurocode requires the highest web width reductions and is the only document that specifies different k-factors depending on duct type.

2.3.2 Construction Requirements

Post-tensioning ducts of any type, size, or number may be included in the web of a girder as per the contractor's or designer's specifications provided that the ducts themselves adhere to certain material standards and are appropriately placed and secured during fabrication. The following sections describe the main features of the ducts and bridge construction provisions that must be adhered to, with a particular emphasis on AASHTO requirements.

2.3.2.1 Duct Materials and Sizing

The AASHTO LRFD Bridge Construction Specifications, 3rd Ed. (2010) and the AASHTO LRFD Bridge Design Specifications, 6th Ed. (2012) outline the major types and dimensions of post-tensioning duct that are suitable for use. Metal (steel) or high-density polyethylene (HDPE) plastic ducts are permitted. Section 10.8.2 of the Bridge Construction Specifications requires that "semi-rigid [metal] ducts shall be corrugated and, when tendons are to be inserted after the concrete has been placed, their minimum wall thickness shall be as follows: 26 gage for ducts less than or equal to 2.625-in. diameter, 24 gage for ducts greater than 2.625-in. diameter." Where plastic ducts are incorporated, the ducts must adhere to the thickness requirements listed in §10.8.3-1 (Table 2-2). Also, §5.4.6.1 of the Design Specifications implies that bond between plastic ducts and grout or concrete may be an issue, recommending that a study of bonding should be performed where plastic ducts are used. The specifications, do not however, suggest how bonding should be checked.

Table 2-2: HDPE Duct Thickness Requirements (Adapted from AASHTO LRFD Bridge Construction Specifications, 3rd Ed. (2010))

Duct Diameter (in.)	Duct Thickness (in.)
0.9	0.08
2.375	0.08
3.0	0.10
3.35	0.10
4.0	0.12
4.5	0.14
5.125	0.16
5.71	0.16

Additional information is provided regarding selection of duct size. In general, §5.4.6.2 of the Design Specifications state that the inside cross-sectional area of a duct must be at least twice the area of the prestressing strands contained within. Further, δ cannot exceed 0.4. Although not specified, it is assumed that the inner diameter of the duct should be considered when checking this provision. The requirement is known largely to exist to ensure that there is space for adequate concrete placement around ducts during casting. Whether the limiting value of 0.4 for δ plays any role in influencing shear capacity is questionable.

2.3.2.2 Duct Spacing

Codes require that if multiple ducts are to be used vertically in line in the web of a girder, the ducts must be physically separated by a specified distance for adequate constructability. This is principally required to ensure that acceptable concrete placement and consolidation may be achieved, eliminating the accumulation of voids on the underside of ducts after vertical casting of members. (Corven and Moreton 2004). Meanwhile, codes do not explicitly include provisions to address the ramifications of violating duct spacing requirements on shear strength. It is implied that if vertical spacing provisions for multiple ducts are satisfied then the effective web width for shear may be taken as that for a single duct.

There are two major sources of guidance on the vertical spacing of ducts in a girder web, noted here. Section 5.10.3.3.2 of the AASHTO Design Specifications calls for a minimum vertical duct clear spacing within non-curved girders as the greater of "1.5 in. or 1.33 times the maximum size of [the concrete] coarse aggregate." The Florida Department of Transportation (FDOT) Structures Design Guidelines Manual (2012) is an alternate source outlining a unique duct spacing for spliced girder applications. This document calls for a minimum center-to-center duct spacing as the greater of "4-inches, [the] outer duct diameter plus 1.5 times [the] maximum aggregate size, or [the] outer duct diameter plus 2-inches."

2.3.2.3 Duct Support

Post-tensioning ducts must be supported at specified elevations and in the profile detailed in the plans within the reinforcing cage prior to casting. Section 5.4.6.1 of the AASHTO Design Specifications refers designers to §10.4.1.1 of the AASHTO Construction Specifications for information about duct support. Section 10.4.1.1 of the Construction Specifications states that "polyethylene duct…shall be tied to stirrups at intervals not to exceed 2.0 ft, and metal duct…shall be tied to stirrups at intervals not to exceed 4.0 ft." Long lengths of plastic duct must be tied down more frequently due to their increased flexibility compared to metal ducts. Securing the ducts in place is critical to prevent shifting or floating during concrete placement. AASHTO does not indicate the exact means by which to support ducts, but standard practice and suggestions provided in the Federal Highway Administration (FHWA) Post-Tensioning Manual (Corven and Moreton 2004) offer choices. According to this document, tie wire may be used to directly attach ducts to stirrups so long as "it is not tightened so much as to distort the rebar cage or crimp the duct." Alternatively, ducts may be rested on bar supports – pieces of reinforcement installed through the web and tied to stirrups. Various shapes including straight, U-, L-, and Z-bars are commonly utilized as supports.

2.3.3 Application of AASHTO LRFD Shear Design Provisions

As part of TxDOT Project 0-6652, a preliminary database of 40 results was developed from five research studies reported on the shear testing of full-scale post-tensioned girders with ducts in the web. The works of Krauss, Heimgartner, and Bachmann (1973), Chitnuyanondh (1976), Rezai-Jorabi and Regan (1986), Hars and Muttoni (2006), and Lee, Cho, and Oh (2010) were consulted. Utilizing the reported properties and details of the girders tested, expected nominal shear strengths of the girders were computed using MCFT formulas outlined in the AASHTO LRFD Bridge Design Specifications. These calculations were performed for three cases:

- Web width reduction according to the general shear provisions
- Web width reduction according to the shear provisions for segmental girders
- Assuming no reduction for ducts

The measured failure shear for each girder reported, herein designated as V_{test}, was compared to the calculated nominal shear strengths for the three cases mentioned, referred to as V_{calc}. In Table 2-3, the ranges and average ratios of V_{test}/V_{calc} for each set of girders are listed. A ratio of V_{test}/V_{calc} below one suggests that the code equations overestimated shear capacity; a ratio in excess of unity denotes a conservative result.

Table 2-3: Results and Conservatism of MCFT Calculations for Past Shear Tests on I-Girders Containing Ducts

Source	No. of Tests	δ_{avg}	V_{test}/V_{calc}								
			Unreduced			*AASHTO 2012 General*			*AASHTO 2012 Segmental*		
			Range	*Avgerage*	*% Unconservative*	*Range*	*Avgerage*	*% Unconservative*	*Range*	*Avgerage*	*% Unconservative*
Krauss, Heimgartner and Bachmann (1973)	11*	0.2	1.24 - 2.34	1.57	0%	1.32 - 2.41	1.67	0%	1.35 - 2.48	1.70	0%
Chitnuyanondh (1976)	8	0.44	1.03 - 1.47	1.31	0%	1.25 - 1.66	1.50	0%	1.59 - 2.11	1.76	0%
Rezai-Jorabi and Regan (1986)	8	0.42	0.71 - 1.15	0.95	63%	0.76 - 1.25	1.03	50%	0.78 - 1.33	1.06	38%
Hars and Muttoni (2006)	6	0.49	0.69 - 1.03	0.86	67%	0.80 - 1.14	0.98	50%	0.82 - 1.20	1.03	33%
Lee, Cho, and Oh (2010)	7	0.25	1.56 - 1.91	1.73	0%	2.09 - 2.80	2.39	0%	2.10 - 2.83	2.42	0%

*Includes 3 Ungrouted Tests

The most important observation to draw from the previous beam research is that while the incorporation of a web width reduction improves shear capacity estimates, the reductions specified in AASHTO are not great enough to ensure conservative results in all instances. For seven of the 40 girder tests (i.e. 17.5%), V_{test}/V_{calc} was found to be below unity when utilizing general design k-factors. Meanwhile, five tests (i.e. 12.5%) failed at a load lower than calculated when using the k-factors for segmental girder design. As a whole, eight of the 40 girder tests (i.e. 20%) would be considered unconservative if a web width reduction was not employed at all. Thus, the effective web width formula is marginally achieving its intended purpose. The AASHTO code equations are underestimating the reduction in shear capacity caused by ducts in webs by up to 20%.

All beams failing below MCFT-expected capacities had a value of δ above 0.4. Not all tests on beams with δ above 0.4 in the literature were unconservative, but the fact that some tests were low provides some credence to a claim that the AASHTO duct size limit may influence shear capacity.

It is also important to mention that all of the beam tests had steel ducts in the web. As was indicated earlier, the AASHTO code does not distinguish between types of ducts.

As will be described later, elements with plastic ducts are likely to perform worse than those with steel ducts for shear applications. As part of the current research project, tests on girders with plastic ducts may result in values of V_{test}/V_{calc} below unity.

2.4 PANEL AND PRISM TESTING

The compression testing of concrete panels or prisms with embedded ducts has often been used as a supplement to full-scale girder testing in many past research endeavors. These tests have been small and easy to perform and are intended to generate results applicable to full-scale beams. The designation of “panel” or “prism” is somewhat arbitrary, but can otherwise be attributed to the dimensions of the specimen’s loading surface. Prisms typically have square loading surfaces while panels are more rectangular (Figure 2-2). In any event, panels/prisms are proportionally-scaled representations of a portion of a girder web subjected to shear-induced compression for studying the mechanism of web crushing in elements containing post-tensioning ducts. Findings have also been used to develop equations to estimate girder capacity, such as the effective web width formula with varied k-factors. Ideally, panel/prism testing can at the very least provide qualitative or relative quantitative results to understand how web crushing behavior and capacities in girders may change depending on variations in construction or design parameters.

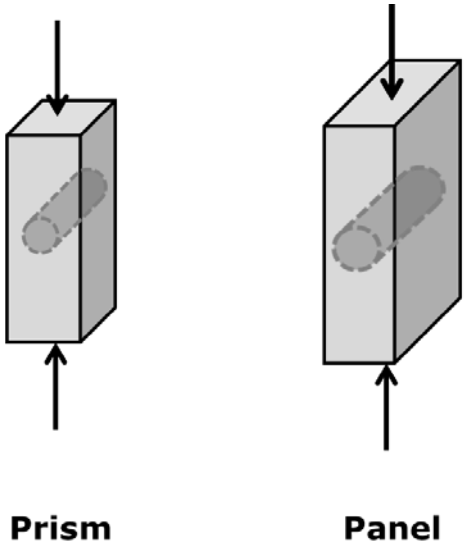

Figure 2-2: Prism vs. Panel

2.4.1 Impetus for Testing in Present Study

The major reason for testing panels with ducts was to develop an efficient and cost-effective study to help guide the design and logistics of full-scale girder fabrication. Compared to girders, panels are easier to fabricate and test, and they are much more suitable for quickly introducing a wide array of test variables that could not otherwise be investigated in large beams. The ultimate goals of the testing program were to not only gather more information on the influence of having a post-tensioning duct on web crushing strength, but to explore the role and impact of varying material properties and construction decisions. From the results of numerous panel tests, it should be possible to get an indication of beam behavior under a variety of circumstances.

2.4.2 Compressive Strut Representation

As is well described by truss models and compression field theory approaches for shear analysis, the behavior of concrete beams acting under the influence of shear can be simplified to the behavior of an interconnected matrix of compressive struts and tension

ties. At any location along the length and depth of the member, a sectional element is subjected to shear stresses resulting from shear forces and normal stresses due to the flexural behavior of the beam. By utilizing concepts of solid mechanics, these shear and normal stresses can be resolved into principal tensile and compressive stresses acting at some angle of inclination relative to a horizontal plane. The inclined principal tensile stresses are further resolved into vertical and horizontal components and appropriately resisted by the transverse and longitudinal steel provided in the beam acting as ties. Meanwhile, the inclined principal compressive stresses are separately handled via the concrete in the web, discrete portions of which are typically analyzed as struts.

Concrete panels or prisms tested under uniaxial compression are intended to represent a single strut or webbed portion of an I-girder resisting shear-induced compressive stresses (Figure 2-3). Ultimately, a common shear failure, in the absence of issues with anchorage, bond, or horizontal shear, is determined by the lesser of the compressive capacity of the web or the yield capacity of the transverse reinforcement. The presence of a duct complicates computations of the strut capacity. Consequently, it is advantageous to model such a critical component like the strut in isolation as a compressively-loaded prism or panel to determine the influence of ducts.

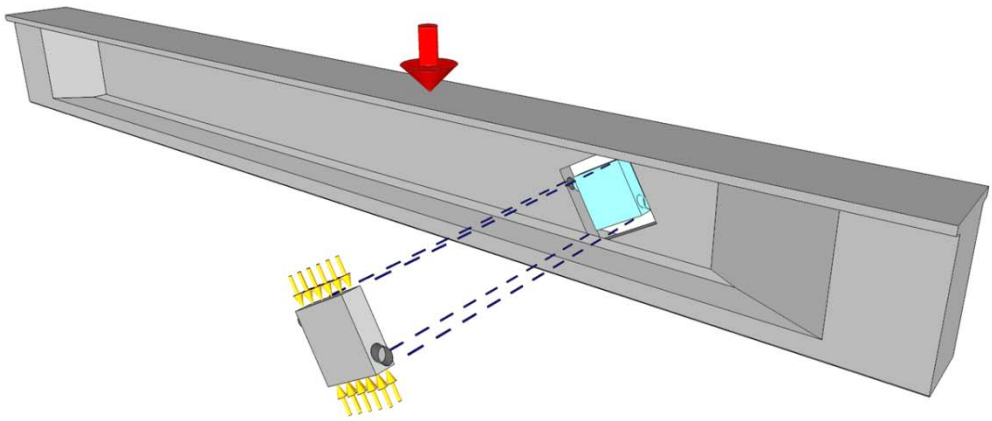

Figure 2-3: Panel as a Representation of a Compressive Strut with a Duct

2.4.3 Formulation of Web Width Reduction Factor and k-factors

In an effort to compare past experimental results from panel/prism testing, many researchers have quantified a parameter referred to here as the web width reduction factor, which normalizes the compressive capacity of ducted tests specimens. For all subsequent discussion in this document, the web width reduction factor is also defined as η_D, as given by Muttoni, Burdet, and Hars (2006). The web width reduction factor is simply the ratio of the measured compressive capacity of a panel/prism containing a duct to the measured compressive capacity of an otherwise identical, solid panel/prism without a duct. Capacity may be based on the applied load or applied stress at failure. Thus, the web width reduction factor formula may be explicitly written as:

$$\eta_D = \frac{(ducted\ panel/prism\ failure\ load/applied\ stress)}{(control\ panel/prism\ failure\ load/applied\ stress)} \qquad \textbf{Equation 2-7}$$

The factor indicates the fraction or percentage of the gross concrete section available to resist crushing when there is a duct. The value of η_D obtained through experimentation depends on numerous variables such that no table or matrix can adequately define all possible values. Additionally, this factor is, in its most basic form, the ratio of two experimentally obtained numbers. These are the reasons why code provisions for beam shear capacity do not directly utilize a fractional reduction of the gross web width and rather adopt the formula-derived effective web width with a k-factor.

There are two ways in which k-factors have been or can be obtained. First, regardless of whether research has been conducted on girders or panels/prisms, quantified k-factors have often been determined through exercises in curve fitting with test data. These values were obtained to ensure that web crushing capacities calculated using the effective web width would accurately reflect experimental results. Second, k-factors can be mathematically derived by relating the effective web width and web width reduction factor. If directly applied to code equations, the web width reduction factor would exist as a multiplier on the gross web width to convert it into an effective web width as:

$$b_{eff} = \eta_D * b_w$$ **Equation 2-8**

Using Equations 2-1 and 2-8, η_D can be directly correlated to the k-factor in the general effective web width formula as:

$$\eta_D = 1 - k\delta$$ **Equation 2-9**

where:

δ = duct diameter-to-web thickness ratio

Rewriting Equation 2-9, k-factors can be determined as:

$$k = \frac{1-\eta_D}{\delta}$$ **Equation 2-10**

2.4.4 Review of Past Web Crushing Research

Web crushing in girders containing post-tensioning ducts has been a growing topic of research interest since the 1960s, as the desire to engineer more efficient, longer-span bridges with post-tensioning has increased. Most studies performed to understand the girder shear performance and estimate crushing capacity with ducts present have been conducted on small-scale panel or prism specimens, compressively loaded to gauge the impact of an embedded discontinuity. Factors contributing to web crushing reductions in the presence of ducts have been analyzed. Although many behavioral aspects of web crushing have been assessed, certain mechanisms have not been fully analyzed for every potential construction or design scenario. Moreover, as was seen with design codes, researchers have not been able to generate singular, agreed upon computational ways to estimate crushing capacity.

A historical background of seven principal research investigations performed in the past 50 years on web crushing of ducted specimens is provided. The testing programs and major findings from each of these studies are outlined, many of which provided guidance for the current study with regard to experimental setup and selection of test variables or parameters requiring attention.

2.4.4.1 Gaynor (1961)

The main focus of Gaynor's research was to consider how the compressive strength of drilled cores or molded cylinders would change if a piece of reinforcement were embedded perpendicularly to the loading axis. Although his work was not performed in the field of crushing behavior in specimens containing ducts, Gaynor's research was largely referenced by Leonhardt (1969) and uncovered the general phenomenon behind the reduction in capacity in specimens of future studies. Gaynor conducted a series of compression tests on 6 x 12 in. cylinders with either one or multiple, 0.5-in. or 1-in. deformed bar(s) placed perpendicularly to the loading axis at various eccentricities from the centroid of the section. Ultimately, he found that the presence of reinforcement in a cylinder reduces its compressive capacity somewhat. Although no clear conclusions could be made about bar eccentricity, Gaynor's results showed that a larger amount of reinforcement (i.e. larger sizes of bars) reduced compressive capacity more. Most importantly, his findings were evidence that a discontinuity in the structural properties of a concrete section can hurt capacity.

2.4.4.2 Leonhardt (1969)

Leonhardt worked to extend the research performed by Gaynor (1961), looking at compressive strength reductions of concrete elements not only in the case of embedded reinforcement but in the case of embedded post-tensioning ducts. Rather than experimenting on cylinders, Leonhardt advanced to using relatively large, compressively-loaded concrete panels. He considered a variety of test parameters including grouting of ducts, singular or multidirectional duct eccentricity (from the section centroid), duct inclination, and use of multiple ducts horizontally aligned.

Leonhardt's testing program consisted of compression tests on 52 panels, some of which were solid sections and others which contained either steel bars or corrugated, steel ducts 50 mm (1.97-in.) in diameter. Most of the panels measured 68 x 30 x 15 cm (26.77 x 11.81 x 5.91 in.), with load applied at the faces measuring 68 x 15 cm (26.77 x 5.91 in.). A few panels were made larger to accommodate tests with multiple ducts across the

section width. The panels with single ducts had a δ of 0.33 (50 mm duct in a 15 cm thickness).

Test results showed that that the eccentricity and inclination of an embedded component (duct or reinforcement) make little difference on how much compressive strength is reduced. Testing also proved that a section with two ducts horizontally in line separated by at least one duct diameter performs better than that with one duct of double the diameter.

Leonhardt was possibly the most influential researcher in looking at the effects of ducts on web crushing capacity. Notably, he illustrated and described the mechanism of compressive stress flow deviation and thus capacity reduction. He also developed some of the earliest effective width formulas for the shear design of girders in the presence of ducts. His formulas called for k-factors of 1.0 and 0.67 (or 2/3) when using empty or grouted ducts, respectively. These k-factors reflected the fact that sections with empty ducts perform worse than those with grout. As mentioned by Clarke and Taylor (1975), Leonhardt did not provide any experimental evidence supporting the use of the k-factor of 2/3 in the grouted duct formula. Also, Leonhardt suggested that a capacity reduction would only be necessary if δ were greater than 0.1.

2.4.4.3 Clarke and Taylor (1975)

A series of small prism tests to verify Leonhardt's effective web width formulas was conducted with the additional goal of studying the effects of duct inclination. A number of 100 x 100 x 500 mm (3.94 x 3.94 x 19.69 in.) solid and ducted prisms were tested, with load applied to the square surfaces. Ducts were 20, 40, or 45 mm (0.79-, 1.57-, or 1.77-in.) in diameter and were created from molded steel sheathing. The ducts were either grouted or left empty and angled at 45, 60, 75, or 90° to the loading axis.

Clarke and Taylor confirmed Leonhardt's findings and showed that Leonhardt's effective web width formulas were valid. As had been suggested by Leonhardt, duct inclination was not found to significantly influence the compressive capacity. A k-factor of 1.0 for cases using empty ducts was found to be acceptable. The k-factor of 2/3 for use

in cases with grouted ducts was verified by experimental evidence. Test results were found to correlate well with theoretical values computed using a modified effective web width formula considering the ratio of grout to concrete elastic moduli:

$$b_{eff} = b_w - d_d + d_d\left(E_g / E_c\right) \qquad \textbf{Equation 2-11}$$

where:

d_d = duct diameter (same as ϕ used earlier)

E_g = elastic modulus of grout

E_c = elastic modulus of concrete

Given a modular ratio of exactly 3.0, a k-factor of 2/3 would be obtained. Clarke and Taylor's experimentation utilized a ratio of moduli slightly higher than 3.0, and they found that the test results and theoretical calculations matched adequately.

2.4.4.4 Chitnuyanondh (1976); Campbell, Batchelor, and Chitnuyanondh (1979); Campbell and Batchelor (1981)

Chitnuyanondh, et al. performed a series of compression tests on prisms to complement a web crushing study on prestressed I-girders. These tests were mostly conducted on 6 x 6 x 24 in. specimens with 6 x 6 in. loading surfaces. Single or double cavities, 3-in. in diameter, were cast into these specimens to represent the discontinuities from post-tensioning ducts. For prisms with two cavities, the voids were separated by a clear spacing of either 1.5-in. or 3-in. In some specimens, 0.25-in. spiral reinforcement with a 0.875-in. pitch and a 4.5-in. diameter was placed around the cavities. The spiral reinforcement was used for grouted and ungrouted prisms, and in cases with one or two cavities.

The researchers found that using spiral reinforcement around cavities improved prism compressive capacity compared to non-reinforced panels in both grouted and ungrouted cases. Ultimately, the reinforcement helped more for those prisms with empty

cavities. When using two cavities, reinforcement only improved capacity significantly when the cavities were separated by less than a full diameter.

Chitnuyanondh explained that providing spiral reinforcement boosts capacity. A prism with a duct first splits into two equal, slender halves due to the tension produced from compression stress flow deviation. Then, these pieces of the entire specimen fail by a combination of axial load and flexure that develops due to a net eccentric compressive load applied to each segment. This is depicted in Figure 2-4. Under this combination of axial load and flexure, the two prism halves fail with a total load less than would be predicted based on the pure axial compressive strength of the net prism section at the level of the duct. Ultimately, the spiral reinforcement works by holding the splitting halves together.

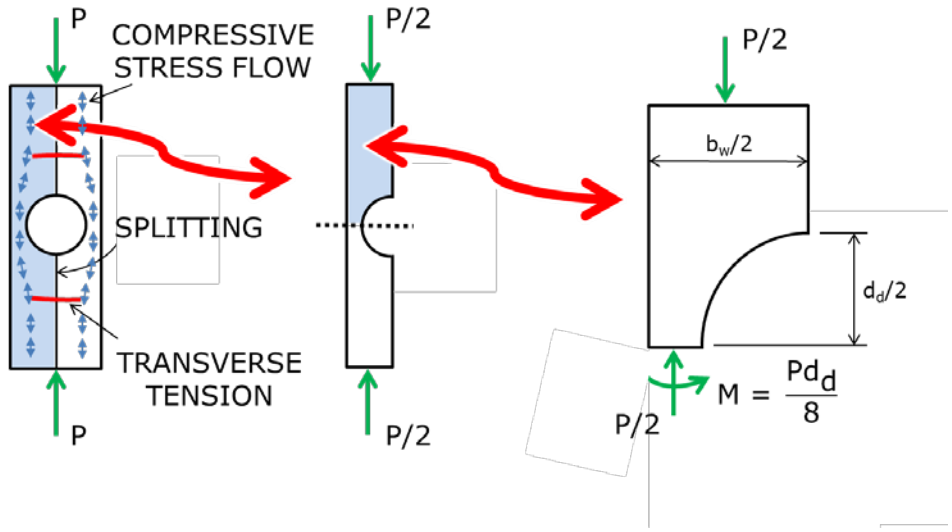

Figure 2-4: Main Failure Mechanism of Panels/Prisms (Adapted from Campbell and Batchelor (1981))

The researchers found that grouted prism results were predicted well using the effective web width formula and reductions proposed by Leonhardt (1969), but that his equation for empty ducts was overly conservative. Rather than use prism test results to determine new k-factors, the researchers consulted beam test results from their study to

come up with recommendations. They did this because they noted that prisms likely underestimate beam capacity since stirrups in tension in a full girder should help resist outward bending of the web containing a duct. Strain measurements from beam tests were utilized along with stress-strain relationships to compute web width reduction factors for the cases of grouted and empty ducts. New k-factors of 0.75 and 0.33 for empty and grouted ducts were derived.

Chitnuyanondh, Campbell, and Batchelor also looked at an assortment of prism and panel test data existing at the time to generate new potential effective width formulas. They noted that the trend in web width reduction with increasing δ for prisms with grouted ducts is nonlinear. Equation 2-12 was found to fit the data:

$$b_e = b_w - \frac{1}{3}d_d - \frac{1}{2}\frac{d_d^2}{b_w} \qquad \textbf{Equation 2-12}$$

where:

b_e = effective web width

Also, the researchers provided a lower bound, parabolic equation for the effective web width of elements with empty ducts to account for combined axial and flexural effects:

$$b_e = b_w - 2d_d + \frac{d_d^2}{b_w} \qquad \textbf{Equation 2-13}$$

2.4.4.5 Rezai-Jorabi and Regan (1986)

A series of panel tests were conducted by Rezai-Jorabi and Regan to complement their shear tests on I- and T-beams with inclined tendons. They looked at the effects of ducts in girder webs with and without grout while utilizing different values of δ. A total of 15 panels were tested (only six were reported) on solid and steel-ducted specimens. The researchers incorporated steel ducts with diameters of 32, 75, and 100 mm (1.26-, 2.95-, 3.94-in.) in panels that were 200 mm (7.87-in.) thick, thus giving values of δ of

0.16, 0.375, and 0.5. Reported information does not indicate the concrete strength of these specimens or the full dimensions of the loading surfaces.

The reported results from this study showed no reduction in capacity for a prism with a grouted duct at a δ of 0.16, barely any reduction at a δ of 0.375, and some larger reduction at a δ of 0.5. Conversely, capacity was greatly reduced at all values of δ when ducts were empty. Rezai-Jorabi and Regan also observed that the prisms maintained high strain concentrations near the duct and lower strains near the prism surface, verifying findings of Leonhardt (1969).

Rezai-Jorabi and Regan developed a new, nonlinear formulation to estimate η_D with empty ducts, and recommended new k-factors for the basic, linear effective web width formula. The new equation provided was:

$$\eta_D = \cos^3\left(\frac{\pi}{2} \cdot \frac{d_d}{b_w}\right) \qquad \textbf{Equation 2-14}$$

The researchers claimed that it yielded a minimally-affected capacity at low values of δ, still gave a downward trend in capacity with increasing δ, and ultimately yielded a capacity of zero for a δ of 1.0. For the regular effective web width formula, k-factors of 0.5 and 1.3 were suggested for use with grouted and empty ducts, respectively. The researchers increased the latter k-factor from 1.0 (used in codes at the time) to 1.3 as they found that 1.0 was unconservative for a δ above 0.35.

2.4.4.6 Ganz, Ahmad, and Hitz (1992)

This was the first investigation of the compressive behavior of panels with HDPE ducts due to their growing utilization for corrosion protection and to provide a low-friction environment for post-tensioning. The aim was to determine if shear provisions for using grouted ducts in post-tensioning applications would apply to both plastic and steel ducts. Although this research was conducted to apply to offshore applications, the findings also apply to bridge applications.

A total of 14 prisms were tested including six solid prisms and eight comprising two each of the following: empty cavities, grouted cavities, grouted steel ducts, and grouted HDPE ducts. Most of the prims measured 250 x 250 x 500 mm (9.84 x 9.84 x 19.69 in.) in dimension (only two solid specimens differed slightly to look at the panel height-to-width ratio). The ducts and cavities in all prisms were 50 mm (1.97-in.) in diameter, yielding a δ of 0.2. All plastic ducts were non-corrugated and grouted. High-strength concrete [70 MPa (10.2 ksi)] was used with ratios of grout-to-concrete strength on the order of one-half to two-thirds.

The results did not show significant differences in capacity for any of the types of panels where grout was used. Variations in failure load were insignificant between solid prisms, those with grouted cavities, or those with grouted steel ducts. The prisms with grouted plastic ducts failed at loads about 6% lower than those for solid panels, but this was deemed within the normal scatter of results and thus unimportant. Only the prisms with empty cavities failed at significantly different loads than the solid panels (about 20% less). Transverse deformations measured in the prisms verified these findings. Deformations were not much different between panels with grouted cavities or ducts of either type. Transverse deformations in the panels with empty cavities were about twice those in grouted elements.

It is also important to note that the investigators recognized that the results from this study might not match for panels with larger values of δ. They claimed, however, that based on the results, code standards in existence at time of their report were “quite conservative” for grouted ducts.

2.4.4.7 Muttoni, Burdet, and Hars (2006)

This is the most recently published investigation on panel testing, aimed primarily at addressing web crushing behavior when using HDPE ducts. The panels tested were the largest since Leonhardt’s study (1969). They were scaled appropriately to represent a large portion of an actual girder web, included corrugated plastic ducts, and were also the first known to include web reinforcement required by design.

A total of 16 panels measuring 600 x 600 x 125 mm (23.6 x 23.6 x 4.9 in.) were tested. These were loaded on the entire face. Twelve of the panels were fabricated in the laboratory, with another four removed from an existing bridge girder to investigate the effects of previous cracking on web crushing strength. Laboratory-created specimens were either solid or included empty steel, grouted steel, or grouted HDPE ducts. Tests were not performed on panels with empty HDPE ducts. These specimens included vertical and horizontal, #2.5 bars spaced at 5.9-in. with ducts having diameters of 2.44-in. (steel) or 2.48-in. (plastic). These dimensions yielded an average δ of 0.50. Seven 0.6-in., seven-wire prestressing strands were included in all ducted panels. A normal-strength concrete with a 28-day strength of approximately 5,200 psi was used, while the grout incorporated had a strength near 4,000 psi.

The main finding from this study was that use of HDPE ducts can reduce crushing capacity much more so than using steel ducts, at least in elements with a large δ. The average capacity of steel-ducted panels with grout was about 13% less than the average solid control capacity, which was determined to be consistent with past research results. However, the average capacity of plastic-ducted panels with grout was about 37% less than the average control capacity. Meanwhile, capacities were worse for panels with previous cracking. Also, the impact of duct inclination when using HDPE ducts was considered and found to affect capacity very little.

The researchers noted that while Eurocode 2 is the only code that distinguishes between difference in duct type and the code in general is the most conservative overall, changes could be made. They suggested that k-factors in Eurocode 2 should be changed to 0.4 from 0.5 for steel ducts, to 0.8 from 1.2 for plastic ducts, and kept at 1.2 for all empty ducts. Also, the researchers pointed out that reinforcement through the thickness of the panel (or girder web) can be helpful, just as recommended in Eurocode 2 and by Chitnuyanondh (1976). They did not, however, say how to accomplish this.

2.4.5 Comparison of Existing Test Results

The results of the panel and prism testing from the literature were compiled into a database, the bulk of which are briefly addressed and analyzed here. Tests containing steel or plastic ducts or cavities for which web width reduction factors and values of δ could be ascertained from the literature or computed from reported data are considered. Tests with incomplete information or those looking at the effects of embedded reinforcement or steel rods rather than ducts were not included. In Figure 2-5, η_D vs. δ for all tests with grouted steel or plastic ducts is plotted. In Figure 2-6, the same relationships are plotted for tests with empty ducts or cavities. Each of these graphs illustrates the scatter of data concurrently with plots of estimated values of the web width reduction factor using k-factors given by the major shear design codes referenced in this chapter. Codes conservatively predict values of η_D when data points are above the appropriate, indicated plots. The validity of other web width reduction formulas recommended by researchers was not included.

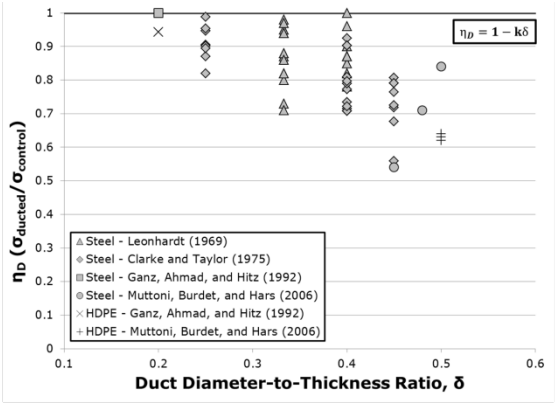

ACI 318-11 (k = 0)

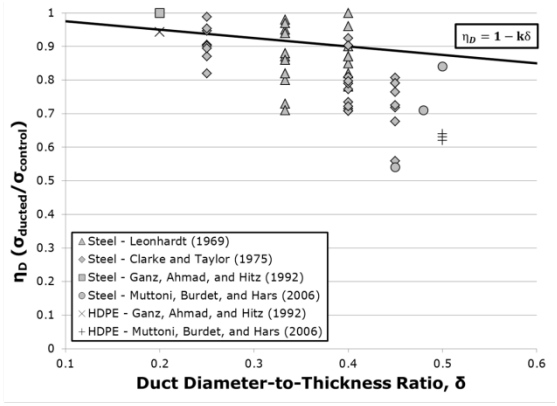

AASHTO 2012 General (k = 0.25)

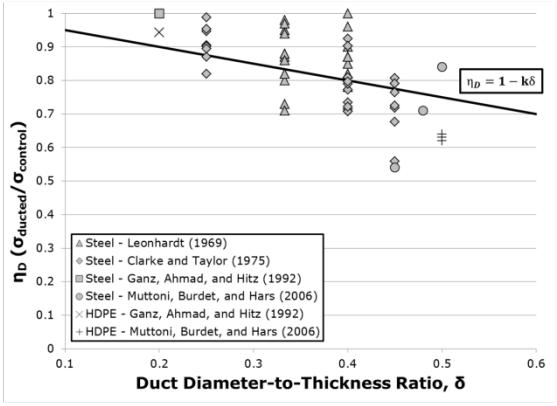

AASHTO 2012 Segmental (k = 0.5)

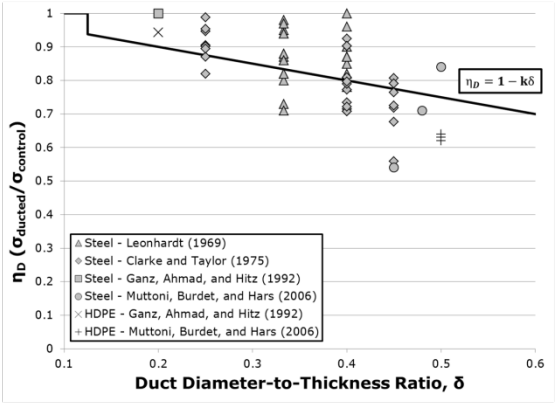

JSCE No. 3 2002 (k = 0.5)

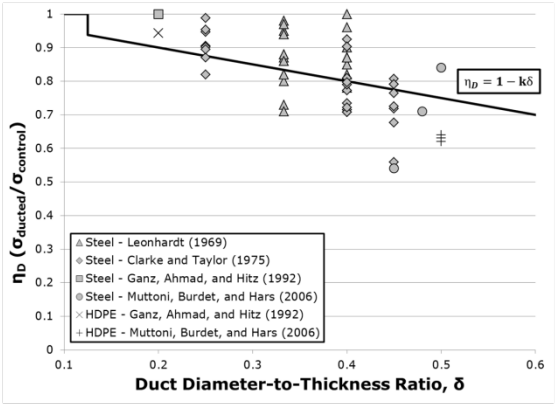

Eurocode 2 2004 - Steel (k = 0.5)

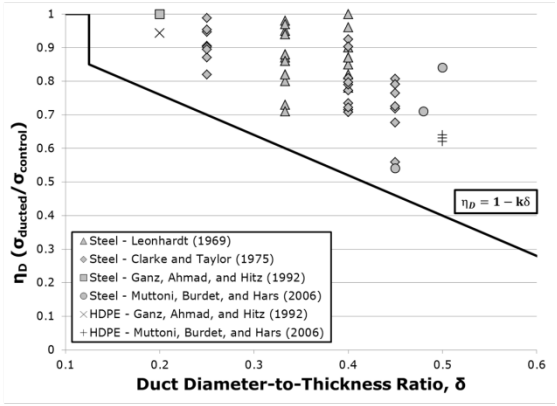

Eurocode 2 2004 – HDPE (k = 1.2)

Figure 2-5: η_D vs. δ for Grouted Panel/Prism Tests in the Literature with Expected Reduction Factors from Code

ACI 318-11 (k = 0)

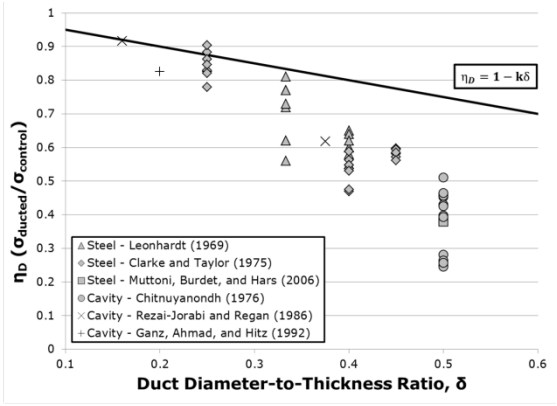

AASHTO 2012 General (k = 0.5)

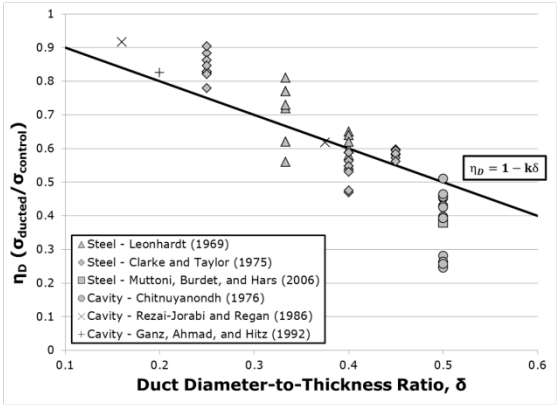

AASHTO 2012 Segmental (k = 1)

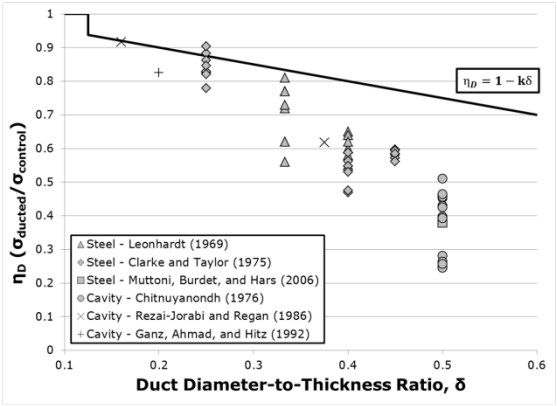

JSCE No. 3 2002 (k = 0.5)

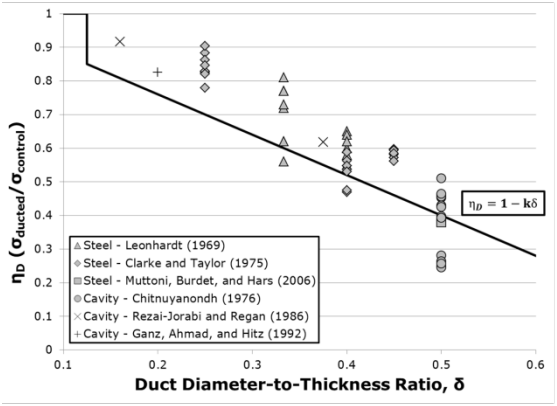

Eurocode 2 2004 (k = 1.2)

Figure 2-6: η_D vs. δ for Ungrouted Panel/Prism Tests in the Literature with Expected Reduction Factors from Code

Evidently, the data indicate a general decreasing trend in η_D with increasing δ, whether a specimen is grouted or not. It is unclear whether this trend is linear, as is implied by codified web width reduction formulas. The data may appear to support a parabolic trend, with η_D falling fasting at higher values of δ, but it is difficult to fully justify a clear trend given the wide scatter of η_D values for the same δ. Meanwhile, without any data points for a δ less than 0.125, this lower limiting ratio above which web width reduction must be considered (according to Eurocode and JSCE) cannot be validated. Also, data above the upper limit of 0.4 for δ from AASHTO do not readily affirm the likelihood of significantly poorer web crushing behavior beyond that limit.

As would be expected given the earlier discussion of code k-factors, the web width reduction formula using the k-factor from the general provisions of AASHTO does a very poor job of estimating or bounding panel/prism crushing capacity. More than half of all grouted specimens failed with η_D values less than predicted by AASHTO, and the η_D values of only two ungrouted specimens are conservatively estimated.

On the other hand, the formula using Eurocode k-factors was much better in predicting capacities. Only the web width reduction formula for grouted plastic ducts with a k-factor of 1.2 conservatively predicts η_D values for all of the pertinent tests. In fact, using a k-factor of 1.2 generates conservative estimates of η_D for all grouted specimens. This prediction is, however, overly conservative in a number of cases, including those with plastic ducts. Although not conservative in a number of cases, the formula for steel ducts using the k-factor of 0.5 from Eurocode, JSCE and the segmental girder provisions of AASHTO appears to give a reasonable average of η_D for grouted prisms/panels across the entire range of values for δ. Meanwhile, the formula using the k-factor of 1.2 from Eurocode predicts a majority, although not all, of the η_D values for ungrouted tests.

2.4.6 Summary of Tests Previously Conducted

A number of design and construction considerations were investigated in panel and prism tests of past studies. It is imperative to assemble a list of these factors or

specimen types in order to identify what information has been thoroughly gathered or assessed and need not be confirmed nor expanded in this project. The following outlines panel test parameters which have been sufficiently examined:

- Duct inclination and eccentricity
- Multiple ducts in line vertically and horizontally
- Panels/prisms with cavities and steel ducts
- Low to intermediate values of δ in panels with steel ducts

Although a great deal of work has been done in the field of ducted prism and panel testing, the effects of a substantial number of test parameters have not been explored at all or sufficiently. The following points highlight the areas lacking in experimental results and form the basis for much of the test program in the present study:

- As seen in Figure 2-7, there has been highly limited testing on panels with plastic ducts and no confirmation of previous results in that regard. Only five specimens with plastic ducts were investigated. These were only grouted specimens, and one used an atypical, non-corrugated plastic duct.

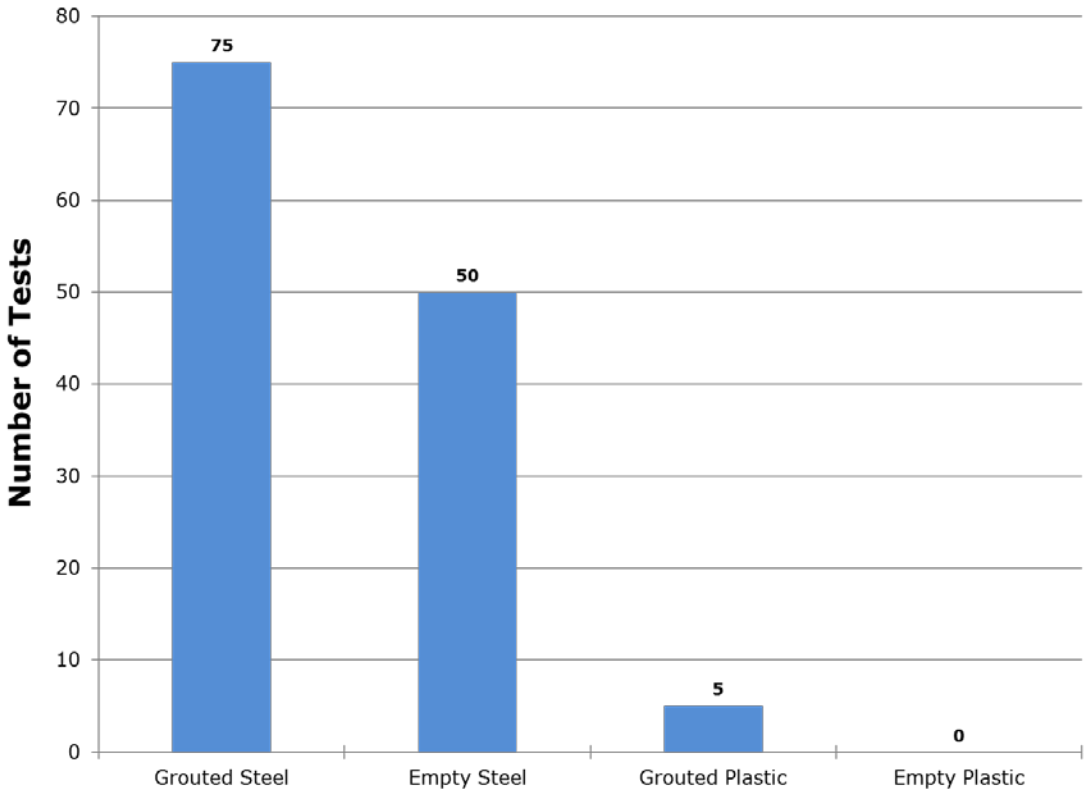

Figure 2-7: Summary of Test Types Previously Conducted

- Testing was not carried out in any studies on the effects of concrete or grout strengths or the ratio of the two. Also, the effects of ducts in webs were rarely considered when using very high concrete strengths. In Figure 2-8, the ranges of concrete strengths (whether measured with cubes or cylinders) utilized in past research studies are shown. With the exception of one test specimen, no prior testing has been conducted with high-strength concretes of 10 ksi.

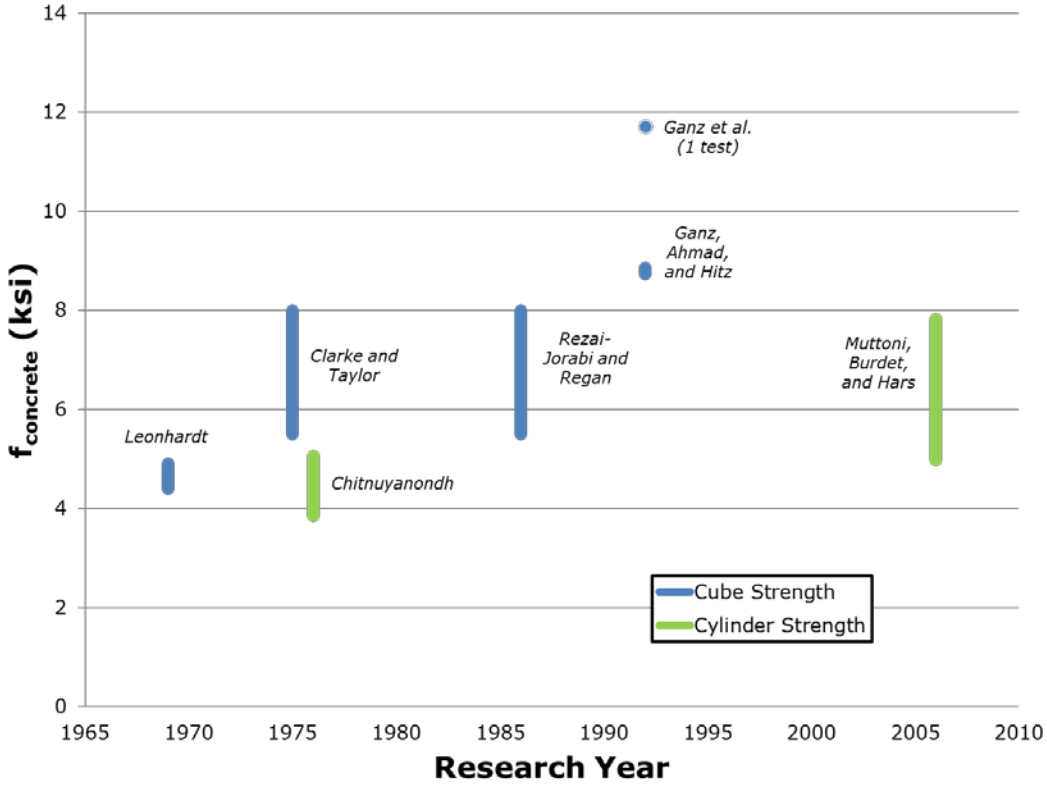

Figure 2-8: Historical Perspective of Panel/Prism Concrete Strength

- Providing transverse reinforcement through the thickness of a panel to resist splitting was only investigated with continuous spiral reinforcement of one size around grouted or empty cavities. Through-thickness reinforcement was not considered in any form or with steel or plastic ducts.
- Looking at a historical plot of average panel sizes tested over time (Figure 2-9), the largest panels tested were about 120 in^2 in cross-section – those tested by Leonhardt (1969) and Muttoni, Burdet, and Hars (2006). The thickness of panels was occasionally altered in some tests within a single study, but the effects of size were not emphasized by the researchers.

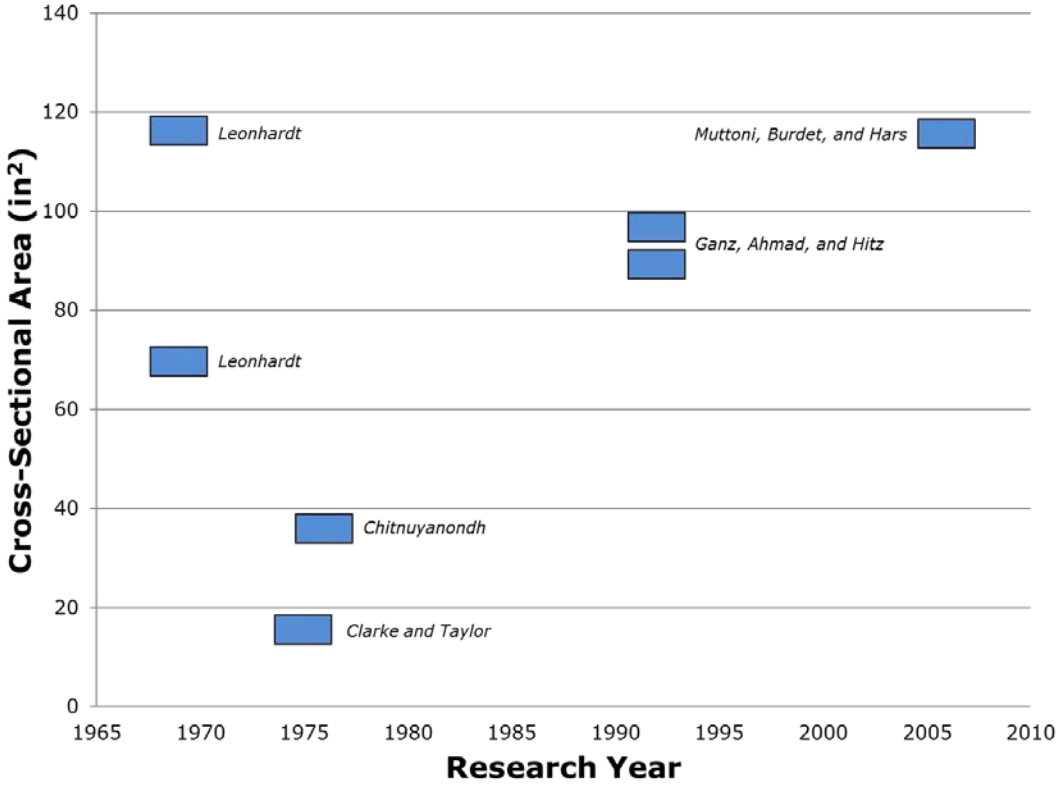

Figure 2-9: Historical Perspective of Panel/Prism Size

- In general, test variables have been considered through multiple studies rather than within the same study. Recommended equations for effective web widths have often been formulated comparing test data between test specimens with different properties from multiple studies. These specimens varied in size and fabrication technique.

2.5 CHAPTER SUMMARY

The influence of post-tensioning ducts on web crushing and shear capacities of I-girders was explained. Ducts behave as discontinuities in the structural framework of a web leading to deviations in shear-induced compressive stress flow paths and ultimately, reductions in web crushing capacity which may further limit overall shear capacity.

Various concrete design codes used worldwide attempt to account for this reduction by using effective web widths for shear calculations to account for ducts. There is a lack of consistency from one code to the next, some being more conservative than others while explicitly specifying more design parameters that may be influential when determining appropriate reductions. Ultimately, American code provisions, namely AASHTO, have been found to give some of the most unconservative estimates of shear strength in post-tensioned girders.

Research was conducted to understand the mechanism of web crushing and estimate shear capacities for girders with ducts in the web. Compression testing was performed on small-scale prisms and panels with embedded ducts to gauge relative capacities and ideally predict behavior in full-scale girders with a select number of testing variables. Through their investigations, researchers attempted to advance and clarify empirical formulations for estimating capacity along the same lines as those used in design codes. Despite some success in these endeavors, formulaic approaches to estimating capacity remain disparate, and a number of design and construction parameters that may affect capacity have yet to be examined.

The following chapters detail the test program and results of the current study which is based on past investigations and aims to provide missing data.

CHAPTER 3
Experimental Program

3.1 OVERVIEW

A total of 100 prismatic, concrete panel specimens with and without embedded post-tensioning ducts were constructed and analyzed at the Ferguson Structural Engineering Laboratory (FSEL) at The University of Texas at Austin. In this chapter, the general experimental setup and procedures followed during the course of this study are documented.

The process of fabricating panels is outlined. The efforts taken to efficiently produce specimens and prepare them for testing are explained. Materials and methods of construction are defined for general purposes. More in-depth information about materials and methods used in specialized test cases is covered in Chapter 4, where the results of these tests are discussed. Next, the high-capacity, uniaxial compressive testing machine designed and constructed at FSEL to conduct the panel tests is described. The functionality of each component of the test frame and the operation of the setup as a whole are detailed. Finally, the standard operating procedures for testing are conveyed, with clearly delineated procedures for pre-, early-, and late-stage load application.

3.2 PANEL FABRICATION

A total of 100 panels were produced in the lab, each nominally measuring 5-, 7-, or 9-in. thick and 24 x 24 in. in plan. In all, nine 5-in., eighty-one 7-in., and ten 9-in. panels were constructed and tested. The actual measured dimensions of each panel are given in Appendix A.

The panels were fabricated in sets of nine, or ten in one case, with each set typically consisting of two solid concrete specimens without a duct and seven specimens containing a post-tensioning duct. The solid panels of each set were used as controls against which the behavior of the panels with ducts could be compared. The seven

remaining panels of each set provided a means of exploring the effects of the parameters selected.

3.2.1 Specimen Dimensions

As previously discussed, some of the most recent panel tests were conducted on approximately 24 x 24 x 5 in. specimens in Switzerland by Muttoni, Burdet, and Hars (2006). The initial specimens tested in this study were designed to match those produced by the Swiss researchers and to emulate their results. Additionally, 24-in. deep steel forms were readily available at FSEL. Given this background, all panels in this study were 24 x 24 in.

The panel thickness varied between 5-, 7-, and 9-in. The transition from 5- to 7-in. was deemed necessary to match the 7-in. web thickness typical of Texas I-Girders (Tx Girders) used by the Texas Department of Transportation. The subsequent increase to 9-in. was implemented to simulate the compressive behavior of a thickened Tx Girder web (containing a duct) that would be needed to provide sufficient girder shear capacity. Finally, thickness was limited by the capabilities of the loading frame and safety concerns associated with explosive failures of high-strength concrete compression elements. The expected failure loads for the largest panels to be tested were expected to fail at 1500-2000 kips.

3.2.2 Formwork

Each of the panels was fabricated in the lab using a formwork setup shown in Figure 3-1. Two 24-in. deep steel side forms were bolted to a plywood base soffit. The side forms were separated by a distance of 5-, 7-, or 9-in. to produce the desired panel thicknesses. A number of interior, wooden form spacers were constructed and bolted down between the side forms to create 24-in. long segments for casting individual panels (Figure 3-2). The spacers contained removable, interchangeable end caps, as seen in Figure 3-3, with holes of varying sizes and configurations bored out so that sections of post-tensioning duct could be inserted and held in place between spacers during concrete

placement. Lastly, as shown in Figure 3-4, 0.25-in. thick steel spreader tie bars were bolted to the side forms in order to keep the side forms adequately tied together to maintain uniform specimen thicknesses.

Figure 3-1: Formwork for Panel Casting

Figure 3-2: Panel Form Spacers

Figure 3-3: Spacer End Caps

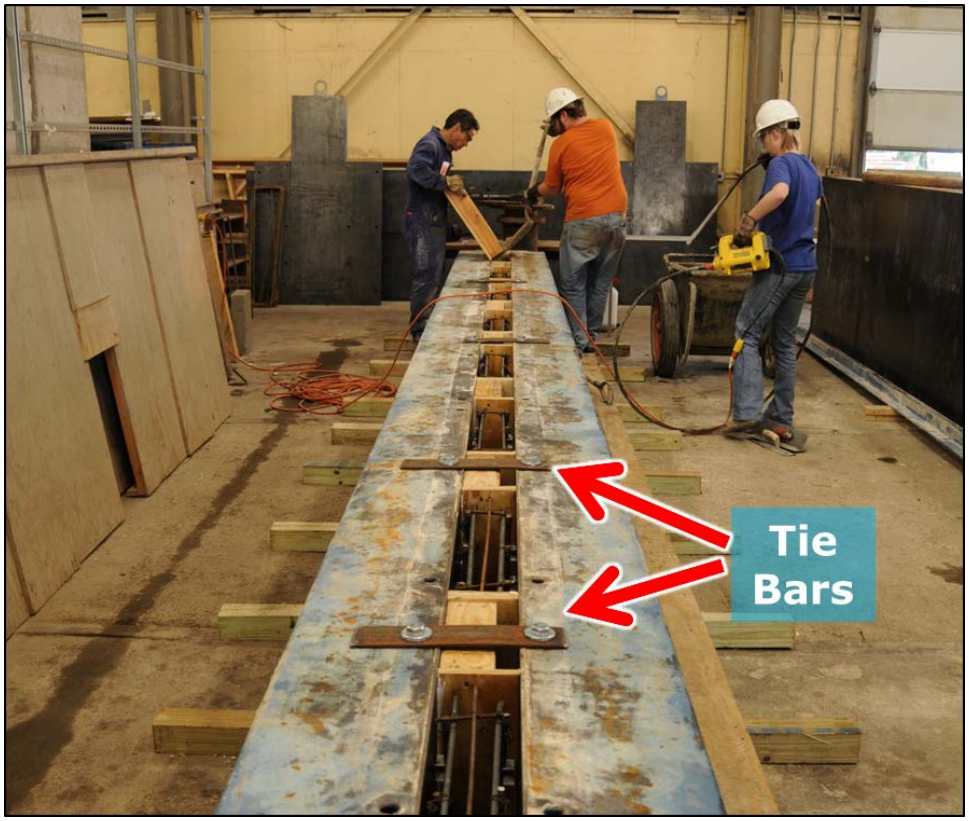

Figure 3-4: Side Form Tie Bars

For the final set of panels cast, special interior spacers were fabricated, as seen in Figure 3-5. This formwork permitted casting panels with different thicknesses using the same concrete.

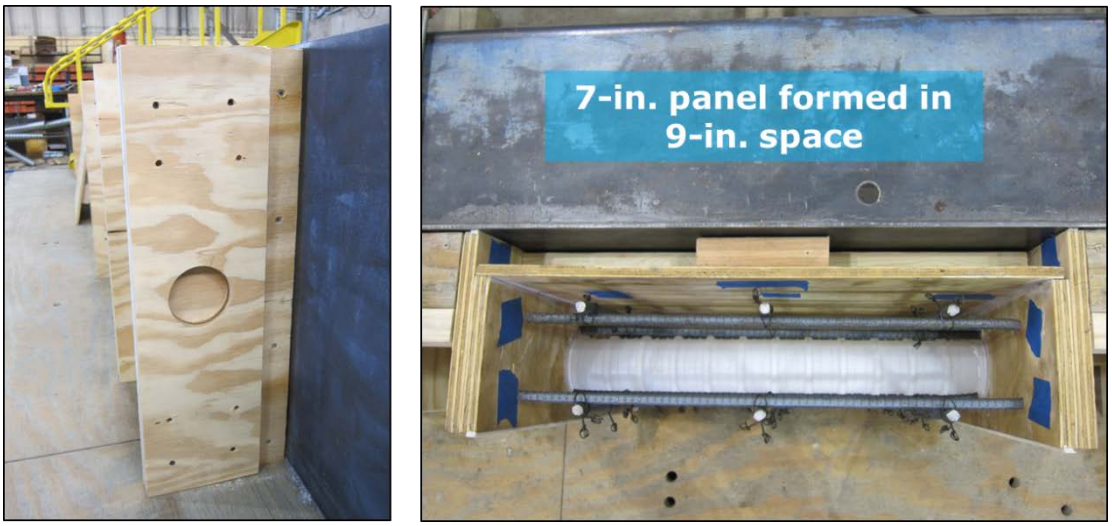

Figure 3-5: Modified Panel Form Spacers for Panel Size Variation in Same Set

3.2.3 Panel Layout and Reinforcement

The basic layouts for the majority of ducted and control panel specimens are detailed in Figure 3-6. With the exception of three cases, single, straight lengths of plastic or steel duct were placed at mid-depth and mid-thickness of panels (i.e. at a section's geometric centroid). The other three ducted specimens utilized two pieces of duct with different vertical space between the ducts. All of the ducts were oriented perpendicular to the loading direction. Duct inclination at angles other than 90° was not considered in this study.

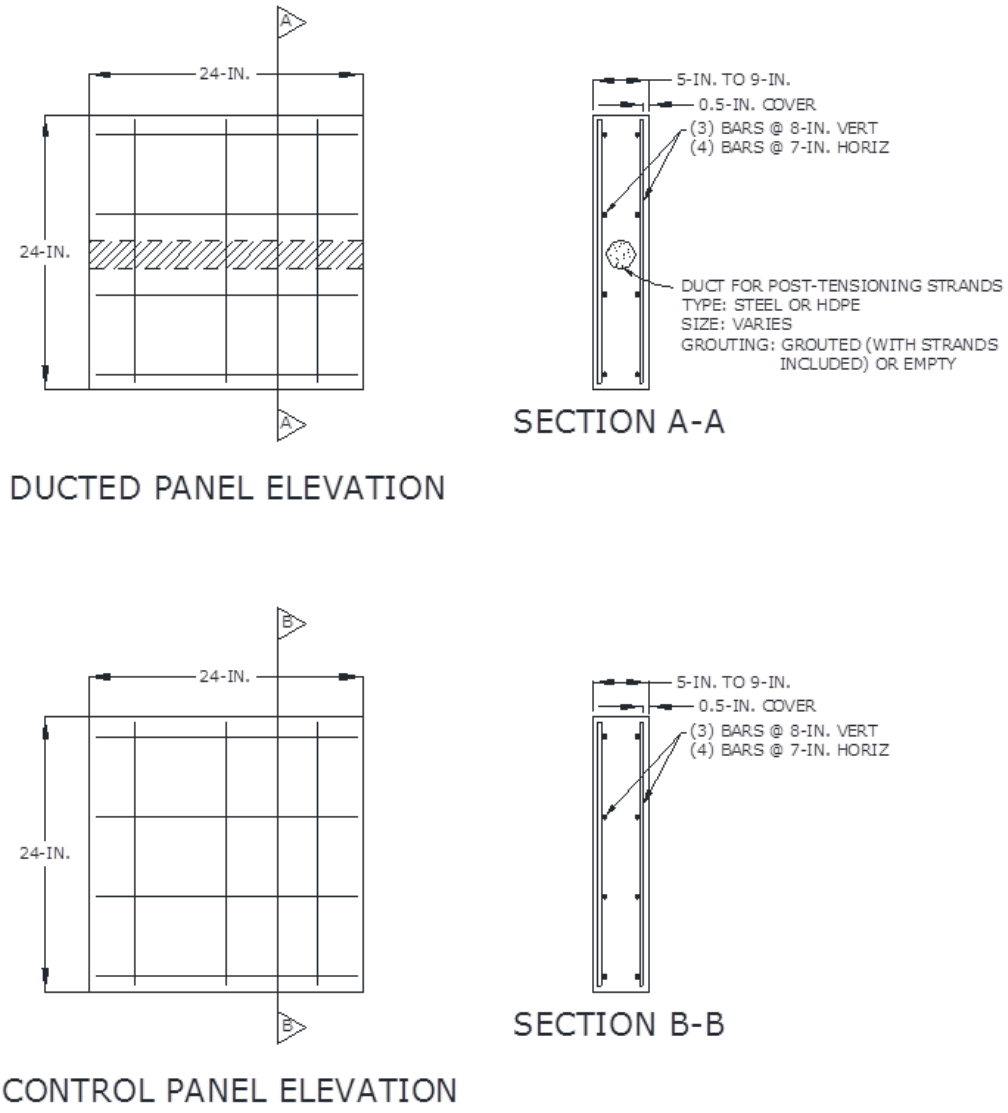

Figure 3-6: Basic Panel Reinforcement and Duct Layouts

Each panel was reinforced with two layers of reinforcement tied in a two-directional mesh. The bars placed vertically (and perpendicular to the duct) were meant to model the stirrups in a girder passing through a strut region. Three vertical bars spaced at 8-in. were used in order to match the typical 8-in. stirrup spacing in standard Tx Girders.

The four horizontal bars (parallel with the duct) were added for construction purposes to help hold the vertical bars in place. In the first two sets of panels, the two layers of reinforcement were tied together with small, straight pieces of #2 reinforcing bars through the panel thickness and subsequently tied to the duct. For all other panels, the layers of reinforcement were tied down to #2 bars placed in-between the interior form spacers (Figure 3-7). The clear cover was 0.5-in. for all panels and reinforcement patterns.

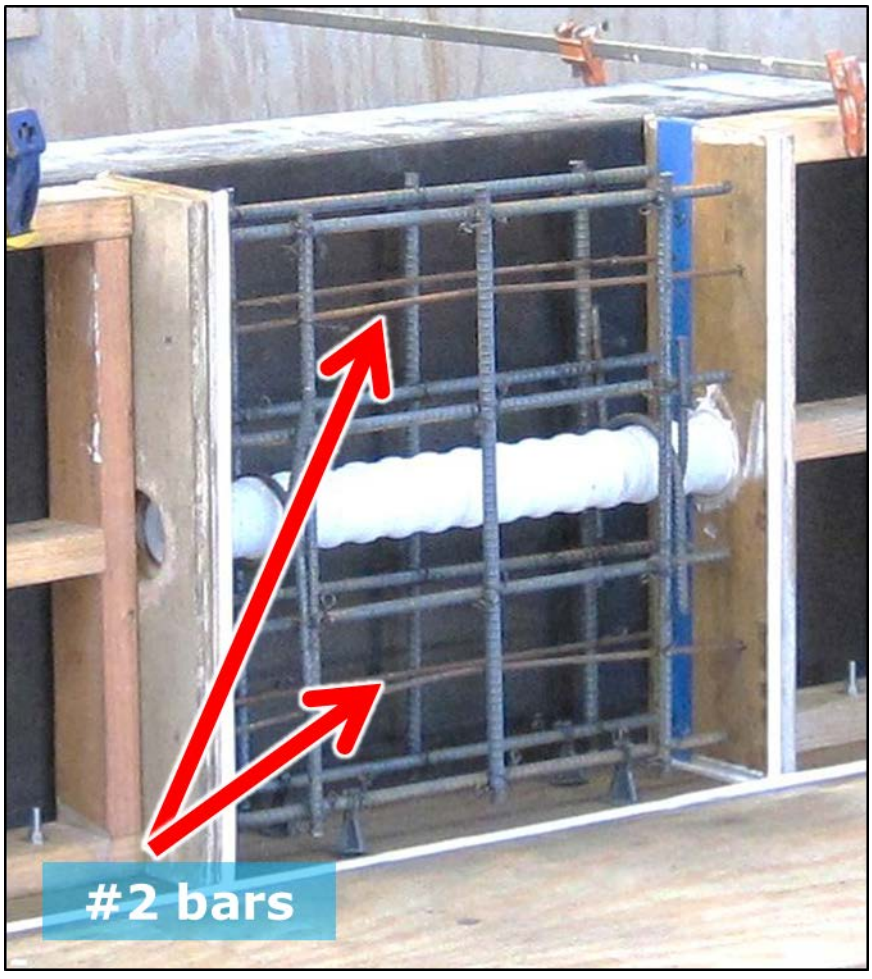

Figure 3-7: #2 Bars for Mesh Reinforcement Support

Additional reinforcement was included in some panels through the panel thickness at various points along the length of the duct but away from the duct. The shapes, locations, orientations, and purposes of these bars are discussed in Chapter 4.

3.2.4 Casting and Grouting

Each set of panels was vertically cast and care was taken to ensure good consolidation of concrete, especially beneath the ducts. No external vibration was used, but internal vibration was employed to minimize the possibility of voids around the ducts (Figure 3-8). The casting direction was the same as the eventual loading direction.

Figure 3-8: Panel Casting and Internal Vibration Procedure

In Figure 3-9, the final stage of the casting operation is shown. At the end of each concrete placement, exposed surfaces of fresh concrete were hand troweled and covered with plastic sheeting for specimen curing.

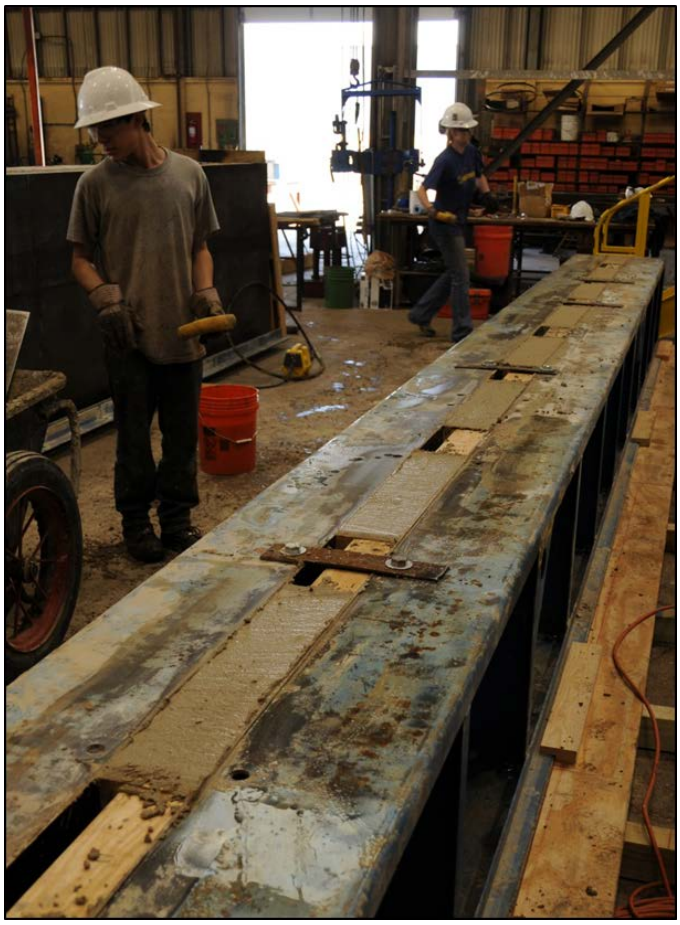

Figure 3-9: End of Casting

A complete set of test specimens is shown in Figure 3-10. The panels were normally removed from the formwork about two days after casting and were stored on the laboratory floor for approximately a week before grouting the ducts.

Figure 3-10: Completed Panel Set Cured and Removed from Forms

A vertical grouting operation was employed. Each panel was tilted upright with one of the exposed duct ends capped with plywood. A small amount of gypsum hydrostone was poured into the ducts to harden and seal the duct end so that no grout would leak out. Sets of bundled lengths of prestressing strand were placed in each duct, and then grout was hand-mixed and poured into each duct (Figure 3-11). Low-bleed, well-mixed batches of grout were used to achieve a good consistency without voids along the duct.

Figure 3-11: Duct Grouting Procedure

3.2.5 Application of Gypsum Hydrostone to Panel Ends

Part of the effort to assure even load application or bearing stresses on the panels involved the application of thin, uniform layers of gypsum hydrostone cast against each loading surface of the specimens. A lifting harness, depicted in Figure 3-12, was developed to assist in this process and greatly expedite testing.

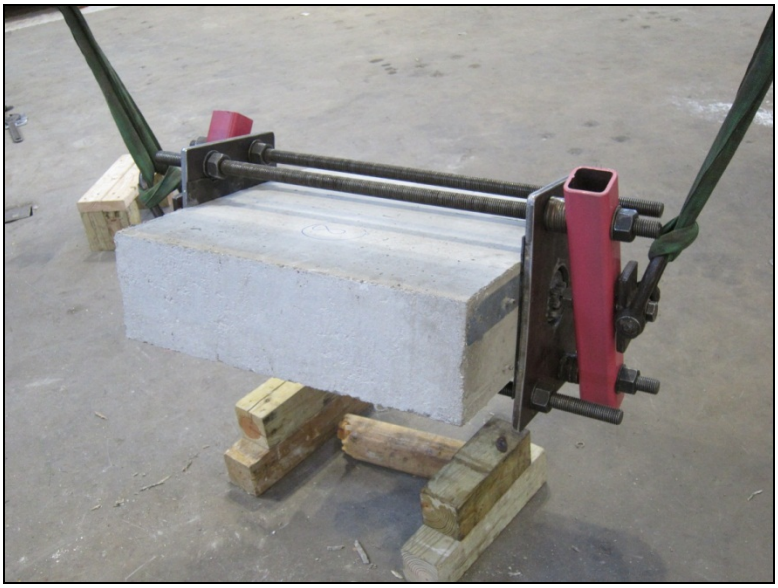

Figure 3-12: Rotating Panel Lifting Harness

The lifting harness was clamped to the sides of a panel around openings for ducts so that the panel could be safely lifted and placed into a bed of liquid hydrostone on a level steel plate (Figure 3-13a). After the hydrostone hardened, the panel could be lifted up and rotated 180° using the rotating harness to allow hydrostone to be applied to the other surface. This entire process was fast and ensured that the hydrostone would not crack during panel transport. In Figure 3-13b, a panel with hydrostone applied to one surface is being moved from the hydrostone platform.

Figure 3-13: End-Capping Panels with Gypsum Hydrostone

3.3 TEST MATERIALS

The following subsections detail the primary materials used in panel fabrication. Targeted material properties are presented here while measured properties may be found for each specimen in Appendix A.

3.3.1 Concrete

Two concrete mix designs were utilized. The first was chosen to achieve a 28-day design strength of 5,500 psi, used for the first set of panels and a later set analyzing the effect of grout strength versus concrete strength. The second mix was selected to reach 10,000 psi using a Type I cement with similar proportions as a Type III, 10,000 psi mix used for Tx Girders. This mix was used for constructing all other panels. Exact mix proportions are presented in Table 3-1.

Table 3-1: Concrete Mix Designs

Mix Design	#1	#2
Used For Panel Sets:	1, 5	2-4, 6-11
Target f'_c (psi)	5,500	10,000
Batch Size (yds)	3	3
Batch Proportions		
Type I Cement (lbs)	1269	1776
Sand (lbs)	4533	4245
D-Rock - 3/8-in. max agg. (lbs)	5604	5160
Class F Fly Ash (lbs)	309	600
Water (gal)	57.2	61.5
Set Retarder (oz)	24	47
High-Range Water Reducer (oz)	71	143

3.3.2 Grout

Three types of pre-packaged grout were used to achieve a range of compressive strengths. The first was a general application, non-shrink grout with sand used with a modified water-to-grout ratio to attain a low-strength mix emulating that used in the Swiss tests. This grout was only used for the first set of panels with a water-to-grout ratio of 0.30. The other two grouts were TxDOT-approved for post-tensioning applications: a sand- and cement-based product and a silica-fume-enhanced product. The majority of specimens utilized the former with a water-to-grout ratio of approximately 0.33, which typically yielded compressive strengths below 6,500 psi. The latter grout was primarily used in specimens to achieve strengths above 10,000 psi at a water-to-grout ratio of approximately 0.24. Throughout the remainder of this document, these two grouts are often referred to as regular-strength and high-strength grouts, respectively.

3.3.3 Mild Reinforcement and Prestressing Strands

Primary reinforcement for each test specimen consisted of Grade 60, #3 or #4 bars used as vertical/horizontal mesh reinforcement, #3 bars for through-thickness

reinforcement, and #2 bars utilized to hold other bars in place. The #3 bars were only used as mesh reinforcement in a few of the initial panels tested.

Ordinary, 0.5-in. prestressing strands with an ultimate tensile strength of 270 ksi were placed in the ducts prior to grouting. Given the short lengths of strand used, they were obviously not tensioned. The strands existed to represent any barrier to stress flow through a duct within the panels as might be seen in a girder. Table 3-2 indicates the number of strands placed in each of the duct diameters.

Table 3-2: Number of Strands Placed in Grouted Ducts

Duct Diameter (in.)	# of Strands
2.375	7
3	9
3.375	12
4	17

3.3.4 Post-Tensioning Ducts

Cylindrical, corrugated metal and high density polyethylene (HDPE) ducts were used in this study (Figure 3-14). The metal ducts are thin-walled, galvanized steel with angled corrugations. The HDPE ducts are thick-walled, low-friction plastic with thick, concentric ribs perpendicular to the longitudinal axis formed during the extrusion processes used in manufacturing the ducts. Additional protrusions exist parallel to the duct axis for those plastic ducts with a nominal diameter of 3.375-in. and greater. The steel and plastic ducts used had nominal interior diameters of 2.375-, 3-, 3.375-, and 4-in. All discussions of and calculations performed with results from this study utilize the nominal interior duct diameter rather than the exterior or outer diameter (which accounts for duct thickness).

Figure 3-14: HDPE and Steel Ducts

3.4 TEST VARIABLES

A number of variables were considered in the design of each test specimen. Various material properties and construction options were explored to reflect a wide range of possible conditions that might be or that are already utilized in practice. The goal was to assess the absolute or relative influence of each variable on the panel compressive strength. The following list includes all of the major design parameters investigated during the course of this study:

- Duct material (steel, HDPE)
- Bond characteristics of ducts
- Grout strength
- Concrete strength
- Duct diameter-to-thickness ratio
- Through-thickness reinforcement, including amount, location, and shape
- Multiple ducts (two)

- Panel thickness

An in-depth description of each of the test variables is provided in Chapter 4, including discussion about how test specimens were designed. It is important to note that the majority of specimens were designed to examine the effects of parameters independently; however, some panels were fabricated with the intent to observe the direct combined effect of multiple variables.

3.5 TEST FRAME

A self-reacting, uniaxial compression testing machine was designed at FSEL for panel testing (Figure 3-15). The design and construction of this equipment was carried out by the research team on Project 0-6652. The test frame was developed primarily for use with the current study, but with the understanding that it might be a valuable asset for future research endeavors. The following subsections describe the general use and purpose of the machine, its main working components, and its operation. The intent here is to briefly familiarize the reader with how the test setup works. Design calculations and construction drawings that were utilized during assembly are not included.

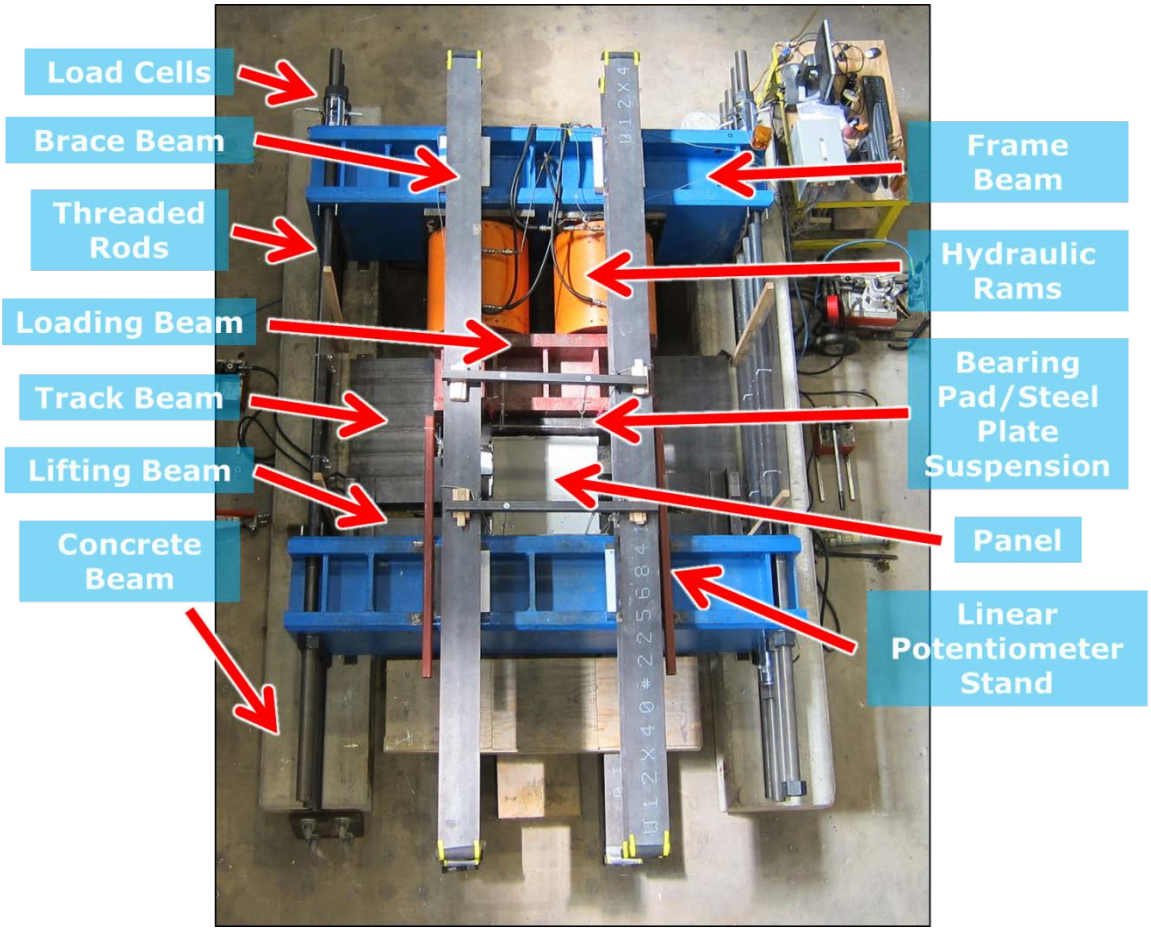

Figure 3-15: Aerial View of Compression Test Frame

3.5.1 General

The test frame was designed to be able to apply up to four million pounds in compression. This load limit was dictated by the 2-million-pound capacities of two hydraulic rams available at FSEL. It was anticipated that the largest panel load the test frame would have to impose would be for a 9-in. thick solid control panel (9 x 24 in.) with a concrete mix that could be much stronger than the nominal 10,000 psi specified and could be as high as 13,000 psi. It was assumed that a panel might fail at or above

100% of the concrete cylinder strength. The highest load would likely be 2800 kips and would provide a failure margin for the test frame of 1.43.

As a whole, the test frame was also designed to be stiff enough to minimize the differential, flexural, and axial deformations of the principal elements of the frame. This was especially important to ensure uniform load on each specimen.

3.5.2 Self-reacting Mechanism of Test Frame

The test frame was designed to be completely self-reacting, requiring no connection to the laboratory foundation. The decision to create a self-reacting test setup greatly simplified design. Further, the frame could be located anywhere in the laboratory. Due to the high loads the test frame was capable of producing and the lack of redundancy of the self-reacting system, special attention had to be given to safety in the operating mechanisms of the machine. It was imperative that the test specimen was the weakest element of the system, failing at a load well below those that could possibly cause yielding or fracture of any of the individual steel elements of the test frame or exceed the capacity of the loading rams. Thus, some of the individual components were designed with a high factor of safety.

The test frame was designed to be simple – symmetrical with axially-loaded elements and no moment transfer between components. Figure 3-16 illustrates the general load path and force on the elements of the frame. This diagram illustrates only axial load or reactions on the elements.

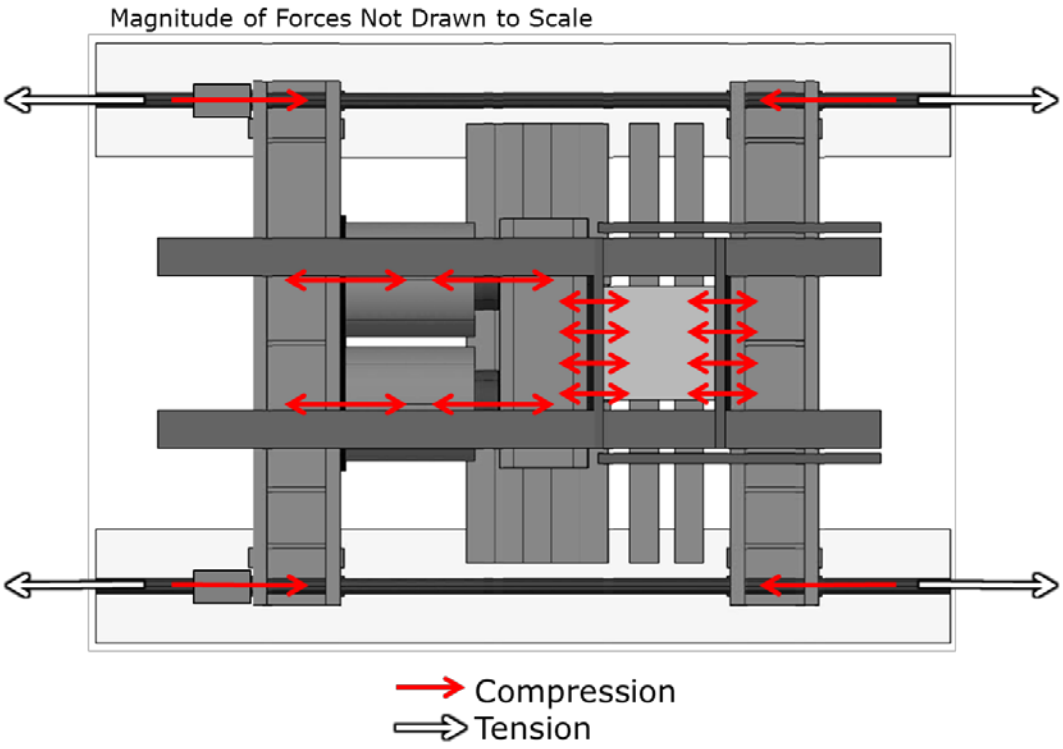

Figure 3-16: Load Path of Self-Reacting Test Frame (Adapted from Schmidt 2011)

3.5.3 Test Frame Components

The principal components of the test frame referred to through this document include the frame beams, threaded rods, brace beams, concrete beams, Teflon tracks, track beam, loading beam, lifting beam, bearing pads and steel plates, linear potentiometer stands, hydraulic rams, and load cells. The components are labeled in Figure 3-15.

3.5.3.1 Frame Beams

The frame beams were built-up steel sections with large flexural capacities. These sections were designed to minimize deflections. Each beam consisted of two 10-foot-long W14x426 steel sections welded together at their flanges with 0.75-in. deep groove welds.

These sections were further stiffened by the attachment of 1-in. thick steel plates on either side via full-length, 0.75-in. fillet welds. 3.5-in. diameter holes were fabricated at the ends of the frame beams to accommodate threaded rods. The beam webs were stiffened along their entire lengths and especially at locations of load transfer. Multiple 1-in. thick, full-depth stiffeners were welded on both sides of the two webs of each beam near the ends (where rods were located) and at bearing points for specimens or hydraulic rams.

3.5.3.2 Threaded Rods

Eight 3-in. diameter, high-yield, coarsely-threaded rods provided the tensile elements of the test frame. The rods passed through the frame beams, and nuts at the ends of the rods were tightened and adjusted to ensure simultaneous engagement of all rods. Each rod had a 670 kip yield capacity, all-in-all guaranteeing elastic behavior well beyond the highest anticipated panel failure loads.

3.5.3.3 Brace Beams

Four W12x40 sections were attached above and below the frame beams to maintain the overall alignment of the test frame and its components. Although referred to as ‘brace’ beams, these sections were not utilized in any manner to supply resistance to structural instability or provide a means to improve the load-carrying capacity of the frame. With the goal of applying a uniform load to the test specimens, it became necessary to achieve a means of ensuring a parallel configuration of moving parts. The brace beams facilitated this geometric behavior by physically tying the frame beams together, thus preventing either from independently rotating. This became especially important when operating at very high loads. In such instances, elements of the test frame were susceptible to shift under the high-energy impact of panel failure.

The connection between a brace beam and frame beam is pictured in Figure 3-17. The brace beams were loosely bolted to the frame beams. Long-slotted holes oriented in the loading direction were drilled in each brace beam at the connection points near one

end of the test frame. This allowed the frame beams to move under load while still maintaining proper alignment and without transfer of load through the brace beams. Additionally, sheets of Teflon were placed between the brace beams and frame beams at the connections to eliminate the generation of friction during loading.

Figure 3-17: Connection Between Frame Beam and Brace Beam

3.5.3.4 Concrete Beams

A pair of 15-foot-long concrete beams was utilized to elevate the primary components of the test frame off the ground and provide a means of clearance for the lower brace beams.

3.5.3.5 Teflon Tracks

In an effort to maintain a test setup in which there would be no loss of load between the points of load application and load measurement (at the rods), Teflon-mounted steel plates were placed between the frame beams and underlying concrete support beams (Figure 3-18). By providing a Teflon-on-Teflon boundary between these large elements, the frame beams could freely slide on top of the concrete under the application of load, thus eliminating any loss of load to friction and ensuring that the final

load measurements based on the tension in the rods would accurately reflect the true failure load of each specimen.

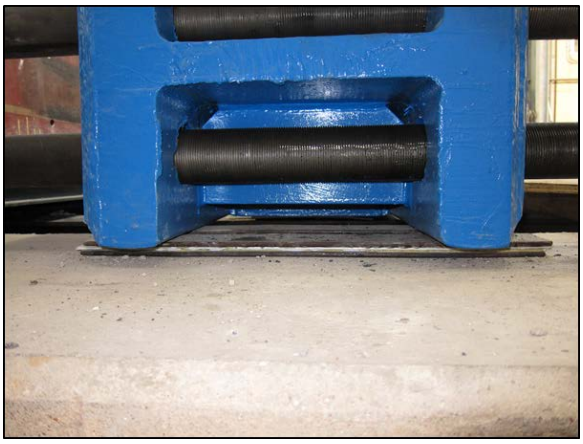

Figure 3-18: Teflon Track

3.5.3.6 Track Beam

Due to the design of the test frame as a horizontally-reacting machine and the elevation of the frame atop the concrete beams, a mechanism was needed to support the loading beam. The track beam consisted of five W12x40 sections placed directly adjacent to one another and made composite that spanned across the concrete beam supports. At approximately the third points along the spans of the individual sections lied 1-in. thick steel plates welded to link the sections together and provide an elevated track upon which the load beam could sit and slide in proper alignment with the rams. A layer of 0.125-in. thick Teflon was adhered to the track plates to provide a very low friction sliding surface for the loading beam.

3.5.3.7 Loading Beam

A highly-stiffened, wide-flange section was utilized to uniformly transmit load from the hydraulic rams to the specimens. This beam was selected for two primary reasons. For one, the length of the section available adequately fit within the boundaries

of the test frame established by the frame beams and rods. Secondly, the widths of the flanges were appropriately large enough to engage the entirety of the heads of the hydraulic rams as well as the thicknesses of panels tested.

This element was also required to be stiff enough to limit flexural deflections so that the load on the specimen would be uniformly distributed. Ten equally-spaced, 1-in. thick stiffeners were added to the member to achieve this goal. Small pieces of 0.125-in. thick Teflon were attached to the flanges of the loading beam prior to placing the beam on and aligning it with the Teflon-faced tracks of the track beam (Figure 3-19).

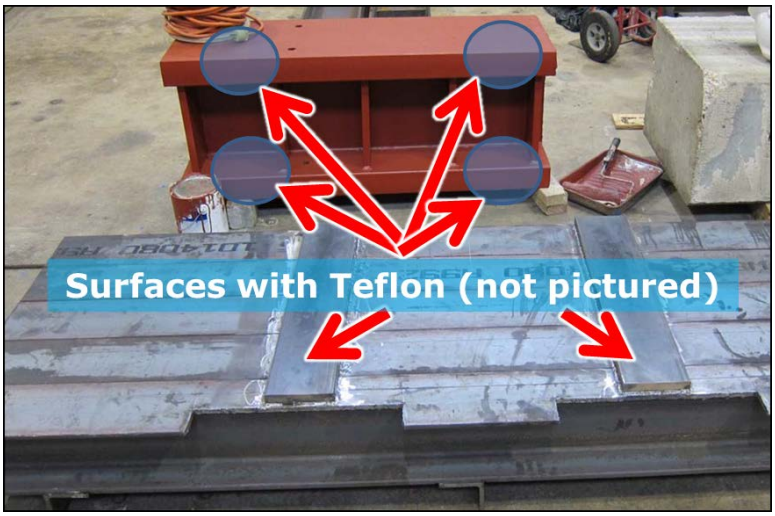

Figure 3-19: Teflon Mounting of Track Beam and Loading Beam

3.5.3.8 Lifting Beam

Two W12x40 beams were used to position the test specimens in the loading frame (Figure 3-20). After load was applied to the specimen, the beams were lowered so they were no longer in contact with the specimens. Small hydraulic rams were extended or retracted to position the panels. Four 1-in. thick Teflon/PVC pads were bolted to the top surface of the lifting beam to aid in centering the test specimens when positioned on this beam.

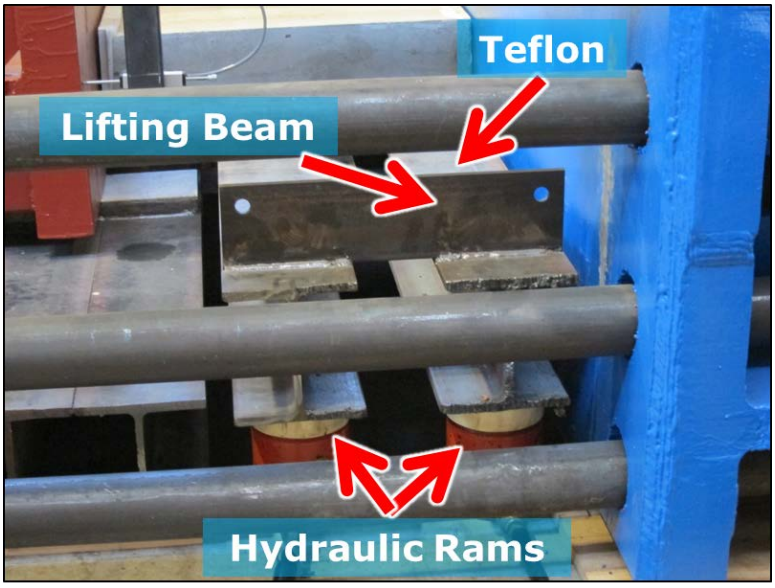

Figure 3-20: Operation of Lifting Beam

3.5.3.9 Bearing Pads and Steel Plates

A uniform distribution of force to the loading surfaces of each specimen was facilitated through the use of reinforced, elastomeric bearing pads and 0.25-in. thick steel plates. The 9-in. wide bearing pads were placed against the loading beam and frame beam at the two loading surfaces to account for any remaining unevenness of the contact surfaces (after the hydrostone end-capping procedure). Additionally, 0.25-in. thick steel plates were placed between the test specimen and each bearing pad to ensure a well-spread distribution of forces across the bearing pads and prevent undesirable deformations of the pads. The pads and plates were centered and kept in place via adjustable cable suspension from the upper brace beams.

3.5.3.10 Linear Potentiometer Stands

A pair of L-frames constructed from thick-walled, HSS sections were temporarily welded to the specimen-end frame beam on either side of the test specimen to support

linear potentiometers (Figure 3-21). The instrumentation was used for measuring the deflection (shortening of the panel under load) between the frame beam and the loading beam. The stands were placed such that they would not interfere with the advancement of the loading beam during load application, but could break away from the rest of the test frame and not sustain damage when the panel failed.

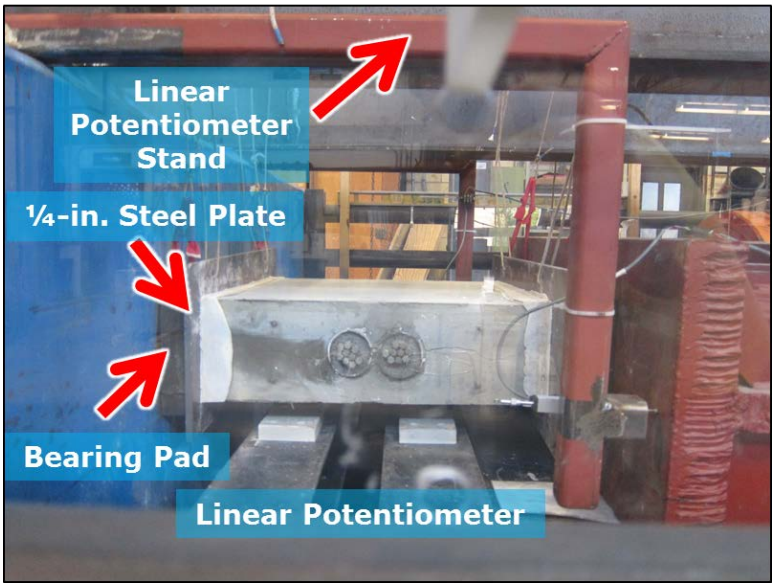

Figure 3-21: Linear Potentiometer Stands

3.5.3.11 Hydraulic Rams

Two 2-million pound capacity hydraulic rams applied load to the test specimens. Each ram was secured to a 2-in. thick steel plate that was subsequently bolted to the frame beam with high-strength, A490 bolts.

3.5.3.12 Load cells

The failure load for a single panel test was calculated as the sum of individual load readings from each of the center-hole load cells placed on the threaded rods. Each

load cell was situated on a rod at the ram-end frame beam as shown in Figure 3-22. The data from all load cells were added to determine the compression applied to the test panel.

Figure 3-22: Load Cells

3.5.4 Instrumentation

As previously mentioned, eight load cells were used to collect the load applied to the test specimens. In addition to determining this load, values from individual load cells were periodically compared and averaged to check if forces were being symmetrically distributed through the test frame. A pressure transducer was connected to each of the inflow hydraulic lines attached to the rams. The measured pressures from these devices were converted to applied load and compared with the load cell readings as a secondary check of load distribution. Lastly, two linear potentiometers were used at either side of the test frame to measure the relative movement between the specimen-end frame beam and loading beam. While the measurements obtained were not accurate measures of specimen deflection (compression of bearing pads was also considered), loading

symmetry could be verified and estimated load-deflection plots could be generated to estimate stress-strain behavior of the test panels.

3.6 EXPERIMENTAL PROCEDURE

Testing of each panel was carried out through a multi-stage operating procedure. Steps were taken to minimize operator variability and obtain the most accurate and precise results possible.

3.6.1 Test Frame Maintenance

Prior to loading any of the test specimens, all elements of the test frame were checked. The measures taken at this time included:

- Tightening all nuts on the rods
- Confirming that the bolts between brace breams and frame beams were adequately loose to allow for easy slippage in slotted holes
- Re-aligning the Teflon tracks beneath the frame beams
- Centering the bearing pads and steel plates side-to-side and vertically against the loading beam and specimen-end frame beam while appropriately tying these pieces down using high-tensile strength towing line
- Centering the loading beam from side-to-side so the rams could engage the beam evenly
- Ensuring the existence of adequate space to lower the test panel into position

Once the listed tasks were completed, a panel (with hydrostone applied to the loading surfaces) was placed in the test frame and final adjustments were made. One face of the panel was placed against one of the steel plates and was centered in the load frame. The small rams beneath the lifting beam were extended to lift the panel to the appropriate position where it was centered vertically on the plates/bearing pads. The large hydraulic rams were then extended to close any gap that might exist between the panel and steel

plate(s). The extensions of the rams were measured and loading rates were adjusted to make sure that each ram would engage the panel simultaneously.

3.6.2 Initial Loading Stage and Instrumentation Check

Initial loading operations for each test were carried out to verify that the test frame and instrumentation were working correctly. First, the rams were extended until the total load applied to the panel reached 30 kips. Pressure transducer readings were monitored to ensure that they were recording evenly. The linear potentiometer readings were compared. These comparisons were made to determine if the load was being applied uniformly and all instrumentations were functioning. Load cell readings were also compared. Given the presence of eight load cells, each of the load cells should have measured approximately three to four kips to provide a total load of 30 kips. If the load cell readings were different than expected, the nuts on the rods were tightened or loosened as needed to even the load cell readings.

Safety precautions were developed to protect the researchers and bystanders during failure of the test specimen. The failure was highly explosive and provided little warning, so sheets of flexible polycarbonate or plywood were placed over the test frame to prevent heavy and jagged shards of concrete from flying through the air (Figure 3-23).

Figure 3-23: Test Frame Safety Precautions

3.6.3 Loading to Failure

Loading to failure was carried out at load rate between 0.5-1 kips/sec. In some cases, cracking resulted in minor drops in recorded load followed by further increases in load. In all cases, failure was indicated by a substantial drop in load-carrying capacity of the specimen, most often with little warning, accompanied by a loud noise and violent disintegration of parts or the entirety of the cross-section. Pieces of reinforcement were typically mangled or buckled after failure. Additionally, ducts were often seen to be severed or split apart with pieces of strand dislodged and grout either cracked or crushed. The precise nature of the failure and observed details of the state of the destroyed specimen were indicative of its structural behavior and the effect of certain variables on the behavior.

3.7 CHAPTER SUMMARY

As part of a larger study on the influence of post-tensioning ducts in the web of an I-girder on shear strength, a considerable number of small-scale concrete panels with and without embedded ducts were constructed and tested in uniaxial compression to observe trends in load-response behavior and estimate web crushing strength. Sets of panels were engineered at the Ferguson Structural Engineering Laboratory from preliminary design through to building, casting, grouting, and pre-test setup. The design of the panels incorporated a wide array of test variables and parameters understood or expected to have potential impact on the crushing capacity of webs containing ducts. The panels were load-tested using a specially-designed, 4-million-pound testing machine. In-depth descriptions of the test variables considered in this study are provided in Chapter 4 along with the results of pertinent panel tests. An evaluation of quantitative trends in crushing capacity is covered in Chapter 5, based on the results of this study. Also at that time, the discussion of panel testing will segue into comparisons with girder testing.

CHAPTER 4
Test Parameters and Results

4.1 OVERVIEW

A total of 100 panel specimens were tested. In most instances, each set of panels was designed to address the influence of one parameter on the compressive capacity of the panels. Generally, each set of panels was tested 28 days after from casting and at least 21 days after grouting. The panels within each set were all tested within a period of one to two weeks to minimize material variability. Only six panel tests did not provide useful results.

The major test parameters examined in this study are displayed in Figure 4-1. The means by which design variations were achieved are discussed along with the reasons for such modifications. Abridged results of panel tests principally relevant to each test parameter are presented where appropriate. In most cases, the experimental results are given in one of two forms: the actual failure loads of the panels in question or more commonly, the corresponding web width reduction factors (η_D). For thoroughness, a value of η_D is computed as the applied failure stress of a ducted panel, σ_{ducted}, divided by the average applied failure stresses of the control specimens, $\sigma_{\text{control,}}$ from the same set. Although calculating η_D values using applied stresses varies little from results using failure loads, the true measured dimensions of the panels are accounted for as accurately as possible. All specimens are referred to by a designation such as P1-1, where the first number indicates the panel set and the second indicates the panel number within that set. The complete data for all panel tests is provided in Appendix A. There, the reader may find detailed information regarding casting and grouting operations, fabrication details, material properties, and test results unique to individual specimens.

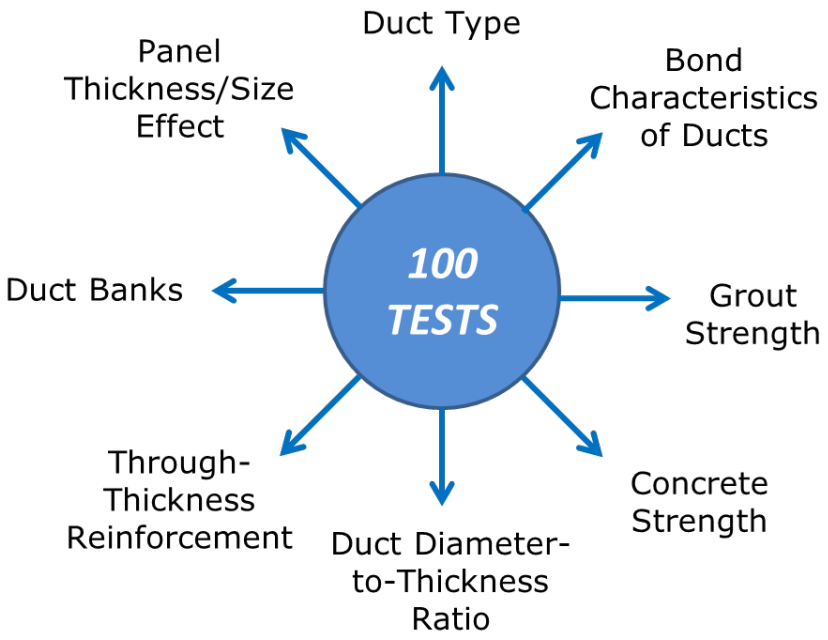

Figure 4-1: Primary Panel Test Parameters

4.2 INITIAL PANEL TESTS

The first set of a panels cast were tested with the intention of verifying the proper working condition of the test frame and validate past research results. These panels were 5-in. thick and were fabricated using a medium-strength concrete and low-strength grout to emulate the specimens tested by Muttoni, Burdet, and Hars (2006). Both plastic and steel ducts were used with an interior nominal diameter of 2.375-in. The layout of primary mesh reinforcement was kept approximately the same as in the tests by Muttoni et al. The duct orientation was also kept at 90°. The final results of these tests were compared to prior findings. Any problems encountered with the initial operation of the test frame were rectified before proceeding with future panel testing.

4.2.1 Shake-Down Tests

The first three tests (P1-1, P1-2, and P1-4) conducted were used to refine operation of the test frame. The results of these tests were discarded due to observations

of poor distribution of applied load and instrumentation errors. At the onset of the test program, procedures for using bearing pads in the test setup and applying hydrostone to panels were not yet finalized. Two of three controls cast and an ungrouted, plastic-ducted panel failed prematurely due to crushing of the edges of the panels. These panels were not well aligned in the test frame and did not have very flat loading surfaces. At the same time, load cell and pressure transducer readings were not well correlated.

Adjustments were made to the test frame and testing procedures after the first specimens failed improperly. All subsequent tests in the first panel set were carried out after the flaws previously encountered were corrected.

4.2.2 Comparison with Results of Muttoni, Burdet, and Hars (2006)

Six tests from the first panel set (one control and five ducted panels) were compared to those from the work of Muttoni et al. In Figure 4-2, η_D values calculated for similar tests from the two sources are compared. No comparison could be made for a panel with an empty, plastic duct. Overall, the only difference between the two sets of panels was the material properties. Measured concrete and grout strengths are also shown in Figure 4-2.

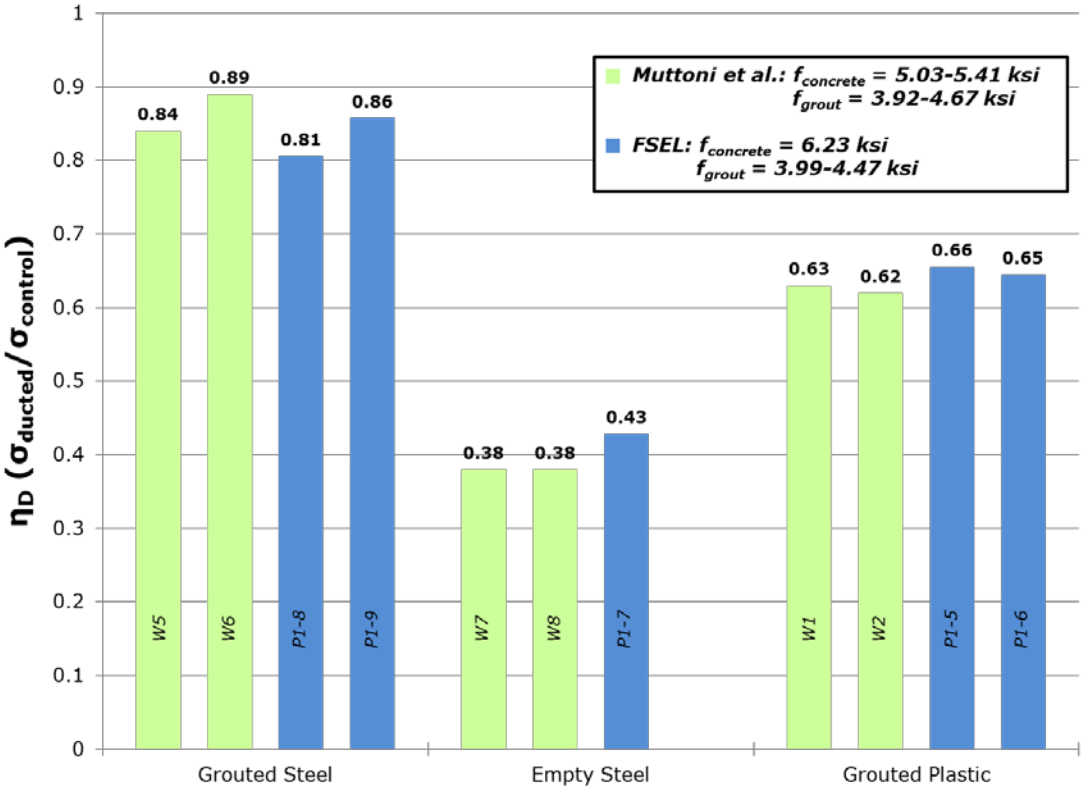

Figure 4-2: Comparison of 5-in. Panel Results and Tests by Muttoni et al.

The results from this set of panels agreed well with the past findings. Panels with empty ducts performed poorer than those with grouted ducts, and panels with plastic ducts had lower capacities than those with steel ducts.

The good comparison between results from the two studies confirmed the test procedure used in this study. The remaining tests of this investigation were conducted using the practices developed during testing of the initial panels.

4.3 EXPERIMENTAL RESULTS FOR TEST VARIABLES/PARAMETERS

The following subsections cover the bulk of test results obtained from the remainder of the panel tests as they apply to the discussion of each test variable investigated.

4.3.1 Duct Type

Corrugated steel and plastic ducts were used in this study. Limited prior testing by Muttoni et al. (2006) conducted on panels with plastic ducts indicated a large reduction in compressive capacity compared to steel ducts. This small but compelling information and a lack of consideration of duct type by most code shear equations prompted the need to further investigate the behavioral differences of panels with differing duct types.

The impact of a chosen duct type was continually assessed during this study. Plastic and steel ducts were used for panels of all thicknesses and for those used to study other test variables including duct diameter-to-web thickness ratios, grout strength, and use of through-thickness reinforcement. As will be described, a specimen with a plastic duct always failed at a lower load than a comparable one with a steel duct. For the sake of brevity, the remainder of the discussion in this section will focus on the behavioral differences between 7-in. panels using different duct types. The specimens covered here had a 3-in. diameter duct, high-strength concrete, normal-strength grout, and no through-thickness reinforcement. In this way, the impact of duct type alone will be addressed. Any unique effects of changing duct types while modifying some other variable are described in subsequent sections of this chapter, as appropriate.

The resulting η_D values computed for the tests covered are compared in Figure 4-3 which illustrates the aforementioned difference in load-carrying capacity when using different duct types. Despite minor differences in concrete or grout strengths, panels with the same duct type are shown together. The η_D values were very similar for each group. On average, the panels with plastic ducts exhibited a decrease in η_D of 0.18 compared to those with steel ducts.

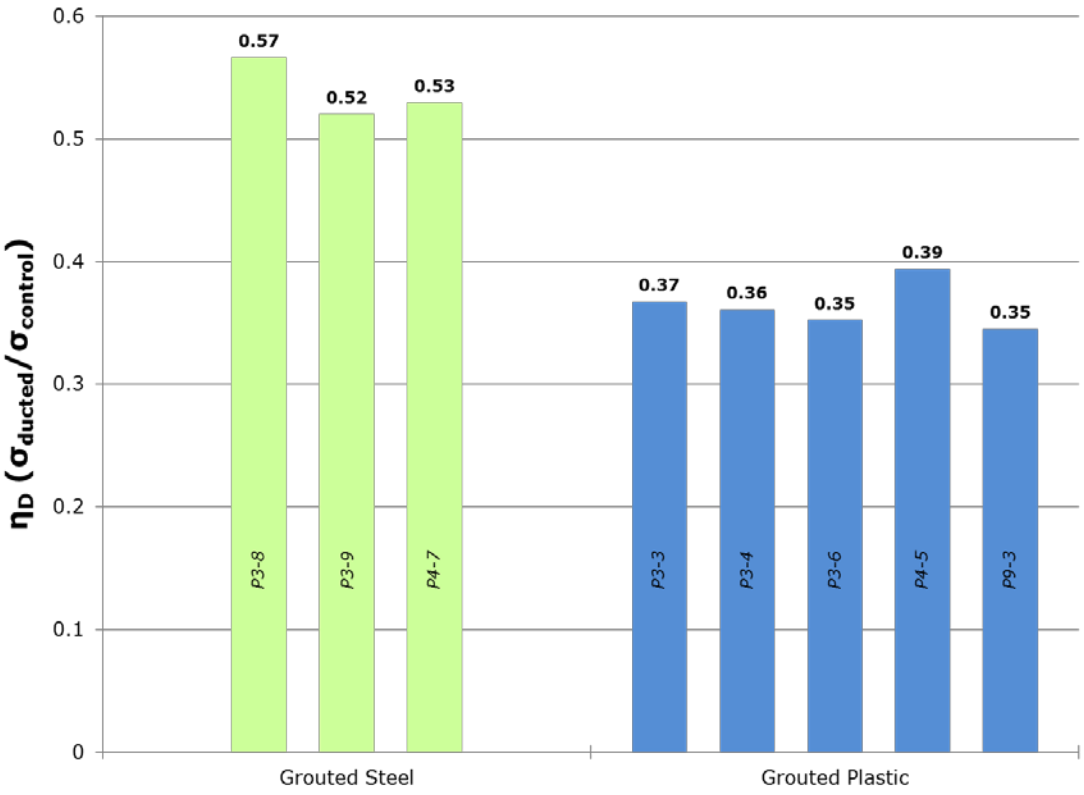

Figure 4-3: Comparison of Plastic- and Steel-Ducted Panel Results

Regardless of duct type, each specimen ultimately failed by the initiation of splitting of the specimen near mid-thickness and near the duct rather than by crushing (Figure 4-4). This splitting was relatively abrupt, typically with little to no warning of impending failure. An example of this load-deflection behavior is seen in Figure 4-5. Initially, deflections increased rapidly under minimal load during specimen seating until the specimen's loading surfaces and the bearing pads became fully engaged. Under continued loading, deflections increased – quickly at first and more gradually at higher loads. Ultimately, the slope of the load-deflection curve did not change much, if at all, when a panel failed. The splitting of panels was accompanied by the expulsion of concrete at the sides of the panels and buckling of the reinforcement in the direction of loading.

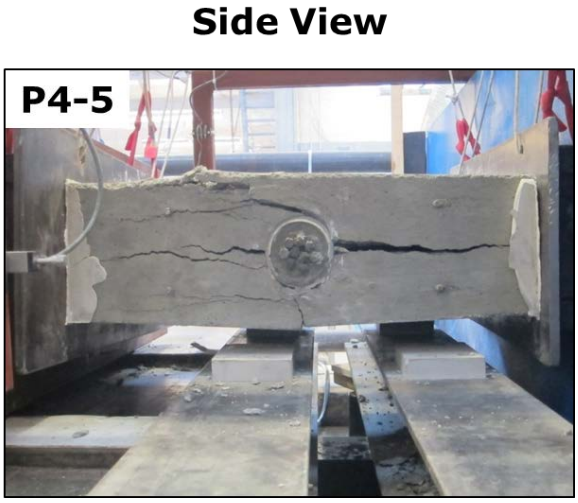

Figure 4-4: Tensile Splitting of Panels

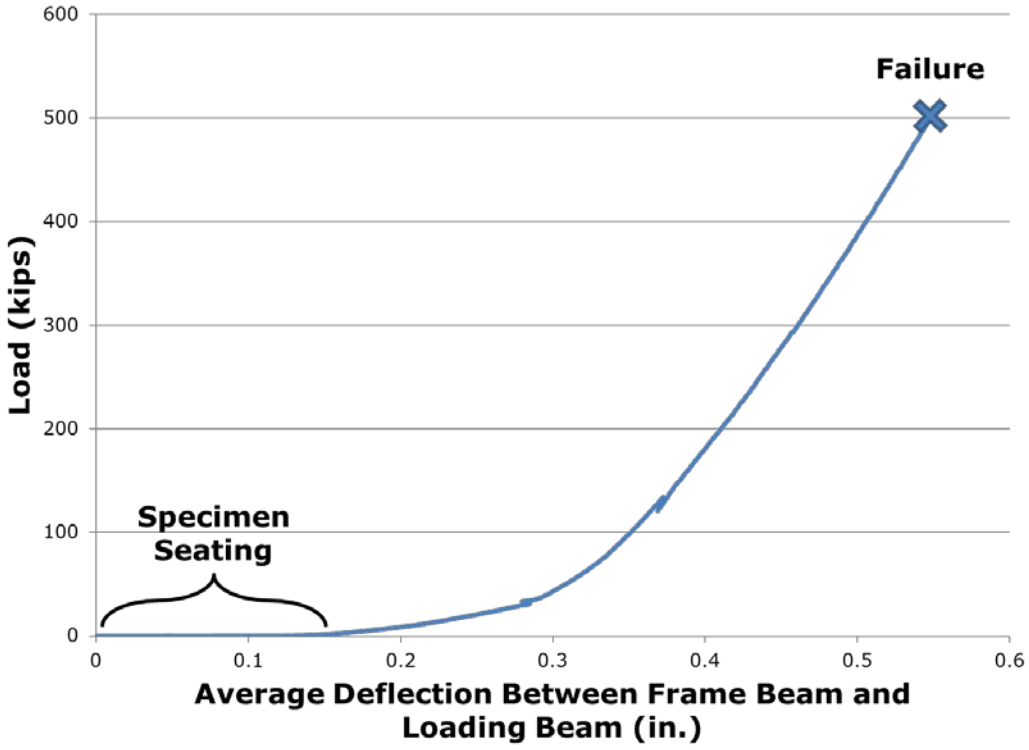

Figure 4-5: Example Load-Deflection Plot

The primary link to understanding the difference in capacities depending on duct type used lies in the observed sequence of cracking up to failure. In many cases, panels with plastic ducts split in half exhibiting complete separation or debonding between the duct and surrounding concrete (Figure 4-6a). The duct did not always remain completely intact though, and the grout was often seen to be partially cracked; however, this was mostly the result of the energy release when the panel failed rather than a characteristic of failure itself. On the other hand, the panels with steel ducts almost never experienced debonding between the concrete and duct. In some cases, the failure could be categorized as a complete mid-thickness splitting failure, with the duct itself being severed and cracking propagating through the grout (Figure 4-6b). In other instances, splitting still dominated at failure, although cracks propagated from mid-thickness at panel ends toward the outer duct edges while leaving the duct and grout undamaged (Figure 4-6c).

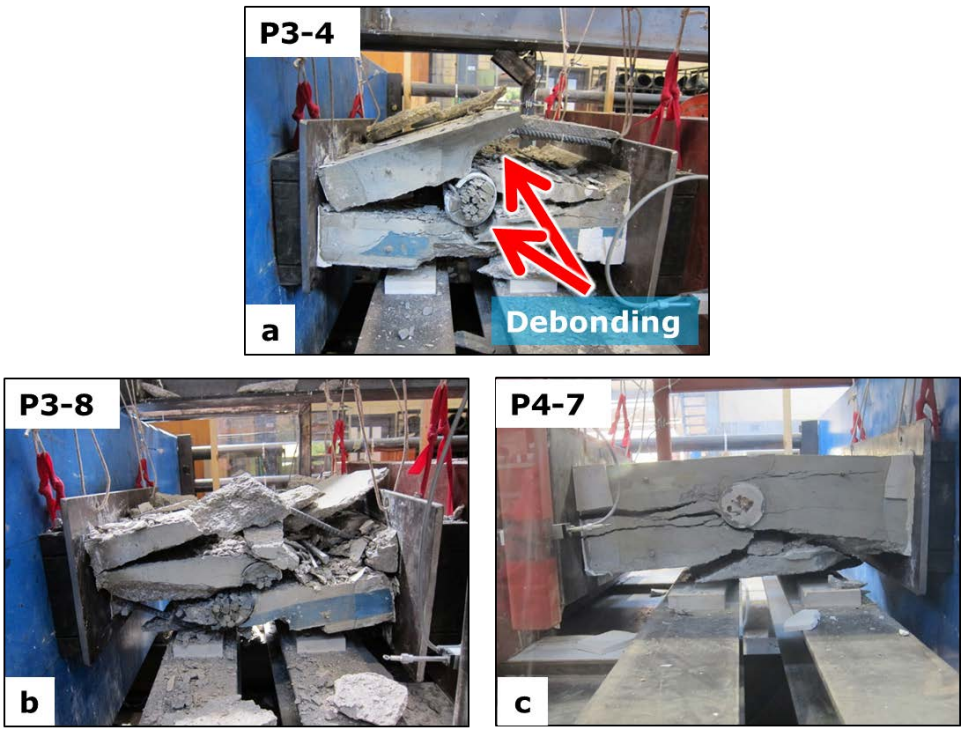

Figure 4-6: Common Failures of Plastic- or Steel-Ducted Panels

The implication of these failure mechanisms is that the standard flow of compressive stresses in a panel with a grouted duct is inhibited when debonding between the duct and concrete occurs. The ability to transmit stresses through the duct and allow the grout to carry some of the load is stopped or limited when debonding occurs. The steel-ducted panels maintained adequate bond and carried additional load. The plastic-ducted panels exhibited debonding, where failure was essentially a consequence of the panel shifting its load response from that for a panel with a fully bonded and grouted duct to that for a panel behaving as though the duct were empty. Without a means of transferring load from the concrete to grout, compressive stresses will suddenly begin flowing completely around the duct (as for panels with empty ducts), and high tensile stresses will develop. Because the tests were load-controlled, the applied loads on these specimens remained constant during the shift from the bonded to unbonded states. At those loads, the increased tensile stresses led to a sudden failure.

The question of why the plastic ducts debonded from the concrete and steel ducts was likely associated with the chemical and/or physical properties of the duct materials. An investigation of chemical bond between concrete and either steel or plastic was not attempted here. Regarding the physical nature of HDPE and steel, it is known that HDPE has a lower coefficient of friction. It is plausible that this smooth, low friction material would not mechanically bond to concrete very well, or at least as well as steel.

Physical attributes of the ducts themselves, namely the size and shape of the corrugations, might play a role in explaining bond behavior as well. The corrugations on both types of ducts are deliberately fabricated to provide a means of mechanical interaction between the ducts and surrounding concrete. Steel ducts have corrugations that are not as wide, protruding, or widely spaced as those for plastic ducts. Additionally, corrugations are diagonally wound around steel ducts while the plastic duct corrugations are perpendicular to the longitudinal axis of the duct due to the extrusion process used in duct fabrication. In panels, the plastic duct corrugations are parallel to the direction of loading. Under the application of load, it would seem likely that surrounding concrete

could just slide forward along these parallel corrugations. The angled steel corrugations would better resist such movement.

General proof testing of physical bond between concrete and plastic or steel ducts was not within the scope of this study, but may be valuable to conduct. All-in-all, there is clearly some value in the recommendation by the AASHTO Bridge Design Specifications (2012) to investigate bond between materials when using plastic ducts. Further evaluation of bond in the context of panel testing is addressed as follows.

4.3.1.1 Effects of Bond

In order to verify that the principal discrepancies between panels with plastic ducts and panels with steel ducts were due to issues of duct-to-concrete bonding, a number of panel tests were conducted with attempts to either break or improve the bond between the ducts and concrete. A bond breaker was applied to panels with steel ducts so that the surface provided no adhesive bond capacity. A panel with a plastic duct coated with the same bond breaker was tested to gauge how much chemical bond actually existed between the duct and concrete. Also, a panel with an abraded plastic duct was tested to examine the possibility of improving bond characteristics.

The entire exterior surface of the 3-in. steel ducts used in two panel tests were coated with a thin layer of melted wax in order to break the bond between the ducts and concrete. The wax was melted and evenly applied using a heat gun. This was done to ensure that the nominal thickness of the ducts would not be impacted and that there would be a uniform layer of wax on the duct (Figure 4-7).

Figure 4-7: Application of Wax Bond Breaker to Steel Ducts

Testing of these panels resulted in failures more typical of panels with plastic ducts than those with normal steel ducts. Each panel with a waxed steel duct exhibited a splitting and debonding failure where the duct remained undamaged and the grout did not crack. The first panel (P4-9) debonded from the concrete and failed with an η_D of 0.42 (Figure 4-8a). This value is almost the same as the upper-bound results of previously-tested panels with grouted plastic ducts, which had failed with an η_D closer to 0.40. The second panel (P4-8) provides added perspective. In this case, part of the duct remained bonded to the concrete at a location where the wax was unintentionally removed during concrete placement (Figure 4-8b). This panel failed with an η_D of 0.49. This was higher than that for the other panel but lower than that for typical steel-ducted panels failing with an average η_D of about 0.54. Clearly, the results from using a bond breaker verify that bond is a major contributing factor to the difference in compressive capacity when using different duct types.

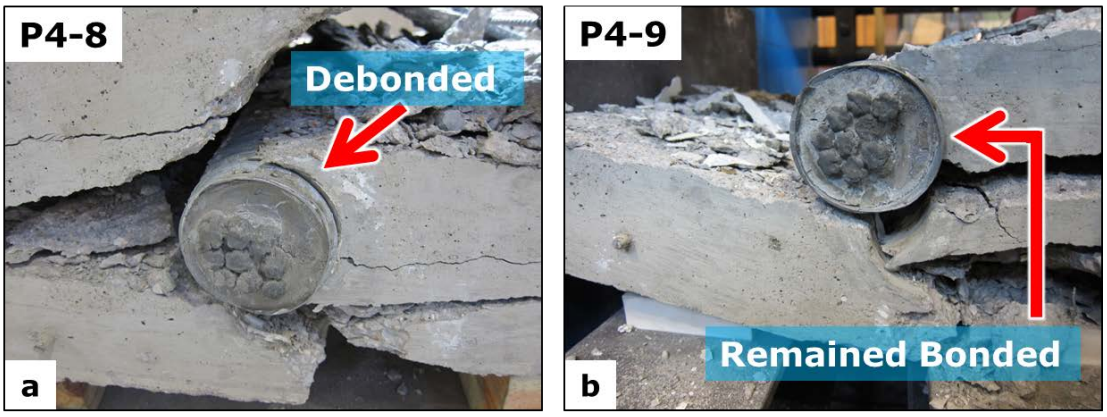

Figure 4-8: Failures of Panels with Waxed, Steel Ducts

The wax bond breaker was also applied to one plastic duct to investigate if the bond between the duct and concrete was possibly more mechanical in nature than chemical. The panel with the waxed plastic duct (P4-6) failed no differently than typical plastic-ducted panels. This panel failed with an η_D of 0.39, within the normal range of other panels with plastic ducts. The wax should have all but eliminated any chemical bond existing between the ducts and concrete. Since, the wax did not worsen the failure capacity of this panel, it indicates that there was little chemical bond to begin with.

An additional panel was tested that contained a plastic duct shown in Figure 4-9, whose surface was scored using 80 grit sandpaper to provide a roughened surface to possibly improve mechanical bond. The procedure used did not improve performance; this panel (P7-9) failed at an η_D of 0.37. Other ways of improving bond of plastic ducts may be possible; however, determining a viable solution would likely involve significant alterations to construction and/or duct manufacturing practices. Thus, the role of bond will have to be taken into consideration in design procedures.

Figure 4-9: Sanded, Plastic Duct

4.3.2 Effects of Empty or Grouted Ducts

The presence or lack of grout in a duct plays a large role in influencing the compressive stress flow around the duct and consequently the level and location of tensile stresses produced that lead to reduced capacities. When an empty duct is present, compressive stresses within a member will flow from the load points around the duct to where concrete exists. Obviously, the void space within the duct is incapable of carrying any load and thus the concrete itself must essentially carry the entirety of the load. When a duct is grouted, on the other hand, the concrete does not have to endure all of the load. Grout is a stiff, load-carrying material that helps carry some of the applied compressive stress on the section. The resultant flow of stresses becomes more balanced, thus the severity of the force flow deviation and generation of tension is mitigated.

Tests conducted in this study confirmed that the use of grout improves crushing capacity. In Figure 4-10, the results of 7-in. specimens with both empty or grouted, steel or plastic ducts are compared. As evidenced, including grout increased the capacities of both plastic- and steel-ducted panels. Interestingly, the panels with empty plastic or steel ducts failed at nearly identical loads. Conversely, the panels with grouted, steel ducts showed marked improvement over their plastic counterparts. The η_D values for panels

with steel ducts improved 0.33 on average when adding grout over a value of 0.22 for an ungrouted panel. Meanwhile, the inclusion of grout increased η_D for plastic-ducted panels by only 0.15 on average over a value of 0.21 for an ungrouted panel.

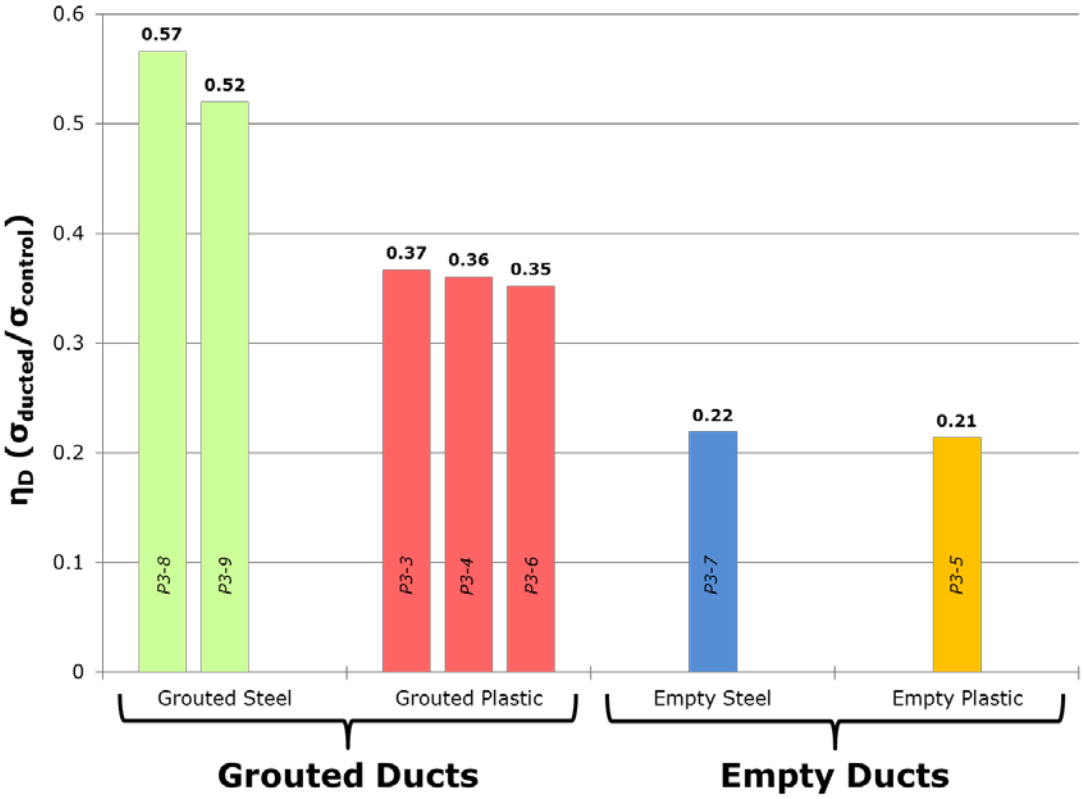

Figure 4-10: Comparison of Results for Panels with Empty or Grouted Ducts

These results suggest that the type of duct has extremely little to no relevance on the behavior of a panel with no grout. The duct has no substantial load-carrying capacity. Ultimately, the compressive capacity of a ducted panel without grout is no different than a concrete member with an empty cavity.

Whereas the type of duct is seemingly irrelevant for a panel with an empty duct, the same cannot be said of a panel with a grouted duct. The impact of duct type was addressed earlier; however, these findings reaffirm that the difference in bond

characteristics between plastic and steel ducts is consequential. It is important to recognize that load can only be transferred from one structural component to another given an appropriate means of connection between the two. In a grouted panel, the duct principally serves as a barrier between the surrounding concrete and grout. Load must be transferred from the concrete outside the duct to the grout within and thus relies on adequate bond or mechanical interlock between the duct and surrounding media. As revealed earlier, a steel duct bonds better to concrete than does a plastic duct, hence the reason why the grouted, steel-ducted panels exhibited higher capacities than their plastic-ducted counterparts. At the other end of the spectrum, without any grout in the duct, bond characteristics are meaningless and therefore so are duct types.

4.3.3 Effects of Grout Strength

The strength of grout is important in controlling the compressive stress flow around a duct. As for any composite structural member or system of individual members resisting load, the load is proportioned between components according to their relative stiffnesses. In the case of panel testing, the relative stiffnesses of the concrete and grout will largely influence the direction of stress flow and overall panel behavior. The influence of the ratio between grout and panel concrete strengths was investigated.

A single set of panels was designed to analyze the impact of varying grout strength. The goal was to test specimens with a wide range of grout-to-concrete strength ratios both above and below unity. The highest grout strengths normally obtained during this study were often not significantly higher than the 10 ksi concrete design strength. Thus, for these specimens, a low concrete strength was selected to achieve ratios of grout-to-concrete strength greater than 1.0. The measured concrete strength was 3.62 ksi. The grout strengths used were 2.3 ksi, 5.49 ksi, and 10.62 ksi resulting in grout-to-concrete strength ratios of 0.64, 1.52, and 2.93, respectively. Plastic and steel ducts were paired with each of the grout strengths.

The results of six grout strength tests are compared in Figure 4-11. As expected, increasing the grout strength (or grout-to-concrete strength ratio) boosted capacities in all

cases. For the plastic-ducted panels, increasing the grout strength from 2.3 ksi to 5.49 ksi did not improve the capacity significantly (η_D increased from 0.60 to 0.64). However, a further increase up to 10.62 ksi did generate a large rise in η_D from 0.64 to 0.81. Increasing the grout strength seemingly had a more profound effect on the steel-ducted panels. Each increase in grout strength yielded a large rise in capacity. Overall, η_D of the panel with the highest strength grout improved from 0.82 to 1.09 compared with the lowest strength grout. Moreover, some of the steel-ducted panels actually failed at higher loads than the controls. Despite these observations, the differences in η_D values may not be characteristic of behavior in all cases. More testing is needed to validate trends.

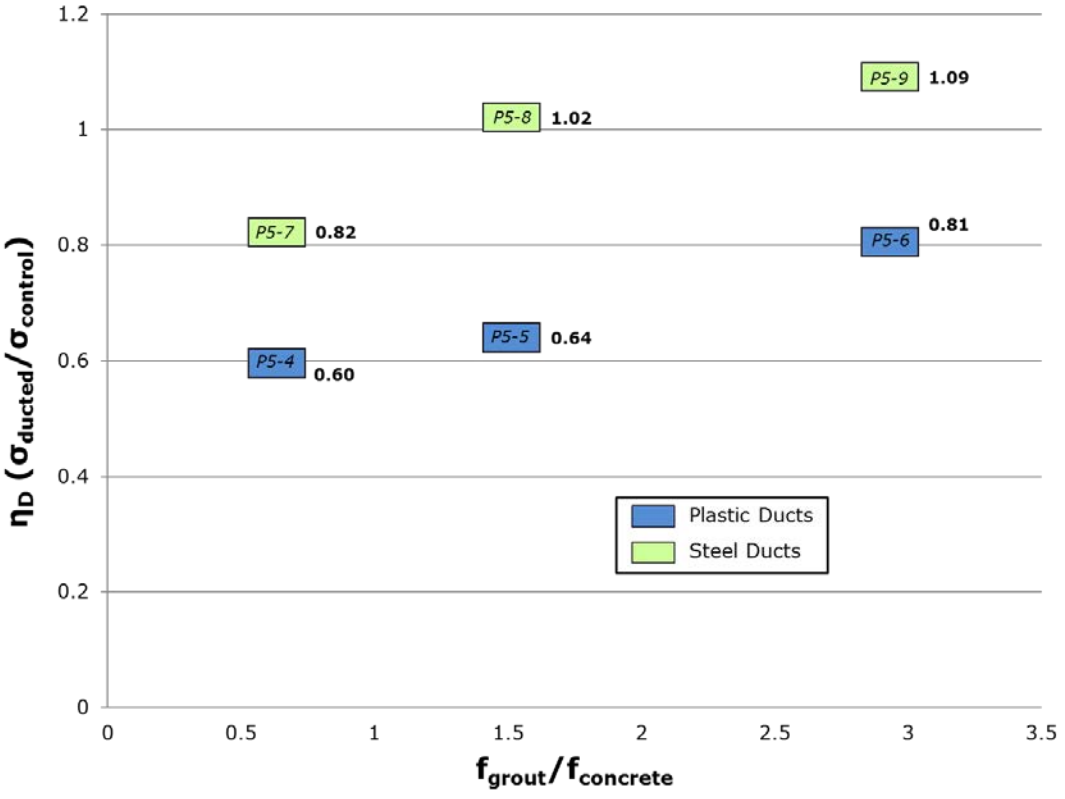

Figure 4-11: Results of Modifying Grout-to-Concrete Strength Ratio at a Low Concrete Strength

Reiterating suggestions from other researchers, as grout strength/stiffness increases, it should theoretically attract a greater portion of the compressive load assuming that the concrete strength/stiffness remains the same. Compressive stresses would tend to flow toward the grouted duct as the grout strength/stiffness increased relative to that for the concrete. Consequently, the tension generated everywhere within the panel would drop, especially in the vicinity of the duct. From equilibrium, any deviation of stress flow from a straight path would still result in the presence of tensile stresses across the thickness of the panel. However, with very strong/stiff grout, the field of tension would get shifted away from the duct.

The failure behaviors of the panels with varying grout strength confirm expectations and help explain why the plastic-ducted panels required such a high grout strength to see substantial gains in capacity while the steel-ducted panels did not. In Figure 4-12, the three steel-ducted panels are shown after failure. As grout strength increased, there was a progression from common splitting in the vicinity of the duct to a combination of splitting and diagonal cracking at the ends of the panels. The crack patterns began to mimic the flow of compressive stresses (perpendicular to tensile stresses) inward toward the grout that was stiffer than the surrounding concrete (Figure 4-13). Because of good bond between the steel ducts and concrete, this crack pattern was apparent and distinct changes in capacity were noted as the field of tension migrated away from the duct.

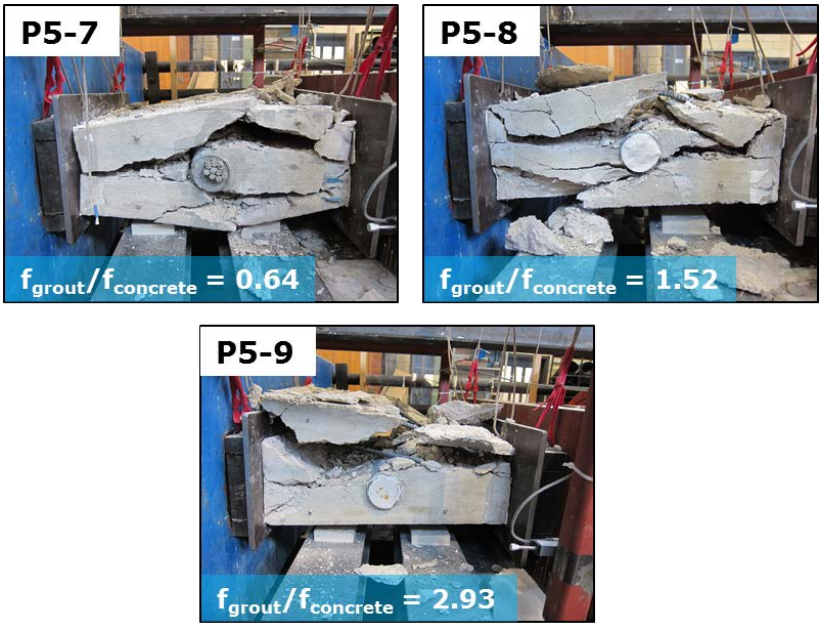

Figure 4-12: Failures of Steel-Ducted Panels with Modified Grout-to-Concrete Strength Ratios

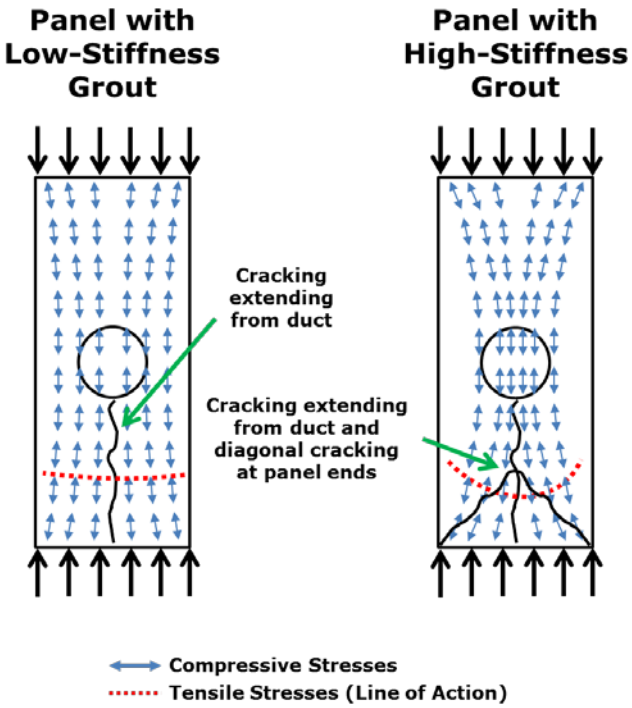

Figure 4-13: Crack Patterns in Panels with Different Grout Stiffnesses

Meanwhile, the tests with plastic ducts showed debonding even as grout strength increased. Clearly, the grout strength needed to be high enough to move the tension field far enough from the duct to delay the inevitable debonding between the duct and concrete. Hence, panels with plastic ducts did not exhibit a large increase in capacity with higher grout strength as did the panels with well-bonded, steel ducts.

The benefits of an increased grout strength are apparent; however, the level of improvement in capacities in panels described may or may not be applicable to all cases. Additional specimens were used to address the impact of a higher grout strength when using a high concrete strength (near 10 ksi). P8-7 had a 3-in. plastic duct in a 7-in. thickness, no through-thickness reinforcement, and a high grout-to-concrete strength ratio of 1.22. This panel failed with an η_D of 0.32, no improvement over the typical range of 0.35 to 0.4 seen for similar panels with a grout-to-concrete strength ratio nearly half as much (i.e. around 0.6). This data is consistent with that from the panels with a low concrete strength, where little change was seen in the capacities of plastic-ducted panels when increasing grout-to-concrete strength ratios from 0.64 to 1.52 (slightly more than two times). Other panels had varied sizes of steel ducts in 7-in. thick panels with an equal amount of through-thickness reinforcement and either regular- or high-strength grouts. Despite the presence of reinforcement and changing duct sizes, pairs of individual panels with the same ducts and different grout strengths can be compared here (Figure 4-14). For these panels, the grout-to-concrete strength ratio was adjusted from 0.55 to 1.13. This led to increases in η_D of 0.15, 0.12, and 0.19 for the panel pairs with 2.375-, 3-, and 4-in. ducts, respectively. These increases were about the same as the change in η_D of 0.20 with slightly more than double the grout-to-concrete strength ratio (from 0.64 to 1.52) for the low concrete strength, steel-ducted panels.

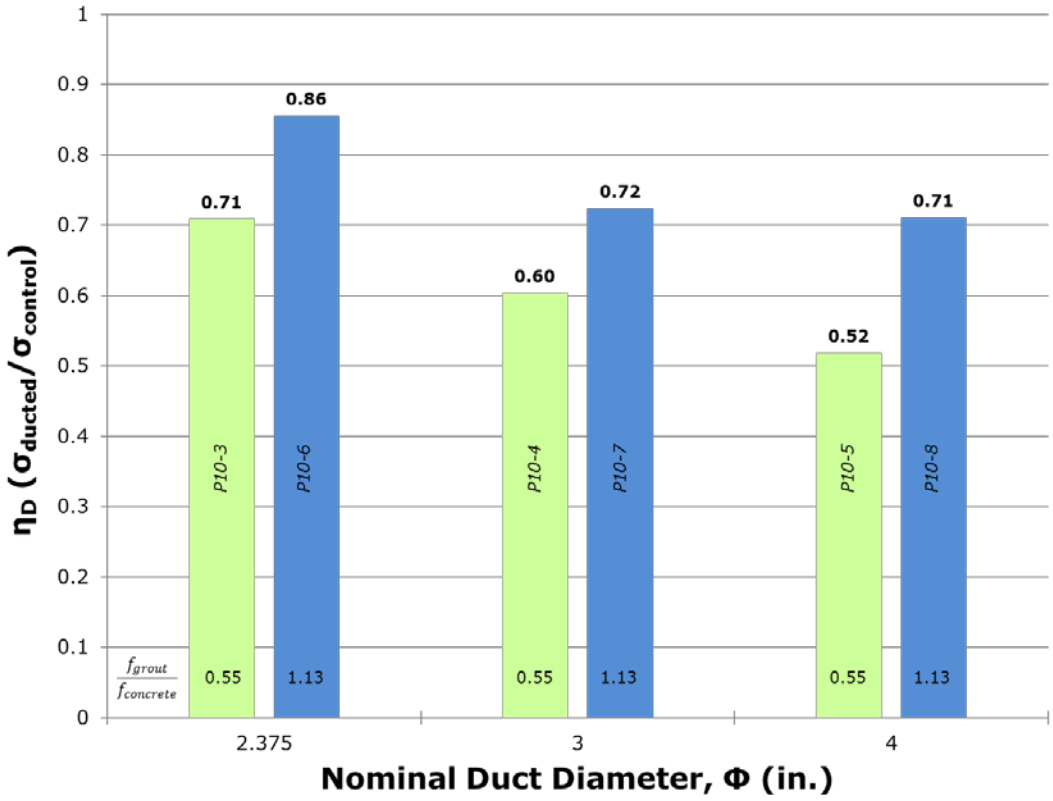

Figure 4-14: Results of Modifying Grout-to-Concrete Strength Ratio in Steel-Ducted Panels with a High Concrete Strength

No definite quantitative trend can be established from the data collected regarding grout-to-concrete strength ratio. It is not clear what type of strength increase might have resulted with grout-to-concrete strength ratios in-between those used or below the minimum ratios used. Increasing grout strength benefited the capacities of panels with either plastic or steel ducts. However, within practical limits, a higher grout strength is only beneficial for panels with steel ducts. The useful grout strength limit in this case would likely be similar to the concrete strength used (around 10 ksi), which was not typically exceeded in this study for the grouts used.

4.3.4 Effects of concrete strength

In many instances, the η_D values for panels with similar grout strengths or grout-to-concrete strength ratios but different concrete strengths were not equivalent. The η_D values tended to decrease as the compressive strength of the concrete increased. This trend was best noted in two sets of grouted test specimens. The first of these panel sets had a grout strength of 5.29 ksi with a concrete strength of 9.39 ksi (0.56 grout-to-concrete strength ratio). The second set used multiple grout strengths and a concrete strength of 3.62 ksi. One grout was 5.49 ksi, nearly equivalent to that for the first panel set. A second grout was selected to give a grout-to-concrete strength of 0.64, similar to that for the other set. In Figure 4-15, average results for the plastic- or steel-ducted panels of these two sets are compared on the basis of similar grout strength and similar grout-to-concrete strength ratio. In all cases, panels with the lower-strength concrete yielded higher η_D values.

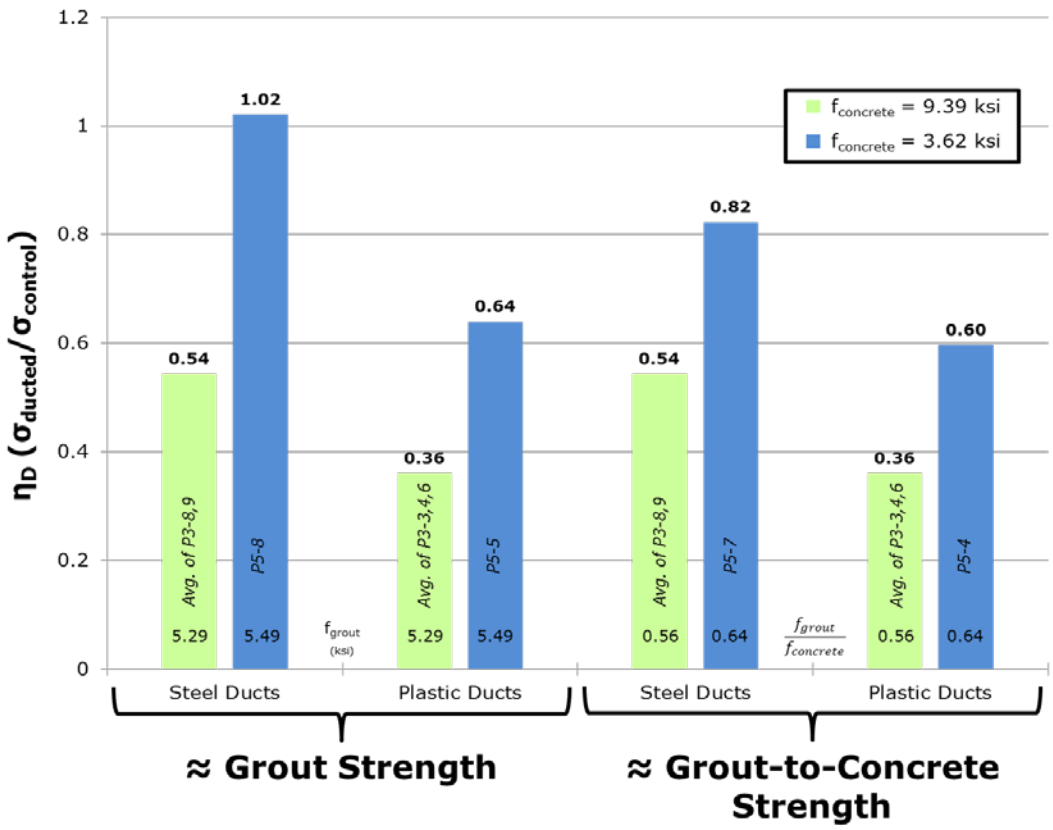

Figure 4-15: Comparison of Panels with Different Concrete Strengths

One important role of concrete strength in influencing panel capacity is that it directly correlates with stiffness which consequently affects the compressive stress deviation in a ducted panel. An increase in concrete strength (or decrease in grout-to-concrete strength ratio) will be matched with greater stiffness and more load attracted toward the concrete surrounding the duct. Thus, the stress flow deviation should be greater, and the amount of tension produced across the thickness should increase for the same applied compressive load. At the same time, concrete with a heightened strength will be capable of resisting a greater amount of tension. These two effects offset each other, although it is unclear by how much. Thus, it is not possible to claim that the rise in

tension produced is the main cause for a lower panel capacity with rising concrete strength.

The drop in η_D with increasing concrete strength can best be explained by two other essential roles played by the concrete properties. First, the concrete's compressive strength alone dictates the capacity of a solid control. Second, the concrete's tensile strength serves as the main limiting factor in the ultimate failure of a specimen with a duct. While, a higher concrete strength is known to increase both the tensile and compressive resistances of a member, the tensile capacity only increases as a function of the square root of the compressive strength. As a result, an increase in concrete strength will boost compressive capacity far more than tensile capacity. Given their reliance upon the appropriate strength properties, the control and ducted panel capacities will differ more as concrete strength rises. Hence, the ratio of the two capacities (i.e. η_D) drops.

The results of panel testing suggest that crushing capacity is not likely based on a one-to-one ratio of grout strength to concrete strength. Both are critical, and the interaction of the two is essential, but at the very least, the strength of the concrete appears to have added importance. For future analysis purposes, it may be appropriate to treat grout and concrete strength separately.

Transitioning from a low- or normal-strength concrete to a high-strength concrete only illustrates the relative impact of concrete strength. No testing was performed on typical panels (with a 3-in. duct in a 7-in. thickness) with intermediate concrete strengths. Thus, an exact quantitative trend cannot be established to fully capture the effects of concrete strength for a complete range of possible strengths. It is unknown whether η_D gradually decreases with increasing concrete strength or abruptly changes at some particular strength that defines a difference between a "high-capacity" or "low-capacity" behavior. In any case, large differences in concrete strength have a profound impact on panel capacity.

The effect of concrete strength is not as clear-cut when working with strengths around 10 ksi and small differences of less than about 2 ksi. Results for a set of 7-in. thick plastic- and steel-ducted panels with concrete between 8.0 ksi and 9.0 ksi were

compared with a set of similar panels with concrete between 9.0 ksi and 10.0 ksi (Figure 4-16). The differences in concrete strength between the sets were small (1.22 ksi for plastic-ducted panels and 0.79 ksi for steel-ducted panels). The grout-to-concrete strength ratios were similar. The η_D values for panels with the same duct type were within a range of 0.05. Given the inherent variability of concrete and experimental test results, these values are not different enough to establish any particular relationship based on material strength.

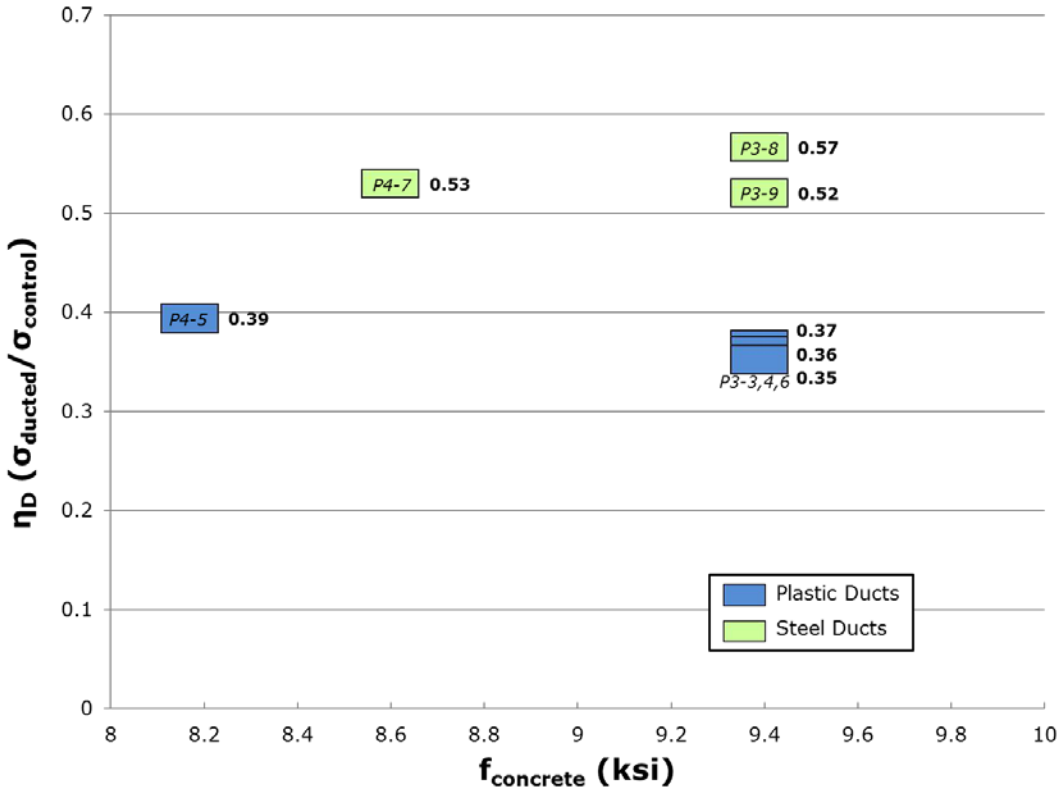

Figure 4-16: Effect of Small Changes in Concrete Strength

4.3.5 Duct Diameter-to-Thickness Ratio

All code provisions related to the web width reduction factor take into account the ratio of the duct diameter to the girder web width (or panel thickness), δ, as the primary variable. Despite the emphasis placed on this value, changing δ was not a primary test parameter in this study. A compendium of prior panel and prism test results exists from which numerous conclusions have been drawn about the importance of δ. Tests with varying values of δ in this study were conducted for two reasons: 1) to verify the trend of declining compressive capacity with an increasing δ, and 2) to evaluate the limiting maximum δ of 0.4 in the AASHTO LRFD specifications.

It is important to note that δ was only varied in 7-in. thick panels. The commentary provided should be applicable to any situation in which panels of the same thickness are compared. Later in this chapter, the special importance of panel thickness will be covered. Details will be provided explaining why panels with differing values of δ and non-equivalent thicknesses cannot be compared on the same basis outlined here.

The quantity δ controls the deviation angle of compressive stress flow around the duct as influenced by the grout. Obviously, given the same thickness and other things being equal including grout and concrete strengths, a larger δ will give way to a greater stress deviation and more tension. This ultimately leads to a larger drop in load-carrying capacity. This behavior is illustrated in Figure 4-17.

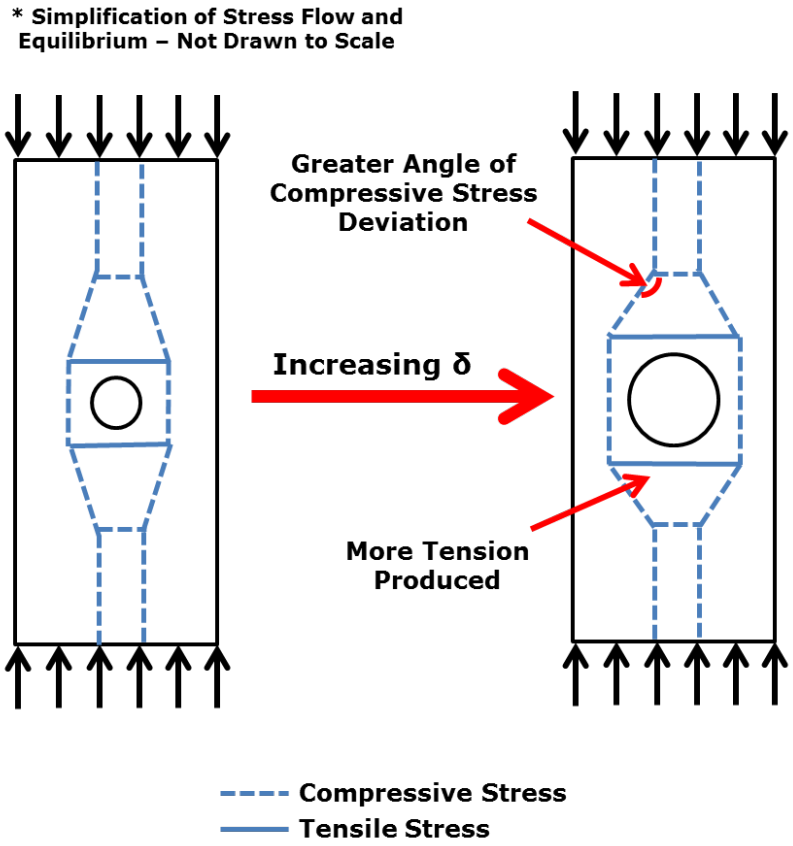

Figure 4-17: Behavior of Panels with Increasing δ

The 7-in. thick plastic-ducted panels with 2.375-, 3-, or 3.375-in. duct diameters, no through-thickness reinforcement, high-strength concrete, and regular-strength grout are considered. The nominal values of δ are 0.34, 0.43, and 0.48. The measured values of δ, material strengths, and failure information for these panels are summarized in Table 4-1. Slight differences in concrete and grout strengths exist but may be considered inconsequential for this discussion.

Table 4-1: Results of Plastic-Ducted Panels with Varying δ

Specimen	$f_{concrete}$ (ksi)	f_{grout} (ksi)	Φ (in.)	Nominal δ	Measured δ	η_D
P7-8	10.6	4.9	2.375	0.34	0.37	0.43
P3-3	9.4	5.3	3	0.43	0.43	0.37
P3-4	9.4	5.3	3	0.43	0.43	0.36
P3-6	9.4	5.3	3	0.43	0.43	0.35
P4-5	8.2	4.7	3	0.43	0.42	0.39
P9-3	10.2	6.3	3	0.43	0.43	0.35
P8-3	11.2	6.0	3.375	0.48	0.48	0.28

The reported test results show a decline in capacity with increased δ. With an increase in δ of about 0.1, the panels with 3-in. ducts on average show a decline in η_D of about 0.07 compared to that for the panel with the 2.375-in. duct. For a panel with a 3.375-in. duct, there is a similar decline in η_D. This trend of η_D decreasing at an increasing rate with respect to δ follows the trend from previous research (Figure 4-18).

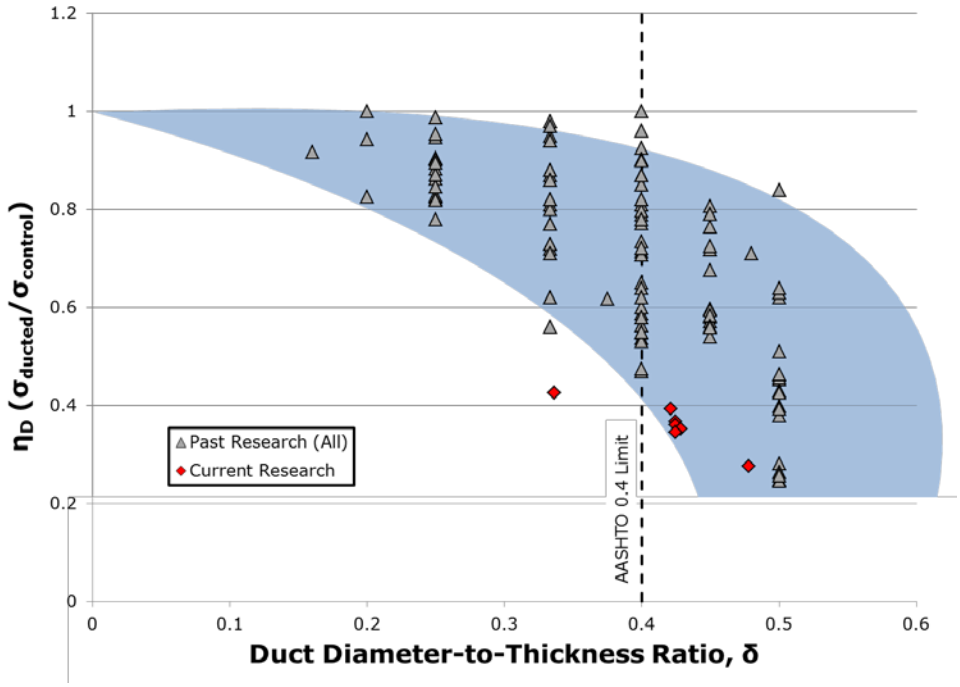

Figure 4-18: Relationship Between η_D and δ

Based on the few panel test results obtained from this study, the 0.4 limit may or may not be considered appropriate as shown in Figure 4-18. In this case, a change in the limit would depend on several factors. Given the exceedingly low values of η_D for all panels with plastic ducts, it is difficult to justify a 7-in. thick girder with a 3-in. duct (δ = 0.42) performs significantly better than one with a 2.375 in. duct (δ = 0.34). In other words, permitting an η_D of around 0.45 (δ = 0.34) is not likely to be considered much improvement over an η_D of 0.4 (δ = 0.42). On the other hand, tightening this limit (e.g. changing the limit to 0.3 or less) would be far too restrictive for girder construction, as web widths would have to increase given the same required duct size for post-tensioning. Such a provision would likely negate some of the benefits of using spliced girders. Further evaluation of this limit is necessary and should be conducted using results from full-scale girder shear tests.

It should also be noted that the tests were conducted in this study looking at different values of δ when using steel ducts as well. A set of 7-in. panels utilized steel ducts with 2.375-, 3- and 4-in. diameters to yield nominal values of δ of 0.34, 0.43, and 0.57, respectively. Two panels using each duct size were fabricated, with one including regular-strength grout and the other high-strength grout. Each panel incorporated through-thickness reinforcement. Consequently, there are no unreinforced baselines with which to compare to plastic-ducted panels, and using the reinforced panels to investigate the 0.4 limit is not feasible. The results of the reinforced tests are used, however, to confirm basic trends in specimen capacity.

Figure 4-19 shows the results of the reinforced, steel-ducted panel tests. As anticipated, given the same grout strength, there is a downward trend in capacity with increasing δ. With so limited a number of data points, it is not possible to claim this trend to be significant.

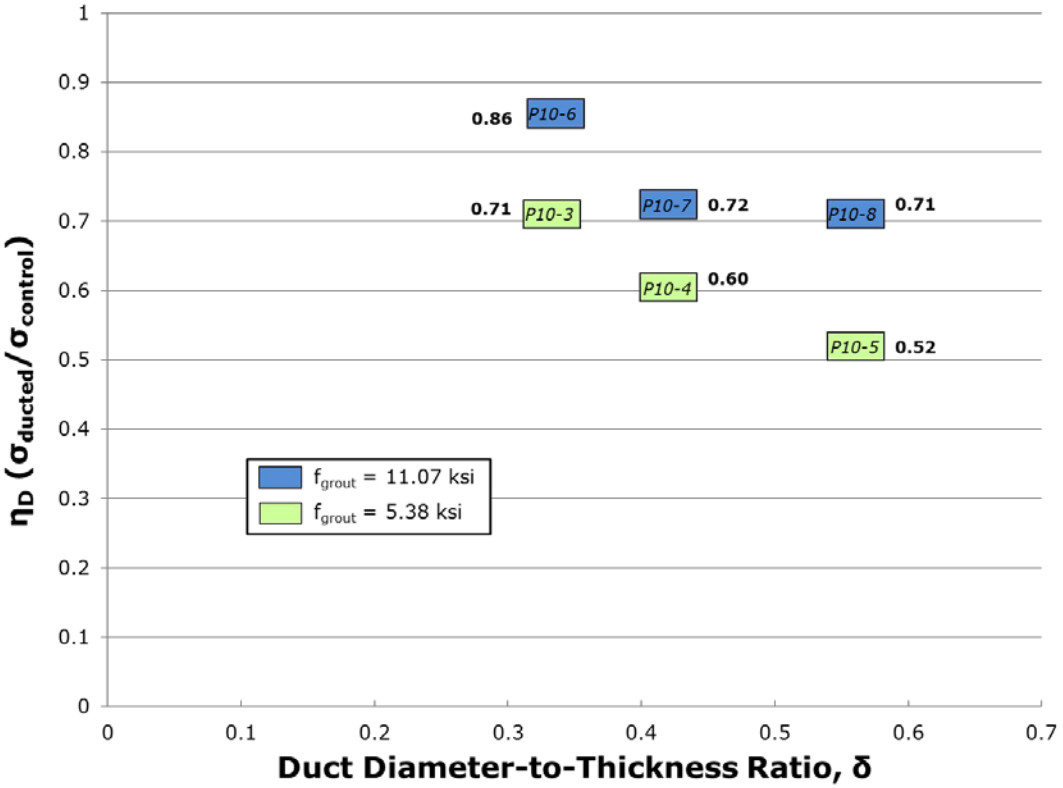

Figure 4-19: Results of Steel-Ducted Panels with Varying δ and Grout Strength

4.3.6 Effects of through-thickness reinforcement

A large number of panel tests were conducted over the course of this study to examine the potential benefits of incorporating reinforcement to resist tension generated across the panel thickness.

The deviation of compressive stress flow through a ducted web results in the generation of internally equilibrating tensile stresses forming across the width of the web. This can be seen from a simple illustration of the compressive stress flow around a duct or using strut and tie modeling. Obviously, the amount of tension introduced depends on the extent of the compressive stress flow deviation. By geometry and recognition of equilibrium, an increased angle of stress deviation results in higher tensile stresses.

Ultimately, tension that is produced must be resisted by the concrete, the grout (given appropriate bond with the duct and between the duct and the concrete), and any reinforcement in the direction of the tensile stresses (across the thickness). Concrete and grout are weak in tension. In girders, a slight amount of reinforcement is provided at locations through the web to support the ducts, but not to necessarily resist this tension. Due to the way the ducts were supported in the panels for casting, bar supports were not necessary. Adding additional reinforcement for strength purposes was not originally considered or expected to even be useful.

The benefits of including through-thickness reinforcement in the panels and the need to pursue additional investigation were only realized due to a construction convenience. During initial panel fabrication, construction was found to be quite difficult because there was no way to easily keep the two mats of primary mesh reinforcement vertically level or parallel to one another for casting. To stabilize the mats of reinforcement, they were initially tied together using short, 4-in. pieces of #2 reinforcing bars located approximately 1.5-in. away from the edge of the panel (attached to the outer horizontal bars) in each corner (Figure 4-20). In this case, the reinforcement was secured to stay in place for casting. As described before, testing of the first set of panels commenced with results found to be consistent with those obtained by Muttoni et al. (2006). Thus, these #2 bars did not seemingly affect capacity.

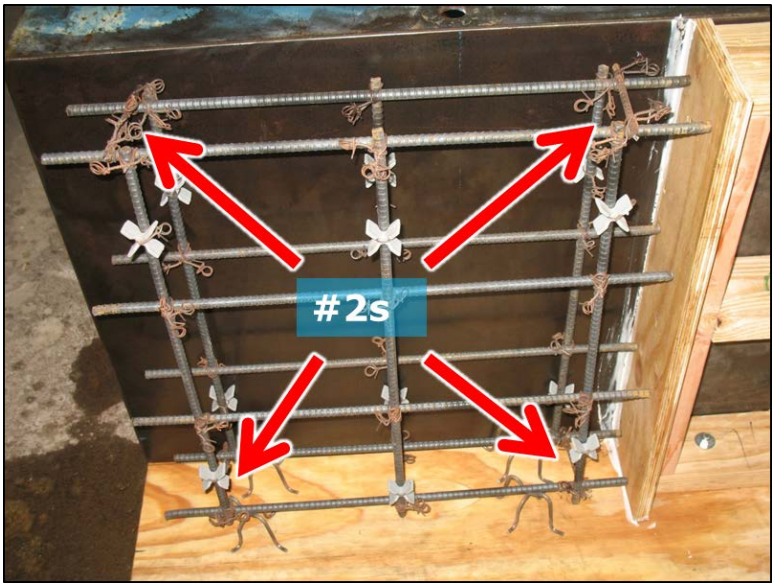

Figure 4-20: Incorporation of #2 Bars in First Panel Set

For the second set of panels (first set of 7-in. thick panels), the #2 bars were used again, but this time they were moved to approximately 9-in. away from the panel edge (or tied to the middle horizontal bars). For construction purposes, this change was helpful and better stabilized the primary reinforcement.

For the third and future sets of panels, the #2 construction bars through the thickness of the panel were omitted. Instead, #2 bars were inserted between the panel spacer forms in the same direction as the horizontal bars of the panel (Figure 4-21). The reinforcement layers were then tied to these #2 bars. These bars were only used for construction purposes in a similar manner as the horizontal bars in the mats of primary reinforcement. These bars were perpendicular to the direction of applied loading on the panels and thus were not intended or expected to provide any means of additional reinforcement to improve compressive capacities.

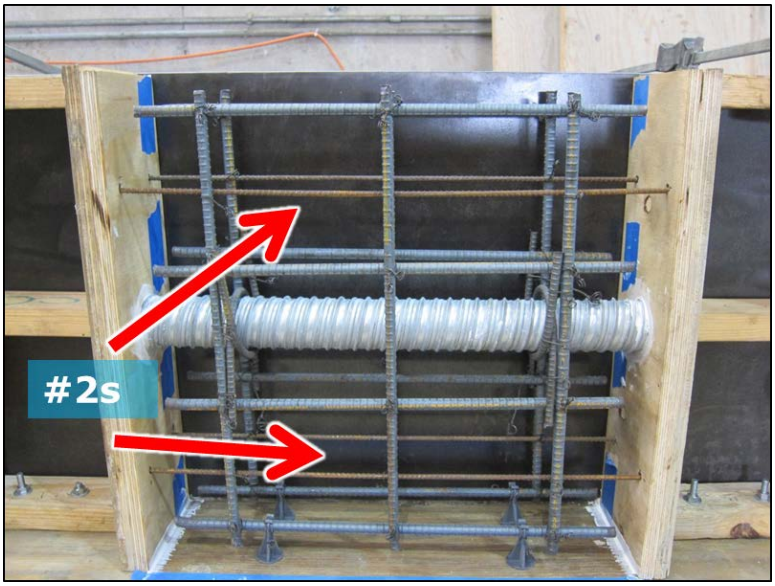

Figure 4-21: Incorporation of #2 Bars in Later Panel Sets

The third set of panels was exactly the same as the second set of panels except for the way in which the #2 bars were used. These specimens were intended to verify the results from the second set of panels. Further, the change in the "secondary" reinforcement was not expected to alter results. Figure 4-22 provides a side-by-side comparison of the results for each of the panels of the second and third sets.

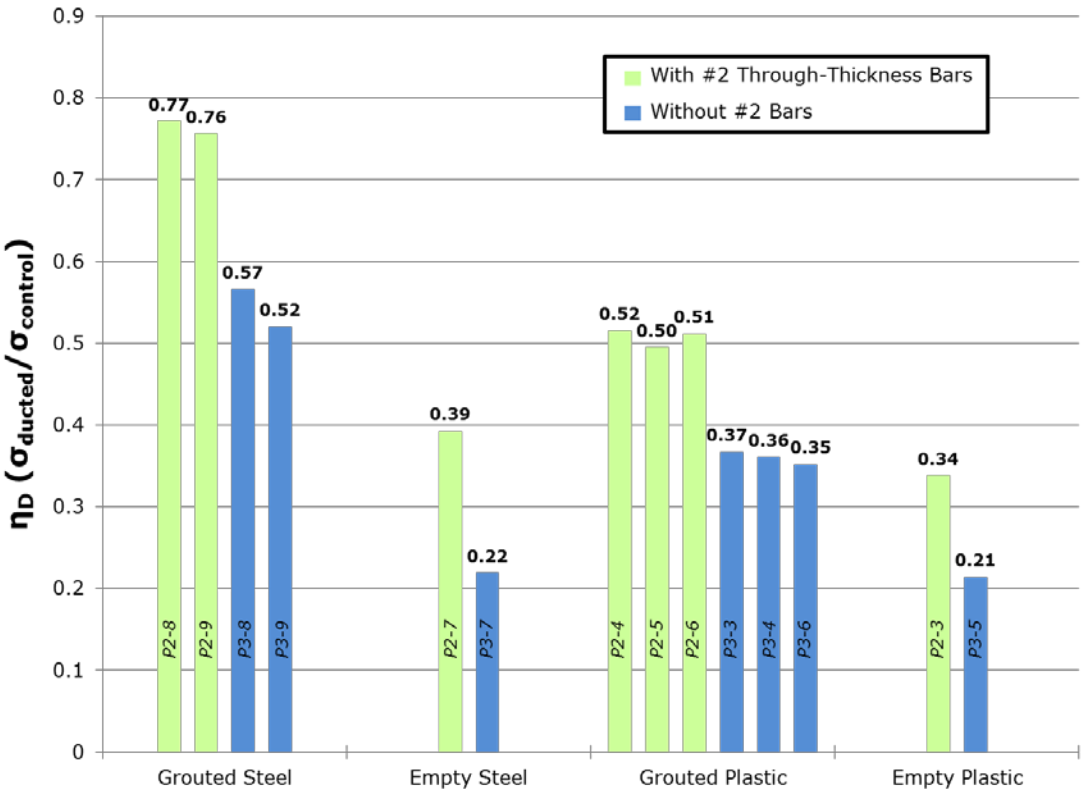

Figure 4-22: Comparison of Panels With or Without #2 Through-Thickness Bars

Unexpectedly, the results from the third set of panels with no through-thickness reinforcement were lower than those from the second set of panels. Upon further inspection, it was discovered that the small #2 bars connecting the layers of panel reinforcement were indeed improving the panel capacities. The #2 bars in one of the panels with a grouted, plastic duct yielded and fractured during testing (Figure 4-23). Despite the short length of these bars, they were able to develop tensile forces and allow the panels to reach higher failure loads.

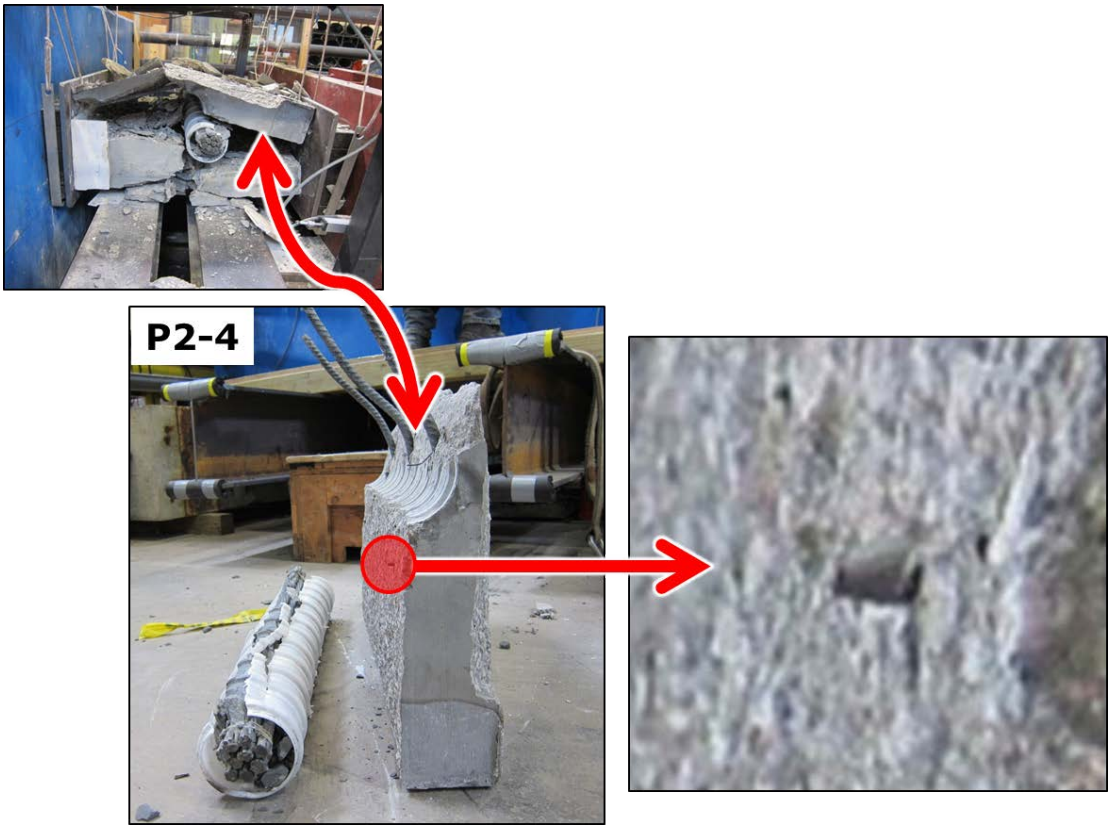

Figure 4-23: Necking and Fracture of a #2 Bar Placed Through the Thickness

From these results, it became apparent that reinforcement placed through the thickness of the panel at even a few discrete locations and close enough to the duct could resist tensile forces and improve compressive capacity. Regardless of how inconsequential the #2 bars might have seemed upon first inspection, this finding aligned with general ideas presented in the literature. As discussed in Chapter 2, Chitnuyanondh (1976) showed improvements in the compressive capacity of prisms when adding spiral reinforcement around cavities. In that case, reinforcement extending through the thickness of the prisms served to resist a splitting failure. Additionally, Eurocode 2 (2004) provisions and Muttoni, Burdet, and Hars (2006) entertained the idea of using transverse reinforcement to resist tensile splitting. Chitnuyanondh, however, was the only researcher to have previously run experiments on specimens with through-thickness

reinforcement to prove such usefulness. The results of the panel tests with and without #2 bars verified Chitnuyanondh's findings.

Many of the subsequent panel tests in this study were performed to better understand the impact of using through-thickness reinforcement and maximize benefits from doing so. Experiments were conducted looking at the best combinations of various amounts, locations, and shapes of reinforcing bars that could be used as through-thickness reinforcement to boost compressive capacity the most.

4.3.6.1 General Behavior of Panels With and Without Through-Thickness Reinforcement

It holds that without any reinforcement provided through the thickness of a panel in the direction of the tension, the panel should exhibit a tensile, splitting failure at a load much lower than that of the control or even a similar ducted panel with reinforcement. Indeed, ducted panels without any through-thickness reinforcement always failed by means of tensile splitting. This failure mechanism was readily observed during testing and from post-failure images. Failure was initiated by cracking at mid-thickness of a panel next to the duct. Cracking was parallel to the direction of loading (or perpendicular to the direction of tension). In some instances, the crack would form, accompanied by a slight decline in load. Load could increase, but usually never higher than the previous peak. This behavior was more often seen for panels with lower concrete strengths. In most instances, however, the panels failed instantly upon initial cracking. This was especially true of high-strength panels that had large loads applied. A failed panel usually exhibited a large crack directly through its center with two halves of the panel separated from each other.

Ducted panels with through-thickness reinforcement often failed in a different manner. The presence of the reinforcement allowed the panel as a whole to resist tension as well as provide a mechanical restraint against the panel completely splitting in half. During loading, these panels often exhibited tensile cracking (again usually initiated near the duct and near mid-thickness), but the panels did not instantly fail. Instead, the panels

were able to continue picking up load. Ultimately, the panel failures were more indicative of a crushing failure, with partially crushed ducts, cracked or crumbled grout and numerous small cracks around the duct. Despite more crushing failures, panels with through-thickness reinforcement still failed at loads much lower than those of solid controls. The panels were still negatively impacted by the presence of tension. Tensile cracks, including those at the center of the panels, were observed. Other cracks formed near the loaded ends, where no through-thickness reinforcement was placed.

4.3.6.2 Effects of Reinforcement Amounts/Size

The consequences of altering the amount or location of through-thickness reinforcement along a length of duct were investigated. The ultimate goal of this portion of the study was to determine the best locations for the through-thickness reinforcement for ease of construction and to attain the greatest benefit in counteracting tensile splitting.

With the exception of the aforementioned use of #2 bars, all through-thickness reinforcement used in this study consisted of #3 bars. Hence, individual bar size was not modified. This choice primarily stemmed from the inability to tightly bend larger bars or place them in an already congested, narrow space.

For tests considering variation in reinforcement amounts, only one reinforcement configuration was used. This standard (‘normal’) layout consisted of two pieces of hairpin-bent reinforcement (with a bend diameter of 4-in.) hooked around the duct in either direction of loading located at discrete points along the duct’s length (Figure 4-24). The bent portion of each individual piece was meant to resist tension through the panel thickness on a single side of the duct. In no case described here were multiple pieces of reinforcement bundled on the same side of the duct to potentially increase the amount of reinforcement at a single location. The potential benefits of bundling multiple bars on the same side of a duct will be addressed later.

Figure 4-24: 'Normal' Hairpin Configuration

Each piece of reinforcement was placed such that the portion resisting tension was located at a specified distance away from the duct. The importance of the proximity of each piece of through-thickness reinforcement to the duct will be covered in more detail in the next section. For clarity, the results of only those panels with reinforcement placed at identical distances from the duct will be compared. The three distances used for panels will be referred to as 'close', 'midway,' and 'far' to reflect location; actual measurements will be provided later.

Four different combinations of reinforcing locations along the duct were considered (Figure 4-25). The first two combinations consisted of sets of bars tied to either all three or only the outer two primary, vertical reinforcing bars. These layouts were considered to reflect likely use of through-thickness reinforcement attached to each or only every other stirrup in a girder. One set of panels incorporated both layouts with bars at all three locations from the duct. A third layout consisted of only one set of bars connected to the middle vertical reinforcing bar. In P7-6, this scheme was used with bars located 'close' to the duct to attain a lower bound capacity in the presence of through-thickness reinforcement. The final combination of locations placed five sets of bars along

the length of the duct, equally spaced at 4-in. Three sets were tied to the vertical reinforcing bars and the other two were tied in-between to horizontal reinforcing bars where possible. It should be noted, of course, that this configuration is impractical for actual girders which lack horizontal reinforcement and where through-thickness reinforcement can only be tied to stirrups. The use of so many sets of bars was only done to determine an upper bound value on capacity and reflect behavior of continuous reinforcement around a duct (i.e. a spiral). The use of many discrete reinforcing locations was an alternative to using spiral reinforcement, which would have been very difficult to support and place within the layers of primary reinforcement. In P4-3 and P4-4, five sets of bars located either 'far' from or 'close' to the duct were used.

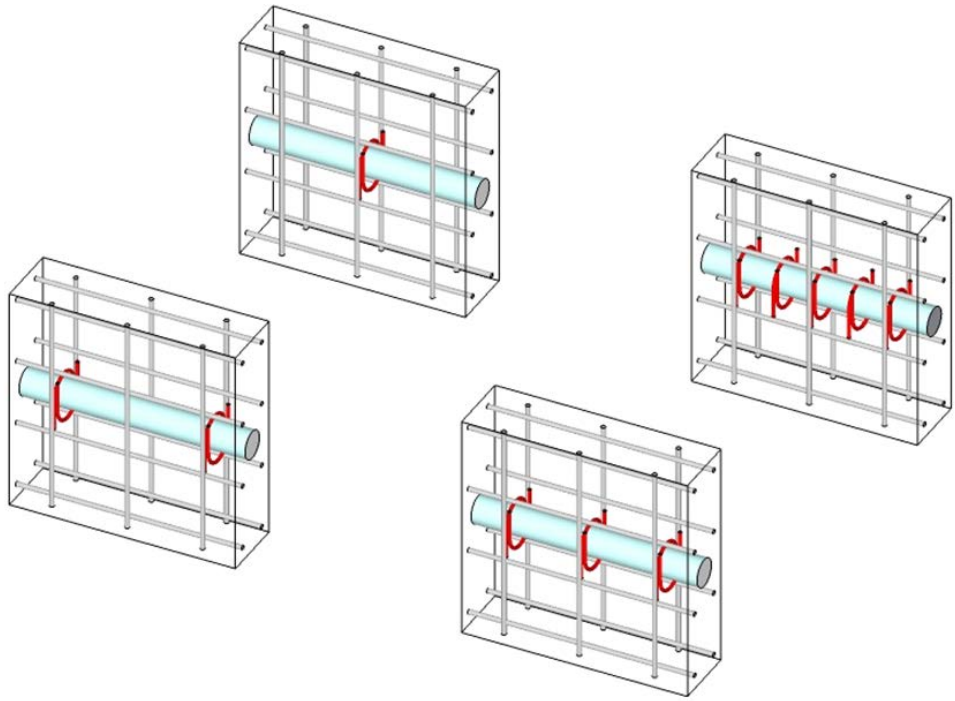

Figure 4-25: Four Combinations of Locations for Placing Through-Thickness Reinforcement Along the Duct Length

Results of tests with through-thickness reinforcement at different locations are compared in Figure 4-26 given reinforcement located at the same distance from the duct. These tests were conducted on 7-in. panels with 3-in. plastic ducts and normal-strength grout. Results from different sets are compared for similar concrete and grout properties.

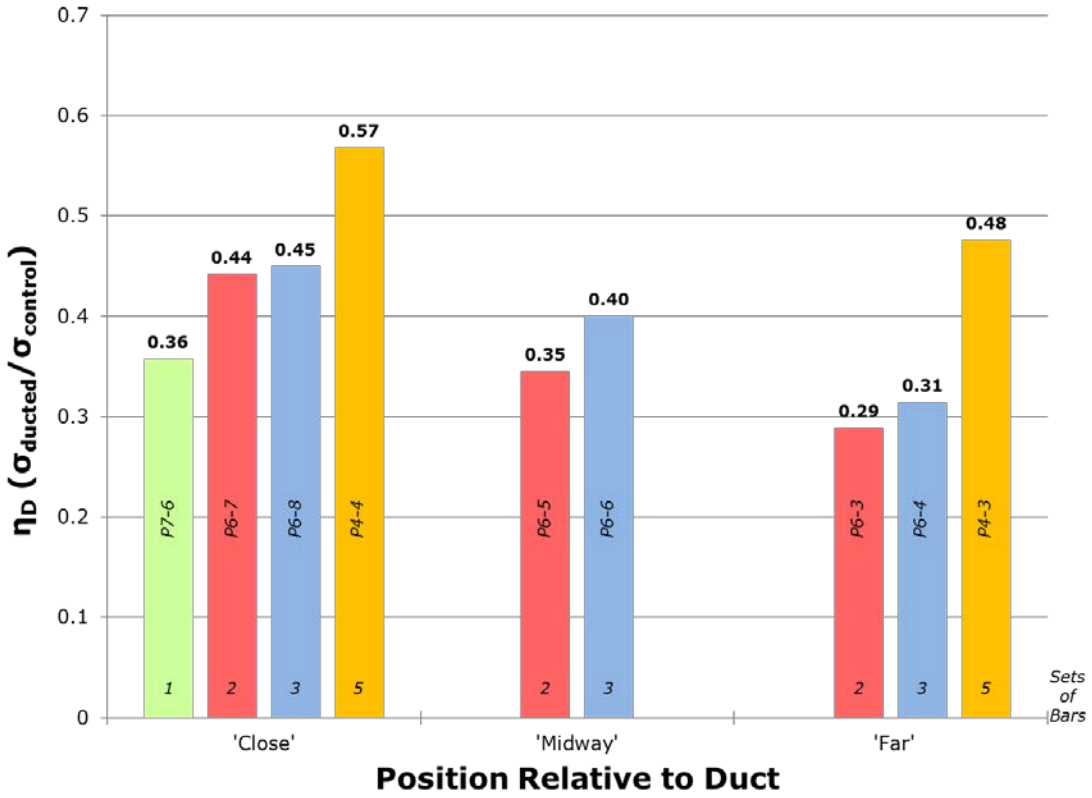

Figure 4-26: Comparison of Results for Panels with Varied Amounts of Through-Thickness Reinforcement

Regardless of how far the reinforcement was from a duct, there was little difference between reinforcing two or three locations. In no case did η_D increase by more than 0.05. As such, a change in η_D was within normal test result variation. It cannot be conclusively stated that adding through-thickness reinforcement at every vertical bar (or stirrup) location is any better than at alternating locations. The use of two or three sets of

bars, however, was clearly advantageous over using only one set in the middle of a panel. P7-6, with only one set of bars, failed at a load much lower than its counterparts, and more importantly with an η_D of 0.36, exactly in the typical range of non-reinforced 7-in. panels with 3-in. plastic ducts. Reinforcement in this case was not distributed well enough to resist tensile splitting across the entire cross section of the specimen.

The specimens with five sets of through-thickness reinforcement showed the most interesting behavior of these tests. Numerically, P4-3 showed an increase in η_D of 0.18 compared to the average η_D of the panels with two or three sets of bars at the 'far' position. P4-4 showed an increase in η_D of 0.12 compared to the average η_D of the panels with two or three sets of bars at the 'close' position. These boosts in capacity were coupled with a change in failure behavior. Rather than just split near mid-thickness, hold together, and then crack at the sides at the level of the duct, the panels crushed with some increased spalling on the sides near the duct after initial cracking (Figure 4-27). Evidently, the large percentage of through-thickness reinforcement was adequate in resisting splitting and keeping the panel stitched together so that it could crush rather than fail via eccentric loading of two slender halves of the original whole.

Figure 4-27: Failures of Panels with Five Sets of Hairpins

The most intriguing finding here was the capacity of the panel with the five 'close' sets of bars (P4-4). This panel failed with an η_D of 0.57. If one were to estimate the pure uniaxial compressive capacity of a panel based only on the net concrete section at the location of the duct (i.e. 4-in. out of 7-in. total with a 3-in. duct), the resulting capacity would be exactly 57% (or 4/7) of the control capacity. As has been previously discussed, panels with plastic ducts exhibit debonding between the concrete and duct resulting in an inability for load to continue to be carried by the grout. In this event, the maximum feasible capacity of a panel would only be that for the net concrete section at the level of the duct. Thus, it appears that the goal to ascertain the upper bound capacity for panels with plastic ducts and through-thickness reinforcement was indeed achieved.

The effects of differing through-thickness reinforcement locations along the length of the duct were not considered for panels with steel ducts, ducts of diameters other than 3-in., or when using reinforcement layouts other than the 'normal' one. Thus, for nearly all tests including through-thickness reinforcement following those described in this section, sets of bars were only used at the outer two vertical bar locations. It was assumed that in these cases, including an additional set of bars in the middle of a panel would not be of any vital importance, as determined before.

4.3.6.3 Effects of Reinforcement Location Relative to a Duct

The importance of the proximity of through-thickness reinforcement to the duct (in the direction of loading) was considered. Typically, any reinforcement embedded in the thickness of a girder web to support the duct would be in contact with the duct. Different reinforcing distances were utilized in the panel tests to capture behavior in the cases of reinforcement placed against the duct, placed near locations of the #2 bars from the second set of panels, and at other locations. The primary goal was to determine if reinforcement proximity mattered when considering the location of tensile stresses due to compressive stress deviation.

In the sixth set of panels, capacities when using through-thickness reinforcement at different distances away from the duct were compared. These panels included only

3-in. plastic ducts, normal-strength grout, and used the ‘normal’ hairpin layout. Four distances were chosen as measured from the interior surface of a duct to the surface of a through-thickness bar at the interior of its bend. These included bars placed against the duct and bars at the aforementioned ‘close,’ ‘midway,’ and ‘far’ positions. In Figure 4-28, the latter three scenarios and images of each during construction are detailed. Bars in the ‘close’ position were placed to match the locations of through-thickness #2 bars from the second panel set. Bars in the ‘far’ position were placed because more reinforcement could only be easily added to the panels at the specified location with #2 support bars in the way. Bars in the midway position were placed exactly in-between those in the ‘close’ and ‘far’ spots.

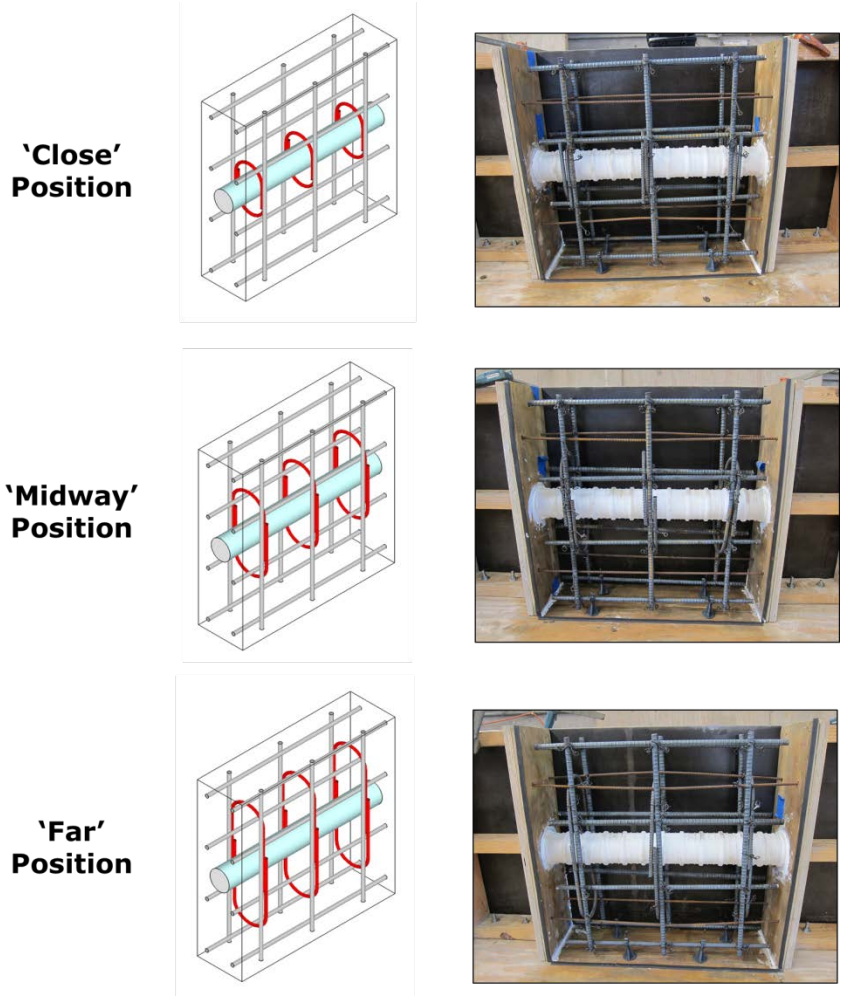

Figure 4-28: Relative Placements of Through-Thickness Reinforcement to the Duct

In Figure 4-29, the results of the tests based on distance between the duct and reinforcement are shown. Two separate sets of data are shown depending on whether two or three sets of reinforcement were used along the length of duct. In either case, there was an upward trend in capacity as through-thickness reinforcement was moved closer toward the duct. The η_D values for panels with reinforcement 'far' or 'midway' from the duct were no higher than those for panels without reinforcement. No significant change was noted in capacity when placing the reinforcement against the duct or just slightly away

from it in the ‘close’ position. Overall, these results imply that through-thickness reinforcement will have an impact only if placed near the duct.

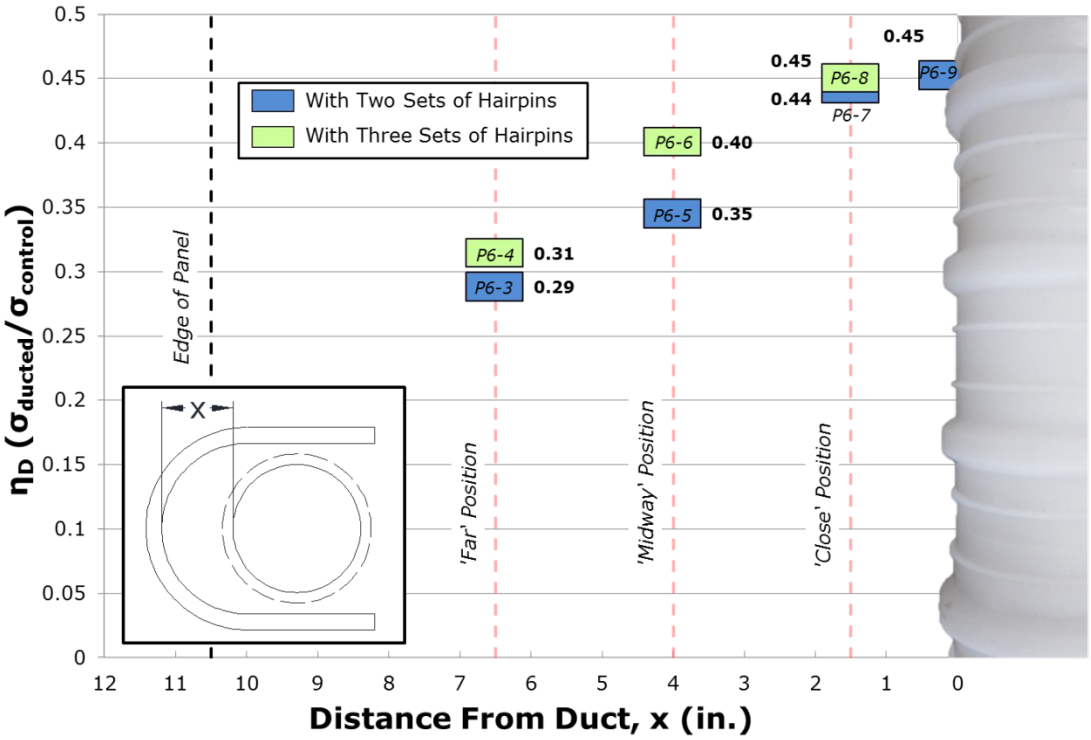

Figure 4-29: Results of Panels with Hairpins Located Various Distances From Duct

The failure behaviors of the panels discussed were similar but illustrate some slight differences. As for all reinforced panels, mid-thickness cracking occurred, but load increased without the two halves of a panel suddenly separating. For the panels with bars located ‘far’ from the duct, failure involved some crushing of the concrete around the ducts and of the ducts themselves along with cracking at the sides of the panel near the duct (Figure 4-30). This behavior was similar for panels with bars at the ‘midway’ position. The presence of cracking near the duct verified general panel behavior as outlined by Chitnuyanondh (1976). At splitting, a panel acts as two separate, eccentrically-loaded halves failing in combined axial load and flexure. Half of a panel

bending outward would produce tension at the outer fibers with the greatest tensile stress located exactly in the middle near the duct. The presence of through-thickness reinforcement enabled this cracking to be observed by holding the panel together whereas in panels without this reinforcement, the explosiveness of an unrestrained splitting failure precluded visual confirmation of such a secondary failure mechanism. Meanwhile, panels with bars 'close' or against the duct exhibited increased crushing behavior compared to those with bars placed farther from the duct (Figure 4-31).

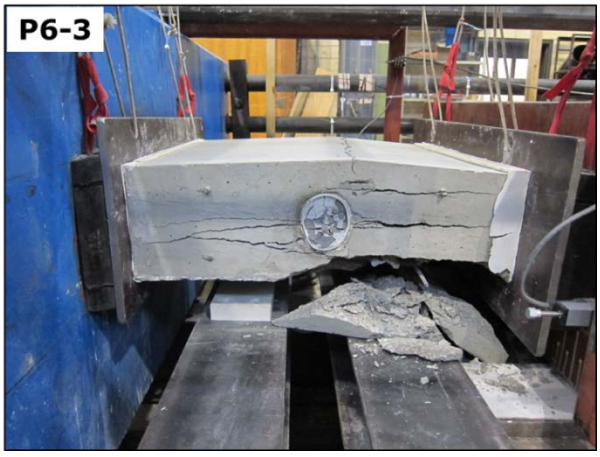

Figure 4-30: Failure of Reinforced Panel with Cracking at Level of Duct

Figure 4-31: Failure of Panel with Reinforcement Near the Duct

These results suggest that the greatest use of through-thickness reinforcement may not be to prevent cracking, but to mechanically hold the panel together after initial cracking so that it continues to carry compressive loads. In Figure 4-32, the basic differences in the progression of failure for panels with or without through-thickness reinforcement are depicted. As has been described, a panel with no through-thickness reinforcement splits in half upon failure. Reinforcement across the thickness will resist tension, but once the panel splits, compressive stresses should flow directly into the two panel halves rather than deviate around the duct and develop more tension. In other words, the tension causing the initial splitting crack should largely dissipate rather than increase after the crack forms. Regardless, the tensile resistance provided by the reinforcement will keep the panel from experiencing a brittle failure and allow it to continue carrying load. Theoretically, the two slender halves of the panel are loaded eccentrically, and will ultimately fail by a combination of axial load and flexure with cracking seen at panel sides near the duct. Any reinforcement through the thickness should, at this point, work to restrain each panel half from flexing outward. Ideally, the reinforcement is most efficient if located near the point of maximum flexure (i.e. the middle of the panel near the duct). In such a case, more load can be sustained.

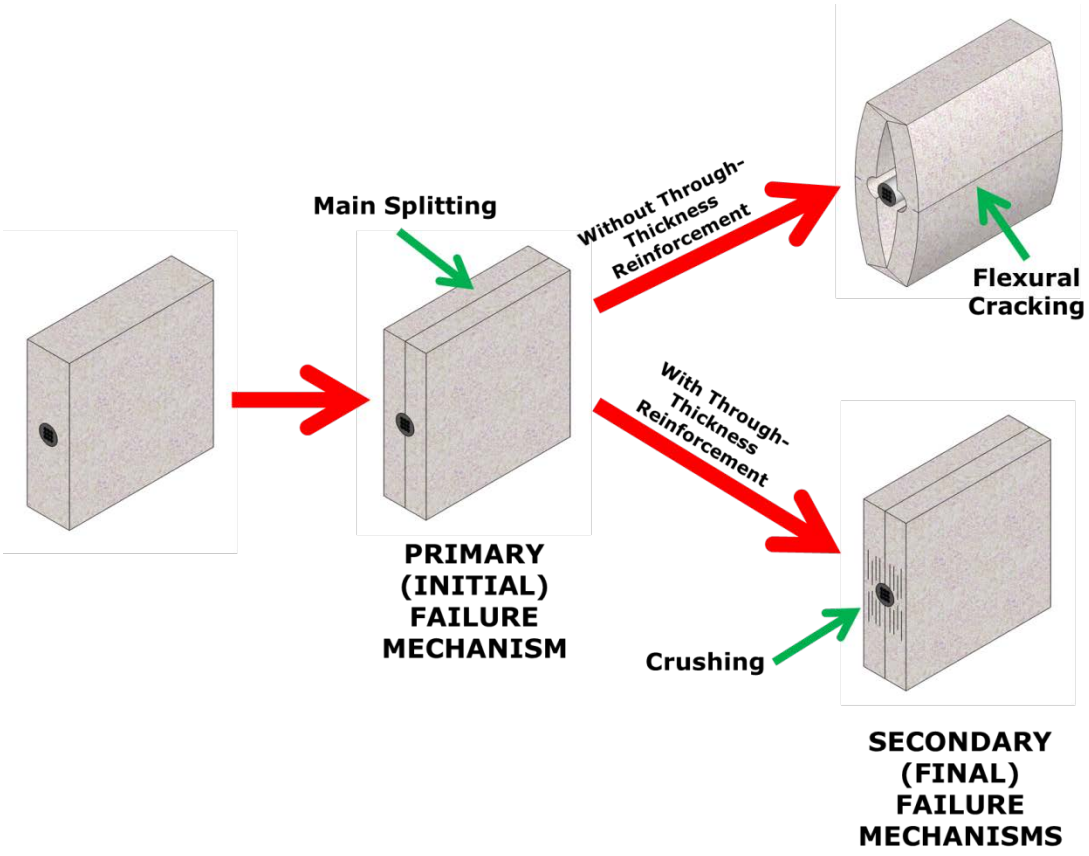

Figure 4-32: Progression of Failure for Panels With or Without Through-Thickness Reinforcement

Two additional panels were cast to understand the relationship between capacity and location of reinforcing from the duct. These panels (P8-8 and P8-9) were fabricated with 3-in. plastic ducts, but they were filled with high-strength grout. This was done to see how through-thickness reinforcement would help if the stress flow deviation significantly changed, and thus the generated tension field were shifted further from the duct. In P8-8, two sets of 'normal' through-thickness bars at the 'close' position were used. P8-8 failed at a load of 743 kips (η_D = 0.45). P8-9 included two sets of bars at the 'far' position, and it failed at 758 kips (η_D = 0.46). Clearly, the distance between the bars and duct did not matter when using a stronger grout. Placing bars closer to where the tension field was located was not advantageous in this case. In fact, the panels failed with

the same values of η_D as did previous panels with bars close to the duct when using normal-strength grout.

As a whole, the results outlined here indicate that the simplest and most beneficial location for through-thickness reinforcement is against the duct. Doing so is the easiest for construction (and already done when using bars as duct supports) and provides the greatest benefit to capacity. This is true regardless of grout strength. Ultimately, the best location of through-thickness reinforcement in relation to the duct has little to do with where tension is greatest across the thickness due to compressive stress deviation. Instead, the ideal location is based on where reinforcement will best keep the gross cross-section tied together and restrict non-crushing mechanisms of failure.

The findings from this portion of the study were used to design additional panels. In subsequent panel tests, different configurations of through-thickness reinforcement were placed against ducts of any type.

4.3.6.4 Effects of Reinforcement Shape

Design codes do not specify the need for through-thickness reinforcement in the web of a post-tensioned girder as a means of supplying load-carrying capacity or crack control. Despite a lack of such provisions, this reinforcement is still often included for facilitating the proper placement of a duct inside a beam. As discussed in Chapter 2, ducts must be supported, but there are numerous ways to do so. Many challenges arise during construction while attempting to suspend a duct at the appropriate elevations and with designated profiles. The ends of a duct terminate at embedded anchorages and the connection must be internally sealed for grouting operations. Internal suspension of a duct is only possible by tying the duct to stirrups within the beam. Ordinary tie wire will not support extremely flexible ducts, especially those made from plastic.

Pieces of reinforcement extending through the girder web are often tied to stirrups to provide a means of support for the duct. As described in Chapter 2, reinforcement used in this case is not a requirement but an acceptable alternative to supporting ducts with tie wire. No industry standard exists regarding the shape of these supporting bars; however,

current practice reveals some similarities in their specification for use in post-tensioned girder projects. All duct supporting bars are designed to be readily attached to stirrups. The supporting bars must have a relatively flat portion that extends through the web beneath the duct with bents at right angles to tie to the stirrups.

In order to fully gauge the relative impact of through-thickness reinforcement and standardize detailing, a set of panels was designed with the goal of investigating the impact of the orientation and shape of the reinforcement. Prior to the construction of this panel set, all but one of the panels tested with through-thickness reinforcement contained the ‘normal’ hairpin configurations described earlier consisting of overlapping pieces of hairpin-bent reinforcement with a bend diameter of 4-in. Of special interest were reinforcing schemes consisting of reinforcement shapes commonly used in the field, like inverted hairpins or Z-bars, or variations that might be easier to install.

4.3.6.4.1 Through-Thickness Reinforcement Layouts

Overall, six primary through-thickness reinforcement configurations were investigated in this study to determine if any one combination of reinforcement shape and orientation excelled over any others in improving the compressive capacity of a panel containing a duct. The variations were only used with plastic ducts. The six configurations are shown in Figure 4-33.

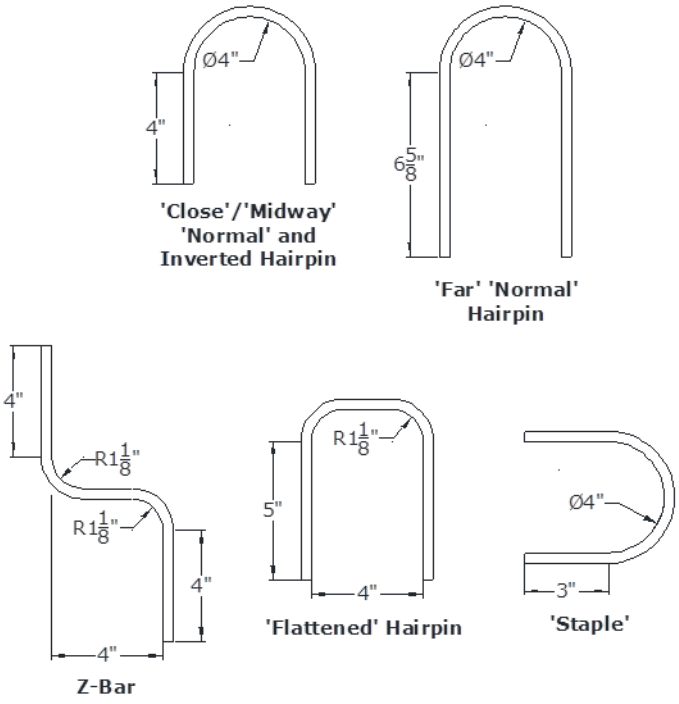

Figure 4-33: Shapes and Dimensions of Through-Thickness Reinforcing Bars

4.3.6.4.1.1 'Normal' Hairpins

The 'normal' hairpin configuration was used in the majority of through-thickness reinforcement tests conducted in this study. This configuration met all necessary code requirements for bar bending, utilized ideal placement of bars and was easy to place. Reinforcement consisted of #3 bars with a 4-in. diameter interior bend and 4-in. minimum straight leg lengths. The bend diameter was selected to ensure that bent bars could accommodate the largest diameter ducts used. Regardless of proximity to the duct or placement along the length of the duct, each reinforcement location consisted of two hairpins crossing each other, hooked around the duct with legs oriented in the direction of loading. These provided a means of resisting splitting stresses on either side of the duct where forces developed.

4.3.6.4.1.2 Inverted Hairpins

The inverted hairpin configuration was designed as a simple orientation modification to the ‘normal’ hairpin scheme mainly to determine if the direction of installing the hairpins mattered. On occasion, panels tested with ‘normal’ hairpins showed signs of distress upon failure, suggesting that the orientation of the panels might be hindering the panel from reaching a higher capacity. In Figure 4-34 this post-failure shape of a ‘normal’ hairpin is illustrated, showing that the hairpin legs are no longer straight and parallel to each other as they were originally constructed but are rather angled away from the bend. Due to the nature of hooking the hairpin around the duct, the hairpin legs were directly in the vicinity of the largest component of the tension field developed in the panel. Consequently, the tension may have led to the legs pushing outward and inducing a prying effect on the outer fibers of the panel leading to a premature loss of capacity. Thus, in an effort to determine if this was the case, the inverted hairpins were not hooked around the duct. Rather, the bend was butted against the duct on either side with legs still in the direction of loading but extending away from the duct (Figure 4-35). This was intended to move the legs further from the region of highest tension.

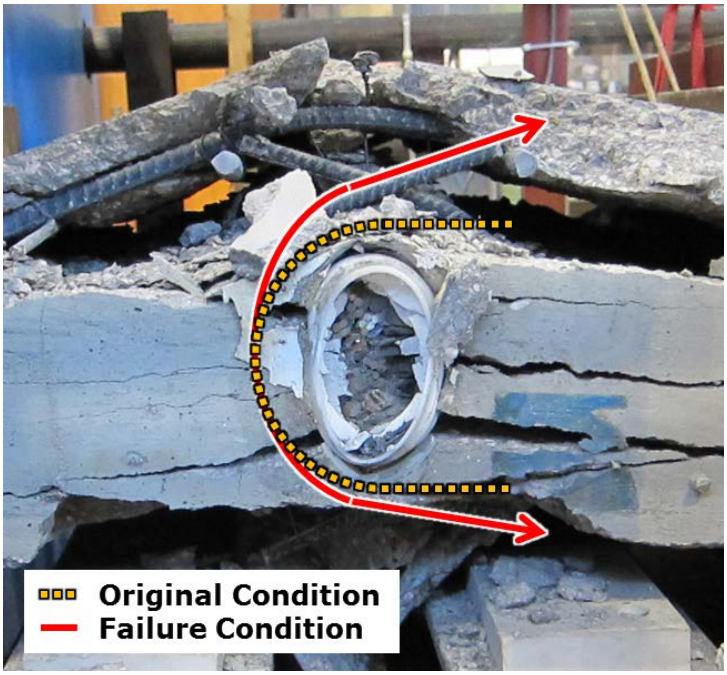

Figure 4-34: Typical Failure Condition of 'Normal' Hairpins

Figure 4-35: Inverted Hairpin Configuration

4.3.6.4.1.3 'Flattened' Hairpins

The 'flattened' hairpin setup (Figure 4-36) was created as a minor alteration of the physical shape, but not orientation, of the 'normal' hairpin scheme. Rather than have each individual piece of reinforcement continuously bent into one arc, the flattened hairpins were bent at two locations to provide a flat portion that was placed against the duct instead of a curved portion. Each bend was kept at the minimum code-required radius, and a 4-in. spacing between the legs of each piece of reinforcement was maintained.

Figure 4-36: 'Flattened' Hairpin Configuration

4.3.6.4.1.4 Single-side, Inverted Hairpins

This configuration consisted of 'normal' hairpins placed against only one side of the duct to emulate bars supporting a duct at the appropriate elevation in a girder (Figure 4-37). The primary goal of this scheme was to determine if placing through-thickness

reinforcement on only one side of the duct would have as much, or any, benefit compared to reinforcing both sides.

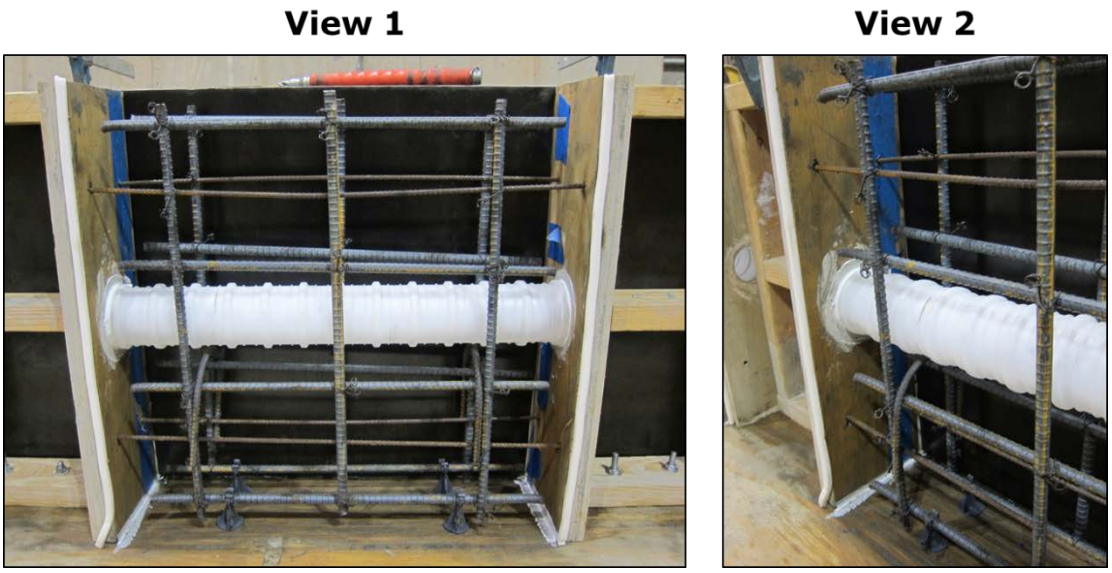

Figure 4-37: Single-Side, Inverted Hairpin Configuration

4.3.6.4.1.5 Z-Bars

The Z-bar configuration consisted of pairs of reverse, double-bent bars placed around the duct and secured to vertical bars. Each piece was fabricated with the same minimum bend radii as for the flattened hairpins; however, the two legs were bent in opposite directions. This configuration was somewhat easier to place than any of the hairpin variations. The Z-bars were installed in pairs such that the legs of the two bars overlapped on one side of the duct (Figure 4-38).

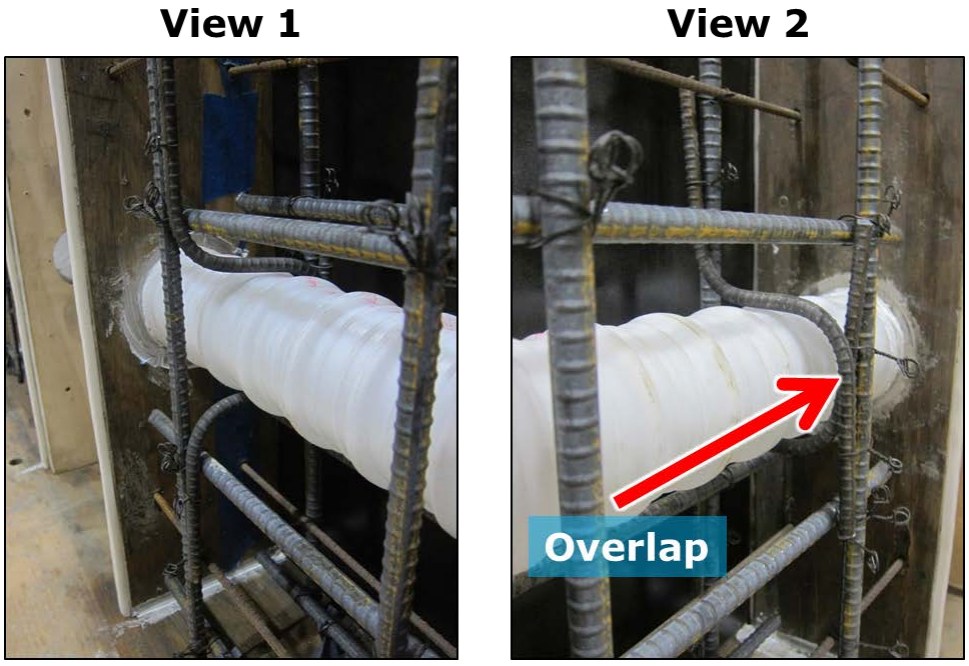

Figure 4-38: Z-Bar Configuration

4.3.6.4.1.6 'Staples'

This setup incorporated hairpin-bent pieces of reinforcement with the same 4-in. diameter bend as previously used, the difference being that these pieces were inserted through the thickness of the panel from the sides rather than above and below the duct in the direction of loading (Figure 4-39). While fitting the 'staples' into a congested region of a reinforcement cage was slightly simpler than the 'normal' hairpins, securing the 'staples' was more cumbersome. The bent portion of the reinforcement had to be tied very securely to the vertical bars. The legs of opposite bars were tied together, but they were not tied to any main horizontal or vertical bars.

Figure 4-39: 'Staple' Configuration

4.3.6.4.2 Comparison of Results With Different Reinforcement Shapes

The ninth set of panels included six specimens each with one of the six through-thickness reinforcement configurations and a seventh, unreinforced panel as a baseline. Only 3-in. plastic ducts and normal-strength grout were used in this set of 7-in. thick panels.

Figure 4-40 shows the η_D values for each of these seven ducted panels. As seen previously, the presence of through-thickness reinforcement against the duct improved panel capacity somewhat, although the use of different reinforcement schemes yielded differing capacities.

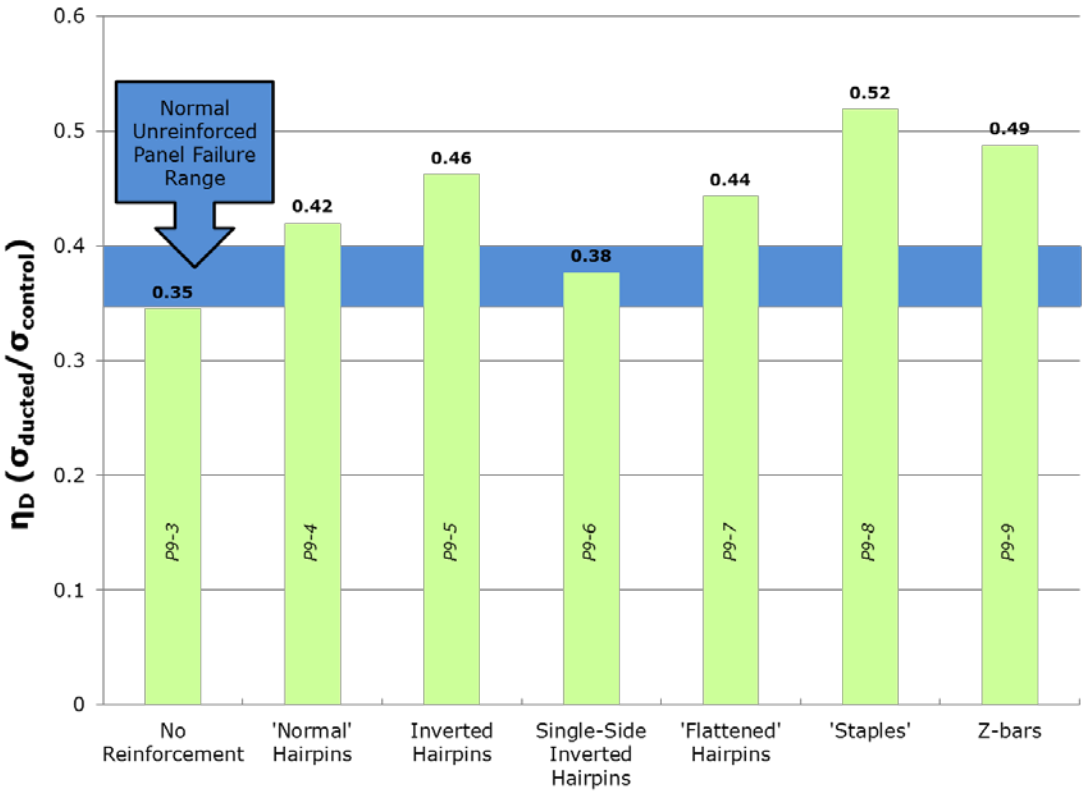

Figure 4-40: Comparison of Panel Results with Varied Shapes and Orientations of Through-Thickness Reinforcement

Noteworthy findings regarding use of the unique through-thickness reinforcement configurations are as follows:

- The panels with inverted hairpins and flattened hairpins performed only slightly better than ‘normal’ hairpins. There was no evidence from these tests that the legs of the ‘normal’ hairpins were bending outward and lowering capacity as previously mentioned.
- Not surprisingly, the panel with inverted hairpins on one side of the duct had a capacity between that for the unreinforced panel and that for the panel with inverted hairpins on both sides of the duct. In this case, the reinforcement helped somewhat as crushing behavior was observed in the reinforced side for the panel.

Ultimately, though, the panel principally failed via splitting of the unreinforced side (Figure 4-41).

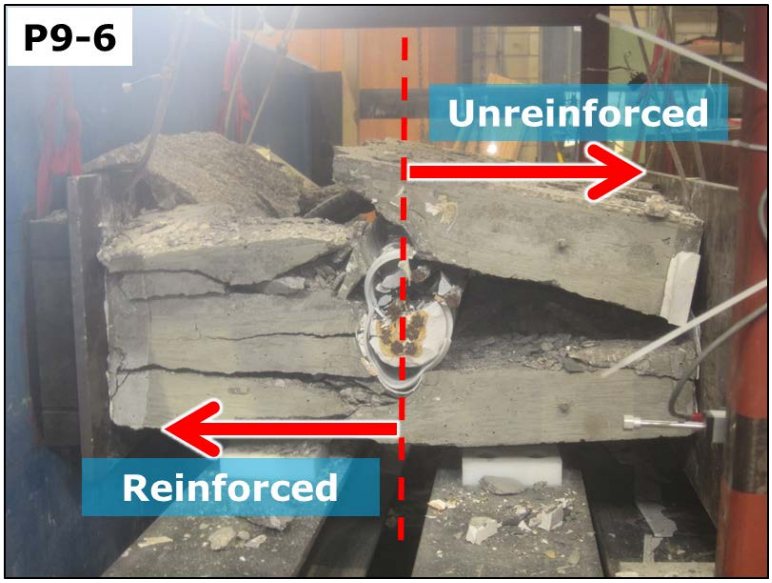

Figure 4-41: Failure of Panel with Single-Side, Inverted Hairpins

- The panels with Z-bars and 'staples' did not differ significantly in their capacities, but use of these configurations generated the highest overall panel capacities. The primary difference between using the 'staple' scheme and others was that two bars were placed on each side of the duct rather than one, thus doubling the effective amount of reinforcement at individual locations without having to use larger size bars. Using either of these schemes may be worth additional consideration, although the difficulty in tying staples to stirrups may negate their efficacy. Rather, it may be advantageous to investigate increasing the number of pieces of reinforcement placed against the duct at discrete locations using the 'normal' or inverted hairpin configurations.

It is important to note that reinforcement must be placed on both sides of the duct. Ultimately, the shape or orientation was less important than the amount of reinforcement crossing the splitting plane. Otherwise, ease of fabrication should be given top consideration in selecting a form of reinforcement.

4.3.6.5 Other Considerations When Using Through-Thickness Reinforcement

The use of through-thickness reinforcement was considered in conjunction with varying δ. Ultimately, through-thickness reinforcement was found to be beneficial for most practical values of δ, not just for a δ of 0.42 (3-in. duct in a 7-in. thickness). This was confirmed through the testing of additional plastic-ducted panels. An unreinforced, 7-in. panel (P7-8) with a 2.375-in. plastic duct (δ = 0.34) failed at an η_D of 0.43 A comparable panel with reinforcement (P8-5) failed at an η_D of 0.5. Meanwhile, an unreinforced, 7-in. panel (P8-3) with a 3.375-in. plastic duct (δ = 0.48) failed at an η_D of 0.28. Its counterpart with reinforcement (P8-4) reached an η_D of 0.31. As was seen in panels with 3-in. ducts, these panels showed improvements in capacity when through-thickness reinforcement was added. However, η_D only marginally improved when using the larger duct. It is probable that as the duct becomes larger and the amount of concrete cover is reduced, a more substantial amount of through-thickness reinforcement would be necessary to hold a section together under increasing tension.

Through-thickness reinforcement was also used in a set of panels with steel ducts, in which differing values of δ and different grout strengths were also considered. The value of δ was not varied for steel-ducted panels without through-thickness reinforcement in this study. Thus, there is no basis on which to compare these panels with those using ducts other than 3-in. in diameter. The capacity of the panel with a 3-in. duct, normal-strength grout, and ‘normal’ hairpins from these tests (P10-4) can be compared to the average capacity of the three previously-tested, unreinforced panels with 3-in. steel ducts (P3-8, P3-9, and P4-7). With an η_D of 0.6, the reinforced panel maintained a higher capacity than its unreinforced counterparts which had an average η_D of 0.54. This result suggests that through-thickness reinforcement may indeed be beneficial when using steel

ducts. However, with an already substantially higher η_D for panels with steel versus plastic ducts, an increase in η_D with through-thickness reinforcement is more beneficial for plastic-ducted panels than for steel-ducted ones. More testing would likely be needed to fully gauge the impact of through-thickness reinforcement for steel-ducted panels.

Additionally, the benefits of using through-thickness reinforcement were determined when using empty plastic or steel ducts. An ungrouted, 7-in. panel with a 3-in. plastic duct and sets of 'normal' hairpins against the duct tied to each vertical bar was fabricated (P8-6). This panel failed with an η_D of 0.25, a slight improvement over an η_D value of 0.21 for an unreinforced, ungrouted panel (P3-5). An ungrouted, 7-in. panel with a 3-in. steel duct and sets of 'normal' hairpins against the duct tied to the outer two vertical bars was also constructed (P10-9). This panel failed with an η_D of 0.35, a significant improvement over 0.22, the η_D value of its unreinforced counterpart (P3-7). These results suggest that through-thickness reinforcement can improve capacity even when no grout is used. More testing is needed to confirm if the η_D values obtained in these instances are typical.

4.3.7 Duct Banks

Three tests were performed with multiple ducts vertically in line to verify if limiting duct spacing requirements are sufficient so that no modification to web crushing strength for a single duct is necessary. Each of the tests had two 3-in. diameter ducts spaced at various distances and filled with regular-strength grout. One specimen was fabricated with two ducts placed against each other with a center-to-center spacing of 3-in. (Figure 4-42a), providing only the space created by the duct corrugations for concrete placement and reducing the surface area for bonding. Another specimen contained ducts separated by two duct diameters center-to-center or 6-in. (Figure 4-42b). The last had a center-to-center duct spacing of three diameters or 9-in. (Figure 4-42c).

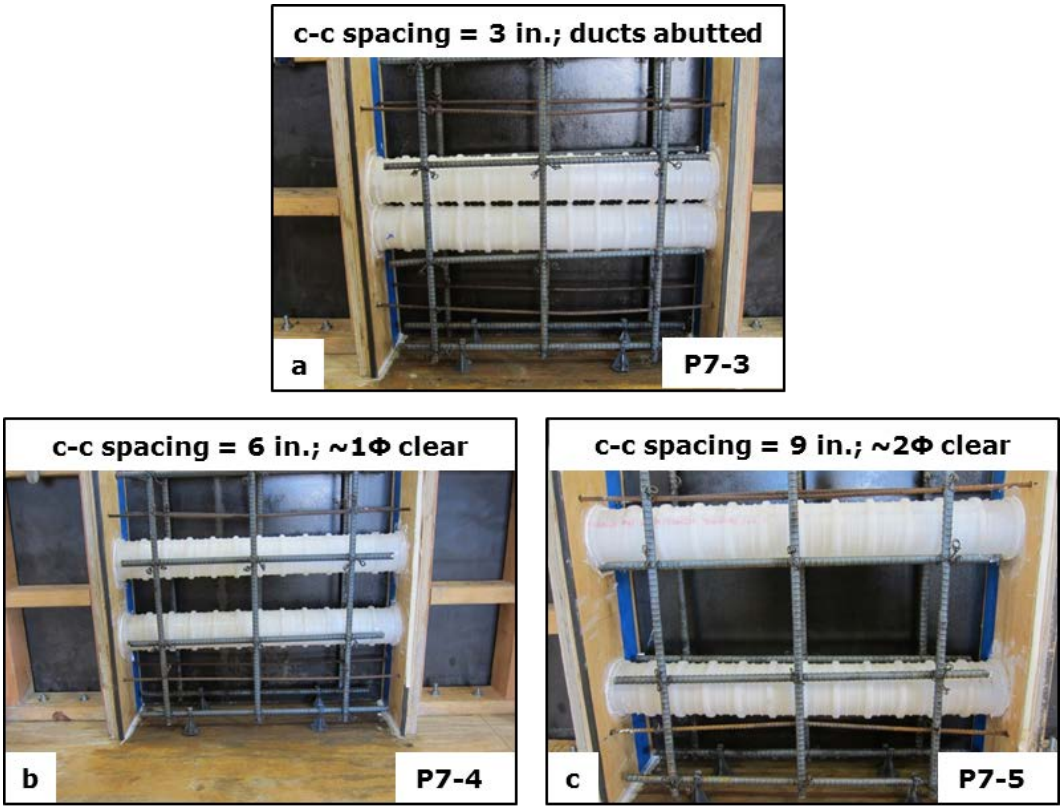

Figure 4-42: Duct Spacing for Panels with Multiple Ducts

Given the duct and panel dimensions and concrete materials used for these tests, the required duct spacing according to AASHTO (2012) and FDOT Structures Design Guidelines (2010) provisions outlined in Chapter 2 were determined (Table 4-2). Based on the requirements, the duct spacing used in the specimen with adjacent ducts did not satisfy the requirements of both references.

Table 4-2: Required Duct Spacing For Typical Design

Design Document	Spacing Taken as Maximum of: (in.)	Calculated Spacing (in.)	Duct Spacing Required (in.)
AASHTO (2012) – based on clear spacing	1.5	1.5	1.5 (= 5.0 center-to-center)
	1.33 x Coarse Aggregate Size	0.49875	
FDOT Structures Guidelines (2012) – based on center-to-center spacing	4	4	5.5
	Outer Duct Diameter + 1.5 x Coarse Aggregate Size	4.0625	
	Outer Duct Diameter + 2	5.5	

Notes
* Coarse aggregate is 0.375-in.
* Outer duct diameter is 3.5-in.

The strengths of the first two panels (P7-3 and P7-4) did not differ significantly, but the associated web-width reduction factor for each fell below that for the majority of tests with a single 3-in. diameter plastic duct. These panels failed with η_D values of 0.32 and 0.31. The third panel with ducts spaced three diameters apart center-to-center (P7-5) failed at an η_D of 0.37 and fell in the normal range for panels with single plastic ducts.

Each of the panels exhibited cracking at around 65-75% of the final load. This behavior was rarely seen in panels with single ducts which typically failed upon first cracking. Crack patterns are shown in Figure 4-43. In each case, splitting cracks formed along the center of the panel from the outer ends of the ducts. In the panel with adjacent ducts (P7-3), minor crushing of the concrete between the ducts was noted (Figure 4-43a). The panel with the 6-in. duct separation (P7-4) experienced cracking between ducts at mid-thickness (Figure 4-43b). The panel with the 9-in. duct spacing (P7-5) had parallel cracks between the ducts in in line with the outer edges of the ducts (Figure 4-43c). Failure of each of these panels is also shown in Figure 4-43. At failure, each of the panels exhibited some level of debonding paired with interior cracking at or very near the duct edges as though the ducts and concrete between were behaving as one unit and the outside concrete split from that unit (Figure 4-44).

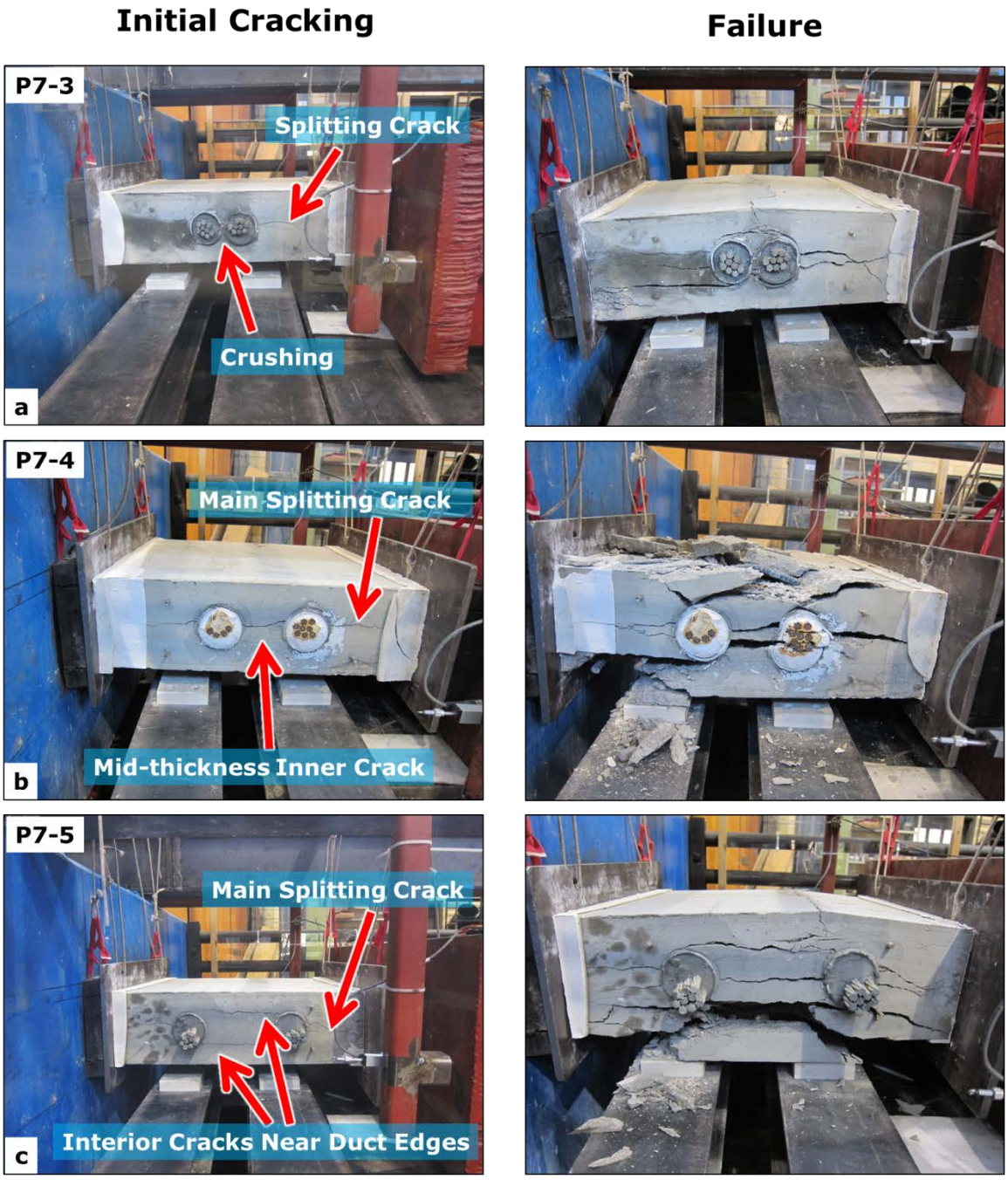

Figure 4-43: Initial Cracking and Failures of Panels with Multiple Ducts

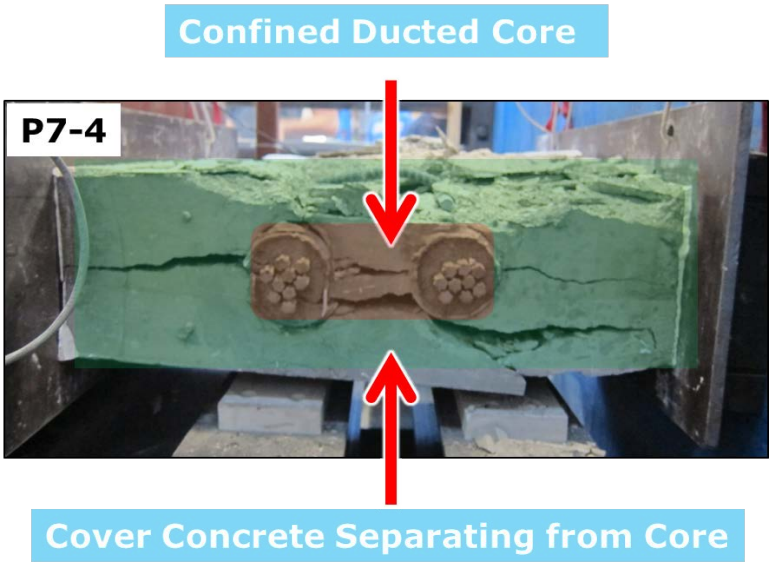

Figure 4-44: Separation of Concrete Core Between Multiple Ducts

Overall, failure of these panels appears to be best explained by the interaction of two mechanisms: 1) separation between the cover concrete and the core concrete located between the ducts and 2) debonding between the ducts and concrete. It has already been described how failure of single-duct panels typically commenced whereby the cracked and debonded panel could be treated as two slender, eccentrically-loaded halves incapable of resisting the resulting flexure. This concept could be extended to the failure of multi-duct panels. As illustrated in Figure 4-45a, the innermost fibers of the halves of a single-duct panel directly contact the plastic duct. Under load, these pieces would tend to bend outward and pull away from the rest of the panel, and the loss of bond between the concrete and duct after first cracking would preclude the generation of restraint against this movement. On the other hand, Figure 4-45b indicates that a tensile force restraining outward movement of the panel segments develops in a multi-duct panel due to the continuity between the cover and core concrete between the ducts. Until cracking between the cover and concrete between the ducts develops, additional load can be carried.

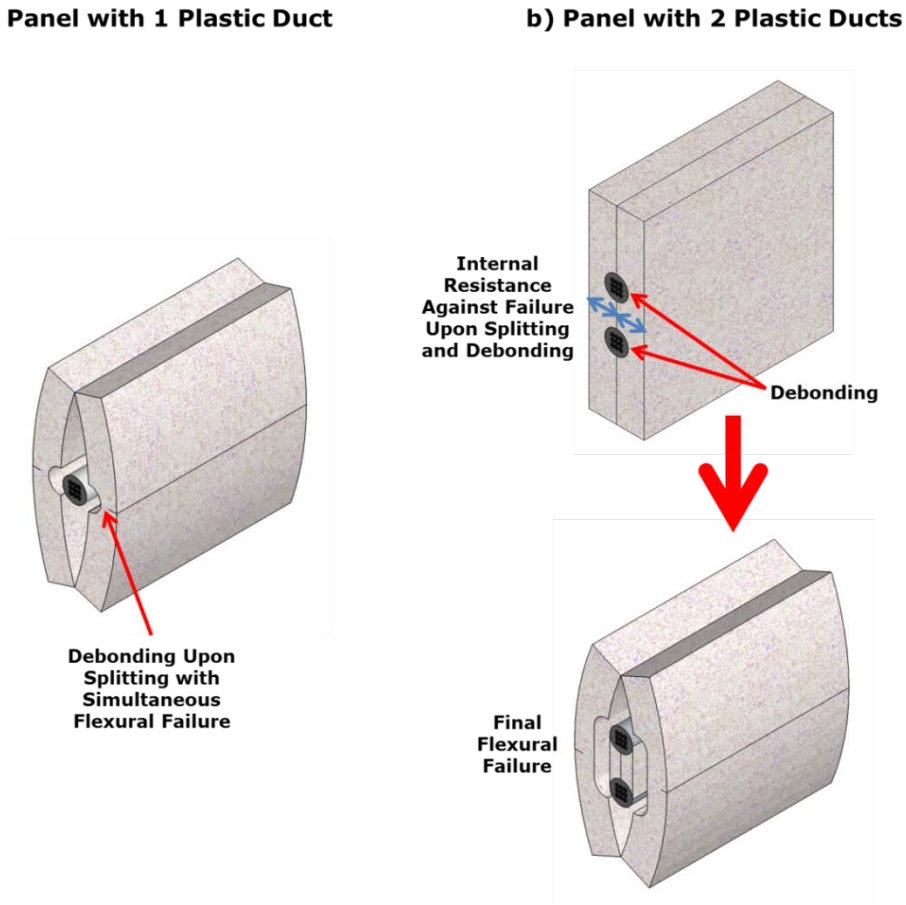

Figure 4-45: Difference in Failure Behaviors for Panels with One or Two Ducts

Overall, the results of these tests show that a panel with multiple ducts spaced at least three inner duct diameters center-to-center will be as strong as that with a single duct. The amount of concrete between the ducts in this case minimizes stress deviations and provides adequate tensile resistance against the separation of cover.

4.3.8 Size Effect

One of the primary objectives of this study was to investigate the effect that increasing the web thickness would have on reducing the effect of post-tensioning ducts on the web crushing capacity of an I-girder. Initial test results illustrated differences between the 5-in. thick panels of the first panel set and many comparable 7-in. panels of

the third panel set. Despite inconsistencies in concrete and grout strengths between the 5- and 7-in. panels, results of these panel tests indicated that η_D decreases significantly when transitioning to thicker specimens while δ changes little. This trend is evident when comparing the results of similar panels in Figure 4-46.

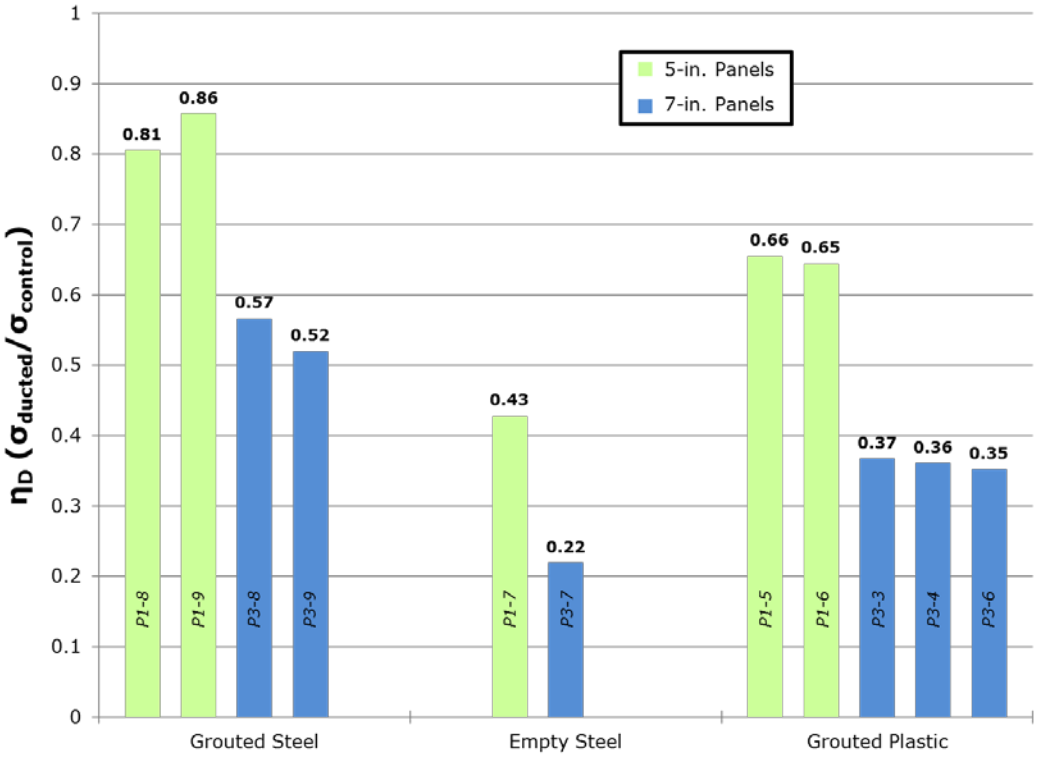

Figure 4-46: Comparison of 5- and 7-in. Panels

The reduction in η_D with increasing panel thickness raises questions regarding the accuracy of code equations. The database of previous research was examined to assess the validity of the study's results shown in Figure 4-46. It was noted that existing equations primarily assume that δ is the only dimensional quantity affecting the web crushing strength. Further, these formulas were often calibrated to and validated by the failure loads of panels with gross cross-sectional areas well below those of the 7-in. and 9-in. thick panels tested in this study. In fact, the largest panels previously tested included

the 5-in. thick panels tested by Muttoni et al. (2006), and their results were in accordance with capacity predictions utilizing the k-factors from Eurocode 2 (2004) – the most conservative of all codes consulted. Ultimately, it is not surprising that those test results and the results of the initial 5-in. panels of this study with nearly identical cross-sectional areas and very similar material properties were so well matched.

The early comparisons between the 5-in. and 7-in. panels suggested the possibility that not only does the direct relationship between the duct diameter and web thickness play a role in web crushing strength, but the actual thickness of a girder web may have an effect independent of the duct. This potential size effect could not be adequately assessed with the lack of data on a larger panel thickness. Consequently, a set of panels was specifically designed to evaluate the size effect.

This set consisted of 5-, 7-, and 9-in. thick controls and ducted panels with similar values of δ, all utilizing the same batches of concrete and grout. In total, 12 panels were cast in which four of each thickness were fabricated. Within each subset of four panels, two were solid, one contained a steel duct, and the other had a plastic duct. None of the panels contained through-thickness reinforcement, and each ducted panel was grouted with a regular-strength grout. Combinations of duct sizes and panel thicknesses were selected to achieve a consistent δ from one panel to the next. With all materials the same and near-equivalent values of δ, any differences in failure loads could be attributed almost solely to the change in thickness. Figure 4-47 depicts the range of panel sizes and ducts tested. The panel thickness, duct diameter, and resulting ratio of the two dimensions are provided for each panel in Table 4-3.

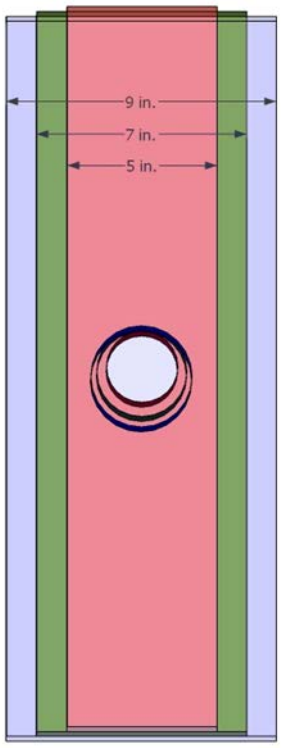

Figure 4-47: Variety of Panel Sizes Tested

Table 4-3: Results From Tests with Varying Thicknesses

Nominal Thickness (in.)	Specimen	Duct Type	Φ (in.)	Nominal δ	Failure Load (kips)	η_D
5	P11-8	Plastic	2.375	0.48	518.2	0.62
5	P11-9	Steel	2.375	0.48	709.5	0.84
7	P11-5	Plastic	3	0.43	500-525*	0.36**
7	P11-6	Steel	3	0.43	785.1	0.54
9	P11-2	Plastic	3.375	0.38	528.2	*0.31****
9	P11-3	Steel	3.375	0.38	750.3	*0.44****

* Estimated failure load range based on previous 7-inch panel results
** η_D taken as average for P3-3,4,6, P4-5 and P9-3
*** Calculated η_D based on actual 9-inch failure load and estimated control

The failure loads and associated web width reduction factors for the panels with varying thicknesses are also provided in Table 4-3. Given comparable results from earlier testing, only one 5-in. thick panel and one 7-in. thick panel were tested as controls. Two

9-in. thick control panels failed at much lower loads than expected (similar to those for the 7-in. thick controls). It was found that the bearing pads experienced significant shear deformations that resulted in eccentric loading, flexural cracking, and premature failure of the 9-in. control panels (Figure 4-48). Based on the other control panels that reached an average of 84% of the reported cylinder strength, the 9-in. control panels should have failed at approximately 1700 kips. Using that value, η_D values for the ducted 9-in. panels are presented in Table 4-3. Also, the 7-in. panel with the plastic duct in this set of tests failed at a much higher load than similar panels previously tested, and the values from those tests are given in Table 4-3.

Figure 4-48: Bearing Pad Failure During 9-in. Control Tests

Based on current code equations, all web thickness sizes with a similar δ should give approximately the same η_D. The experimental results obtained here are inconsistent with this concept. With increasing panel thickness, the η_D values dropped.

The failure loads of the panels (with the same type of duct) were similar for different panel thicknesses despite differences in the ratio of failure load to that of a

control panel. This implies that approximately the same amount of tension was produced across the thickness of the panel for each size thus limiting crushing capacity by nearly the same amount. This is not surprising; with a similar δ, the relative duct area to concrete area at the level of the duct is constant and thus the resultant spread of compressive force should be the same. Thus, the tensile forces generated should be similar.

Clearly, these findings show that a dichotomy exists when it comes to formulating an expression for η_D. The value is obtained from the testing of two specimens that fail in a different manner. It depends on the failure load of a ducted member and the failure load of a solid control test with the same thickness. In other words, failure of a panel is a function of its own thickness. In the case of ducted panels, the thickness is accounted for in δ, which appears to be the primary dimensional quantity differentiating panel capacity. For solid panels, capacity is directly proportional to the gross area in the direction of loading and thus directly related to thickness. Thus, increasing the thickness of a control panel will always increase its capacity, but doing so to a ducted panel may or may not increase capacity depending on how or if the duct size is altered. In the end, η_D is not meant to only be treated as being proportional to the duct diameter and inversely proportional to the control thickness. More accurately, η_D should be directly proportional to δ for the ducted panel and inversely proportional to the thickness of the control.

Current shear equations use web width reduction factors to modify strengths by relative amounts rather than directly considering an absolute crushing capacity as a strength limit. While an absolute capacity would not require the need to make comparisons, it would not be as convenient as a multiplier. Despite the usefulness of a multiplier, such a quantity must accurately reflect the differences between the original and modified capacities. Problematically, the results of the size effect tests performed in this study suggest that the web width reduction factor (or multiplier) is formulated incorrectly in codes. Current web width reduction factor formulas address δ, but do not account for any additional impact from the thickness of a solid web. In essence, this is no different than assuming that all members under consideration are sized the same. As it

stands now, two girders with the same δ but different web thicknesses would yield the same web width reduction factor. When applied to the full web width of each girder, the resulting shear-compression capacity of the thicker-webbed girder would be computed to be incorrectly higher than the thinner-webbed girder. In this case, the code equations for a larger member would actually yield a more unconservative result, even though a designer would be led to opt for a thicker-webbed member to increase shear capacity.

4.4 CHAPTER SUMMARY

The results and qualitative analysis of 100 compressive tests performed on ducted and solid panels to reflect crushing behavior of post-tensioned girder webs were presented. The effects of major parameters considered to have a potential impact on girder web crushing capacity were highlighted. The principal findings from the study on ducted panels are summarized as follows:

- Duct Type: The use of plastic ducts reduces crushing capacity more than when using steel ducts. This is a consequence of poor bonding between concrete and plastic ducts. No adequate means of improving bond was determined in this study.
- Duct Grouting: Elements with grouted ducts always maintain a higher capacity than those with empty ducts.
- Size Effect: A significant size effect exists when determining the η_D values of ducted elements with varying thicknesses. For the same duct diameter-to-thickness ratio, a thicker element will maintain a lower η_D than will a thinner element. This is because the absolute capacity of a solid control increases with thickness, but the absolute capacity of any sized element with the same duct diameter-to-thickness ratio is constant. Apart from a division between duct types in many instances, η_D formulations for all codes do not consider web thickness and are unconservative in terms of the size effect.
- Through-Thickness Reinforcement: The use of through-thickness reinforcement improves crushing capacity. It prevents a member from failing upon initial tensile splitting by providing some tensile resistance and mechanically holding a

specimen together so that additional load may be applied. Through-thickness reinforcement would help the most if used continuously around the duct. As this is likely not very construction-friendly or economical, use of reinforcement at discrete locations along the length of the duct is recommended. Discrete reinforcement only needs to be tied to every other vertical bar/stirrup; adding additional bars at tie-down points does not noticeably increase capacity any more. Through-thickness reinforcement improves strength most and is easiest to use when tied against and on both sides of the duct. Multiple pieces of reinforcement can be extended through the thickness of the ducted element at the same location on each side of the duct to possibly improve capacity more than when using only one bar. Regardless, the shape of bars used did not significantly influence the crushing capacity of panels, and geometry of the bars should be chosen on the basis of ease of fabrication and installation.

- Grout Strength: Crushing capacity is improved with an increasing grout strength relative to concrete strength. This effect is limited in elements with plastic ducts when the grout strength is not substantially higher than the concrete strength (an improbability for most practical applications). On the other hand, capacity changes in elements with steel ducts are more readily seen regardless of whether or not the grout-to-concrete strength ratio is greater than unity.
- Concrete Strength: Relative capacities (i.e. η_D values) decrease with increasing concrete compressive strength. This is because the compressive strength of a control increases faster than the tensile strength of concrete which influences ducted member capacity.
- Duct Banks: An element containing multiple ducts vertically in line can perform as well as that with a single duct if the ducts are spaced at least three diameters apart center-to-center.

The findings from panel testing are largely expected to be well-adapted to post-tensioned girder testing with ducts in the web, at least from a qualitative standpoint. In the next chapter, new k-factors to use with effective web width formulas and a new comprehensive, quantitative formula to estimate crushing capacity for panels (and possibly girder webs) will be derived from the panel results outlined here. At the same time, further discussion will be provided on how well these panel test results and future girder test results may match.

CHAPTER 5
Panel Test Result Analysis and Girder Comparisons

5.1 OVERVIEW

The crushing behavior of an I-girder web with a post-tensioning duct has been studied through panel testing; however, the results have not been calibrated against results from tests of full-scale girders. The findings from this study were quantitatively assessed to develop adjustments to equations for shear capacity taking web crushing into account. First, trends in the web width reduction factors obtained from testing were determined using curve-fitting techniques to generate lower-bound k-factors that may be adopted in place of those currently used in codes. This procedure is consistent with the approach used by past researchers. Then, an alternate means of determining web crushing capacity is provided which considers the reduction in capacity due to the presence of a duct in terms of a member's tensile splitting resistance rather than the compressive resistance of a web with a duct.

Finally, a discussion is presented on the transition from panel to girder testing to determine shear capacity. The relationship between panel behavior and girder behavior with ducts in the web is explored. Similarities in behavior of panels and girders are discussed along with an assessment of the test parameters investigated in panel testing that would be important to include in girder testing. Finally, a short commentary on the results of an initial ducted girder test is presented to support this discussion.

5.2 EVALUATION OF EXISTING CODE K-FACTORS

Prior to attempting to formulate new k-factors based on panel test results from this study, it is imperative to assess the adequacy of those factors as employed in current shear design codes. Here, only test results for panels with single ducts, no modified bond

conditions, and no through-thickness reinforcement are used in considering the usefulness of those factors.

In Figure 5-1, values of η_D for 5-, 7-, and 9-in., grouted, steel- and plastic-ducted panels are plotted against δ. Plots of calculated η_D values using k-factors specified in various codes are shown. Code web width reduction factors are conservative for data points above lines representing code η_D values. With the exception of two of the 7-in. steel-ducted panel tests using grout-to-concrete strength ratios above 1.0, no results are conservatively estimated by the AASHTO general shear provisions. For 5-in. panels, only Eurocode 2 conservatively estimates η_D for the test panels. Meanwhile, codes give very poor estimates of η_D for thicker panels. Only the results of 7-in. plastic- and steel-ducted panels using a low concrete strength (3.62 ksi) are conservatively estimated by some codes. The web width reduction factors are not sufficiently evaluated by any code for any 7-in. panels with higher concrete strengths or for any 9-in. panels.

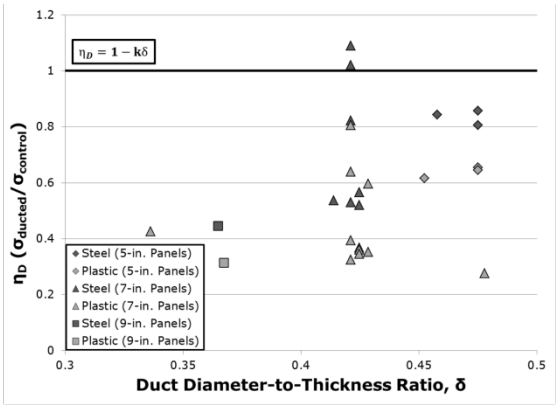

ACI 318-11 (k = 0)

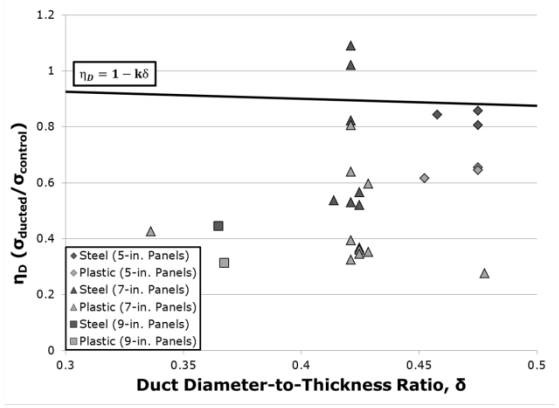

AASHTO 2012 General (k = 0.25)

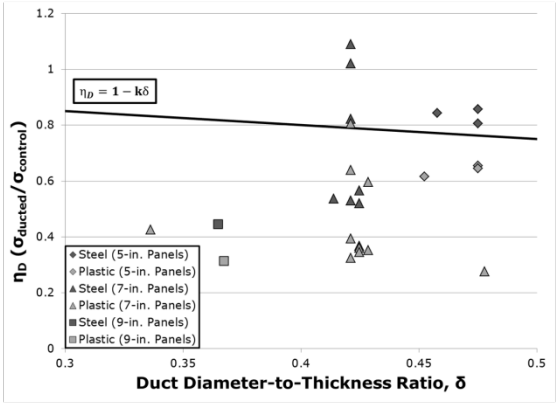

AASHTO 2012 Segmental (k = 0.5)

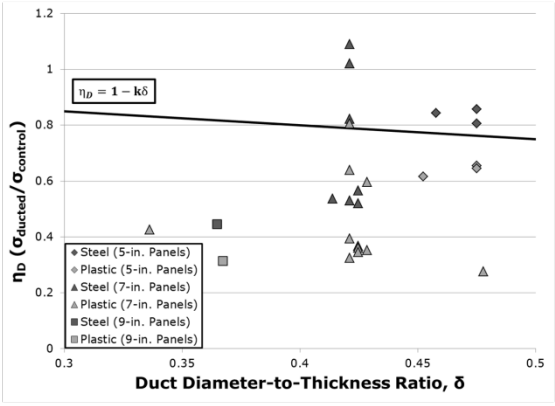

JSCE No. 3 2002 (k = 0.5)

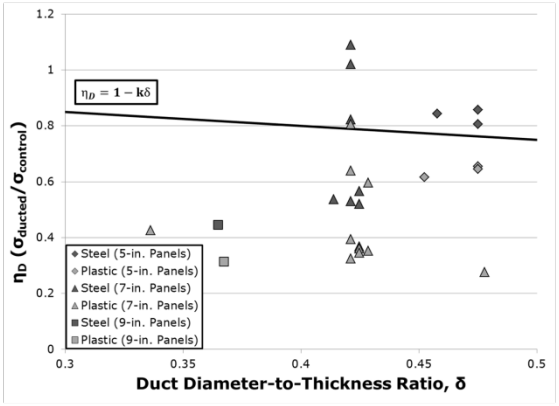

Eurocode 2 2004 - Steel (k = 0.5)

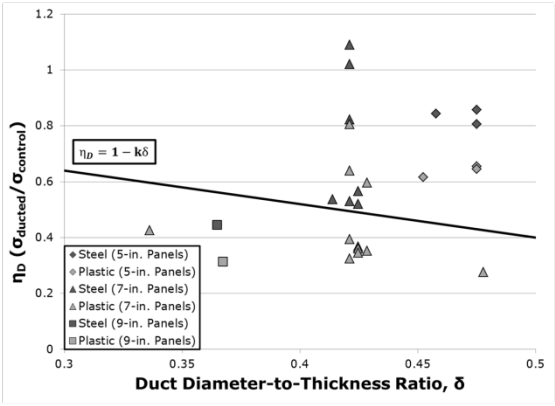

Eurocode 2 2004 – HDPE (k = 1.2)

Figure 5-1: η_D vs. δ for Grouted Panel Tests with Expected Reduction Factors from Code

The three results from ungrouted panel tests along with code estimates of η_D are summarized in Table 5-1. Only Eurocode 2, with an increased k-factor of 1.2, correctly estimated η_D for the single 5-in. steel-ducted panel tested. The values of η_D for the two thicker, ungrouted panels were well below code predictions.

Table 5-1: η_D for Ungrouted Panel Tests with Expected Reduction Factors from Code

		P1-7 (5-in. Steel) δ = 0.48	P3-7 (7-in. Steel) δ = 0.43	P3-5 (7-in. Plastic) δ = 0.43
	Experimental η_D	0.43	0.22	0.21
Code η_D	*ACI 318-11*	1.0	1.0	1.0
	AASHTO 2012 General	0.76	0.79	0.79
	AASHTO 2012 Segmental	0.52	0.57	0.57
	JSCE No. 3 2002	0.76	0.79	0.79
	Eurocode 2 2004	0.42	0.48	0.48

5.3 COMPUTATION OF NEW K-FACTORS

The results from the current study are used to determine new k-factors that adjust the effective web width to give conservative estimates of web crushing capacities. New k-factors are derived and presented for cases in which grouted or empty ducts of either primary duct type are used in members with varying thicknesses. Situations in which through-thickness reinforcement is utilized are also considered.

5.3.1 Grouted Panels

The majority of testing in the present study was done on panels with grouted ducts. As such, much of the work in developing new k-factors is based on test results on such specimens. First, k-factors are evaluated for use with either steel or plastic ducts and for web thickness for which data was not available to the code writers. Additionally, adjustments are suggested for the inclusion of through-thickness reinforcement.

5.3.1.1 Accounting for Size Effect

The first priority in selecting new k-factors based on panel tests was to consider the effect of varying specimen thickness on crushing capacity. The results of the size

effect tests reported in Chapter 4 were used to derive a set of k-factors that could fit all data on average. In Figure 5-2, plots of η_D versus δ based on the web width reduction factor formula using these k-factors are shown along with subsets of 5-, 7-, and 9-in. steel-and plastic-ducted panel test results. There is not enough data to determine a maximum or minimum limitation on δ. Only the results of single-ducted panels of high-strength concrete and without through-thickness reinforcement are shown. Compared with code k-factors, these k-factors lead to better predictions of η_D for each type of panel.

Although the derived k-factors can be used to obtain accurate average estimations for η_D, some data are not conservatively estimated. In order to obtain k-factors that could be used to conservatively estimate η_D for all data, additional data refinement was attempted. In Figure 5-3, conservative k-factors factors were selected in rounded, "code-friendly" increments of 0.25.

The rounded k-factors work well to conservatively estimate η_D and reflect some key findings in this study. A value of 0.5 for the case of steel ducts in 5-in. thick elements is no different than that given by most design codes. The factor of 1.0 for use of plastic ducts in members of the same thickness is less conservative than that of 1.2 from Eurocode, but confirms the Eurocode value. Further, a value of 1.0 is the same as original research-developed k-factors for use with empty ducts. Although the scenario in question here deals with grouted ducts, it has been discussed that after debonding between plastic ducts and concrete occurs, subsequent behavior of a panel is essentially no different than that for a panel containing an empty duct. Finally, the size effect is clearly captured by increasing k-factors for thicker webs. A k-factor of 2.0 is selected for both 7- and 9-in. plastic-ducted elements. With more data points for 9-in. thick panels, the value is likely to change.

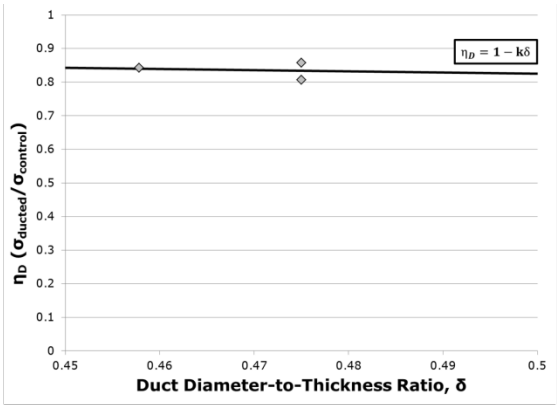

Steel, 5-in. (k = 0.35)

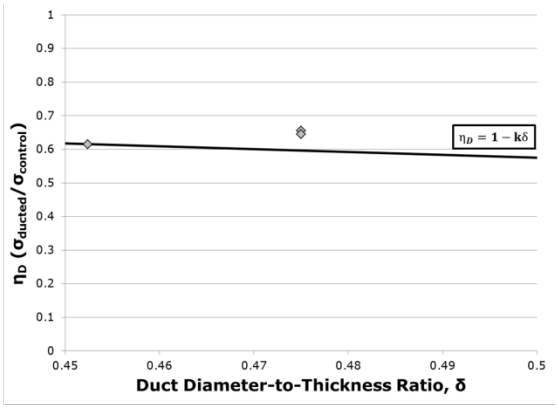

Plastic, 5-in. (k = 0.85)

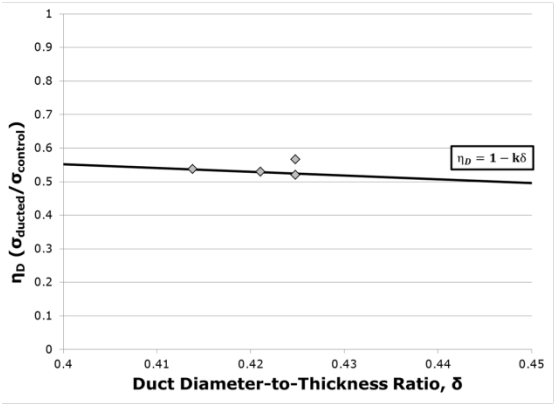

Steel, 7-in. (k = 1.12)

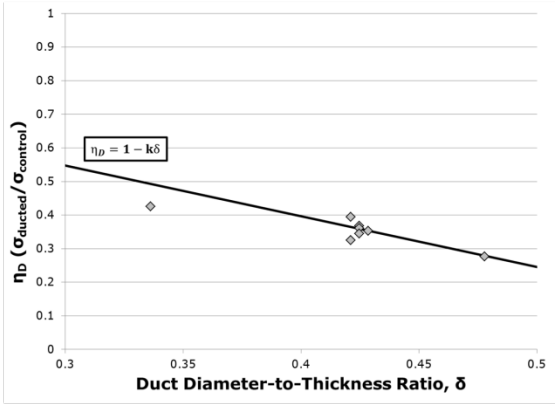

Plastic, 7-in. (k = 1.51)

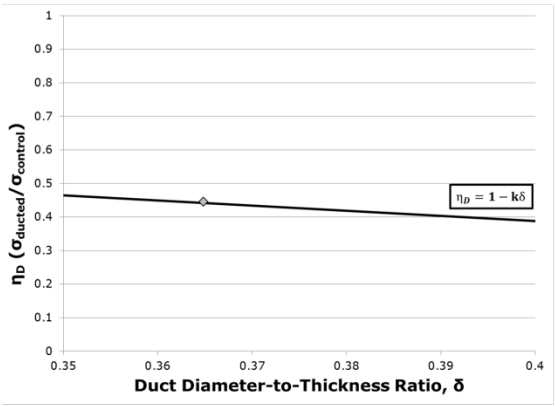

Steel, 9-in. (k = 1.53)

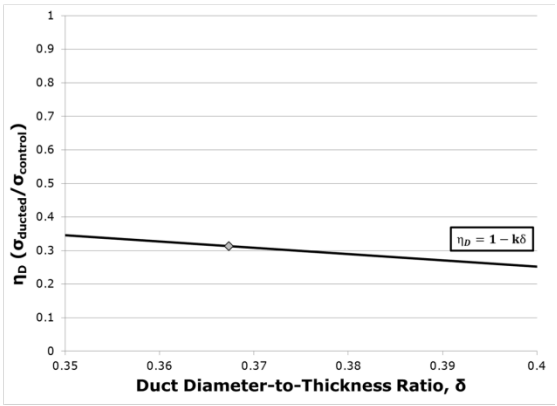

Plastic, 9-in. (k = 1.87)

Figure 5-2: Application of k-factors for Grouted Cases with Consideration of Panel Thickness

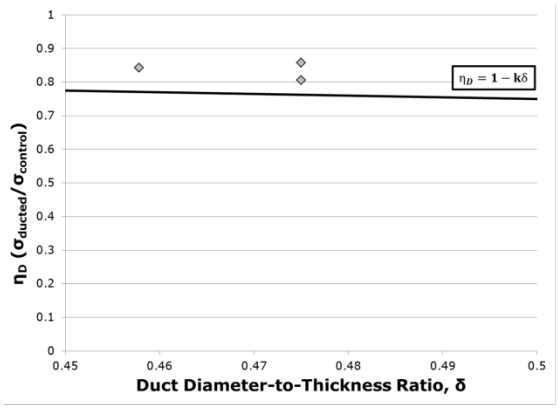

Steel, 5-in. (k = 0.5)

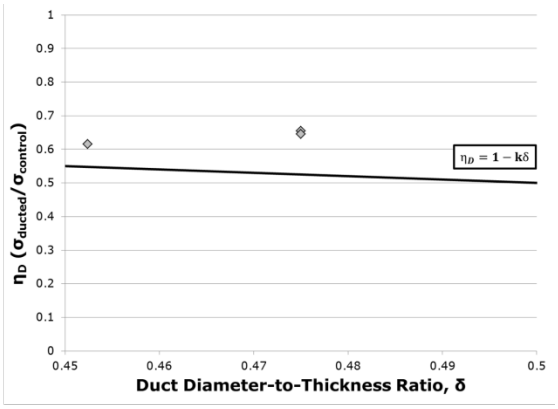

Plastic, 5-in. (k = 1.0)

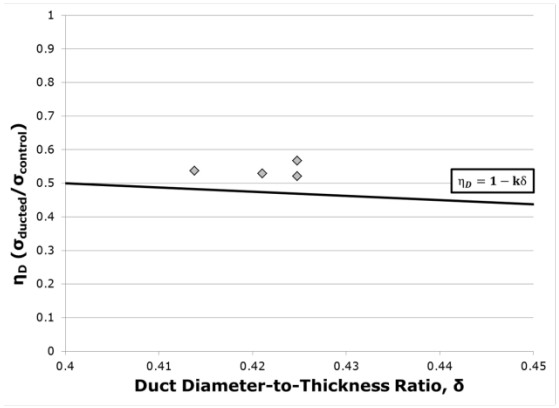

Steel, 7-in. (k = 1.25)

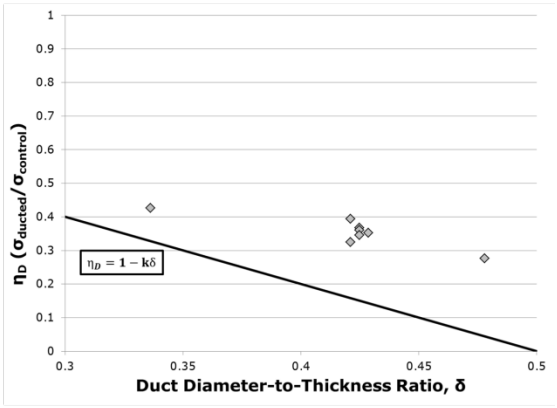

Plastic, 7-in. (k = 2.0)

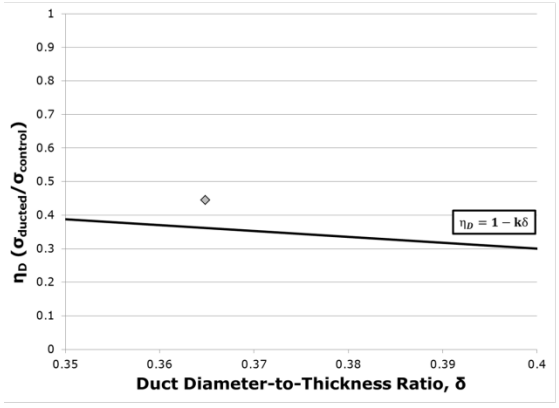

Steel, 9-in. (k = 1.75)

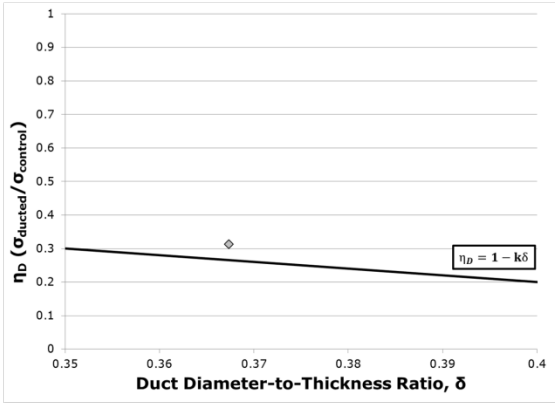

Plastic, 9-in. (k = 2.0)

Figure 5-3: Selection of New k-factors for Grouted Cases

5.3.1.2 Accounting for Through-Thickness Reinforcement

After developing new k-factors for the general cases of grouted, steel- and plastic-ducted elements of varying sizes, potential modifications to these factors are considered for through-thickness reinforcement. As was described in Chapter 4, the greatest benefits of through-thickness reinforcement in panels were seen when transverse bars were placed relatively close to the duct on both sides and tied to vertical bars. Panels fitting these criteria are considered here, regardless of concrete or grout strengths or δ. Only panels with #2 bars through the thickness are not accounted for.

Tests with through-thickness reinforcement were only conducted on 7-in. panels. As such, modifications to k-factors to account for this reinforcement may not apply to elements with other thicknesses. In Figures 5-4 and 5-5, pertinent results on reinforced, plastic- and steel-ducted panels are displayed. Estimates of η_D with the k-factors of 1.25 and 2.0 derived before for use of the duct types in 7-in. specimens are shown. Obviously, these estimates are conservative, but on the verge of being too much so. A variety of single multipliers below 1.0, referred to as reinforcement factors (designated by r) were applied (in increments of 0.05) to the base k-factors for unreinforced cases to give potential modified k-factors to use in reinforced cases. The smallest value of r that can be multiplied by the base k-factors to still ensure conservative estimates of η_D is 0.8 for both plastic- and steel-ducted specimens.

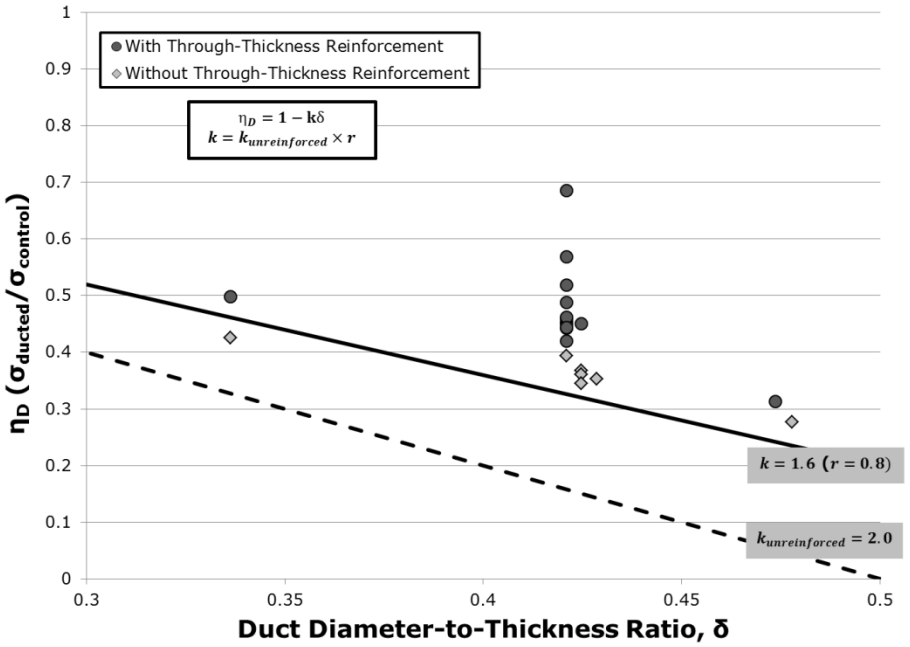

Figure 5-4: Adjustment of k-factor for 7-in. Plastic-Ducted Panels with Through-Thickness Reinforcement

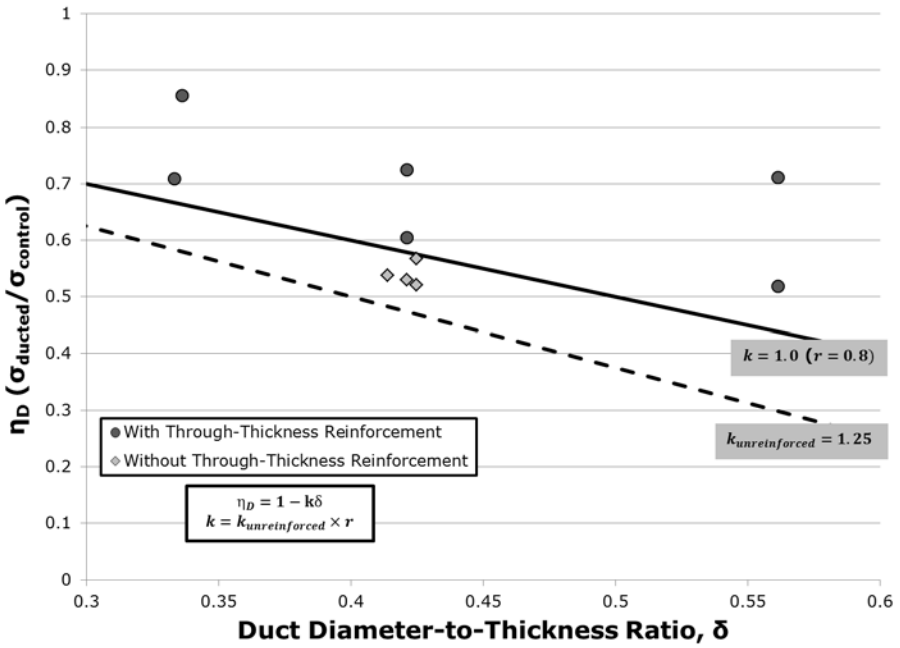

Figure 5-5: Adjustment of k-factor for 7-in. Steel-Ducted Panels with Through-Thickness Reinforcement

In using an r of 0.8, k-factors for cases in which plastic or steel ducts are used become 1.6 and 1.0, respectively. The k-factor of 1.0 implies that with just a small amount of through-thickness reinforcement around steel ducts, one can fully rely on the crushing capacity of the net section of concrete at the level of the duct. The same cannot be said when using plastic ducts. The k-factor of 1.6 indicates that most tests with plastic ducts did not incorporate enough through-thickness reinforcement across the length of duct to be able to utilize a factor of 1.0. It is important to remember, though, that some data did show that providing a significant amount of through-thickness reinforcement around plastic ducts (e.g. five sets of hairpins in P4-4) could enable one to account for crushing of the net section of concrete at the duct (i.e. use a k-factor of 1.0). In the end, the fact that a k-factor of 1.0 could be used confirms Eurocode's allowance of such a value if enough transverse reinforcement is provided around a duct.

5.3.2 Ungrouted Panels

Using the results of ungrouted 5- and 7-in. panels without through-thickness reinforcement, plots of estimated η_D values using k-factors of 1.25 and 2.0 are shown in Figure 5-6. These k-factors apply when using either plastic or steel ducts. There is limited data on panels with empty ducts to validate the use of these k-factors. There is also insufficient data on ungrouted panels with through-thickness reinforcement to determine usable k-factors in such cases.

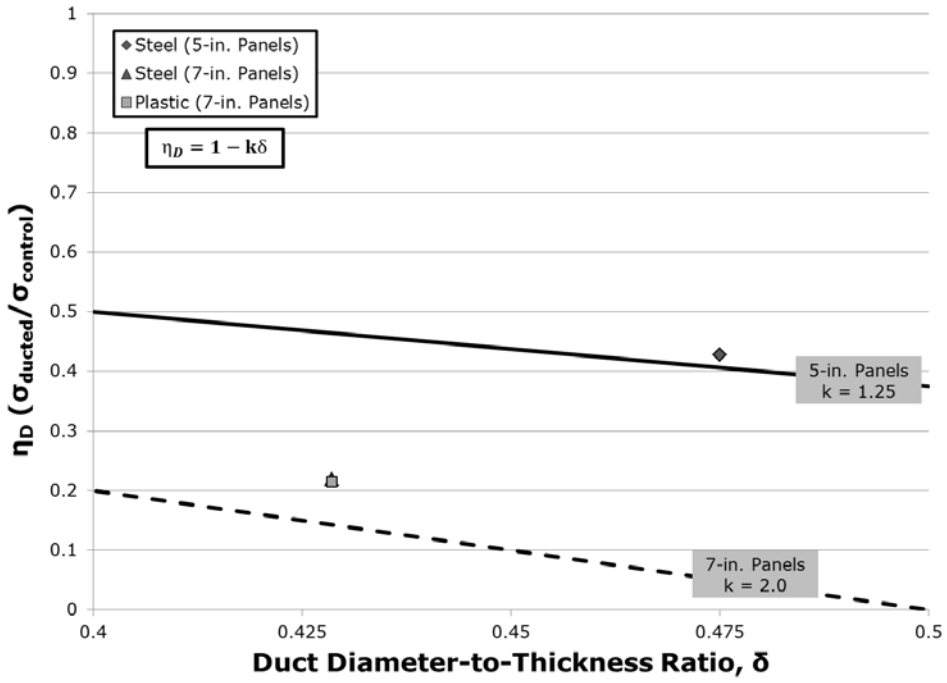

Figure 5-6: Selection of k-factors for Ungrouted Cases

5.3.3 Summary of New k-Factors and Recommendations

A variety of new k-factors have been derived from panel test results of this study for recommended use when working with ducted elements. In Table 5-2, these k-factors are summarized. Factors have been selected for a combination of duct type, grouting, and element thickness. The values can be adjusted for the inclusion of through-thickness reinforcement. Linear interpolation is recommended to choose an appropriate k-factor for panel thicknesses between those listed.

Table 5-2: Summary of New k-factors (From Panel Tests)

	Grouted Ducts*		Empty Ducts
Thickness (in.)	*Steel*	*Plastic*	*Steel/Plastic*
5	0.5	1	1.25
7	1.25	2	2
9	1.75	2	---

* *If adequate through-thickness reinforcement is provided, multiply k-factors by 0.8 for grouted cases*

5.4 NEW WEB WIDTH REDUCTION FACTOR FORMULA

As has been discussed, the standard web width reduction factor formula is based on the ratio of the crushing capacity of a ducted panel to that of a solid control. Using this method of determining η_D is quite challenging given the lack of homogeneity in materials and the effects of tensile stresses generated across the specimen width. As a result, code formulas for the effective web width provide conservative estimates of ducted member capacity with k-factors that apply to typical design cases, but material properties are not considered. While this approach may be simple, there is potential for calculated web width reduction factors to be overly conservative.

An alternative approach to evaluating web width reduction factors is presented here. The approach developed accounts for the range of parameters investigated in this study and directly utilizes some material properties to consider the effects of tension in a panel. Such a calculation may be described using the following formula and Figure 5-7:

$$\eta_D = \frac{ducted\ failure\ load}{control\ failure\ load} = \frac{\alpha\sqrt{f_c}h_{eff}w}{\beta f_c t w} \qquad \textbf{Equation 5-1}$$

where:

α = factor for tensile strength of concrete in a ducted element

f_c = concrete cylinder strength [psi]

h_{eff} = effective depth of element [in.]

w = width of element parallel to direction of duct [in.]

β = fraction of cylinder strength for compressive strength of a concrete element

t = element thickness [in.]

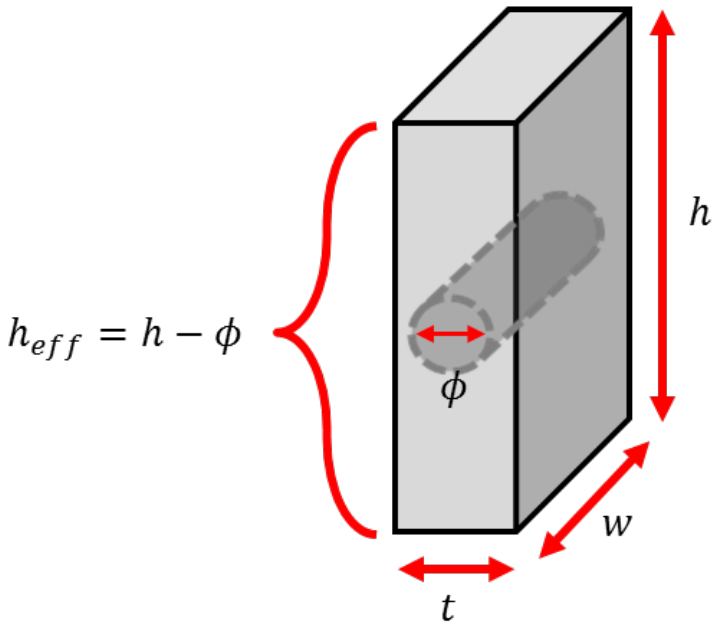

Figure 5-7: Designated Panel Dimensions

In Equation 5-1, the control failure load is equal to the uniaxial compressive capacity of the panel – a product of the concrete's cylinder strength and the gross cross-sectional area of the loading surface modified by β to reflect the relationship between the in situ strength of concrete and the cylinder strength. Based on the testing of all control specimens during this study, the value of β was found to average 0.84, which is essentially the same as a value of 0.85 that is used in most codes.

The ducted member's crushing capacity is not taken as some portion of the uniaxial compressive capacity. Instead, it is taken as the compressive capacity when the lateral tensile force reaches a critical level. The tensile force is based on the square root of the concrete's cylinder strength and the area on which tensile stresses are developed (i.e. through the thickness). In this equation, the area under the influence of tensile load is

considered to be the product of a panel's width (parallel to the duct) and its effective depth (perpendicular to the duct). The effective depth is defined as:

$$h_{eff} = h - \Phi$$ **Equation 5-2**

where:

h = full depth of element perpendicular to the duct [in.]

Essentially, the effective depth is used as a simplification here, whereas only the concrete outside of the ducted portion of a panel is assumed to be able to resist tension. The duct, grout, and concrete at the immediate sides of the duct are not treated as being able to resist tension themselves. Ultimately, this may be more of a reasonable assumption when dealing with plastic ducts as opposed to steel ducts considering that plastic ducts debond from concrete upon panel failure. However, in any case, this is a conservative estimation.

Regardless of panel type, the existence of tensile stresses through the thickness was explained to be the primary instigator of failure. Panels without grout fail exclusively by tensile splitting. Those with grout still fail mostly due to an initial tensile splitting without significant evidence of crushing. The inclusion of through-thickness reinforcement was shown to promote an increase in noticeable crushing behavior of panel specimens as opposed to a display of pure tensile splitting. However, it is important to recognize that these reinforced panels showed signs of both tensile and compressive distress upon failure. The failure of these specimens could best be described as mixed-mode, falling between failure modes displayed by unreinforced specimens with ducts (splitting) and controls (pure crushing). Despite the effects of tension surrounding the duct being somewhat mitigated, the through-thickness reinforcement was not a salve capable of eliminating these forces. Tensile forces continued to exist in the specimen and limit its overall compressive capacity, albeit clearly not as substantially as in unreinforced panels. For these reasons, it is convenient and suitable to simplify any

quantification of ducted panel compressive capacity as a measure of "equivalent" through-thickness tensile capacity.

Within Equation 5-1, the magnitude of the "equivalent" tensile capacity is primarily captured in the factor α. Essentially, α considers the influence that tension produced transverse to a compressive strut has on reducing the strut's compressive capacity given the presence or lack of through-thickness reinforcement and the magnitude of stress deviation around the duct based on geometric and material properties of the system. In full, α accounts for the impact of:

- Duct Type
- Grouting
- Grout and Concrete Strengths
- Duct Diameter-to-Thickness Ratio
- Through-Thickness Reinforcement

Ultimately, it is simpler to examine the relative impact of variables and components on overall crushing strength through the use of a function with a comparative multiplier like α rather than formulate an equation isolating the exact amount of capacity contribution from individual system components. In a system with four principal components (concrete, reinforcement, grout, and a duct), it is far more complicated to mathematically determine the component interactions than in a much more well-known ordinary reinforced concrete system (consisting of just concrete and reinforcement).

In order to make a determination of α, it is important to begin by noting that this quantity may be able to be found using a continuous function of parameters or else taken from a set of discrete values. Based on the web width reduction factor formula given in Equation 5-1, α may be computed from panel test results of this study as:

$$\alpha = \frac{P_{ducted}}{\sqrt{f_c} h_{eff} w} \qquad \textbf{Equation 5-3}$$

where:

P_{ducted} = ducted panel failure load [lbs]

The original expectation from the analysis of results was to determine if a continuous trend for α existed with respect to any algebraic combination of quantifiable test parameters, namely grout-to-concrete strength ratio, panel thickness, and δ. This process was initiated by first examining trends in α versus each of these parameters individually. No results from panels with through-thickness reinforcement, multiple ducts, or altered duct bond conditions were considered.

In Figure 5-8, α is plotted versus the grout-to-concrete strength ratios for steel- and plastic-ducted panels. Only 7-in. panels with 3-in. ducts are considered. Just as η_D improved with increasing grout-to-concrete strength ratios, α exhibits an increasing trend with a higher strength ratio. However, there is reason to believe that α would not be greatly varied over a range of practical grout-to-concrete strength ratios (i.e. below approximately 1.0). Thus, a continuous trend for α based upon strength ratios is not meaningful.

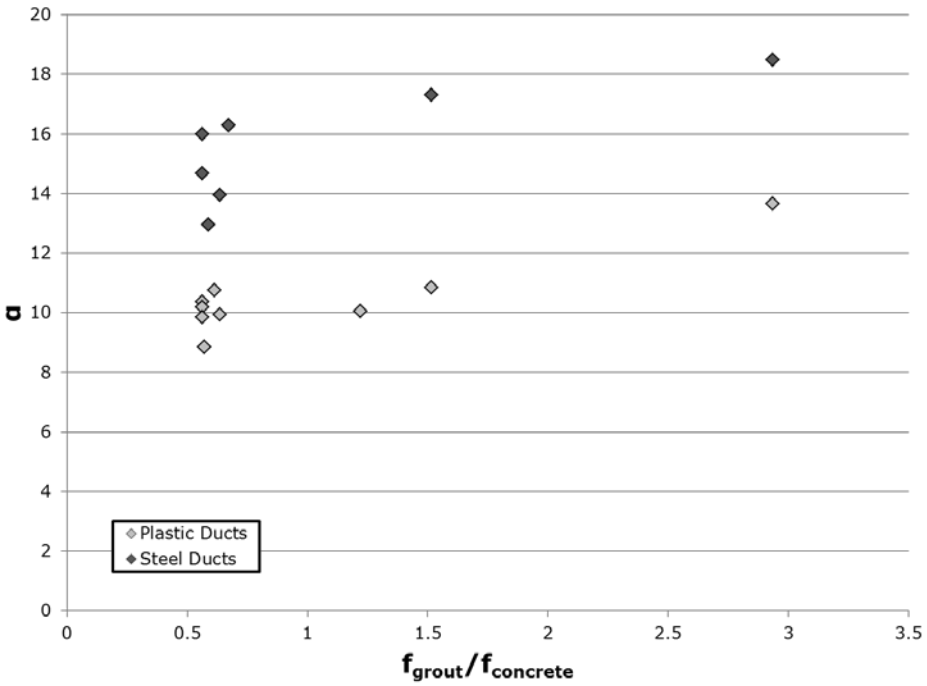

Figure 5-8: α vs. Grout-to-Concrete Strength Ratio

In Figure 5-9, α is plotted versus panel thickness. Only results of panels with the same combination of thickness and duct size used in the set of panels with varying thicknesses are shown. Evidently, there is a nearly constant relationship between α and the thickness of plastic-ducted panels. Conversely, there is far more scatter in the data for steel-ducted panels that may imply somewhat of a rise in α with increasing panel thickness.

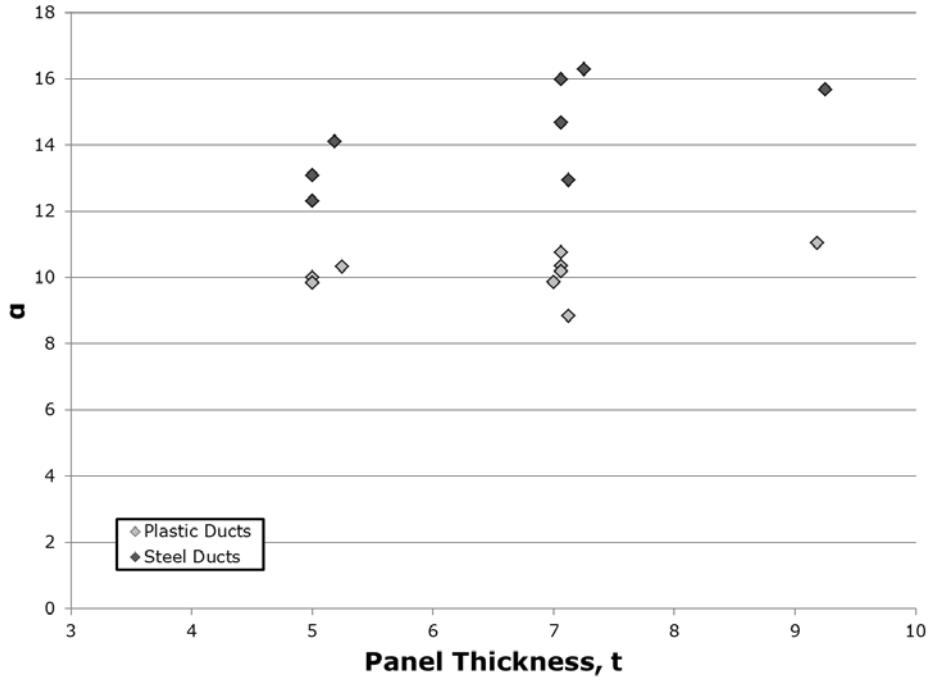

Figure 5-9: α vs. Panel Thickness

Lastly, α is compared to δ in Figure 5-10. Only results from 7-in. panels with high-strength concrete and normal-strength grout are assessed. As has been discussed previously, δ was not the widely modified during the course of this study. As such, there is an absence of sufficient data and scatter in the plot to support a trend for α here.

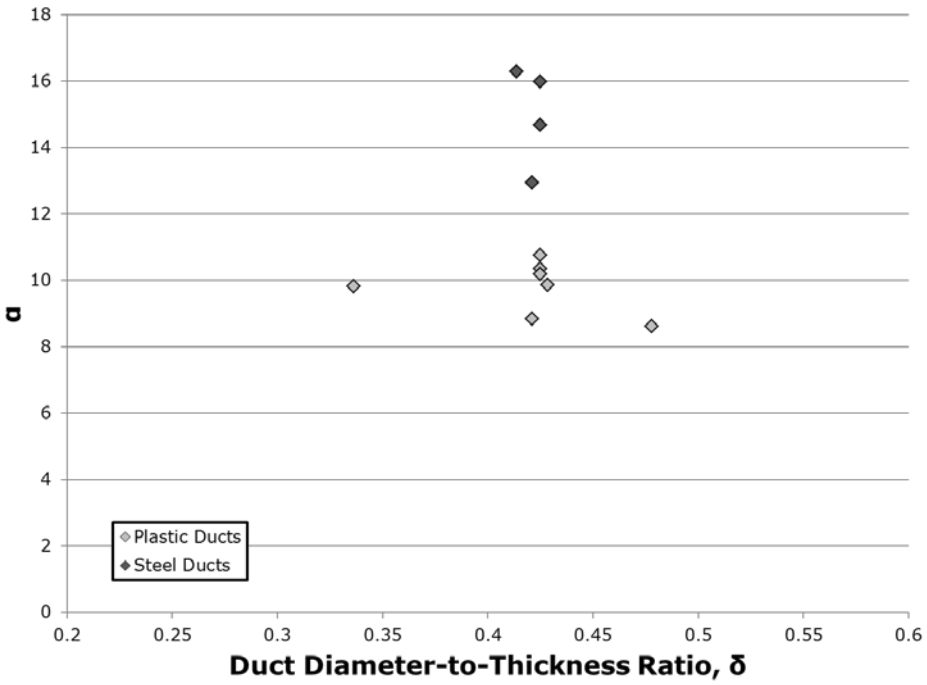

Figure 5-10: α vs. δ

Overall, while α may depend on the grout-to-concrete strength ratio, panel thickness, and/or δ, it is difficult to distinguish a continuous relationship between these quantities. In many of these cases, there is a lack of widespread data to support anything other than a slight hint of a varying or constant trend.

Given the inability to confirm any type of continuous trend in α with quantitative parameters, the choice was made to explore possible discrete values of α for the same general combinations of duct type, grouting, and reinforcing used in k-factor determination. In Figures 5-11 and 5-12, values of α are displayed from panels when

using either plastic or steel ducts, respectively. Data are separated in the events of using grouted ducts, with or without through-thickness reinforcement. Data for panels with empty ducts are limited and not included. Panels of all thicknesses and with all values of δ are considered together. For each case considered, the minimum, maximum, and average values of α are provided.

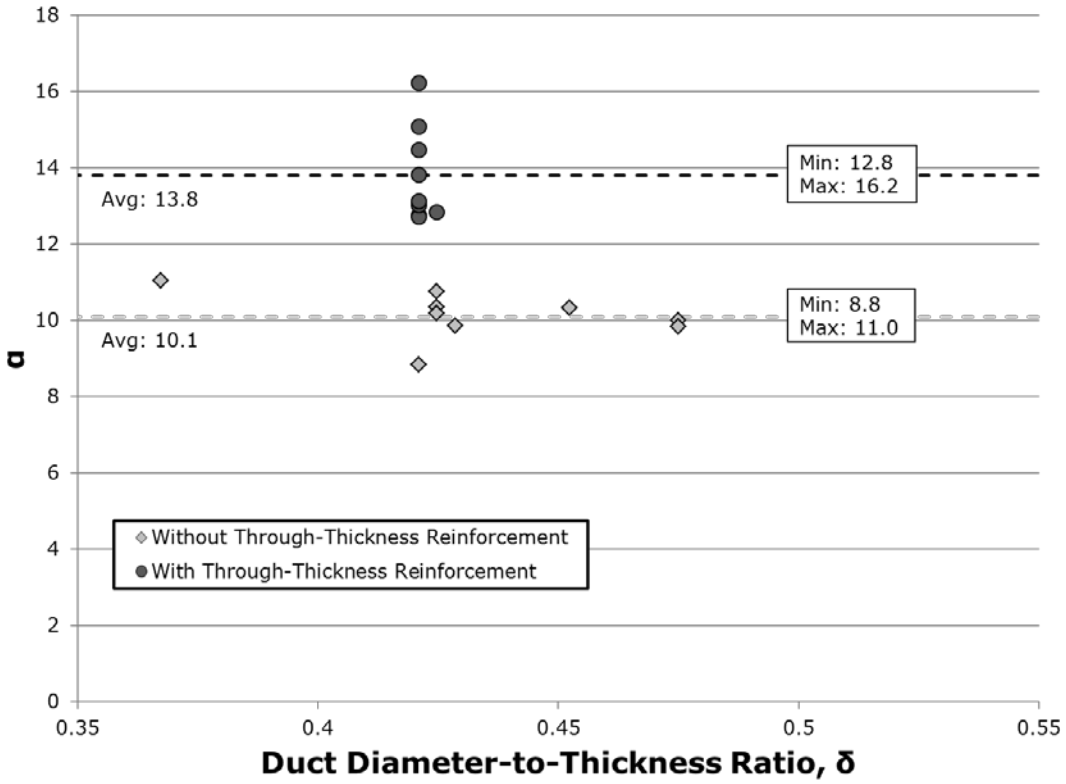

Figure 5-11: α for Cases with Grouted, Plastic Ducts

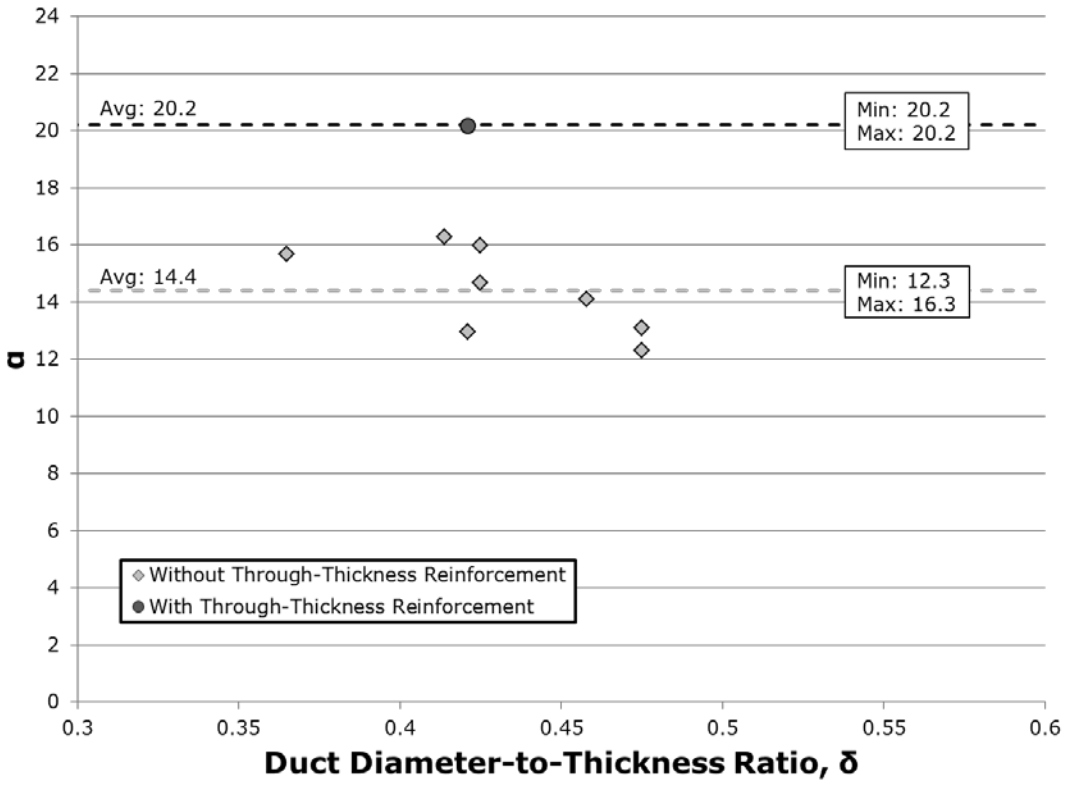

Figure 5-12: α for Cases with Grouted, Steel Ducts

Values of α are similar to each other for panels with either duct type and no grout or reinforcement. This is obviously consistent with the fact that these panels failed with similar η_D values. It is noteworthy that the value of α is about 6.0 for each of these panels. This is perhaps not surprising since the testing of an ungrouted panel is, in practice, little different than a split cylinder test giving a tensile resistance of $6\sqrt{f_c}$.

In all other comparable cases, α is higher for steel-ducted panels. Values of α increase when transitioning from the ungrouted case with the inclusion of grout or through-thickness reinforcement. These values increase slightly more so when grout is added. Interestingly, the addition of grout to unreinforced, plastic-ducted panels has roughly the same impact on α as does the inclusion of reinforcement in ungrouted, steel-ducted panels. Meanwhile, the addition of grout to unreinforced, steel-ducted panels has

about the same effect on α as does the addition of reinforcement in grouted, plastic-ducted panels.

It is still somewhat difficult to choose singular values of α based on the data provided. Some scatter, although not necessarily a significant amount, exists for α in certain cases. Then, only a minimal number of data points are shown for many cases. Finally, the effects of δ are not strongly considered. Despite these shortcomings, reasonable values of α can be selected for potential use and are summarized in Table 5-3. These values are selected in whole number increments for convenience. They are equivalent to the average values of α given for each combination of parameters having been rounded down. These values are empirical and remain exploratory – more test data and refinement is needed to guarantee acceptable use.

Table 5-3: Summary of Selected Values of α (From Panel Tests)

	Steel Ducts	**Plastic Ducts**
	Grouted	***Grouted***
Without Through-Thickness Reinforcement	14	10
With Through-Thickness Reinforcement	20	13

5.5 TRANSITION FROM PANEL TO GIRDER TESTING

It is important to remember that panel testing is a supporting tool for understanding the crushing behavior of members with ducts in the web, but girder testing is needed to fully assess shear capacity. Since the focus of this study was not on the girder testing portion of TxDOT Project 0-6652, a substantial discussion of how well or accurately the panels represent the girders to be tested is left for future work. Only a single, preliminary girder test from the project is briefly looked at here. The possible shortcomings of panel testing and reasons for which panel and girder tests may yield different results can, however, be addressed. Further, while panel test results may not

show a complete picture of post-tensioned girder web behavior, they can be used to estimate values from girder tests that incorporate some of the most influential test parameters.

5.5.1 Limitations of Panel Testing

All results of panel testing are not intended nor expected to be applicable to full-scale girders. The panels themselves are meant to simulate accurate-scale representations of a portion of an I-girder acting as a compressive strut in carrying shear forces from a point of load application to the supports. Of course, a thin-rectangular section of concrete subjected to pure compressive loads as fabricated and load-tested in the laboratory does not actually exist in the field. A compressive strut does not exist in isolation from the remainder of the structure nor under such ideal loading conditions. Boundary conditions for the region of the actual girder acting as a compressive strut presumably will play the largest role in establishing the web crushing capacity of a full girder compared to the compressive capacity of a panel. Whereas the panels are free from external restraint except at points of compressive load application, true struts exist in a composite of concrete and steel and are bounded continuously by flanges.

All along, the primary intended goals of the panel testing program were to establish qualitative and, where possible, quantitative trends. Through the modification of particular properties and construction details, changes in the behavior of each specimen could be studied. With this in mind, two highly important issues must be addressed.

Firstly, the panel test results do not provide an absolute numerical reduction in web crushing capacity of a full girder. For instance, while the load-carrying capacity of a 7-in. panel with a 3-in. plastic duct, no through-thickness reinforcement, and a moderate grout-to-concrete strength ratio is approximately 35-40% of that for a solid panel, the actual web crushing capacity of post-tensioned girder may not be as low as 35-40% of that for an ordinary pre-tensioned girder.

Secondly, a number of the variables tested during the course of this study proved highly influential in affecting panel capacity; however, the improvements made to the

design of the panels may have a reduced or even negligible effect in full-scale girders. Variations in panel specimen design were carefully selected to match design or construction alterations that might actually already be utilized in or could be adopted by a girder. Despite this, some design changes may be more suited to loading of panels than girders. A critical example of this may be the inclusion of through-thickness reinforcement. In panel tests, the principal role of the reinforcement was to keep the specimen from splitting in half upon tensile cracking and enable it to continue carrying compressive force. Spreading of compressive stress through a loaded girder and a panel test comprises a similar deviation of stress around the duct with accompanied cross-tensile forces for equilibrium. Without a means of counteracting this tension and the splitting inherent, the web of the girder would likely be cleft apart. In contrast to the panels, though, the compressive strut of a girder will likely experience some restraint to splitting due to different boundary conditions and the presence of stirrups. Notably, a girder web is continuously connected to thick flanges, and multiple struts that are stressed differently interact.

An important consideration is that panel testing lacks the redundancy inherent in a full-scale girder. A panel is the singular element in the overall local structural system being investigated. Upon loading the panel to its maximum compressive capacity, failure is initiated, and nothing can be done to subsequently improve the strength of the entire system. In relating panels and beams, strict adherence to panel testing procedures and results would lead to an implication that failure of a complete beam is initiated and defined by a single strut attaining a specified compressive loading. This is an incorrect assessment of actual girder behavior. Panel testing does not account for the probability of load redistribution within a girder, especially when considering that successive struts are not equally stressed and maintain varied resistances largely in the presence of nonuniform moments.

As a corollary to the previous points, the panel tests conducted in this study were only a subset of an endless range of possible experiments that could have been run. Experimentation with each and every combination of variables or parameters that might

be incorporated was and would continue to be impractical. Consequently, results and trends established in Chapter 4 and this chapter should be appreciated, but again, not necessarily taken as absolute in every case.

5.5.2 Recommendations for Girder Testing

Girder tests should include four major parameters that were investigated in panel tests to better gauge web crushing capacities. Duct materials, duct diameter-to-thickness ratios, web thicknesses (i.e. size effect), and the use of through-thickness reinforcement should all be considered. Duct banks are not a necessity for girder testing at this time. Modifying concrete or grout strengths is not practical or seemingly necessary according to panel tests when working with strengths in ranges typical of these girders.

5.5.3 Expectations for Girder Testing

As an overview, particular qualitative trends from panel tests can be expected to influence girder web crushing capacity with a high probability. Undoubtedly, girders with empty ducts will behave poorer than those with grouted ducts. It is likely that girders with plastic ducts will maintain lower web crushing capacities than those with steel ducts. Also, web crushing capacity should decrease with increasing duct diameter-to-thickness ratio, at least beyond some ratio.

5.5.4 Preliminary Girder Testing

As part of TxDOT Project 0-6652, the transition from panel to girder testing was initiated with the fabrication and testing of a standard, pretensioned, 46-in. deep Tx Girder (Tx46) with a 7-in. web and a 3-in. diameter plastic post-tensioning duct added. The duct was placed with a straight profile at mid-depth of the girder, and supported by attaching it to stirrups with tie wire without the use of bar supports through the web thickness. The duct was grouted and strands were included in the duct; however, no post-tensioning force was applied. The grout and concrete strengths were similar to those used

for the majority of panel tests. Provision of additional construction details is beyond the scope of this document.

During shear testing of the Tx46 girder, first cracking in the test region was observed to be parallel to and at the level of the duct rather than inclined as is more common. The girder eventually failed by web crushing with spalling of concrete at this location (Figure 5-13).

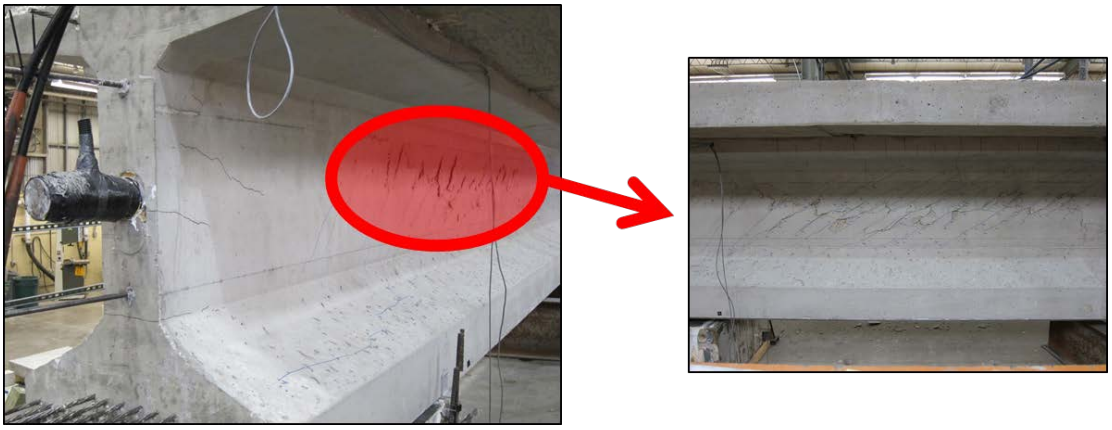

Figure 5-13: Failure of Tx46 Girder with a Duct in the Web

Results and quantitative analysis from this test are only briefly touched upon here. The failure shear load for this girder, V_{test}, was compared to the calculated shear capacity, V_{calc}, obtained with AASHTO MCFT general shear formulas. Various values of V_{calc} were computed using different k-factors, including that given by the general provisions of AASHTO (k = 0.5) and a value of 1.4 calculated from an η_D of 0.4 representative of common plastic-ducted panel failures. With a k-factor of 0.5, V_{test}/V_{calc} was found to be 0.93. With a k-factor of 1.4, V_{test}/V_{calc} was computed as 1.48, a very conservative value but an acceptable factor of safety for shear. A value for V_{test}/V_{calc} of 1.01 was calculated with a k-factor of 1.0. In other words, the failure shear load was accurately predicted by AASHTO calculations assuming that the shear capacity (i.e. web crushing capacity in this case) could be determined based upon only the net

section of concrete at the level of the duct. This was of course found to be the case for plastic-ducted panels with a large amount of through-thickness reinforcement. Ultimately, this finding supports the idea that the boundary conditions of a compressive strut in a girder can help to resist strut splitting and act in the same way as through-thickness reinforcement does in a panel.

5.6 CHAPTER SUMMARY

Panel test results from this study were quantitatively analyzed and experimentally-obtained values of the web width reduction factor were found to be poorly estimated using existing k-factors in current design codes. New k-factors were derived from the results, taking into account not only duct type and grouting, but also the influence of member thickness. The presence of through-thickness reinforcement was also considered, where it was determined that a simple multiplier placed on a k-factor for unreinforced cases could give a more appropriate yet still conservative factor to use. These modified (and lowered) k-factors reflect the benefits of using just a minimal amount of reinforcement in panels near a duct, but it was revealed that more reinforcement could lead to acceptable use of a k-factor of 1.0 as suggested in the literature.

In addition to the k-factor approach for estimating crushing capacity, a new formula was developed to determine capacity based on the “equivalent” transverse tensile resistances of ducted panels. This procedure accounts for the same basic parameters as in the k-factor approach, but is meant to ideally estimate web width reduction factors more directly and accurately without being overly conservative.

Lastly, the link between panel and girder testing was explored. It was explained that trends and behaviors seen in panel testing would potentially be evidenced to some degree during girder testing, although reductions in shear (i.e. web crushing) capacities due to ducts would likely not be as severe. This was verified with a brief look at the first plastic-ducted girder tested following the panel study.

CHAPTER 6
Conclusions and Recommendations

6.1 SUMMARY OF RESEARCH STUDY CONDUCTED

The presence of a post-tensioning duct in the web of a concrete I-girder may reduce the shear capacity due to web crushing. As a prelude and supplement to the shear testing of post-tensioned girders for TxDOT Project 0-6652, a study of concrete panels containing embedded post-tensioning ducts was conducted. These panels were intended to be representations of diagonal compression struts in a girder web subjected to uniaxial, compressive loads.

A comprehensive literature review was conducted at the beginning of the study to understand to impact of using ducts. The provisions of various concrete design codes used throughout the world for girder webs with ducts were studied. It was determined that girder shear capacities are typically adjusted by designing with an effective web width which is equivalent to the gross web width less some portion of the summation of duct diameters within the web that depends on the presence or lack of grout and, on occasion, the duct type. Reductions in the web width may be determined using a fraction referred to as a k-factor. The k-factors differ between many codes, with American codes often specifying some of the least conservative k-factors.

In many past studies of web crushing behavior in post-tensioned girders, ducted panel or prism tests were performed. Researchers used their results to determine capacity reductions for ducted members. These investigators found that crushing capacities are reduced because ducts serve as discontinuities in webs leading to the deviation of principal compressive stress flow and development of tensile stresses through the thickness. Although much work has been done with panel or prism testing, there remains a lack of information from large-scale tests, elements with high concrete strengths, and elements with plastic ducts.

In this study, 100 ducted and solid control panels were tested to confirm past findings, fill in gaps in knowledge, and consider ways in which to improve web crushing capacity. The end goal of this study was to guide research on the shear testing of full-scale girders. Variables considered in the panel tests included: duct type, grouting, concrete and grout strengths, duct diameter-to-thickness ratios, use of through-thickness reinforcement, use of multiple ducts, and specimen thickness.

From the results of panel testing, trends related to the various test parameters were established. A new set of k-factors for use with effective web width formulas were computed to conservatively estimate crushing capacities. Also, a new equation to estimate the web width reduction factor was created to more directly capture the influence of the tensile splitting failure mode of ducted elements.

6.2 RESEARCH FINDINGS

It was shown that, in general, panels with steel ducts have a higher capacity than those with plastic ducts due to the susceptibility of plastic ducts debonding from concrete. Panel thickness matters more than just influencing the duct diameter-to-web thickness ratio, as web width reduction factors drop as thickness increases. Concrete and grout strengths can affect capacity – panels with low concrete strengths or with grout strengths in excess of concrete strengths can have higher capacities than others. However, these material strengths are relatively unimportant given practical ranges of strengths used in girder construction. Using a small but well-distributed and efficiently placed amount of through-thickness reinforcement helped to keep a panel from splitting and enabled it to handle additional load. This amounted to incorporating bars tied to at least the outer vertical bars in panels. Even higher capacities could be achieved if through-thickness reinforcement could be incorporated continuously. In any case, an increase in capacity was achieved by using any shape or orientation of reinforcement as long as part of the reinforcement close to the duct extended through the member thickness above and below the duct. Lastly, duct banks did not reduce the capacity if the ducts were adequately spaced.

6.3 CONCLUSIONS

Many of the factors found to influence panel strength are not considered at all or at least as in-depth in code formulations for web width reduction factors or effective web widths. The use of plastic ducts and effects of member thickness are not adequately addressed. New k-factors for use in code equations were derived, distinguishing between duct types, grouting, and member thickness. The values given are more conservative than those currently adopted by code. These may be utilized with the understanding that reductions in estimated crushing capacity are likely not as severe in girders as in panels. Adjustments to these k-factors will be needed when ducted girder tests are performed. The alternate web width reduction formula that was developed will also require refinement for adequacy and acceptance.

6.4 RECOMMENDATIONS FOR FUTURE RESEARCH

Additional tests should be conducted on panels for validation of strength calculations. More testing should be conducted on 9-in. specimens to better establish the influence of increasing specimen thickness.

The primary focus of future work with regard to shear/web crushing reductions with ducts included in member webs should be on full-scale, post-tensioned girder testing. The shear-testing phase of 62-in. deep I-girders as part of TxDOT Project 0-6652 will explore the behavior of entire members with embedded ducts. Experimentation with these girders needs to include at least three of the most important test parameters determined through panel testing: duct type, member thickness, and the incorporation of through-thickness reinforcement. A fourth parameter, grouting, would be useful to consider, although it may not be worth exploring within the overall scope of the project. Trends and numerical results from girder testing must ultimately be compared to the panel test results to determine if panel tests truly reflect full member behavior. Lastly, the results from girder testing should be used to make any necessary refinements to the k-factors or alternate web width reduction factor formula.

APPENDIX A
Panel Test Data

A.1 EXPLANATION OF INFORMATION

The complete set of data for the 100 panel tests performed in this study is provided in this appendix. Information pertaining to each test is given in five areas:

- *Basic Specimen Information* – Indicates the type of specimen (control or ducted), duct type, grouting, and dates of casting, grouting, and testing.
- *Specimen Dimensions* – Indicates nominal loading surface dimensions, actual specimen thickness and width, panel depth, effective depth, duct diameter(s) and measured duct diameter-to-thickness ratio.
- *Material Properties* – Indicates the concrete and grout strengths, grout-to-concrete strength ratio, and yield strength of primary reinforcement.
- *Failure Information* – Gives failure load, applied stress at failure, and calculated web width reduction factor.
- *Other Information* – Indicates special details unique to each specimen including use of #3 bars as primary reinforcement rather than #4 bars (only for a few cases in Set 1), use of modified duct bond conditions, use of through-thickness reinforcement, or invalidation of test results.

A.2 APPENDIX NOTATION

The following symbols and notations are used in this appendix:

$f_{concrete}$ = average concrete strength during testing

f_{grout} = average grout strength during testing

$f_{y,steel}$ = yield strength of primary reinforcement

h = depth of specimen (parallel to loading direction)

h_{eff} = effective depth (= specimen depth - duct diameter)

$P_{failure}$ = specimen failure load

δ = measured duct diameter-to-thickness ratio

η_D = web width reduction factor (= applied failure stress of ducted specimen / average applied failure stresses of controls in same set with same concrete strength)

$\sigma_{failure}$ = applied stress at failure (= failure load / area of loading surface)

A.3 SET-BY-SET DATA

Data for all panel tests are provided in this section as they pertain to each test set.

A.3.1 Set 1

Basic Specimen Information

Specimen Type	Duct Type	Grouting	Date Cast	Date Grouted	Date Tested
Control	---	---	12/20/2010	---	5/6/2011

Specimen Dimensions

Nominal Loading Surface Dimensions	Actual Thickness	Actual Width	h	Duct Diameter(s)	h_{eff}	δ
24 x 5 in.	5 in.	24 in.	24 in.	---	---	---

P1-1

Material Properties

$f_{concrete}$	f_{grout}	$f_{grout}/f_{concrete}$	$f_{y,\ steel}$
6.23 ksi	---	---	64 ksi

Failure Information

$P_{failure}$	$\sigma_{failure}$	η_D
380.0 kips	3.2 ksi	---

Other Information

*Data not accepted - instrumentation and test frame error

*Includes #3 bars for primary reinforcement

Basic Specimen Information

Specimen Type	Duct Type	Grouting	Date Cast	Date Grouted	Date Tested
Control	---	---	12/20/2010	---	5/17/2011

Specimen Dimensions

Nominal Loading Surface Dimensions	Actual Thickness	Actual Width	h	Duct Diameter(s)	h_{eff}	δ
24 x 5 in.	5 in.	24 in.	24 in.	---	---	---

P1-2

Material Properties

$f_{concrete}$	f_{grout}	$f_{grout}/f_{concrete}$	$f_{y,\ steel}$
6.23 ksi	---	---	67 ksi

Failure Information

$P_{failure}$	$\sigma_{failure}$	η_D
568.0 kips	4.7 ksi	---

Other Information
*Data not accepted - instrumentation and test frame error
*Includes #3 bars for primary reinforcement

Basic Specimen Information

Specimen Type	Duct Type	Grouting	Date Cast	Date Grouted	Date Tested
Control	---	---	12/20/2010	---	6/7/2011

Specimen Dimensions

Nominal Loading Surface Dimensions	Actual Thickness	Actual Width	h	Duct Diameter(s)	h_{eff}	δ
24 x 5 in.	5 in.	24 in.	24 in.	2.375 in.	21.625 in.	---

P1-3

Material Properties

$f_{concrete}$	f_{grout}	$f_{grout}/f_{concrete}$	$f_{y,\ steel}$
6.23 ksi	---	---	66 ksi

Failure Information

$P_{failure}$	$\sigma_{failure}$	η_D
625.2 kips	5.2 ksi	---

Basic Specimen Information

Specimen Type	Duct Type	Grouting	Date Cast	Date Grouted	Date Tested
Ducted	Plastic	Empty	12/20/2010	---	5/10/2011

Specimen Dimensions

Nominal Loading Surface Dimensions	Actual Thickness	Actual Width	h	Duct Diameter(s)	h_{eff}	δ
24 x 5 in.	5 in.	24 in.	24 in.	2.375 in.	21.625 in.	0.475

P1-4

Material Properties

$f_{concrete}$	f_{grout}	$f_{grout}/f_{concrete}$	$f_{y,\ steel}$
6.23 ksi	---	---	64 ksi

Failure Information

$P_{failure}$	$\sigma_{failure}$	η_D
239.0 kips	2.0 ksi	0.38

Other Information
*Data not accepted - instrumentation and test frame error
*Includes #3 bars for primary reinforcement

P1-5

Basic Specimen Information

Specimen Type	Duct Type	Grouting	Date Cast	Date Grouted	Date Tested
Ducted	Plastic	Grouted	12/20/2010	5/31/2011	6/9/2011

Specimen Dimensions

Nominal Loading Surface Dimensions	Actual Thickness	Actual Width	h	Duct Diameter(s)	h_{eff}	δ
24 x 5 in.	5 in.	24 in.	24 in.	2.375 in.	21.625 in.	0.475

Material Properties

$f_{concrete}$	f_{grout}	$f_{grout}/f_{concrete}$	$f_{y,\ steel}$
6.23 ksi	4.30 ksi	0.69	65 ksi

Failure Information

$P_{failure}$	$\sigma_{failure}$	η_D
409.6 kips	3.4 ksi	0.66

P1-6

Basic Specimen Information

Specimen Type	Duct Type	Grouting	Date Cast	Date Grouted	Date Tested
Ducted	Plastic	Grouted	12/20/2010	5/31/2011	6/10/2011

Specimen Dimensions

Nominal Loading Surface Dimensions	Actual Thickness	Actual Width	h	Duct Diameter(s)	h_{eff}	δ
24 x 5 in.	5 in.	24 in.	24 in.	2.375 in.	21.625 in.	0.475

Material Properties

$f_{concrete}$	f_{grout}	$f_{grout}/f_{concrete}$	$f_{y,\ steel}$
6.23 ksi	4.47 ksi	0.72	64 ksi

Failure Information

$P_{failure}$	$\sigma_{failure}$	η_D
403.3 kips	3.4 ksi	0.65

Other Information
*Includes #3 bars for primary reinforcement

P1-7

Basic Specimen Information

Specimen Type	Duct Type	Grouting	Date Cast	Date Grouted	Date Tested
Ducted	Steel	Empty	12/20/2010	---	6/6/2011

Specimen Dimensions

Nominal Loading Surface Dimensions	Actual Thickness	Actual Width	h	Duct Diameter(s)	h_{eff}	δ
24 x 5 in.	5 in.	24 in.	24 in.	2.375 in.	21.625 in.	0.475

Material Properties

$f_{concrete}$	f_{grout}	$f_{grout}/f_{concrete}$	$f_{y,\ steel}$
6.23 ksi	---	---	64 ksi

Failure Information

$P_{failure}$	$\sigma_{failure}$	η_D
267.7 kips	2.2 ksi	0.43

Other Information
*Includes #3 bars for primary reinforcement

P1-8

Basic Specimen Information

Specimen Type	Duct Type	Grouting	Date Cast	Date Grouted	Date Tested
Ducted	Steel	Grouted	12/20/2010	5/31/2011	6/8/2011

Specimen Dimensions

Nominal Loading Surface Dimensions	Actual Thickness	Actual Width	h	Duct Diameter(s)	h_{eff}	δ
24 x 5 in.	5 in.	24 in.	24 in.	2.375 in.	21.625 in.	0.475

Material Properties

$f_{concrete}$	f_{grout}	$f_{grout}/f_{concrete}$	$f_{y,\ steel}$
6.23 ksi	3.99 ksi	0.64	67 ksi

Failure Information

$P_{failure}$	$\sigma_{failure}$	η_D
504.0 kips	4.2 ksi	0.81

Other Information
*Includes #3 bars for primary reinforcement

P1-9

Basic Specimen Information

Specimen Type	Duct Type	Grouting	Date Cast	Date Grouted	Date Tested
Ducted	Steel	Grouted	12/20/2010	5/31/2011	6/9/2011

Specimen Dimensions

Nominal Loading Surface Dimensions	Actual Thickness	Actual Width	h	Duct Diameter(s)	h_{eff}	δ
24 x 5 in.	5 in.	24 in.	24 in.	2.375 in.	21.625 in.	0.475

Material Properties

$f_{concrete}$	f_{grout}	$f_{grout}/f_{concrete}$	$f_{y,\ steel}$
6.23 ksi	4.30 ksi	0.69	65 ksi

Failure Information

$P_{failure}$	$\sigma_{failure}$	η_D
536.3 kips	4.5 ksi	0.86

A.3.2 Set 2

P2-1

Basic Specimen Information

Specimen Type	Duct Type	Grouting	Date Cast	Date Grouted	Date Tested
Control	---	---	6/2/2011	---	6/30/2011

Specimen Dimensions

Nominal Loading Surface Dimensions	Actual Thickness	Actual Width	h	Duct Diameter(s)	h_{eff}	δ
24 x 7 in.	6.9375 in.	24 in.	24 in.	---	---	---

Material Properties

$f_{concrete}$	f_{grout}	$f_{grout}/f_{concrete}$	$f_{y,\ steel}$
9.69 ksi	---	---	

Failure Information

$P_{failure}$	$\sigma_{failure}$	η_D
1195.0 kips	7.2 ksi	---

P2-2

Basic Specimen Information

Specimen Type	Duct Type	Grouting	Date Cast	Date Grouted	Date Tested
Control	---	---	6/2/2011	---	7/1/2011

Specimen Dimensions

Nominal Loading Surface Dimensions	Actual Thickness	Actual Width	h	Duct Diameter(s)	h_{eff}	δ
24 x 7 in.	7 in.	23.9375 in.	24 in.	---	---	---

Material Properties

$f_{concrete}$	f_{grout}	$f_{grout}/f_{concrete}$	$f_{y,\ steel}$
9.69 ksi	---	---	66 ksi

Failure Information

$P_{failure}$	$\sigma_{failure}$	η_D
1264.9 kips	7.5 ksi	---

P2-3

Basic Specimen Information

Specimen Type	Duct Type	Grouting	Date Cast	Date Grouted	Date Tested
Ducted	Plastic	Empty	6/2/2011	---	6/29/2011

Specimen Dimensions

Nominal Loading Surface Dimensions	Actual Thickness	Actual Width	h	Duct Diameter(s)	h_{eff}	δ
24 x 7 in.	7 in.	24 in.	24 in.	3 in.	21 in.	0.429

Material Properties

$f_{concrete}$	f_{grout}	$f_{grout}/f_{concrete}$	$f_{y,\ steel}$
9.69 ksi	---	---	66 ksi

Failure Information

$P_{failure}$	$\sigma_{failure}$	η_D
418.5 kips	2.5 ksi	0.34

Other Information
*Includes #2 bars through-thickness in 'close' position at outer two vertical bars

P2-4

Basic Specimen Information

Specimen Type	Duct Type	Grouting	Date Cast	Date Grouted	Date Tested
Ducted	Plastic	Grouted	6/2/2011	6/10/2011	7/1/2011

Specimen Dimensions

Nominal Loading Surface Dimensions	Actual Thickness	Actual Width	h	Duct Diameter(s)	h_{eff}	δ
24 x 7 in.	7.0625 in.	24 in.	24 in.	3 in.	21 in.	0.425

Material Properties

$f_{concrete}$	f_{grout}	$f_{grout}/f_{concrete}$	$f_{y,\ steel}$
9.69 ksi	5.56 ksi	0.57	66 ksi

Failure Information

$P_{failure}$	$\sigma_{failure}$	η_D
643.7 kips	3.8 ksi	0.52

Other Information
*Includes #2 bars through-thickness in 'close' position at outer two vertical bars

P2-5

Basic Specimen Information

Specimen Type	Duct Type	Grouting	Date Cast	Date Grouted	Date Tested
Ducted	Plastic	Grouted	6/2/2011	6/10/2011	7/7/2011

Specimen Dimensions

Nominal Loading Surface Dimensions	Actual Thickness	Actual Width	h	Duct Diameter(s)	h_{eff}	δ
24 x 7 in.	7.0625 in.	24 in.	24 in.	3 in.	21 in.	0.425

Material Properties

$f_{concrete}$	f_{grout}	$f_{grout}/f_{concrete}$	$f_{y,\ steel}$
9.69 ksi	5.56 ksi	0.57	66 ksi

Failure Information

$P_{failure}$	$\sigma_{failure}$	η_D
618.1 kips	3.6 ksi	0.50

Other Information

*Includes #2 bars through-thickness in 'close' position at outer two vertical bars

P2-6

Basic Specimen Information

Specimen Type	Duct Type	Grouting	Date Cast	Date Grouted	Date Tested
Ducted	Plastic	Grouted	6/2/2011	6/10/2011	7/7/2011

Specimen Dimensions

Nominal Loading Surface Dimensions	Actual Thickness	Actual Width	h	Duct Diameter(s)	h_{eff}	δ
24 x 7 in.	7 in.	24 in.	24 in.	3 in.	21 in.	0.429

Material Properties

$f_{concrete}$	f_{grout}	$f_{grout}/f_{concrete}$	$f_{y,\ steel}$
9.69 ksi	5.56 ksi	0.57	66 ksi

Failure Information

$P_{failure}$	$\sigma_{failure}$	η_D
633.3 kips	3.8 ksi	0.51

Other Information

*Includes #2 bars through-thickness in 'close' position at outer two vertical bars

P2-7

Basic Specimen Information

Specimen Type	Duct Type	Grouting	Date Cast	Date Grouted	Date Tested
Ducted	Steel	Empty	6/2/2011	---	6/28/2011

Specimen Dimensions

Nominal Loading Surface Dimensions	Actual Thickness	Actual Width	h	Duct Diameter(s)	h_{eff}	δ
24 x 7 in.	7 in.	24 in.	24 in.	3 in.	21 in.	0.429

Material Properties

$f_{concrete}$	f_{grout}	$f_{grout}/f_{concrete}$	$f_{y,\ steel}$
9.69 ksi	---	---	66 ksi

Failure Information

$P_{failure}$	$\sigma_{failure}$	η_D
486.1 kips	2.9 ksi	0.39

Other Information

*Includes #2 bars through-thickness in 'close' position at outer two vertical bars

P2-8

Basic Specimen Information

Specimen Type	Duct Type	Grouting	Date Cast	Date Grouted	Date Tested
Ducted	Steel	Grouted	6/2/2011	6/10/2011	6/29/2011

Specimen Dimensions

Nominal Loading Surface Dimensions	Actual Thickness	Actual Width	h	Duct Diameter(s)	h_{eff}	δ
24 x 7 in.	7 in.	23 in.	24 in.	3 in.	21 in.	0.429

Material Properties

$f_{concrete}$	f_{grout}	$f_{grout}/f_{concrete}$	$f_{y,\ steel}$
9.69 ksi	5.56 ksi	0.57	66 ksi

Failure Information

$P_{failure}$	$\sigma_{failure}$	η_D
915.3 kips	5.7 ksi	0.77

Other Information

*Includes #2 bars through-thickness in 'close' position at outer two vertical bars

P2-9

Basic Specimen Information

Specimen Type	Duct Type	Grouting	Date Cast	Date Grouted	Date Tested
Ducted	Steel	Grouted	6/2/2011	6/10/2011	6/30/2011

Specimen Dimensions

Nominal Loading Surface Dimensions	Actual Thickness	Actual Width	h	Duct Diameter(s)	h_{eff}	δ
24 x 7 in.	7.0625 in.	24 in.	24 in.	3 in.	21 in.	0.425

Material Properties

$f_{concrete}$	f_{grout}	$f_{grout}/f_{concrete}$	$f_{y,\ steel}$
9.69 ksi	5.56 ksi	0.57	66 ksi

Failure Information

$P_{failure}$	$\sigma_{failure}$	η_D
944.5 kips	5.6 ksi	0.76

Other Information

*Includes #2 bars through-thickness in 'close' position at outer two vertical bars

A.3.3 Set 3

P3-1

Basic Specimen Information

Specimen Type	Duct Type	Grouting	Date Cast	Date Grouted	Date Tested
Control	---	---	6/20/2011	---	7/29/2011

Specimen Dimensions

Nominal Loading Surface Dimensions	Actual Thickness	Actual Width	h	Duct Diameter(s)	h_{eff}	δ
24 x 7 in.	7 in.	23.9375 in.	24 in.	---	---	---

Material Properties

$f_{concrete}$	f_{grout}	$f_{grout}/f_{concrete}$	$f_{y,\ steel}$
9.39 ksi	---	---	63 ksi

Failure Information

$P_{failure}$	$\sigma_{failure}$	η_D
1192.7 kips	7.1 ksi	---

P3-2

Basic Specimen Information

Specimen Type	Duct Type	Grouting	Date Cast	Date Grouted	Date Tested
Control	---	---	6/20/2011	---	8/4/2011

Specimen Dimensions

Nominal Loading Surface Dimensions	Actual Thickness	Actual Width	h	Duct Diameter(s)	h_{eff}	δ
24 x 7 in.	7 in.	23.875 in.	24 in.	---	---	---

Material Properties

$f_{concrete}$	f_{grout}	$f_{grout}/f_{concrete}$	$f_{y,\ steel}$
9.39 ksi	---	---	66 ksi

Failure Information

$P_{failure}$	$\sigma_{failure}$	η_D
1527.2 kips	9.1 ksi	---

P3-3

Basic Specimen Information

Specimen Type	Duct Type	Grouting	Date Cast	Date Grouted	Date Tested
Ducted	Plastic	Grouted	6/20/2011	7/8/2011	7/28/2011

Specimen Dimensions

Nominal Loading Surface Dimensions	Actual Thickness	Actual Width	h	Duct Diameter(s)	h_{eff}	δ
24 x 7 in.	7.0625 in.	24 in.	24 in.	3 in.	21 in.	0.425

Material Properties

$f_{concrete}$	f_{grout}	$f_{grout}/f_{concrete}$	$f_{y,\ steel}$
9.39 ksi	5.29 ksi	0.56	63 ksi

Failure Information

$P_{failure}$	$\sigma_{failure}$	η_D
506.0 kips	3.0 ksi	0.37

P3-4

Basic Specimen Information

Specimen Type	Duct Type	Grouting	Date Cast	Date Grouted	Date Tested
Ducted	Plastic	Grouted	6/20/2011	7/8/2011	7/28/2011

Specimen Dimensions

Nominal Loading Surface Dimensions	Actual Thickness	Actual Width	h	Duct Diameter(s)	h_{eff}	δ
24 x 7 in.	7.0625 in.	24.125 in.	24 in.	3 in.	21 in.	0.425

Material Properties

$f_{concrete}$	f_{grout}	$f_{grout}/f_{concrete}$	$f_{y,\ steel}$
9.39 ksi	5.29 ksi	0.56	66 ksi

Failure Information

$P_{failure}$	$\sigma_{failure}$	η_D
499.9 kips	2.9 ksi	0.36

P3-5

Basic Specimen Information

Specimen Type	Duct Type	Grouting	Date Cast	Date Grouted	Date Tested
Ducted	Plastic	Empty	6/20/2011	3 in.	7/29/2011

Specimen Dimensions

Nominal Loading Surface Dimensions	Actual Thickness	Actual Width	h	Duct Diameter(s)	h_{eff}	δ
24 x 7 in.	7 in.	24.125 in.	24 in.	3 in.	21 in.	0.429

Material Properties

$f_{concrete}$	f_{grout}	$f_{grout}/f_{concrete}$	$f_{y,\ steel}$
9.39 ksi	---	---	66 ksi

Failure Information

$P_{failure}$	$\sigma_{failure}$	η_D
294.2 kips	1.7 ksi	0.21

P3-6

Basic Specimen Information

Specimen Type	Duct Type	Grouting	Date Cast	Date Grouted	Date Tested
Ducted	Plastic	Grouted	6/20/2011	7/8/2011	8/2/2011

Specimen Dimensions

Nominal Loading Surface Dimensions	Actual Thickness	Actual Width	h	Duct Diameter(s)	h_{eff}	δ
24 x 7 in.	7 in.	24.0625 in.	24 in.	3 in.	21 in.	0.429

Material Properties

$f_{concrete}$	f_{grout}	$f_{grout}/f_{concrete}$	$f_{y,\ steel}$
9.39 ksi	5.29 ksi	0.56	66 ksi

Failure Information

$P_{failure}$	$\sigma_{failure}$	η_D
482.4 kips	2.9 ksi	0.35

P3-7

Basic Specimen Information

Specimen Type	Duct Type	Grouting	Date Cast	Date Grouted	Date Tested
Ducted	Steel	Empty	6/20/2011	---	7/29/2011

Specimen Dimensions

Nominal Loading Surface Dimensions	Actual Thickness	Actual Width	h	Duct Diameter(s)	h_{eff}	δ
24 x 7 in.	7 in.	23.9375 in.	24 in.	3 in.	21 in.	0.429

Material Properties

$f_{concrete}$	f_{grout}	$f_{grout}/f_{concrete}$	$f_{y,\ steel}$
9.39 ksi	---	---	63 ksi

Failure Information

$P_{failure}$	$\sigma_{failure}$	η_D
298.8 kips	1.8 ksi	0.22

P3-8

Basic Specimen Information

Specimen Type	Duct Type	Grouting	Date Cast	Date Grouted	Date Tested
Ducted	Steel	Grouted	6/20/2011	7/8/2011	8/3/2011

Specimen Dimensions

Nominal Loading Surface Dimensions	Actual Thickness	Actual Width	h	Duct Diameter(s)	h_{eff}	δ
24 x 7 in.	7.0625 in.	23.9375 in.	24 in.	3 in.	21 in.	0.425

Material Properties

$f_{concrete}$	f_{grout}	$f_{grout}/f_{concrete}$	$f_{y,\ steel}$
9.39 ksi	5.29 ksi	0.56	63 ksi

Failure Information

$P_{failure}$	$\sigma_{failure}$	η_D
778.6 kips	4.6 ksi	0.57

P3-9

Basic Specimen Information

Specimen Type	Duct Type	Grouting	Date Cast	Date Grouted	Date Tested
Ducted	Steel	Grouted	6/20/2011	7/8/2011	8/3/2011

Specimen Dimensions

Nominal Loading Surface Dimensions	Actual Thickness	Actual Width	h	Duct Diameter(s)	h_{eff}	δ
24 x 7 in.	7.0625 in.	24.125 in.	24 in.	3 in.	21 in.	0.425

Material Properties

$f_{concrete}$	f_{grout}	$f_{grout}/f_{concrete}$	$f_{y,\ steel}$
9.39 ksi	5.29 ksi	---	63 ksi

Failure Information

$P_{failure}$	$\sigma_{failure}$	η_D
720.7 kips	4.2 ksi	0.52

A.3.4 Set 4

P4-1

Basic Specimen Information

Specimen Type	Duct Type	Grouting	Date Cast	Date Grouted	Date Tested
Control	---	---	8/2/2011	---	8/24/2011

Specimen Dimensions

Nominal Loading Surface Dimensions	Actual Thickness	Actual Width	h	Duct Diameter(s)	h_{eff}	δ
24 x 7 in.	7.125 in.	23.875 in.	24 in.	---	---	---

Material Properties

$f_{concrete}$	f_{grout}	$f_{grout}/f_{concrete}$	$f_{y,\ steel}$
8.17 ksi	---	---	63 ksi

Failure Information

$P_{failure}$	$\sigma_{failure}$	η_D
1016.9 kips	6.0 ksi	---

P4-2

Basic Specimen Information

Specimen Type	Duct Type	Grouting	Date Cast	Date Grouted	Date Tested
Control	---	---	8/2/2011	---	9/12/2011

Specimen Dimensions

Nominal Loading Surface Dimensions	Actual Thickness	Actual Width	h	Duct Diameter(s)	h_{eff}	δ
24 x 7 in.	7.125 in.	24 in.	24 in.	---	---	---

Material Properties

$f_{concrete}$	f_{grout}	$f_{grout}/f_{concrete}$	$f_{y,\ steel}$
8.60 ksi	---	---	63 ksi

Failure Information

$P_{failure}$	$\sigma_{failure}$	η_D
1143.5 kips	6.7 ksi	---

P4-3

Basic Specimen Information

Specimen Type	Duct Type	Grouting	Date Cast	Date Grouted	Date Tested
Ducted	Plastic	Grouted	8/2/2011	8/8/2011	8/22/2011

Specimen Dimensions

Nominal Loading Surface Dimensions	Actual Thickness	Actual Width	h	Duct Diameter(s)	h_{eff}	δ
24 x 7 in.	7.125 in.	24.0625 in.	24 in.	3 in.	21 in.	0.421

Material Properties

$f_{concrete}$	f_{grout}	$f_{grout}/f_{concrete}$	$f_{y,\ steel}$
8.17 ksi	4.66 ksi	0.57	63 ksi

Failure Information

$P_{failure}$	$\sigma_{failure}$	η_D
487.8 kips	2.8 ksi	0.48

Other Information
*Includes five sets of #3 'normal' hairpins in 'far' position

P4-4

Basic Specimen Information

Specimen Type	Duct Type	Grouting	Date Cast	Date Grouted	Date Tested
Ducted	Plastic	Grouted	8/2/2011	8/8/2011	8/23/2011

Specimen Dimensions

Nominal Loading Surface Dimensions	Actual Thickness	Actual Width	h	Duct Diameter(s)	h_{eff}	δ
24 x 7 in.	7.125 in.	24 in.	24 in.	3 in.	21 in.	0.421

Material Properties

$f_{concrete}$	f_{grout}	$f_{grout}/f_{concrete}$	$f_{y,\ steel}$
8.17 ksi	4.66 ksi	0.57	63 ksi

Failure Information

$P_{failure}$	$\sigma_{failure}$	η_D
581.1 kips	3.4 ksi	0.57

Other Information
*Includes five sets of #3 'normal' hairpins in 'close' position

P4-5

Basic Specimen Information

Specimen Type	Duct Type	Grouting	Date Cast	Date Grouted	Date Tested
Ducted	Plastic	Grouted	8/2/2011	8/8/2011	8/23/2011

Specimen Dimensions

Nominal Loading Surface Dimensions	Actual Thickness	Actual Width	h	Duct Diameter(s)	h_{eff}	δ
24 x 7 in.	7.125 in.	23.9375 in.	24 in.	3 in.	21 in.	0.421

Material Properties

$f_{concrete}$	f_{grout}	$f_{grout}/f_{concrete}$	$f_{y,\ steel}$
8.17 ksi	4.66 ksi	0.57	63 ksi

Failure Information

$P_{failure}$	$\sigma_{failure}$	η_D
401.6 kips	2.4 ksi	0.39

P4-6

Basic Specimen Information

Specimen Type	Duct Type	Grouting	Date Cast	Date Grouted	Date Tested
Ducted	Plastic	Grouted	8/2/2011	8/8/2011	8/26/2011

Specimen Dimensions

Nominal Loading Surface Dimensions	Actual Thickness	Actual Width	h	Duct Diameter(s)	h_{eff}	δ
24 x 7 in.	7.125 in.	24 in.	24 in.	3 in.	21 in.	0.421

Material Properties

$f_{concrete}$	f_{grout}	$f_{grout}/f_{concrete}$	$f_{y,\ steel}$
8.17 ksi	4.66 ksi	0.57	63 ksi

Failure Information

$P_{failure}$	$\sigma_{failure}$	η_D
394.2 kips	2.3 ksi	0.39

Other Information
*Waxed Duct

P4-7

Basic Specimen Information

Specimen Type	Duct Type	Grouting	Date Cast	Date Grouted	Date Tested
Ducted	Steel	Grouted	8/2/2011	8/8/2011	9/9/2011

Specimen Dimensions

Nominal Loading Surface Dimensions	Actual Thickness	Actual Width	h	Duct Diameter(s)	h_{eff}	δ
24 x 7 in.	7.125 in.	24.0625 in.	24 in.	3 in.	21 in.	0.421

Material Properties

$f_{concrete}$	f_{grout}	$f_{grout}/f_{concrete}$	$f_{y,\ steel}$
8.60 ksi	5.06 ksi	0.59	63 ksi

Failure Information

$P_{failure}$	$\sigma_{failure}$	η_D
606.9 kips	3.5 ksi	0.53

P4-8

Basic Specimen Information

Specimen Type	Duct Type	Grouting	Date Cast	Date Grouted	Date Tested
Ducted	Steel	Grouted	8/2/2011	8/8/2011	9/7/2011

Specimen Dimensions

Nominal Loading Surface Dimensions	Actual Thickness	Actual Width	h	Duct Diameter(s)	h_{eff}	δ
24 x 7 in.	7.125 in.	24 in.	24 in.	3 in.	21 in.	0.421

Material Properties

$f_{concrete}$	f_{grout}	$f_{grout}/f_{concrete}$	$f_{y,\ steel}$
8.60 ksi	5.06 ksi	0.59	63 ksi

Failure Information

$P_{failure}$	$\sigma_{failure}$	η_D
563.8 kips	3.3 ksi	0.49

Other Information
*Waxed duct

P4-9

Basic Specimen Information

Specimen Type	Duct Type	Grouting	Date Cast	Date Grouted	Date Tested
Ducted	Steel	Grouted	8/2/2011	8/8/2011	8/23/2011

Specimen Dimensions

Nominal Loading Surface Dimensions	Actual Thickness	Actual Width	h	Duct Diameter(s)	h_{eff}	δ
24 x 7 in.	7.0625 in.	24.1875 in.	24 in.	3 in.	21 in.	0.425

Material Properties

$f_{concrete}$	f_{grout}	$f_{grout}/f_{concrete}$	$f_{y,\ steel}$
8.17 ksi	4.66 ksi	0.57	63 ksi

Failure Information

$P_{failure}$	$\sigma_{failure}$	η_D
431.6 kips	2.5 ksi	0.42

Other Information
*Waxed duct

A.3.5 Set 5

P5-1

Basic Specimen Information

Specimen Type	Duct Type	Grouting	Date Cast	Date Grouted	Date Tested
Control	---	---	8/19/2011	---	9/23/2011

Specimen Dimensions

Nominal Loading Surface Dimensions	Actual Thickness	Actual Width	h	Duct Diameter(s)	h_{eff}	δ
24 x 7 in.	7 in.	23.75 in.	24 in.	---	---	---

Material Properties

$f_{concrete}$	f_{grout}	$f_{grout}/f_{concrete}$	$f_{y,\ steel}$
3.62 ksi	---	---	63 ksi

Failure Information

$P_{failure}$	$\sigma_{failure}$	η_D
515.4 kips	3.1 ksi	---

P5-2

Basic Specimen Information

Specimen Type	Duct Type	Grouting	Date Cast	Date Grouted	Date Tested
Control	---	---	8/19/2011	---	9/28/2011

Specimen Dimensions

Nominal Loading Surface Dimensions	Actual Thickness	Actual Width	h	Duct Diameter(s)	h_{eff}	δ
24 x 7 in.	7.0625 in.	24 in.	24 in.	---	---	---

Material Properties

$f_{concrete}$	f_{grout}	$f_{grout}/f_{concrete}$	$f_{y,\ steel}$
3.62 ksi	---	---	63 ksi

Failure Information

$P_{failure}$	$\sigma_{failure}$	η_D
493.9 kips	2.9 ksi	---

P5-3

Basic Specimen Information

Specimen Type	Duct Type	Grouting	Date Cast	Date Grouted	Date Tested
Ducted	Plastic	Grouted	8/19/2011	9/8/2011	9/22/2011

Specimen Dimensions

Nominal Loading Surface Dimensions	Actual Thickness	Actual Width	h	Duct Diameter(s)	h_{eff}	δ
24 x 7 in.	7.125 in.	24.25 in.	24 in.	3 in.	21 in.	0.421

Material Properties

$f_{concrete}$	f_{grout}	$f_{grout}/f_{concrete}$	$f_{y,\ steel}$
3.62 ksi	2.30 ksi	0.64	63 ksi

Failure Information

$P_{failure}$	$\sigma_{failure}$	η_D
356.0 kips	2.1 ksi	0.69

Other Information

*Includes #3 'normal' hairpins in 'close' position at outer two vertical bars

P5-4

Basic Specimen Information

Specimen Type	Duct Type	Grouting	Date Cast	Date Grouted	Date Tested
Ducted	Plastic	Grouted	8/19/2011	9/8/2011	9/21/2011

Specimen Dimensions

Nominal Loading Surface Dimensions	Actual Thickness	Actual Width	h	Duct Diameter(s)	h_{eff}	δ
24 x 7 in.	7 in.	24.125 in.	24 in.	3 in.	21 in.	0.429

Material Properties

$f_{concrete}$	f_{grout}	$f_{grout}/f_{concrete}$	$f_{y,\ steel}$
3.62 ksi	2.30 ksi	0.64	63 ksi

Failure Information

$P_{failure}$	$\sigma_{failure}$	η_D
302.8 kips	1.8 ksi	0.60

P5-5

Basic Specimen Information

Specimen Type	Duct Type	Grouting	Date Cast	Date Grouted	Date Tested
Ducted	Plastic	Grouted	8/19/2011	9/8/2011	9/26/2011

Specimen Dimensions

Nominal Loading Surface Dimensions	Actual Thickness	Actual Width	h	Duct Diameter(s)	h_{eff}	δ
24 x 7 in.	7.125 in.	24 in.	24 in.	3 in.	21 in.	0.421

Material Properties

$f_{concrete}$	f_{grout}	$f_{grout}/f_{concrete}$	$f_{y,\ steel}$
3.62 ksi	5.49 ksi	1.52	63 ksi

Failure Information

$P_{failure}$	$\sigma_{failure}$	η_D
328.9 kips	1.9 ksi	0.64

P5-6

Basic Specimen Information

Specimen Type	Duct Type	Grouting	Date Cast	Date Grouted	Date Tested
Ducted	Plastic	Grouted	8/19/2011	9/8/2011	9/27/2011

Specimen Dimensions

Nominal Loading Surface Dimensions	Actual Thickness	Actual Width	h	Duct Diameter(s)	h_{eff}	δ
24 x 7 in.	7.125 in.	24 in.	24 in.	3 in.	21 in.	0.421

Material Properties

$f_{concrete}$	f_{grout}	$f_{grout}/f_{concrete}$	$f_{y,\ steel}$
3.62 ksi	10.62 ksi	2.93	63 ksi

Failure Information

$P_{failure}$	$\sigma_{failure}$	η_D
414.3 kips	2.4 ksi	0.81

P5-7

Basic Specimen Information

Specimen Type	Duct Type	Grouting	Date Cast	Date Grouted	Date Tested
Ducted	Plastic	Grouted	8/19/2011	9/8/2011	9/22/2011

Specimen Dimensions

Nominal Loading Surface Dimensions	Actual Thickness	Actual Width	h	Duct Diameter(s)	h_{eff}	δ
24 x 7 in.	7.125 in.	24 in.	24 in.	3 in.	21 in.	0.421

Material Properties

$f_{concrete}$	f_{grout}	$f_{grout}/f_{concrete}$	$f_{y,\ steel}$
3.62 ksi	2.30 ksi	0.64	63 ksi

Failure Information

$P_{failure}$	$\sigma_{failure}$	η_D
422.8 kips	2.5 ksi	0.82

P5-8

Basic Specimen Information

Specimen Type	Duct Type	Grouting	Date Cast	Date Grouted	Date Tested
Ducted	Plastic	Grouted	8/19/2011	9/8/2011	9/26/2011

Specimen Dimensions

Nominal Loading Surface Dimensions	Actual Thickness	Actual Width	h	Duct Diameter(s)	h_{eff}	δ
24 x 7 in.	7.125 in.	24 in.	24 in.	3 in.	21 in.	0.421

Material Properties

$f_{concrete}$	f_{grout}	$f_{grout}/f_{concrete}$	$f_{y,\ steel}$
3.62 ksi	5.49 ksi	1.52	63 ksi

Failure Information

$P_{failure}$	$\sigma_{failure}$	η_D
524.9 kips	3.1 ksi	1.02

P5-9

Basic Specimen Information

Specimen Type	Duct Type	Grouting	Date Cast	Date Grouted	Date Tested
Ducted	Plastic	Grouted	8/19/2011	9/8/2011	9/28/2011

Specimen Dimensions

Nominal Loading Surface Dimensions	Actual Thickness	Actual Width	h	Duct Diameter(s)	h_{eff}	δ
24 x 7 in.	7.125 in.	24 in.	24 in.	3 in.	21 in.	0.421

Material Properties

$f_{concrete}$	f_{grout}	$f_{grout}/f_{concrete}$	$f_{y,\ steel}$
3.62 ksi	10.62 ksi	2.93	63 ksi

Failure Information

$P_{failure}$	$\sigma_{failure}$	η_D
560.5 kips	3.3 ksi	1.09

A.3.6 Set 6

P6-1

Basic Specimen Information

Specimen Type	Duct Type	Grouting	Date Cast	Date Grouted	Date Tested
Control	---	---	9/8/2011	---	10/12/2011

Specimen Dimensions

Nominal Loading Surface Dimensions	Actual Thickness	Actual Width	h	Duct Diameter(s)	h_{eff}	δ
24 x 7 in.	7.0625 in.	24.3125 in.	24 in.	---	---	---

Material Properties

$f_{concrete}$	f_{grout}	$f_{grout}/f_{concrete}$	$f_{y,\ steel}$
9.61 ksi	---	---	63 ksi

Failure Information

$P_{failure}$	$\sigma_{failure}$	η_D
1304.6 kips	7.6 ksi	---

P6-2

Basic Specimen Information

Specimen Type	Duct Type	Grouting	Date Cast	Date Grouted	Date Tested
Control	---	---	9/8/2011	---	10/18/2011

Specimen Dimensions

Nominal Loading Surface Dimensions	Actual Thickness	Actual Width	h	Duct Diameter(s)	h_{eff}	δ
24 x 7 in.	7 in.	23.9375 in.	24 in.	---	---	---

Material Properties

$f_{concrete}$	f_{grout}	$f_{grout}/f_{concrete}$	$f_{y,\ steel}$
9.61 ksi	---	---	63 ksi

Failure Information

$P_{failure}$	$\sigma_{failure}$	η_D
1512.3 kips	9.0 ksi	---

P6-3

Basic Specimen Information

Specimen Type	Duct Type	Grouting	Date Cast	Date Grouted	Date Tested
Ducted	Plastic	Grouted	9/8/2011	9/19/2011	10/10/2011

Specimen Dimensions

Nominal Loading Surface Dimensions	Actual Thickness	Actual Width	h	Duct Diameter(s)	h_{eff}	δ
24 x 7 in.	7 in.	24.25 in.	24 in.	3 in.	21 in.	0.429

Material Properties

$f_{concrete}$	f_{grout}	$f_{grout}/f_{concrete}$	$f_{y,\ steel}$
9.61 ksi	4.81 ksi	0.50	63 ksi

Failure Information

$P_{failure}$	$\sigma_{failure}$	η_D
407.1 kips	2.4 ksi	0.29

Other Information
*Includes #3 'normal' hairpins in 'far' position at outer two vertical bars

P6-4

Basic Specimen Information

Specimen Type	Duct Type	Grouting	Date Cast	Date Grouted	Date Tested
Ducted	Plastic	Grouted	9/8/2011	9/19/2011	10/11/2011

Specimen Dimensions

Nominal Loading Surface Dimensions	Actual Thickness	Actual Width	h	Duct Diameter(s)	h_{eff}	δ
24 x 7 in.	7.0625 in.	24 in.	24 in.	3 in.	21 in.	0.425

Material Properties

$f_{concrete}$	f_{grout}	$f_{grout}/f_{concrete}$	$f_{y,\ steel}$
9.61 ksi	4.81 ksi	0.50	63 ksi

Failure Information

$P_{failure}$	$\sigma_{failure}$	η_D
442.5 kips	2.6 ksi	0.31

Other Information

*Includes #3 'normal' hairpins in 'far' position at all vertical bars

P6-5

Basic Specimen Information

Specimen Type	Duct Type	Grouting	Date Cast	Date Grouted	Date Tested
Ducted	Plastic	Grouted	9/8/2011	9/19/2011	10/11/2011

Specimen Dimensions

Nominal Loading Surface Dimensions	Actual Thickness	Actual Width	h	Duct Diameter(s)	h_{eff}	δ
24 x 7 in.	7 in.	24 in.	24 in.	3 in.	21 in.	0.429

Material Properties

$f_{concrete}$	f_{grout}	$f_{grout}/f_{concrete}$	$f_{y,\ steel}$
9.61 ksi	4.81 ksi	0.50	63 ksi

Failure Information

$P_{failure}$	$\sigma_{failure}$	η_D
482.0 kips	2.9 ksi	0.35

Other Information

*Includes #3 'normal' hairpins in 'midway' position at outer two vertical bars

P6-6

Basic Specimen Information

Specimen Type	Duct Type	Grouting	Date Cast	Date Grouted	Date Tested
Ducted	Plastic	Grouted	9/8/2011	9/19/2011	10/13/2011

Specimen Dimensions

Nominal Loading Surface Dimensions	Actual Thickness	Actual Width	h	Duct Diameter(s)	h_{eff}	δ
24 x 7 in.	7.25 in.	24.0625 in.	24 in.	3 in.	21 in.	0.414

Material Properties

$f_{concrete}$	f_{grout}	$f_{grout}/f_{concrete}$	$f_{y,\ steel}$
9.61 ksi	4.81 ksi	0.50	64 ksi

Failure Information

$P_{failure}$	$\sigma_{failure}$	η_D
580.6 kips	3.3 ksi	0.40

Other Information

*Includes #3 'normal' hairpins in 'midway' position at all vertical bars

P6-7

Basic Specimen Information

Specimen Type	Duct Type	Grouting	Date Cast	Date Grouted	Date Tested
Ducted	Plastic	Grouted	9/8/2011	9/19/2011	10/14/2011

Specimen Dimensions

Nominal Loading Surface Dimensions	Actual Thickness	Actual Width	h	Duct Diameter(s)	h_{eff}	δ
24 x 7 in.	7.125 in.	24.125 in.	24 in.	3 in.	21 in.	0.421

Material Properties

$f_{concrete}$	f_{grout}	$f_{grout}/f_{concrete}$	$f_{y,\ steel}$
9.61 ksi	4.81 ksi	0.50	64 ksi

Failure Information

$P_{failure}$	$\sigma_{failure}$	η_D
631.8 kips	3.7 ksi	0.44

Other Information

*Includes #3 'normal' hairpins in 'close' position at outer two vertical bars

P6-8

Basic Specimen Information

Specimen Type	Duct Type	Grouting	Date Cast	Date Grouted	Date Tested
Ducted	Plastic	Grouted	9/8/2011	9/19/2011	10/17/2011

Specimen Dimensions

Nominal Loading Surface Dimensions	Actual Thickness	Actual Width	h	Duct Diameter(s)	h_{eff}	δ
24 x 7 in.	7.0625 in.	24.25 in.	24 in.	3 in.	21 in.	0.425

Material Properties

$f_{concrete}$	f_{grout}	$f_{grout}/f_{concrete}$	$f_{y,\ steel}$
9.61 ksi	4.81 ksi	0.50	64 ksi

Failure Information

$P_{failure}$	$\sigma_{failure}$	η_D
640.5 kips	3.7 ksi	0.45

Other Information

*Includes #3 'normal' hairpins in 'close' position at all vertical bars

P6-9

Basic Specimen Information

Specimen Type	Duct Type	Grouting	Date Cast	Date Grouted	Date Tested
Ducted	Plastic	Grouted	9/8/2011	9/19/2011	10/17/2011

Specimen Dimensions

Nominal Loading Surface Dimensions	Actual Thickness	Actual Width	h	Duct Diameter(s)	h_{eff}	δ
24 x 7 in.	7.125 in.	23.9375 in.	24 in.	3 in.	21 in.	0.421

Material Properties

$f_{concrete}$	f_{grout}	$f_{grout}/f_{concrete}$	$f_{y,\ steel}$
9.61 ksi	4.81 ksi	0.50	64 ksi

Failure Information

$P_{failure}$	$\sigma_{failure}$	η_D
642.0 kips	3.8 ksi	0.45

Other Information

*Includes #3 'normal' hairpins against duct at outer two vertical bars

A.3.7 Set 7

P7-1

Basic Specimen Information

Specimen Type	Duct Type	Grouting	Date Cast	Date Grouted	Date Tested
Control	---	---	9/27/2011	---	11/8/2011

Specimen Dimensions

Nominal Loading Surface Dimensions	Actual Thickness	Actual Width	h	Duct Diameter(s)	h_{eff}	δ
24 x 7 in.	7 in.	23.9375 in.	24 in.	---	---	---

Material Properties

$f_{concrete}$	f_{grout}	$f_{grout}/f_{concrete}$	$f_{y,\ steel}$
10.15 ksi	---	---	64 ksi

Failure Information

$P_{failure}$	$\sigma_{failure}$	η_D
1217.0 kips	7.3 ksi	---

P7-2

Basic Specimen Information

Specimen Type	Duct Type	Grouting	Date Cast	Date Grouted	Date Tested
Control	---	---	9/27/2011	---	11/17/2011

Specimen Dimensions

Nominal Loading Surface Dimensions	Actual Thickness	Actual Width	h	Duct Diameter(s)	h_{eff}	δ
24 x 7 in.	7 in.	23.9375 in.	24 in.	---	---	---

Material Properties

$f_{concrete}$	f_{grout}	$f_{grout}/f_{concrete}$	$f_{y,\ steel}$
10.62 ksi	---	---	64 ksi

Failure Information

$P_{failure}$	$\sigma_{failure}$	η_D
1219.3 kips	7.3 ksi	---

P7-3

Basic Specimen Information

Specimen Type	Duct Type	Grouting	Date Cast	Date Grouted	Date Tested
Ducted	Plastic	Grouted	9/27/2011	10/5/2011	11/2/2011

Specimen Dimensions

Nominal Loading Surface Dimensions	Actual Thickness	Actual Width	h	Duct Diameter(s)	h_{eff}	δ
24 x 7 in.	7.0625 in.	24.125 in.	24 in.	3 in.	---	0.425

Material Properties

$f_{concrete}$	f_{grout}	$f_{grout}/f_{concrete}$	$f_{y,\ steel}$
10.15 ksi	4.51 ksi	0.44	64 ksi

Failure Information

$P_{failure}$	$\sigma_{failure}$	η_D
401.6 kips	2.4 ksi	0.32

Other Information

*Includes two ducts spaced apart by one duct diameter center-to-center

P7-4

Basic Specimen Information

Specimen Type	Duct Type	Grouting	Date Cast	Date Grouted	Date Tested
Ducted	Plastic	Grouted	9/27/2011	10/5/2011	11/4/2011

Specimen Dimensions

Nominal Loading Surface Dimensions	Actual Thickness	Actual Width	h	Duct Diameter(s)	h_{eff}	δ
24 x 7 in.	7.0625 in.	24.125 in.	24 in.	3 in.	---	0.425

Material Properties

$f_{concrete}$	f_{grout}	$f_{grout}/f_{concrete}$	$f_{y,\ steel}$
10.15 ksi	4.51 ksi	0.44	64 ksi

Failure Information

$P_{failure}$	$\sigma_{failure}$	η_D
378.1 kips	2.2 ksi	0.31

Other Information

*Includes two ducts spaced apart by two duct diameters center-to-center

P7-5

Basic Specimen Information

Specimen Type	Duct Type	Grouting	Date Cast	Date Grouted	Date Tested
Ducted	Plastic	Grouted	9/27/2011	10/5/2011	11/7/2011

Specimen Dimensions

Nominal Loading Surface Dimensions	Actual Thickness	Actual Width	h	Duct Diameter(s)	h_{eff}	δ
24 x 7 in.	7.0625 in.	24.0625 in.	24 in.	3 in.	---	0.425

Material Properties

$f_{concrete}$	f_{grout}	$f_{grout}/f_{concrete}$	$f_{y,\ steel}$
10.15 ksi	4.51 ksi	0.44	64 ksi

Failure Information

$P_{failure}$	$\sigma_{failure}$	η_D
454.9 kips	2.7 ksi	0.37

Other Information

*Includes two ducts spaced apart by three duct diameters center-to-center

P7-6

Basic Specimen Information

Specimen Type	Duct Type	Grouting	Date Cast	Date Grouted	Date Tested
Ducted	Plastic	Grouted	9/27/2011	10/5/2011	11/16/2011

Specimen Dimensions

Nominal Loading Surface Dimensions	Actual Thickness	Actual Width	h	Duct Diameter(s)	h_{eff}	δ
24 x 7 in.	7.0625 in.	24.0625 in.	24 in.	3 in.	21 in.	0.425

Material Properties

$f_{concrete}$	f_{grout}	$f_{grout}/f_{concrete}$	$f_{y,\ steel}$
10.62 ksi	4.86 ksi	0.46	64 ksi

Failure Information

$P_{failure}$	$\sigma_{failure}$	η_D
442.0 kips	2.6 ksi	0.36

Other Information

*Includes #3 'normal' hairpins against duct at middle vertical bar

P7-7

Basic Specimen Information

Specimen Type	Duct Type	Grouting	Date Cast	Date Grouted	Date Tested
Ducted	Plastic	Grouted	9/27/2011	10/5/2011	11/16/2011

Specimen Dimensions

Nominal Loading Surface Dimensions	Actual Thickness	Actual Width	h	Duct Diameter(s)	h_{eff}	δ
24 x 7 in.	7 in.	23.9375 in.	24 in.	3 in.	21 in.	0.429

Material Properties

$f_{concrete}$	f_{grout}	$f_{grout}/f_{concrete}$	$f_{y,\ steel}$
10.62 ksi	4.86 ksi	0.46	64 ksi

Failure Information

$P_{failure}$	$\sigma_{failure}$	η_D
515.8 kips	3.1 ksi	0.42

Other Information
*Includes #3 single-side, inverted hairpins against duct at outer two vertical bars

P7-8

Basic Specimen Information

Specimen Type	Duct Type	Grouting	Date Cast	Date Grouted	Date Tested
Ducted	Plastic	Grouted	9/27/2011	10/5/2011	11/16/2011

Specimen Dimensions

Nominal Loading Surface Dimensions	Actual Thickness	Actual Width	h	Duct Diameter(s)	h_{eff}	δ
24 x 7 in.	7.0625 in.	24.1875 in.	24 in.	2.375 in.	21.625 in.	0.336

Material Properties

$f_{concrete}$	f_{grout}	$f_{grout}/f_{concrete}$	$f_{y,\ steel}$
10.62 ksi	4.86 ksi	0.46	64 ksi

Failure Information

$P_{failure}$	$\sigma_{failure}$	η_D
529.4 kips	3.1 ksi	0.43

P7-9

Basic Specimen Information

Specimen Type	Duct Type	Grouting	Date Cast	Date Grouted	Date Tested
Ducted	Plastic	Grouted	9/27/2011	10/5/2011	11/16/2011

Specimen Dimensions

Nominal Loading Surface Dimensions	Actual Thickness	Actual Width	h	Duct Diameter(s)	h_{eff}	δ
24 x 7 in.	7.0625 in.	23.9375 in.	24 in.	3 in.	21 in.	0.425

Material Properties

$f_{concrete}$	f_{grout}	$f_{grout}/f_{concrete}$	$f_{y,\ steel}$
10.62 ksi	4.86 ksi	0.46	64 ksi

Failure Information

$P_{failure}$	$\sigma_{failure}$	η_D
451.1 kips	2.7 ksi	0.37

Other Information
*Sanded duct

A.3.8 Set 8

P8-1

Basic Specimen Information

Specimen Type	Duct Type	Grouting	Date Cast	Date Grouted	Date Tested
Control	---	---	10/27/2011	---	1/13/2012

Specimen Dimensions

Nominal Loading Surface Dimensions	Actual Thickness	Actual Width	h	Duct Diameter(s)	h_{eff}	δ
24 x 7 in.	7.125 in.	23.875 in.	24 in.	---	---	---

Material Properties

$f_{concrete}$	f_{grout}	$f_{grout}/f_{concrete}$	$f_{y,\ steel}$
11.16 ksi	---	---	64 ksi

Failure Information

$P_{failure}$	$\sigma_{failure}$	η_D
1643.4 kips	9.7 ksi	---

P8-2

Basic Specimen Information

Specimen Type	Duct Type	Grouting	Date Cast	Date Grouted	Date Tested
Control	---	---	10/27/2011	---	1/11/2012

Specimen Dimensions

Nominal Loading Surface Dimensions	Actual Thickness	Actual Width	h	Duct Diameter(s)	h_{eff}	δ
24 x 7 in.	7 in.	23.875 in.	24 in.	---	---	---

Material Properties

$f_{concrete}$	f_{grout}	$f_{grout}/f_{concrete}$	$f_{y,\ steel}$
11.16 ksi	---	---	64 ksi

Failure Information

$P_{failure}$	$\sigma_{failure}$	η_D
1653.7 kips	9.9 ksi	---

P8-3

Basic Specimen Information

Specimen Type	Duct Type	Grouting	Date Cast	Date Grouted	Date Tested
Ducted	Plastic	Grouted	10/27/2011	11/22/2011	1/9/2012

Specimen Dimensions

Nominal Loading Surface Dimensions	Actual Thickness	Actual Width	h	Duct Diameter(s)	h_{eff}	δ
24 x 7 in.	7.0625 in.	24.3125 in.	24 in.	3.375 in.	20.625 in.	0.478

Material Properties

$f_{concrete}$	f_{grout}	$f_{grout}/f_{concrete}$	$f_{y,\ steel}$
11.16 ksi	5.98 ksi	0.54	64 ksi

Failure Information

$P_{failure}$	$\sigma_{failure}$	η_D
456.1 kips	2.7 ksi	0.28

P8-4

Basic Specimen Information

Specimen Type	Duct Type	Grouting	Date Cast	Date Grouted	Date Tested
Ducted	Plastic	Grouted	10/27/2011	11/22/2011	1/9/2012

Specimen Dimensions

Nominal Loading Surface Dimensions	Actual Thickness	Actual Width	h	Duct Diameter(s)	h_{eff}	δ
24 x 7 in.	7.125 in.	24.1875 in.	24 in.	3.375 in.	20.625 in.	0.474

Material Properties

$f_{concrete}$	f_{grout}	$f_{grout}/f_{concrete}$	$f_{y,\ steel}$
11.16 ksi	5.98 ksi	0.54	64 ksi

Failure Information

$P_{failure}$	$\sigma_{failure}$	η_D
516.8 kips	3.0 ksi	0.31

Other Information
*Includes #3 'normal' hairpins against duct at outer two vertical bars

P8-5

Basic Specimen Information

Specimen Type	Duct Type	Grouting	Date Cast	Date Grouted	Date Tested
Ducted	Plastic	Grouted	10/27/2011	11/22/2011	1/10/2012

Specimen Dimensions

Nominal Loading Surface Dimensions	Actual Thickness	Actual Width	h	Duct Diameter(s)	h_{eff}	δ
24 x 7 in.	7.0625 in.	23.9375 in.	24 in.	2.375 in.	21.625 in.	0.336

Material Properties

$f_{concrete}$	f_{grout}	$f_{grout}/f_{concrete}$	$f_{y,\ steel}$
11.16 ksi	5.98 ksi	0.54	64 ksi

Failure Information

$P_{failure}$	$\sigma_{failure}$	η_D
821.3 kips	4.9 ksi	0.50

Other Information
*Includes #3 'normal' hairpins against duct at outer two vertical bars

P8-6

Basic Specimen Information

Specimen Type	Duct Type	Grouting	Date Cast	Date Grouted	Date Tested
Ducted	Plastic	Empty	10/27/2011	---	1/11/2012

Specimen Dimensions

Nominal Loading Surface Dimensions	Actual Thickness	Actual Width	h	Duct Diameter(s)	h_{eff}	δ
24 x 7 in.	7.0625 in.	24.0625 in.	24 in.	3 in.	21 in.	0.425

Material Properties

$f_{concrete}$	f_{grout}	$f_{grout}/f_{concrete}$	$f_{y,\ steel}$
11.16 ksi	---	---	64 ksi

Failure Information

$P_{failure}$	$\sigma_{failure}$	η_D
410.3 kips	2.4 ksi	0.25

Other Information
*Includes #3 'normal' hairpins against duct at all vertical bars

P8-7

Basic Specimen Information

Specimen Type	Duct Type	Grouting	Date Cast	Date Grouted	Date Tested
Ducted	Plastic	Grouted	10/27/2011	11/22/2011	1/13/2012

Specimen Dimensions

Nominal Loading Surface Dimensions	Actual Thickness	Actual Width	h	Duct Diameter(s)	h_{eff}	δ
24 x 7 in.	7.125 in.	24 in.	24 in.	3 in.	21 in.	0.421

Material Properties

$f_{concrete}$	f_{grout}	$f_{grout}/f_{concrete}$	$f_{y,\ steel}$
11.16 ksi	13.62 ksi	1.22	64 ksi

Failure Information

$P_{failure}$	$\sigma_{failure}$	η_D
535.5 kips	3.1 ksi	0.32

P8-8

Basic Specimen Information

Specimen Type	Duct Type	Grouting	Date Cast	Date Grouted	Date Tested
Ducted	Plastic	Grouted	10/27/2011	11/22/2011	1/13/2012

Specimen Dimensions

Nominal Loading Surface Dimensions	Actual Thickness	Actual Width	h	Duct Diameter(s)	h_{eff}	δ
24 x 7 in.	7.125 in.	24 in.	24 in.	3 in.	21 in.	0.421

Material Properties

$f_{concrete}$	f_{grout}	$f_{grout}/f_{concrete}$	$f_{y,\ steel}$
11.16 ksi	13.62 ksi	1.22	64 ksi

Failure Information

$P_{failure}$	$\sigma_{failure}$	η_D
743.1 kips	4.3 ksi	0.45

Other Information

*Includes #3 'normal' hairpins against duct at outer two vertical bars

P8-9

Basic Specimen Information

Specimen Type	Duct Type	Grouting	Date Cast	Date Grouted	Date Tested
Ducted	Plastic	Grouted	10/27/2011	11/22/2011	1/12/2012

Specimen Dimensions

Nominal Loading Surface Dimensions	Actual Thickness	Actual Width	h	Duct Diameter(s)	h_{eff}	δ
24 x 7 in.	7.125 in.	24 in.	24 in.	3 in.	21 in.	0.421

Material Properties

$f_{concrete}$	f_{grout}	$f_{grout}/f_{concrete}$	$f_{y,\ steel}$
11.16 ksi	13.62 ksi	1.22	64 ksi

Failure Information

$P_{failure}$	$\sigma_{failure}$	η_D
757.9 kips	4.4 ksi	0.46

Other Information

*Includes #3 'normal' hairpins in 'far' postiion at outer two vertical bars

A.3.9 Set 9

P9-1

Basic Specimen Information

Specimen Type	Duct Type	Grouting	Date Cast	Date Grouted	Date Tested
Control	---	---	12/20/2011	---	2/2/2012

Specimen Dimensions

Nominal Loading Surface Dimensions	Actual Thickness	Actual Width	h	Duct Diameter(s)	h_{eff}	δ
24 x 7 in.	7.125 in.	24 in.	24 in.	---	---	---

Material Properties

$f_{concrete}$	f_{grout}	$f_{grout}/f_{concrete}$	$f_{y,\ steel}$
10.19 ksi	---	---	64 ksi

Failure Information

$P_{failure}$	$\sigma_{failure}$	η_D
1704.2 kips	10.0 ksi	---

P9-2

Basic Specimen Information

Specimen Type	Duct Type	Grouting	Date Cast	Date Grouted	Date Tested
Control	---	---	12/20/2011	---	2/3/2012

Specimen Dimensions

Nominal Loading Surface Dimensions	Actual Thickness	Actual Width	h	Duct Diameter(s)	h_{eff}	δ
24 x 7 in.	7.125 in.	23.9375 in.	24 in.	---	---	---

Material Properties

$f_{concrete}$	f_{grout}	$f_{grout}/f_{concrete}$	$f_{y,\ steel}$
10.19 ksi	---	---	64 ksi

Failure Information

$P_{failure}$	$\sigma_{failure}$	η_D
1475.0 kips	8.6 ksi	---

P9-3

Basic Specimen Information

Specimen Type	Duct Type	Grouting	Date Cast	Date Grouted	Date Tested
Ducted	Plastic	Grouted	12/20/2011	1/4/2012	1/31/2012

Specimen Dimensions

Nominal Loading Surface Dimensions	Actual Thickness	Actual Width	h	Duct Diameter(s)	h_{eff}	δ
24 x 7 in.	7.0625 in.	24.0625 in.	24 in.	3 in.	21 in.	0.425

Material Properties

$f_{concrete}$	f_{grout}	$f_{grout}/f_{concrete}$	$f_{y,\ steel}$
10.19 ksi	6.25 ksi	0.61	64 ksi

Failure Information

$P_{failure}$	$\sigma_{failure}$	η_D
548.7 kips	3.2 ksi	0.35

P9-4

Basic Specimen Information

Specimen Type	Duct Type	Grouting	Date Cast	Date Grouted	Date Tested
Ducted	Plastic	Grouted	12/20/2011	1/4/2012	1/31/2012

Specimen Dimensions

Nominal Loading Surface Dimensions	Actual Thickness	Actual Width	h	Duct Diameter(s)	h_{eff}	δ
24 x 7 in.	7.125 in.	24 in.	24 in.	3 in.	21 in.	0.421

Material Properties

$f_{concrete}$	f_{grout}	$f_{grout}/f_{concrete}$	$f_{y,\ steel}$
10.19 ksi	6.25 ksi	0.61	64 ksi

Failure Information

$P_{failure}$	$\sigma_{failure}$	η_D
667.8 kips	3.9 ksi	0.42

Other Information

*Includes #3 'normal' hairpins against duct at outer two vertical bars

P9-5

Basic Specimen Information

Specimen Type	Duct Type	Grouting	Date Cast	Date Grouted	Date Tested
Ducted	Plastic	Grouted	12/20/2011	1/4/2012	2/1/2012

Specimen Dimensions

Nominal Loading Surface Dimensions	Actual Thickness	Actual Width	h	Duct Diameter(s)	h_{eff}	δ
24 x 7 in.	7.125 in.	23.9375 in.	24 in.	3 in.	21 in.	0.421

Material Properties

$f_{concrete}$	f_{grout}	$f_{grout}/f_{concrete}$	$f_{y,\ steel}$
10.19 ksi	6.25 ksi	0.61	64 ksi

Failure Information

$P_{failure}$	$\sigma_{failure}$	η_D
734.8 kips	4.3 ksi	0.46

Other Information

*Includes #3 inverted hairpins against duct at outer two vertical bars

P9-6

Basic Specimen Information

Specimen Type	Duct Type	Grouting	Date Cast	Date Grouted	Date Tested
Ducted	Plastic	Grouted	12/20/2011	1/4/2012	2/2/2012

Specimen Dimensions

Nominal Loading Surface Dimensions	Actual Thickness	Actual Width	h	Duct Diameter(s)	h_{eff}	δ
24 x 7 in.	7.0625 in.	24.0625 in.	24 in.	3 in.	21 in.	0.425

Material Properties

$f_{concrete}$	f_{grout}	$f_{grout}/f_{concrete}$	$f_{y,\ steel}$
10.19 ksi	6.25 ksi	0.61	64 ksi

Failure Information

$P_{failure}$	$\sigma_{failure}$	η_D
599.0 kips	3.5 ksi	0.38

Other Information

*Includes #3 single-side, inverted hairpins against duct at outer two vertical bars

P9-7

Basic Specimen Information

Specimen Type	Duct Type	Grouting	Date Cast	Date Grouted	Date Tested
Ducted	Plastic	Grouted	12/20/2011	1/4/2012	2/7/2012

Specimen Dimensions

Nominal Loading Surface Dimensions	Actual Thickness	Actual Width	h	Duct Diameter(s)	h_{eff}	δ
24 x 7 in.	7.125 in.	24.0625 in.	24 in.	3 in.	21 in.	0.421

Material Properties

$f_{concrete}$	f_{grout}	$f_{grout}/f_{concrete}$	$f_{y,\ steel}$
10.19 ksi	6.25 ksi	0.61	64 ksi

Failure Information

$P_{failure}$	$\sigma_{failure}$	η_D
704.9 kips	4.1 ksi	0.44

Other Information

*Includes #3 'flattened' hairpins against duct at outer two vertical bars

P9-8

Basic Specimen Information

Specimen Type	Duct Type	Grouting	Date Cast	Date Grouted	Date Tested
Ducted	Plastic	Grouted	12/20/2011	1/4/2012	2/7/2012

Specimen Dimensions

Nominal Loading Surface Dimensions	Actual Thickness	Actual Width	h	Duct Diameter(s)	h_{eff}	δ
24 x 7 in.	7.125 in.	24 in.	24 in.	3 in.	21 in.	0.421

Material Properties

$f_{concrete}$	f_{grout}	$f_{grout}/f_{concrete}$	$f_{y,\ steel}$
10.19 ksi	6.25 ksi	0.61	64 ksi

Failure Information

$P_{failure}$	$\sigma_{failure}$	η_D
825.2 kips	4.8 ksi	0.52

Other Information

*Includes #3 Z-bars against duct at outer two vertical bars

P9-9

Basic Specimen Information

Specimen Type	Duct Type	Grouting	Date Cast	Date Grouted	Date Tested
Ducted	Plastic	Grouted	12/20/2011	1/4/2012	2/8/2012

Specimen Dimensions

Nominal Loading Surface Dimensions	Actual Thickness	Actual Width	h	Duct Diameter(s)	h_{eff}	δ
24 x 7 in.	7.125 in.	24.25 in.	24 in.	3 in.	21 in.	0.421

Material Properties

$f_{concrete}$	f_{grout}	$f_{grout}/f_{concrete}$	$f_{y,\ steel}$
10.19 ksi	6.25 ksi	0.61	64 ksi

Failure Information

$P_{failure}$	$\sigma_{failure}$	η_D
775.0 kips	4.5 ksi	0.49

Other Information

*Includes #3 'staples' against duct at outer two vertical bars

A.3.10 Set 10

P10-1

Basic Specimen Information

Specimen Type	Duct Type	Grouting	Date Cast	Date Grouted	Date Tested
Control	---	---	1/10/2012	---	2/14/2012

Specimen Dimensions

Nominal Loading Surface Dimensions	Actual Thickness	Actual Width	h	Duct Diameter(s)	h_{eff}	δ
24 x 7 in.	7.125 in.	24 in.	24 in.	---	---	---

Material Properties

$f_{concrete}$	f_{grout}	$f_{grout}/f_{concrete}$	$f_{y,\ steel}$
9.82 ksi	---	---	64 ksi

Failure Information

$P_{failure}$	$\sigma_{failure}$	η_D
1532.6 kips	9.0 ksi	---

P10-2

Basic Specimen Information

Specimen Type	Duct Type	Grouting	Date Cast	Date Grouted	Date Tested
Control	---	---	1/10/2012	---	2/23/2012

Specimen Dimensions

Nominal Loading Surface Dimensions	Actual Thickness	Actual Width	h	Duct Diameter(s)	h_{eff}	δ
24 x 7 in.	7.125 in.	24.1875 in.	24 in.	---	---	---

Material Properties

$f_{concrete}$	f_{grout}	$f_{grout}/f_{concrete}$	$f_{y,\ steel}$
9.82 ksi	---	---	64 ksi

Failure Information

$P_{failure}$	$\sigma_{failure}$	η_D
1777.7 kips	10.3 ksi	---

P10-3

Basic Specimen Information

Specimen Type	Duct Type	Grouting	Date Cast	Date Grouted	Date Tested
Ducted	Steel	Grouted	1/10/2012	1/13/2012	2/13/2012

Specimen Dimensions

Nominal Loading Surface Dimensions	Actual Thickness	Actual Width	h	Duct Diameter(s)	h_{eff}	δ
24 x 7 in.	7.125 in.	24.25 in.	24 in.	2.375 in.	21.625 in.	0.333

Material Properties

$f_{concrete}$	f_{grout}	$f_{grout}/f_{concrete}$	$f_{y,\ steel}$
9.82 ksi	5.38 ksi	0.55	64 ksi

Failure Information

$P_{failure}$	$\sigma_{failure}$	η_D
1173.6 kips	6.8 ksi	0.71

Other Information
*Includes #3 'normal' hairpins against duct at outer two vertical bars

Basic Specimen Information

Specimen Type	Duct Type	Grouting	Date Cast	Date Grouted	Date Tested
Ducted	Steel	Grouted	1/10/2012	1/13/2012	2/13/2012

Specimen Dimensions

Nominal Loading Surface Dimensions	Actual Thickness	Actual Width	h	Duct Diameter(s)	h_{eff}	δ
24 x 7 in.	7.125 in.	23.8125 in.	24 in.	3 in.	21 in.	0.421

P10-4

Material Properties

$f_{concrete}$	f_{grout}	$f_{grout}/f_{concrete}$	$f_{y,\ steel}$
9.82 ksi	5.38 ksi	0.55	64 ksi

Failure Information

$P_{failure}$	$\sigma_{failure}$	η_D
999.7 kips	5.9 ksi	0.60

Other Information
*Includes #3 'normal' hairpins against duct at outer two vertical bars

Basic Specimen Information

Specimen Type	Duct Type	Grouting	Date Cast	Date Grouted	Date Tested
Ducted	Steel	Grouted	1/10/2012	1/13/2012	2/14/2012

Specimen Dimensions

Nominal Loading Surface Dimensions	Actual Thickness	Actual Width	h	Duct Diameter(s)	h_{eff}	δ
24 x 7 in.	7.125 in.	24.375 in.	24 in.	4 in.	20 in.	0.561

P10-5

Material Properties

$f_{concrete}$	f_{grout}	$f_{grout}/f_{concrete}$	$f_{y,\ steel}$
9.82 ksi	5.38 ksi	0.55	64 ksi

Failure Information

$P_{failure}$	$\sigma_{failure}$	η_D
858.6 kips	4.9 ksi	0.52

Other Information
*Includes #3 'normal' hairpins against duct at outer two vertical bars

Basic Specimen Information

Specimen Type	Duct Type	Grouting	Date Cast	Date Grouted	Date Tested
Ducted	Steel	Grouted	1/10/2012	1/13/2012	2/21/2012

Specimen Dimensions

Nominal Loading Surface Dimensions	Actual Thickness	Actual Width	h	Duct Diameter(s)	h_{eff}	δ
24 x 7 in.	7.0625 in.	24.125 in.	24 in.	2.375 in.	21.625 in.	0.336

P10-6

Material Properties

$f_{concrete}$	f_{grout}	$f_{grout}/f_{concrete}$	$f_{y,\ steel}$
9.82 ksi	11.07 ksi	1.13	64 ksi

Failure Information

$P_{failure}$	$\sigma_{failure}$	η_D
1416.1 kips	8.3 ksi	0.86

Other Information
*Includes #3 'normal' hairpins against duct at outer two vertical bars

Basic Specimen Information

Specimen Type	Duct Type	Grouting	Date Cast	Date Grouted	Date Tested
Ducted	Steel	Grouted	1/10/2012	1/13/2012	2/22/2012

Specimen Dimensions

Nominal Loading Surface Dimensions	Actual Thickness	Actual Width	h	Duct Diameter(s)	h_{eff}	δ
24 x 7 in.	7.125 in.	24.0625 in.	24 in.	3 in.	21 in.	0.421

P10-7

Material Properties

$f_{concrete}$	f_{grout}	$f_{grout}/f_{concrete}$	$f_{y,\ steel}$
9.82 ksi	11.07 ksi	1.13	64 ksi

Failure Information

$P_{failure}$	$\sigma_{failure}$	η_D
1199.1 kips	7.0 ksi	0.72

Other Information

*Includes #3 'normal' hairpins against duct at outer two vertical bars

Basic Specimen Information

Specimen Type	Duct Type	Grouting	Date Cast	Date Grouted	Date Tested
Ducted	Steel	Grouted	1/10/2012	1/13/2012	2/23/2012

Specimen Dimensions

Nominal Loading Surface Dimensions	Actual Thickness	Actual Width	h	Duct Diameter(s)	h_{eff}	δ
24 x 7 in.	7.125 in.	24.3125 in.	24 in.	4 in.	20 in.	0.561

P10-8

Material Properties

$f_{concrete}$	f_{grout}	$f_{grout}/f_{concrete}$	$f_{y,\ steel}$
9.82 ksi	11.07 ksi	1.13	64 ksi

Failure Information

$P_{failure}$	$\sigma_{failure}$	η_D
1176.6 kips	6.8 ksi	0.71

Other Information

*Includes #3 'normal' hairpins against duct at outer two vertical bars

Basic Specimen Information

Specimen Type	Duct Type	Grouting	Date Cast	Date Grouted	Date Tested
Ducted	Steel	Empty	1/10/2012	---	2/21/2012

Specimen Dimensions

Nominal Loading Surface Dimensions	Actual Thickness	Actual Width	h	Duct Diameter(s)	h_{eff}	δ
24 x 7 in.	7.125 in.	24 in.	24 in.	3 in.	21 in.	0.421

P10-9

Material Properties

$f_{concrete}$	f_{grout}	$f_{grout}/f_{concrete}$	$f_{y,\ steel}$
9.82 ksi	---	---	64 ksi

Failure Information

$P_{failure}$	$\sigma_{failure}$	η_D
585.2 kips	3.4 ksi	0.35

Other Information

*Includes #3 'normal' hairpins against duct at outer two vertical bars

A.3.11 Set 11

P11-1

Basic Specimen Information

Specimen Type	Duct Type	Grouting	Date Cast	Date Grouted	Date Tested
Control	---	---	2/1/2012	---	3/14/2012

Specimen Dimensions

Nominal Loading Surface Dimensions	Actual Thickness	Actual Width	h	Duct Diameter(s)	h_{eff}	δ
24 x 9 in.	9.25 in.	24 in.	24 in.	---	---	---

Material Properties

$f_{concrete}$	f_{grout}	$f_{grout}/f_{concrete}$	$f_{y,\ steel}$
9.25 ksi	---	---	64 ksi

Failure Information

$P_{failure}$	$\sigma_{failure}$	η_D
1354.6 kips	6.1 ksi	---

Other Information
*Data not accepted - premature flexural failure due to bearing pad deformation

P11-2

Basic Specimen Information

Specimen Type	Duct Type	Grouting	Date Cast	Date Grouted	Date Tested
Ducted	Plastic	Grouted	2/1/2012	2/10/2012	3/13/2012

Specimen Dimensions

Nominal Loading Surface Dimensions	Actual Thickness	Actual Width	h	Duct Diameter(s)	h_{eff}	δ
24 x 9 in.	9.1875 in.	24.125 in.	24 in.	3.375 in.	20.625 in.	0.367

Material Properties

$f_{concrete}$	f_{grout}	$f_{grout}/f_{concrete}$	$f_{y,\ steel}$
9.25 ksi	6.23 ksi	0.67	64 ksi

Failure Information

$P_{failure}$	$\sigma_{failure}$	η_D
528.2 kips	2.4 ksi	---

Other Information
*η_D computed based on estimated control failure load (see Chapter 4)

P11-3

Basic Specimen Information

Specimen Type	Duct Type	Grouting	Date Cast	Date Grouted	Date Tested
Ducted	Steel	Grouted	2/1/2012	2/10/2012	3/13/2012

Specimen Dimensions

Nominal Loading Surface Dimensions	Actual Thickness	Actual Width	h	Duct Diameter(s)	h_{eff}	δ
24 x 9 in.	9.25 in.	24.125 in.	24 in.	3.375 in.	20.625 in.	0.365

Material Properties

$f_{concrete}$	f_{grout}	$f_{grout}/f_{concrete}$	$f_{y,\ steel}$
9.25 ksi	6.23 ksi	0.67	64 ksi

Failure Information

$P_{failure}$	$\sigma_{failure}$	η_D
750.3 kips	3.4 ksi	---

Other Information

*η_D computed based on estimated control failure load (see Chapter 4)

P11-4

Basic Specimen Information

Specimen Type	Duct Type	Grouting	Date Cast	Date Grouted	Date Tested
Control	---	---	2/1/2012	---	3/12/2012

Specimen Dimensions

Nominal Loading Surface Dimensions	Actual Thickness	Actual Width	h	Duct Diameter(s)	h_{eff}	δ
24 x 7 in.	7.25 in.	24 in.	24 in.	---	---	---

Material Properties

$f_{concrete}$	f_{grout}	$f_{grout}/f_{concrete}$	$f_{y,\ steel}$
9.25 ksi	---	---	64 ksi

Failure Information

$P_{failure}$	$\sigma_{failure}$	η_D
1461.5 kips	8.4 ksi	---

P11-5

Basic Specimen Information

Specimen Type	Duct Type	Grouting	Date Cast	Date Grouted	Date Tested
Ducted	Plastic	Grouted	2/1/2012	2/10/2012	3/12/2012

Specimen Dimensions

Nominal Loading Surface Dimensions	Actual Thickness	Actual Width	h	Duct Diameter(s)	h_{eff}	δ
24 x 7 in.	7.125 in.	24.1875 in.	24 in.	3 in.	21 in.	0.421

Material Properties

$f_{concrete}$	f_{grout}	$f_{grout}/f_{concrete}$	$f_{y,\ steel}$
9.25 ksi	6.23 ksi	0.67	64 ksi

Failure Information

$P_{failure}$	$\sigma_{failure}$	η_D
703.2 kips	4.1 ksi	0.48

Other Information

*Data not accepted - outlying data

P11-6

Basic Specimen Information

Specimen Type	Duct Type	Grouting	Date Cast	Date Grouted	Date Tested
Ducted	Steel	Grouted	2/1/2012	2/10/2012	3/12/2012

Specimen Dimensions

Nominal Loading Surface Dimensions	Actual Thickness	Actual Width	h	Duct Diameter(s)	h_{eff}	δ
24 x 7 in.	7.25 in.	23.875 in.	24 in.	3 in.	21 in.	0.414

Material Properties

$f_{concrete}$	f_{grout}	$f_{grout}/f_{concrete}$	$f_{y, steel}$
9.25 ksi	6.23 ksi	0.67	64 ksi

Failure Information

$P_{failure}$	$\sigma_{failure}$	η_D
785.1 kips	4.5 ksi	0.54

P11-7

Basic Specimen Information

Specimen Type	Duct Type	Grouting	Date Cast	Date Grouted	Date Tested
Control	---	---	2/1/2012	---	3/9/2012

Specimen Dimensions

Nominal Loading Surface Dimensions	Actual Thickness	Actual Width	h	Duct Diameter(s)	h_{eff}	δ
24 x 5 in.	5.125 in.	24.125 in.	24 in.	---	---	---

Material Properties

$f_{concrete}$	f_{grout}	$f_{grout}/f_{concrete}$	$f_{y, steel}$
9.25 ksi	---	---	64 ksi

Failure Information

$P_{failure}$	$\sigma_{failure}$	η_D
842.0 kips	6.8 ksi	---

P11-8

Basic Specimen Information

Specimen Type	Duct Type	Grouting	Date Cast	Date Grouted	Date Tested
Ducted	Plastic	Grouted	2/1/2012	2/10/2012	3/9/2012

Specimen Dimensions

Nominal Loading Surface Dimensions	Actual Thickness	Actual Width	h	Duct Diameter(s)	h_{eff}	δ
24 x 5 in.	5.25 in.	24.125 in.	24 in.	2.375 in.	21.625 in.	0.452

Material Properties

$f_{concrete}$	f_{grout}	$f_{grout}/f_{concrete}$	$f_{y, steel}$
9.25 ksi	6.23 ksi	0.67	64 ksi

Failure Information

$P_{failure}$	$\sigma_{failure}$	η_D
518.2 kips	4.1 ksi	0.62

P11-9

Basic Specimen Information

Specimen Type	Duct Type	Grouting	Date Cast	Date Grouted	Date Tested
Ducted	Steel	Grouted	2/1/2012	2/10/2012	3/8/2012

Specimen Dimensions

Nominal Loading Surface Dimensions	Actual Thickness	Actual Width	h	Duct Diameter(s)	h_{eff}	δ
24 x 5 in.	5.1875 in.	24.1875 in.	24 in.	2.375 in.	21.625 in.	0.458

Material Properties

$f_{concrete}$	f_{grout}	$f_{grout}/f_{concrete}$	$f_{y,\ steel}$
9.25 ksi	6.23 ksi	0.67	64 ksi

Failure Information

$P_{failure}$	$\sigma_{failure}$	η_D
709.5 kips	5.7 ksi	0.84

P11-10

Basic Specimen Information

Specimen Type	Duct Type	Grouting	Date Cast	Date Grouted	Date Tested
Control	---	---	2/1/2012	---	3/14/2012

Specimen Dimensions

Nominal Loading Surface Dimensions	Actual Thickness	Actual Width	h	Duct Diameter(s)	h_{eff}	δ
24 x 9 in.	9 in.	23.75 in.	24 in.	---	---	---

Material Properties

$f_{concrete}$	f_{grout}	$f_{grout}/f_{concrete}$	$f_{y,\ steel}$
9.25 ksi	---	---	64 ksi

Failure Information

$P_{failure}$	$\sigma_{failure}$	η_D
1196.5 kips	5.6 ksi	---

Other Information

*Data not accepted - premature flexural failure due to bearing pad deformation

REFERENCES

American Association of State Highway and Transportation Officials (AASHTO) (2010). "AASHTO LRFD Bridge Construction Specifications, 3rd Edition." Washington, DC.

American Association of State Highway and Transportation Officials (AASHTO) (2012). "AASHTO LRFD Bridge Design Specifications: Customary U.S. Units, 6th Edition." Washington, DC.

American Concrete Institute (ACI) Committee 318 (2011). "Building Code Requirements for Structural Concrete (ACI 318-11) and Commentary." American Concrete Institute, Farmington Hills, MI.

British Standards Institute (BSI) (2008). "Eurocode 2: Design of Concrete Structures – Part 1-1: General rules and rules for buildings, BS EN 1992-1-1:2004." London, UK.

Campbell, T.I. and Batchelor, B. (1981). "Effective Width of Girder Web Containing Prestressing Duct." ASCE Journal of the Structural Division, Vol. 107, No. ST5, pp. 733-744.

Campbell, T.I., Batchelor, B., and Chitnuyanondh, L. (1979). "Web Crushing in Concrete Girders With Prestressing Ducts in the Web." PCI Journal, September/October 1979, pp. 70-88.

Chitnuyanondh, L. (1976). "Shear Failure of Concrete I-Beams with Prestressing Ducts in the Web." PhD Dissertation, Queen's University, Kingston, Ontario, Canada.

Clarke, J.L. and Taylor, H.P.J. (1975). "Web Crushing – A Review of Research." Technical Report 42.509, Cement and Concrete Association, pp. 1-16.

Corven, J. and Moreton, A. (2004). "Post-Tensioning Tendon Installation and Grouting Manual." U.S. Department of Transportation Federal Highway Administration, Washington, DC.

Florida Department of Transportation (FDOT) (2012). "Structures Design Guidelines." FDOT Structures Manual, Vol. 1.

Ganz, H. R., Ahmad, A. and Hitz, H. (1992). "Load Transfer Through Concrete Sections With Grouted Ducts." Report No. 242e, VSL International Ltd., Berne, Switzerland.

Gaynor, R. D. (1965). "Effect of Horizontal Reinforcing Steel on the Strength of Molded Cylinders." ACI Journal, July 1965, pp. 837-840.

Hars, E. and Muttoni, A. (2006). "Essais à l'effort tranchant sur des poutres précontraintes à âme mince (Shear tests on prestressed beams with thin webs)." Report No. 01.03-R1, Ecole Polytechnique Fédérale de Lausanne, Lausanne, Switzerland.

Japan Society of Civil Engineers (JSCE) (2002). "Standard Specifications for Concrete Structures." JSCE Guidelines for Concrete, No. 3, Tokyo, Japan.

Krauss, R., Heimgartner, E., and Bachmann, H. (1973). "Versuche über den Einfluss geneigter Spannkabel in teilweise vorgespannten Betonbalken (Experiments on the influence of inclined prestressing tendons in partially prestressed concrete beams)." Report No. 6504-6, Institut für Baustatik Eidgenössische Technische Hochschule Zürich, Zurich, Switzerland.

Lee, S., Cho, J., and Oh, B. (2010). "Shear Behavior of Large-Scale Post-Tensioned Girders with Small Shear Span-Depth Ratio." ACI Structural Journal, March-April 2010, pp. 137-145.

Leonhardt, F. (1969). "Abminderung der Tragfähigkeit des Betons infolge stabförmiger, rechtwinklig zur Druckrichtung angeordnete Einlagen (Reduction of Concrete Compressive Strength due to Rods Inserted Perpendicularly to the Loading)." Festschrift Rüsch, pp. 71-78.

Muttoni, A., Burdet, O.L., and Hars, E. (2006). "Effect of Duct Type on Shear Strength of Thin Webs." ACI Structural Journal, September-October 2006, pp. 729-735.

Rezai-Jorabi, H. and Regan, P.E. (1986). "Shear resistance of prestressed concrete beams with inclined tendons." The Structural Engineer, Vol. 64B, No. 3, pp. 63-75.

Schmidt, K.A. (2011). "Development of a Testing Frame for Studying the Effects of Ducts on the Shear Capacity of Concrete Girders." Report, The University of Texas at Austin, Austin, TX.

VITA

David Michael Wald graduated from J. Frank Dobie High School in Houston, Texas in 2006. He received his Bachelor of Science in Architectural Engineering with Highest Honors from The University of Texas at Austin in May, 2010. In August, 2010, he enrolled in the civil engineering graduate program at The University of Texas at Austin where he worked at the Phil M. Ferguson Structural Engineering Laboratory. He received his Master of Science in Engineering in December, 2012 and is continuing work toward a Doctor of Philosophy.

E-mail: dwald3325@sbcglobal.net

This thesis was typed by the author.